Mechanosensitive adhesive networks guide collective migration of *Xenopus* mesendoderm

Maureen Ann Bjerke

B.A., University of Colorado at Boulder, 2005

A Dissertation Presented to the Graduate Faculty
of the University of Virginia in Candidacy for the Degree of
Doctor of Philosophy

Department of Cell Biology

University of Virginia
May 2014

Abstract

Developing embryos undergo dramatic cell and tissue rearrangements that are required for morphogenesis. These movements have long been thought to be governed by chemical signals encoded by genetic information. However, it has recently become clear that developing tissues also generate forces that are transmitted throughout the tissue, sensed by cells, and transduced into chemical guidance cues. Physical forces may thus act analogously to morphogens, working in a "concentration-dependent" manner and in conjunction with chemical signals to establish the shape and pattern of an embryo. In this dissertation, I explore the mechanisms by which cells sense, integrate, and respond to forces on cadherin- and integrin-based adhesion complexes, and the manner in which the resultant signals guide collective cell migration.

During gastrulation of the *Xenopus* embryo, traction forces are generated by mesendoderm cells as they migrate collectively across an extracellular matrix (ECM) composed of fibronectin. Tissue cohesion is maintained by cadherin-based cell-cell adhesions that resist and balance the traction forces generated by migration. I establish here that anisotropic tension on cadherin adhesions leads to the assembly of a mechanosensitive cadherin adhesion complex containing the intermediate filament protein keratin and the catenin-family protein plakoglobin. The spatial organization of keratin and plakoglobin is dependent on tension at cell-cell adhesions and adhesion to fibronectin. Furthermore, both keratin and plakoglobin are required for force-induced polarization of protrusions in mesendoderm cells. I demonstrate that the integrin associated protein focal adhesion kinase (FAK) is required for multiple morphogenetic events occurring in the early development of the *Xenopus* embryo. FAK is required for

protrusive polarity of migrating mesendoderm cells, organization of keratin filaments and association between plakoglobin and cadherins. I propose that FAK acts by modulating the dynamic balance of traction forces and cell cohesion necessary for polarity within the collectively migrating tissue.

Although mechanical stimuli have emerged as key regulators of development and of pathologic events such as the metastatic invasion of tumor cells, the molecular mechanisms by which forces are sensed are not well understood. I describe here a mass spectrometry based screen designed to discover proteins involved in mechanotransduction by identifying proteins that undergo a conformational change in response to force on cell-cell or cell-ECM adhesions. Initial findings in this screen include proteins involved in the citric acid cycle and glycolysis, suggesting that tension on adhesion complexes may modulate energy production in the cell. These studies now set the stage for continued investigation into the components and mechanisms of adhesion-dependent mechanotransduction. Together the data presented here indicate that regulation of cell polarity in mesendoderm by anisotropic tension generated via the balance of tractive and cohesive forces represents an emergent property of this collectively migrating tissue.

Acknowledgements

This work would not have been possible without the support and generosity of many people to whom I am deeply grateful. First, I would like to thank my advisor, Doug DeSimone, for the guidance he has provided along my path to becoming a scientist. He has given me the opportunity and encouragement to read, to explore, to critique, to create, to argue and to teach. He has also given me room to fail, and then helped me to find my feet again.

I am thankful to all those who have created the scientific community in which I have been immersed for the last several years. To all the past and present members of the DeSimone Lab for making my home away from home a lively and enriching place. To Fred Simon for expert frog care, lab management and home repair advice. To Greg Weber for acting as a mentor, collaborator, sounding board and partner-in-pranks. To the members of my thesis committee, Bettina Winckler, Jing Yu, Martin Schwartz and Ann Sutherland, and to Rick Horwitz and David Castle for advising me, encouraging me and setting me straight. And, to the students and faculty of the Cell Biology department with whom I have enjoyed many enlightening presentations and hallway conversations.

I am truly grateful for the love and support of my family and friends. I am thankful for the enduring friendship of my fellow scientists Bette Dzamba, Tania Rozario, Phoebe Williams, and Jenny Hodges. I can't imagine surviving grad school without the girl's nights, handwritten letters, bicycling adventures and more. I am also thankful to Patty, Pam, Gay, Heather, Robin, Dina, and Tonya for being like sisters to me, brought together by a shared joy in our canine companions. I owe a great debt of gratitude to my family, especially to my parents, Charles and Kathleen, who set me up for success and helped me to pursue my dreams. Finally, I would like to thank my best-friend and husband, Glen Bjerke, for the years of love, light and laughter we have shared thus far. I could not have traveled this road without his constant presence beside me.

Table of Contents

List of Figures

List of Abbreviations

AFM	atomic force microscopy
BAE	basal adhesion extraction
Biotin-HPDP	N-[6-(Biotinamido)hexyl]-3-(2-pyridyldithio)propionamide
CALI	chromophore-assisted light inactivation
C-Cad.Fc	extracellular domain of C-cadherin fused to a human Fc peptide
cFAK	chicken (*Gallus gallus*) FAK
CS-MS	cysteine shotgun mass spectrometry
DMZ	dorsal marginal zone (explant)
ECM	extracellular matrix
EGFP	enhanced green fluorescent protein
FAK	focal adhesion kinase
Fn	fibronectin
FRET	Förster resonance energy transfer
FRNK	FAK-related non-kinase
GAPDH	glyceraldehyde 3-phosphate dehydrogenase
GFP	green fluorescent protein
GTP	guanosine triphosphate
HEPES	4-(2-hydroxyethyl)-1-piperazineethanesulfonic acid
HF-MBS	HEPES-free modified Barth's saline
IAM	iodoacetamide

IP	immunoprecipitation
KIF	keratin intermediate filaments
LC-MS/MS	liquid chromatography in line with tandem mass spectrometry
mBBr	monobromobimane
MBS	modified Barth's saline
MDCK	Madin-Darby canine kidney epithelial cells
MLC	myosin light chain
MO	morpholino
mPAD	microfabricated post array detector
PDGF	platelet derived growth factor
PDMS	polydimethylsiloxane
Pkg	plakoglobin (also known as γ-catenin)
PLL	poly-L-lysine
pLLp	posterior lateral line primordium
RT	room temperature
SDS-PAGE	sodium dodecyl sulfate – polyacrylamide gel electrophoresis
SEM	standard error of the mean
Supe	supernatant
TBS	Tris buffered saline
XCK	*Xenopus laevis* cytokeratin
xFAK	*Xenopus laevis* FAK

Note to the reader

Unless otherwise noted in the figure legends, all data were generated and analyzed by the author, Maureen Bjerke. In some instances data or diagrams were generated in collaboration with others. These data and diagrams are primarily found in Chapter 2 and are noted as such. Some data were collected wholly by Gregory Weber and are included for the sake of clarity. However, even in these instances, the design and analysis of the experiments were conducted cooperatively.

Chapter 1

Introduction

This chapter is based in part on work that is in preparation for publication:

Bjerke MA, Weber GF, and DeSimone DW. Influences of cell-cell contacts on migration. *Journal of Cell Science*

and in part on previously published work:

Weber GF, **Bjerke MA**, and DeSimone DW. 2011. Integrins and cadherins join forces to form adhesive networks. *Journal of Cell Science* 124: 1183-93.

1.1 Influences of cell-cell contacts on migration

Cell migration takes place in many physiological and pathological contexts and in an abundance of different forms. Most cells that migrate within multicelled organisms do so in an environment where stable or transient contacts are made with neighboring cells. The manner and organization with which cells and tissue move is dependent on their environment. Epithelial cells engaged in wound repair migrate as contiguous sheets over a nearly planar surface to fill open space (Friedl and Gilmour, 2009; Vedula et al., 2013). Tumor cells invading stroma densely packed with extracellular matrix (ECM) typically migrate as long cords of cells due to geometric constraints of the environment (Friedl et al., 2012; Wolf et al., 2007). Many neural crest cells migrate individually but transient interactions with one another are often required for directional path-finding (Theveneau and Mayor, 2012). Border cells in the *Drosophila* oocyte migrate as a cluster using interactions with neighboring cells to generate motile force for their migration toward the egg chamber (Montell et al., 2012). This diversity of cell behaviors reveals a variety of migration strategies employed to deal with the general challenges presented by complex 3-D environments comprised of ECM and surrounding tissues.

It is clear that cell-cell contacts are essential for the cohesion of collectively migrating cells, but it is important to consider the many additional consequences and benefits of neighbor association in the regulation of migratory behavior. Cell-cell adhesion proteins like cadherins serve as signaling centers in addition to providing a primary mechanism for holding cells and tissues together. However, other classes of proteins and signaling events also influence and are influenced by cell-cell contacts including gap junctions and surface-bound ligands. While many studies have addressed

influences of the extracellular environment (e.g. ECM, growth factors, chemokines) on migration, I focus here on the ways in which cell-cell contacts influence the behavior of migrating cells. A variety of developmental and pathological systems will be discussed and a particular emphasis placed on the role of cell-cell contacts in the establishment and maintenance of directional polarity.

1.2 Mechanical coupling and tissue geometry

Tissue geometry and mechanical signals have a significant impact on the behavior of migratory tissues as well as single cells migrating through a stationary tissue. Cells in vivo are subject to geometric constraints arising from the 3-D organization of ECM and neighboring cells (Baker and Chen, 2012). Invading clusters of tumor cells typically overcome geometric constraints imposed by ECM via proteolysis and changes in morphology of the migrating cluster (Wolf et al., 2007). However, the mechanisms by which cells cope with spatial constraints imposed by neighboring cells are less clear. What is known is that contacts with neighboring cells influence cell morphology and polarity as well as the generation and transduction of mechanical forces in migrating cells.

Role of adhesive networks in mechanical coupling

In migrating or spreading groups of cells, traction stresses on ECM substrates are balanced by tension across cell-cell adhesions (Maruthamuthu et al., 2011; Trepat et al., 2009). Cadherin mediated cell-cell junctions then facilitate the dynamic propagation of tension through tissues (Maruthamuthu et al., 2011; Serra-Picamal et al., 2012; Trepat et

al., 2009). Cadherin adhesions are required for the organization of traction stresses in groups of cells, as evidenced by a loss of polarity in traction vectors upon disruption of cell cohesion (Mertz et al., 2013). The magnitude and functional significance of mechanical coupling through cadherins likely depend on cell type. Cell groups or tissues that undergo frequent cell rearrangements may be able to dissipate tension, in contrast to cell types in which few such events take place and a build-up of tension is observed (Vedula et al., 2014).

Integrin-mediated substrate tractions and cadherin-mediated cell-cell cohesion can influence one another to form a balanced adhesive network (Weber et al., 2011). Increased traction stresses often lead to increases in tension on cell-cell junctions as described above. However, the strength of cell-cell adhesions may also alter the ability of cells to generate traction forces on a substrate. For instance, groups of ectoderm cells from the blastocoel roof of gastrulating *Xenopus* embryos exert greater traction forces on fibronectin (Fn) than do single ectoderm cells (Dzamba et al., 2009). This behavior illustrates the importance of cell-cell contacts in modulating the interactions of cells with an adhesive substrate. Cells also sense substrate stiffness differently when in contact with one another. The migration rate and coordination of epithelial cell movement into open space are affected by the stiffness of the substrate on which they are migrating (Murrell et al., 2011). The polarity of protrusions and migration vectors within the migrating cell group is more pronounced when the cells are on a stiffer substrate and the degree to which polarity extends to cells behind the leading edge particularly affected by substrate stiffness (Ng et al., 2012). Together these data indicate that the mechanical

linkages between cell-cell and cell-ECM adhesions are critical for the regulation of coordinated cell migration.

Adhesive networks of cell-cell and cell-ECM adhesions are linked within each cell by the cytoskeleton and the intersecting signaling pathways initiated by cell contact and adhesion (Weber et al., 2011). Physical linkages through cytoskeletal connections provide mechanical coupling between adhesive specializations, a function that is likely to be particularly important in collective migration. Supracellular (i.e. across the tissue) actin cabling appears along the leading edge of the migrating sheet, potentially contributing to coordination or mechanical stability of the cell group (Farooqui and Fenteany, 2005). Disruption of cadherin cell-cell adhesions has broad impact on the actin cytoskeleton and cell-matrix adhesions. Supracellular organization of actin filaments is disrupted by disassembly of cadherin adhesions (Mertz et al., 2013). Contractility of the actin cytoskeleton by myosin motor proteins generates tension on the cytoskeleton and distally located adhesions. Myosin function is required for coordinating the effects of substrate stiffness on collective movement and cell-cell adhesion through cadherin-catenin complexes (Boghaert et al., 2012). In addition, inhibition of the intercellular transmission of tension through a tissue via interference with cadherin adhesions can block invasion of tumor cells into that tissue, even if cellular contractility is increased. Thus, the cytoskeleton, cell cohesions and cell-matrix adhesions are all instrumental load-bearing components that enable the mechanical coupling of collectively migrating cells.

Regulation of migration by spatial constraints

Spatial constraints have been shown to alter cell migration rates, either increasing or decreasing rates depending on cell type and the specific organization of the migrating group (Doyle et al., 2009; Vedula et al., 2014, 2012). The size of the area available for cells to migrate into/onto has a significant effect on motile behavior and thus the rate of collective movements (Vedula et al., 2012). Sheets of epithelial cells migrating into a narrow area have high rates of migration and high variations in rates, while a broad advancing tissue front is associated with slower but steadier rates of migration. A correlation is also observed between tissue geometry and coordination of migration velocities. Each of these phenomena are dependent on both cell-cell adhesions and cellular contractility. Interestingly, slower migration is observed in keratinocyte monolayers when induced to form "epithelial bridges" between narrow stripes of ECM (Vedula et al., 2014). This decrease in migration onto a narrow area is thought to be a secondary effect of the tension generated by suspension of cells across ECM free areas. Each of these examples involves confinement mediated by ECM, however, geometric constraints mediated by cell-cell contacts are likely to have similar effects on the behavior and mechanical properties of migrating cells.

During collective migration of the posterior lateral-line primordium (pLLp) cells in zebrafish, spatial constraints are thought to contribute to the morphology and polarity of the tissue (Pouthas et al., 2008). Artificial constraint of migrating lateral line cells in vitro is sufficient to induce sub-cellular localization of organelles and cytoskeletal elements akin to the localization observed in the tissue in vivo. Migration of border cells in the *Drosophila* oocyte provides another striking example of cells migrating in a

geometrically constrained environment. Border cells migrate as a cohesive cluster through a mass of other cells (Montell et al., 2012). Tension generated during migration leads to deformation of the cells in the cluster and to activation of a mechanosensitive signaling pathway that promotes migratory behavior and helps to maintain integrity of the cluster (Somogyi and Rørth, 2004). The movement of mesendoderm cells in the gastrulating *Xenopus* embryo is constrained by both cell-ECM and cell-cell interactions. Mesendoderm cells begin migration as a multi-layered sheet moving onto a Fn matrix. However, at later stages the mesendoderm forms an annular ring and becomes laterally confined as it moves toward the top of the spherical embryo and the ring closes (Davidson et al., 2002). The diminishing open area and narrowing circumference require that the shape or perhaps arrangement of the cells must change, although the mechanisms contributing to this process are not understood. Given the relationships between tissue geometry and mechanical coupling in many other cell types, it is tempting to speculate that mechanical interactions between the migrating cells may be guiding this aspect of tissue morphogenesis.

1.3 Directional cues

Cell-cell contacts influence the generation and maintenance of polarity in many migrating cell types and there are a number of different means by which they do so. Cells in some tissues require geometric or mechanical cues for directionality. Some cells require cell-cell contacts in order to generate and/or respond to chemotactic signals. In other cases, cell adhesion proteins act as specific substrates for migration and may form a pathway for the migratory cells to follow. The following are a few of the many

examples of migration events in which the guidance of migratory direction requires cell-cell contacts.

Directional signaling through tissue geometry

It has long been established that cell-cell contact can inhibit migration and result in retraction or collapse of lamellipodia (Abercrombie and Heaysman, 1954, 1953). It has also been observed that pairs or small clusters of cells are typically polarized such that they extend protrusions away from their contacts with one another (Kolega, 1981). A combination of experimental data gleaned from cells on substrates of confined geometry and from computer modeling suggests that this type of contact inhibition promotes collective migration (Desai et al., 2013). Cells on substrates of confined geometry display cadherin-dependent polarization of both protrusions and internal features such as nucleus-centrosome orientation (Desai et al., 2009; Dupin et al., 2009). Geometric constraints present in a tissue likely lead to more occasions for cell-cell collisions and thus more occasions for contact inhibition to occur. Therefore, directional migration may simply arise from geometric constraints that induce cells to move toward regions that have fewer or no neighboring cells.

Many studies have used in vitro "scratch-wounding" of a monolayer to generate free edges. The migration of cells into the newly open space supports the notion that removal of geometric constraints is sufficient to dictate directional migration. However, this method has the drawback of damaging cells in a way that may induce migration through other means, such as the release of chemical stimuli. In recent years, new techniques have been developed where cells are presented with free space on which to

migrate without significant damage to the cell sheet. In accordance with the earlier studies, free space generated by removal of a barrier is sufficient to induce motility into the open area (Block et al., 2010, 2004; Poujade et al., 2007; van Horssen et al., 2006). The use of acellular barriers for these assays points toward a mechanical model of contact inhibition whereby the lack of tension from the open space is serving as a physical cue and stimulus to migration (Klarlund and Block, 2011).

As epithelial cell sheets begin migrating into open space, cells at the leading edge lose some of their epithelial character (Poujade et al., 2007). The leader cells become protrusive and highly migratory but maintain connections with neighboring cells. Migration velocities among neighboring cells are correlated, even several rows behind the leading edge, indicating transmission of a directional cue. The mechanical pull of the leading edge cells is required for the collective orientation of the migrating cells and the mechanical resistance of the following cells is required to maintain polarity of the leading cells (Reffay et al., 2011). Furthermore, the specification of the leader cell is a consequence of the collective orientation of the migrating tissue, generating a positive feedback loop initiated by the appearance of free space and maintained by mechanical coupling through cell-cell contacts.

Directional signaling via mechanical cues

How do cells respond behaviorally to mechanical forces exerted on them by their neighbors? Maps of calculated intercellular stresses in expanding monolayers of epithelial and endothelial cells correlate with the shape and orientation of the constituent cells (Tambe et al., 2011). Stronger stress anisotropy is correlated with stronger polarity

of cell shape. A number of studies have also demonstrated a tension-dependent correlation of migration velocities among neighboring cells (Reffay et al., 2011; Tambe et al., 2011). The orientation of cells and directional migration in alignment with stress anisotropy is, not surprisingly, dependent on cadherin based cell-cell junctions. However, in some cases cells will orient traction and velocity vectors toward open (but un-fillable) space even when at odds with the local tension anisotropy (Kim et al., 2013). This suggests that a drive to simply fill empty spaces may provide some directionality to endothelial or epithelial cell sheets confronted with open space or a free edge.

Generation of force gradients or anisotropies in tissues is thought to serve as a directional cue akin to chemical gradients (Serra-Picamal et al., 2012). The force landscape within a cell sheet exhibits many spatial variations and fluctuations in magnitude (Tambe et al., 2011). Therefore, mechanical guidance cues may be related to fluctuations or shifts in the overall balance of forces (Fredberg and Trepat, 2011). Cells within an expanding or migrating monolayer have a strong tendency to orient along the maximal principal stress so as to minimize cell-cell shear stresses, and they appear to do so via active remodeling. This type of guidance cue is termed plithotaxis (Fredberg and Trepat, 2011; Roca-Cusachs et al., 2013). Cells thereby sense, respond to and modulate the tension landscape of the tissue. Importantly, each of these activities requires mechanical linkages between cells via cell-cell contacts.

Xenopus mesendoderm cells migrate directionally across a Fn substrate, even when explanted from the embryo and placed in culture (Davidson et al., 2002). The availability of a free edge may guide the polarity of the leading edge cells, as observed in "wounded" epithelial or endothelial monolayers. However, polarity and migratory

behavior are not restricted to a small subset of leading cells at the tissue front. Rather, mesendoderm cells in the following rows of the tissue extend cryptic lamellipodia underneath the cells in front of them (Davidson et al., 2002). Perhaps then the mechanical properties of the cell/tissue environment can be stimuli for directional migration. Indeed, application of force to cadherin adhesions is sufficient to induce polarity of protrusions and directional migration (Weber et al., 2012). Cadherin engagement is necessary but not sufficient to generate polarized cell movements (Weber et al., 2012; Winklbauer and Selchow, 1992). Directional migration is induced specifically by tension transmitted through cell-cell adhesions, a guidance mechanism termed "cohesotaxis" (Roca-Cusachs et al., 2013; Weber et al., 2012).

Directional guidance of zebrafish mesendoderm appears to be similar in many respects to that of X*enopus* mesendoderm. In particular, cells must be in contact with their neighbors in order to migrate directionally (Dumortier et al., 2012). Furthermore, cells need contact with the endogenous prechordal plate tissue, suggesting that directional information is shared among cells in these tissues. Directional migration requires Wnt/PCP and Rac signaling, giving some hint of the pathways involved in the intercellular communication of directional information. It is reasonable to suppose that the mechanical properties of the tissue are influencing the organization and perhaps orientation of the cells via cell-cell contacts. In addition, in migrating epithelial sheets, a spatial correlation has been reported between Rho-family GTPase activity (specifically RhoA) and mapped forces within the migrating group (Reffay et al., 2014). This finding suggests a possible mechanism for the direction of protrusive activity through a feedback loop of force-mediated regulation of Rho-family GTPase activities.

Some types of intercellular organization depend on mechanical interactions between cells but are not necessarily related to the strength of cell-cell adhesions. One such instance is the orientation of cell groups in response to topographic cues on the substrate. Groups of cells exhibit more coordinated behavior on grooved (versus flat) substrates (Londono et al., 2014). Remarkably, cells on flat substrates can receive orientation signals from cells on grooved substrates across a distance of 6-9 cells. These orientation signals appear to be dependent on steric hindrance rather than on mechanical coupling through cell-cell adhesions. It is important to note that the cells in this study were not induced to migrate and may be behave differently if given a migratory stimulus.

Collective chemotaxis

Soluble chemical signals can act to simulate and direct cell migration, a process known as chemotaxis. Many individual and collective cell migration events are dependent on chemotactic signals (Rørth, 2011). Cells in the zebrafish pLLp migrate along a uniform track of the chemokine Sdf1 (also known as Cxcl12a) (David et al., 2002). Although single cells migrate toward increasing gradients of Sdf1, directional migration in the embryo requires an intact tissue (Haas and Gilmour, 2006). Differential expression (Dambly-Chaudière et al., 2007; David et al., 2002) and internalization (Donà et al., 2013) of chemokine receptors within the tissue generate a spatial gradient of chemotactic signal that is sufficient to guide migration. The generation of this chemotactic gradient likely does not depend on direct signals from cell-cell adhesions, but importantly it does require cadherin-mediated organization of the migrating tissue (Aman and Piotrowski, 2011; Donà et al., 2013).

Collective movement of cells in response to chemotactic cues may also have a role in directing migration of *Xenopus* mesendoderm cells. PDGF signaling is required for directionality of groups of mesendoderm cells on native ECM substrates, and inhibition of PDGF signaling inhibits normal gastrulation movements in the embryo (Nagel et al., 2004). However, cells must be in groups in order to be directed by PDGF signaling, suggesting that there may be some similarity to the collective chemotaxis involved in pLLp migration in zebrafish. The observation that intact tissue can migrate directionally on an isometric substrate without PDGF gradients (Davidson et al., 2002) suggests that growth factor signaling may be secondary to or complementary to the directional cues provided through cell-cell junctions.

Cadherins as substrates for migration

Although we most commonly think of cells migrating on extracellular matrix (ECM), some cells (e.g. post-mitotic neural progenitor cells, *Drosophila* border cells) use other cells as a migratory substrate (Montell et al., 2012; Shikanai et al., 2011). Neurons provide a classic example of cells that use cell-cell adhesions as a substrate for migration (Chiba and Keshishian, 1996). Cadherin family adhesion proteins have long been thought to also provide directional information for neural path-finding but there is still only limited evidence to support this hypothesis (Kolodkin and Tessier-Lavigne, 2011; Nern et al., 2008). A second example is the migration of border cell clusters in *Drosophila* oocytes. This migration is dependent on DE-cadherin mediated interactions of the border cells with each other and with the nurse cells through which the cluster migrates (Niewiadomska et al., 1999). If border cells are interacting with both the nurse

cells on which they are migrating and which each other through the same adhesion molecule, how is directional migration generated? Development of front-rear polarity and directional migration of the cell cluster is stimulated by coordinated signaling through two growth factor receptors, EGFR (epidermal growth factor receptor) and PVR (PDGF- and VEGF-receptor related) (Duchek and Rørth, 2001; Duchek et al., 2001; McDonald et al., 2006, 2003). Spatially restricted expression and accumulation of ligands for these receptors guides the border cell cluster toward its target across a substrate of neighboring cells.

1.4 Cytosolic coupling through gap junctions

Although in most migratory events we think of cell-cell contacts in terms of adhesion, there are a number of cell-surface proteins that depend on direct apposition of cell membranes. Gap junctions are a particularly interesting example. Gap junctions are composed of connexin family proteins that form a pore linking the cytoplasms of neighboring cells. These junctions enable fast communication between adjoining cells by allowing transfer of ions and small molecules. Dye transfer studies provide strong evidence for cell-cell communication through gap junctions in migrating cell sheets, invading tumor cells, and between extravasating lymphocytes and endothelia (Defranco et al., 2008; Oliveira et al., 2005; Oviedo-Orta et al., 2002). In wounded epithelia, up-regulation in assembly of gap junctions has been observed, as well as the appearance of gap junctions among myofibroblasts in the wounded tissue (Gabbiani et al., 1978). Calcium waves are also apparent after wounding of epithelial sheets in vitro, and the

transmission of these waves is at least partly dependent on functional gap junctions (Sammak et al., 1997).

Human glioblastoma cells communicate with astrocytes as they invade the brain parenchyma (Oliveira et al., 2005). These interactions are dependent on functional gap junction channels and the presence and functionality of gap junctions correlates with the degree of invasiveness. However, homotypic gap junctional interactions amongst glioblastoma cells negatively regulate invasiveness. One thought is that this inhibition of tumor cell invasion by up-regulation of gap junctions could be due to an increase in cell-cell adhesiveness mediated by connexins. Indeed, one study demonstrated gap junction mediated aggregation of glioma cells upon expression of connexin-32, -40 or -43, suggesting that gap junctions influence the adhesiveness of cells to one another (Lin et al., 2002). The relationship between gap junction mediated adhesion and invasive cell behavior seems to be highly dependent on context. Adhesion of glioma cells to astrocytes via gap junctions appears to be a pre-requisite for invasion of tumor cells rather than a barrier to it (Lin et al., 2002). However, a requirement for gap junctions as adhesive contacts is clearer in other cells and processes such as the radial migration of newborn neurons along radial glia (Elias et al., 2007).

Melanoma cells switch gap junction partners during tumorigenesis, communicating directly with fibroblasts rather than with keratinocytes (Hsu et al., 2000). Change in cadherin type is associated with the switch in cellular partners, suggesting that modulation of cell-cell adhesions may provide new opportunities for heterotypic gap junctional communication. This is not especially surprising given that gap junction formation is known to be dependent, at least in part, on cell-cell adhesive interactions

mediated by other adhesion proteins, particularly cadherins (Frenzel and Johnson, 1996; Jongen et al., 1991).

There are migratory events for which it is clear that gap junction proteins are required, but not known what role they serve. For example, induced expression of connexin-43 in transformed, non-metastatic, mammary epithelial cells increased diapedesis of these cells across an endothelial monolayer, but there was no change in adhesion of individual epithelial cells to the endothelial cell sheet (Pollmann et al., 2005). Another example comes from the study of cardiac neural crest migration. Early work showed dose dependent effects of connexin expression levels on the migration of cardiac neural crest cells (Huang et al., 1998). Increases in connexin expression up-regulated both dye transfer and outgrowth of neural crest cells from explanted tissue. Genetic deletion of α-connexins or treatment with the gap junction inhibitor oleamide resulted in corresponding decreases in intercellular dye transfer and migration. Later reports from the same group suggest that although gap junction proteins are important for guiding directional migration, it is likely that the mechanism is independent of the transfer of signaling molecules between cells (Xu et al., 2006, 2001). Thus, cell-cell connections mediated by gap junctions can modulate cell migration through a number of distinct mechanisms, some of which have yet to be elucidated.

1.5 Maintenance of cell-cell proximity for ligand-receptor signaling

An additional category of signaling events that are dependent on close proximity between cells is that of membrane-bound ligand/receptor interactions such as Eph-ephrin and Notch-Delta signaling. These signaling pathways influence coordination of cellular

behaviors as well as helping to determine cell fates. Ephrin signaling regulates many aspects and modes of cell migration (Poliakov et al., 2004). For example, Eph-ephrin interactions are involved in angiogenic remodeling and possibly in pathogenic angiogenesis as well (Kuijper et al., 2007). Eph-ephrin signaling is also required for migration of neuroblasts out of the subventricular zone (Conover et al., 2000).

Signaling mediated by the interaction of Notch with various ligands such as Delta or Jagged is thought to modulate migratory behavior in many different contexts. Notch signaling is required for induction of an EMT gene expression program in response to hypoxic conditions. Hypoxia induces Notch signaling which in turn acts directly and indirectly to increase levels of the EMT mediator snail-1 (Sahlgren et al., 2008). Ectopic expression of Notch promotes migration of breast cancer cells in culture, likely by regulating cell-cell adhesion and serving as a dissemination cue (Bolós et al., 2013). Furthermore, migration of epithelial or endothelial cell sheets into an open space is impaired by inhibition of Notch signaling and accelerated by activation of the pathway (Chigurupati et al., 2007). However, Notch can also inhibit "protrusive" behavior in some cell types. For example, contact inhibition of cortical neurite outgrowth is regulated by Notch signaling such that inhibition of Notch leads to promotion of neurite extension while antagonism of the pathway stumps outgrowth (Sestan et al., 1999). The mechanisms for these divergent effects of Notch signaling on migration are not yet understood but perhaps may be dependent on the environment of the cell or the type of migration event.

Angiogenesis, proliferation, and differentiation of endothelial cell networks all depend on Notch signaling (Phng and Gerhardt, 2009; Roca and Adams, 2007).

Notch/Dll4 signaling regulates tip cell formation during angiogenesis in mouse retinas (Hellström et al., 2007) and is required to restrict angiogenic behavior to tip cells in zebrafish (Siekmann and Lawson, 2007). Notch can interact with a number of different ligands. Dll4 and Jagged 1 have different spatial expression patterns and antagonistic effects on angiogenesis (Benedito et al., 2009). Notch signaling is required in a similar manner for the normal morphogenesis of the *Drosophila* trachea, serving to restrict cell fates and ERK activation at the tips of tracheal branches. (Ikeya and Hayashi, 1999; Llimargas, 1999; Steneberg et al., 1999)

Notch signaling may regulate some migration events through modulation of cadherin adhesions. Notch activity in the *Drosophila* oocyte is restricted to border cells during their migration and is required for this event (Wang et al., 2007). The mechanism by which Notch regulates migration is not yet known. One possibility is that it modulates cell interactions by regulating cadherin expression through the ETS transcription factor Yan (Schober et al., 2005). In zebrafish, Notch-Delta signaling is required for patterning of neuromast rosettes in the pLLp (Matsuda and Chitnis, 2010). The deposition of the rosettes is an integral element in the morphogenesis of the tissue. Migration of the pLLp tissue is also disrupted when Notch is inhibited. Some evidence indicates that Notch expression correlates cadherin expression, suggesting that modulation of cell-cell-adhesion may be one mechanism by which Notch signaling regulates morphogenesis and migration of the tissue.

1.6 Integration of multiple directional cues

Although I have parsed the roles of cell-cell contacts during collective migration into separate categories, cells in vivo are often exposed to more than one migratory cue. As I have described above, many of these cues are influenced by the presence of cell-cell and must be interpreted by cells simultaneously. Migrating neural crest cells provide a particularly good example of these complexities. Neural crests engage in dynamic short and long range cell-cell interactions that participate in guidance of migration (Teddy and Kulesa, 2004; Theveneau and Mayor, 2013). Many studies have contributed to the development of a model in which neural crest cell migration is guided by a combination of contact inhibition and collective chemotaxis. Directionality is generated by contact inhibition of locomotion for which PCP and Rho-family GTPase signaling are required (Carmona-Fontaine et al., 2008). Similar to the behavior of zebrafish pLLp, neural crest cells can migrate directionally toward the chemokine Sdf1 only when engaged with other cells via N-cadherin (Theveneau et al., 2010). Neural crest cells are also attracted to one another through a "coattraction" mechanism mediated by interactions between complement factor C3a, a secreted chemokine, and its receptor C3aR (Carmona-Fontaine et al., 2011). This attraction between cells requires a high cell density in order to be effective. However, "coattraction" does not require cell-cell contact per se, the cells simply need to be near one another. There is also an interesting interaction between neural crest cells and placodal cells. This interaction involves a "chase" behavior initiated by attraction of the neural crest cells to a chemotactic cue and a "run" behavior mediated by mechanical aversion of the placode cells to the neural crest (Theveneau et al., 2013). Both the "chase" and "run" behaviors are dependent on cadherin mediated

cell-cell contacts. Thus, a chemical cue leads neural crest cells to run into one another or into placodal cells to initiate polarity. Polarity is then maintained by chemokine signaling and further cell-cell contacts.

1.7 Concluding thoughts on the influences of cell-cell contacts on migration

I have presented here a sampling of the myriad ways in which cell-cell contacts influence cell migration events. Nearly every cell migrating in vivo is in contact with neighboring cells at some point during its journey. Some forms of cell-cell contact may have little effect on the behaviour and properties of a migrating cell. However, even transient contacts can form the basis for directional guidance (Theveneau and Mayor, 2012). For many years cell-cell contacts were viewed as antithetical to migration. For instance, it was thought that tumor cells must always undergo an epithelial to mesenchymal transition in order to invade into surround tissues and metastasize. We now know that this is clearly not the case (Friedl and Gilmour, 2009; Friedl et al., 2012). In fact, collective cell migration is an essential feature of early development, organogenesis, wound healing, and metastatic invasion.

Cell-cell contacts do more than simply hold tissues or groups of cells together. This function is certainly important in both static and migrating tissues but interactions mediated by cell-cell adhesions can also cue movement, directionality and identity. The signals mediated by cell-cell contacts take many forms as detailed throughout the preceding pages. The emergence of mechanical coupling and cohesive forces as cues for coordinated movement is a particularly exciting development. Continuing collaborations between physicists, engineers and biologists are needed to deepen our understanding of

the complex interactions between the physical and chemical signals that guide cell migration and morphogenesis.

1.8 Adhesive crosstalk: re-evaluation of concepts and the case for adhesive networks

Knowledge of cell adhesion proteins and the molecules that associate with them has grown rapidly in recent years. Cadherins and integrins are each involved in bidirectional cell signaling events as well as the physical linkages of cells to each other and to the extracellular matrix (ECM). Physical adhesive linkages are crucial for the maintenance of tissue architecture and can also serve instructive roles by enabling cells to sense and respond to changes in their environments. In some cases, this occurs through translation of mechanical inputs into intracellular signals, a process known as mechanotransduction. A simple survey of adhesion-dependent cell signaling pathways reveals that many of the molecular components and functional outputs are common to several different types of adhesion. This leads to questions of how and where these signaling pathways intersect, and what functional consequences result from these interactions? Although other adhesion molecules (e.g. selectins, IgG family cell adhesion molecules) are likely to be involved and can be viewed as additional nodes in an overall cellular adhesive network, the focus here is on integrin-based cell–ECM interactions and cadherin-dependent cell–cell contacts.

The term crosstalk is typically used to represent an interaction(s) between two or more independently initiated signaling pathways, the outcomes of which include the amplification or attenuation of individual pathways, or the initiation of new signals. In

the context of signals transduced through integrins and cadherins these pathways intersect in ways that resemble more closely an integrated network rather than distinct cascades (Fig. 1.1A, B). Integrins and cadherins are both trans-membrane adhesion receptors, have many signaling effector molecules in common, link to common scaffolding and cytoskeletal elements, and share the ability to influence crucial downstream functions, such as cell growth, survival and transcriptional activity. Owing to these common features and molecular associations, cell signaling pathways that depend on cadherins and integrins are likely to interact on multiple levels, and these interactions occur over varying time and length scales. We can distinguish such networks on the basis of both short- and long-range physical associations and cell signaling events. By these criteria we define four general modes of adhesive interactions (Fig. 1.1C-F).

In the most indirect or remote mode of adhesive interactions, signals that originate from one type of adhesion lead to a change in the functional activity of other adhesive contacts elsewhere in the cell (Fig. 1.1C). We term this 'long-range input–output' signaling. For example, cell adhesion to specific ECM proteins or to neighboring cells might lead to changes in gene expression, which could include alterations in levels of adhesion molecules or other proteins involved in regulating adhesion (Onodera et al., 2010). Alternatively, engagement or disengagement of one type of adhesion might modify the functional activities of another by effecting changes in membrane trafficking, cytoskeletal association and/or avidity or binding affinity (Avizienyte et al., 2002).

Another type of interaction between adhesions involves the convergence of independently initiated cell signaling events, often involving downstream effectors that are common to both integrin and cadherin adhesions (Fig. 1.1E). These shared effectors

include non-receptor tyrosine kinases, adaptor and scaffolding proteins, and small GTPases. In addition, cell–cell and cell–matrix adhesions are also linked to the common structural elements that comprise the cytoskeleton. Actin, microtubules and intermediate filaments form distinct, but often spatially overlapping, macromolecular assemblies. These cytoskeletal networks provide physical scaffolds that connect adhesion complexes not only proximally but also at a distance across cells and cell junctions.

The lateral coupling of adhesion receptors can be viewed as a third form of interaction, which involves more short-range associations within the plane of the membrane (Fig. 1.1D). In this instance, however, the proximal interactions of integrin and cadherin do not necessarily involve shared cytoskeletal linkages, or even cell–cell or cell–ECM engagement. Adaptor proteins, such as tetraspanins or growth factor receptors (e.g. the insulin-like growth factor 1 receptor (IGF1R)) can facilitate lateral associations of integrins and cadherins (Canonici et al., 2008; Chattopadhyay et al., 2003). One result of this type of interaction is that integrins promote stability of cell–cell adhesions (Chattopadhyay et al., 2003). Although lateral integrin–cadherin associations are known to occur, their physiological significance remains unclear.

Each of these three modes of adhesive interaction can also converge on a common pathway(s), resulting in a complex feedback loop that, in turn, modulates the functions of one or more of the initiating signals (Fig. 1.1F). For example, Rho GTPases act as both points of convergent signaling downstream of adhesions as well as upstream modifiers of functions of individual adhesion molecules. In the following sections we consider examples of adhesive networking in the context of the four types of general mechanism that are illustrated in Fig. 1.1C-F.

1.9 Mechanisms for integrating adhesive signals

Rho GTPases

Rho family GTPases are central to cell signaling pathways both upstream and downstream of cadherin and integrin adhesions (Huveneers and Danen, 2009; Watanabe et al., 2009), making them prime candidates for mediating integration of adhesion dependent signals. They are known to modulate a wide range of cellular behaviors including cytoskeletal organization, cell polarity, cell proliferation and the formation and maturation of adhesive junctions (Etienne-Manneville and Hall, 2002). Rho GTPases have a primary role in regulating the assembly of integrin based focal adhesions (Hall, 1998). Similarly, the assembly of cadherin-based adherens junctions requires the activity of Rho, Rac and Cdc42 (Van Aelst and Symons, 2002). Rho GTPases must be tightly regulated in the cell given that a certain degree of Rho activity is required for cell-cell adhesion, but increased levels of Rho activity disrupt cadherin adhesions (Zhong et al., 1997).

Adhesion through classical cadherins results in increased Rac1 activity upon engagement but inhibits RhoA activity over the course of a few hours (Noren et al., 2001). The effects of cadherin adhesion on Rho GTPases are known to require the cytoplasmic domain of the cadherin, but the mechanism of signal transduction remains to be established (Noren et al., 2001; Watanabe et al., 2009). A number of proteins bind the cytoplasmic tails of cadherins and some of these have been shown to regulate Rho GTPase activity. p120 catenin binds to the juxtamembrane region of the cadherin tail and when overexpressed can decrease Rho activity while increasing Rac and Cdc42 activity

(Braga and Yap, 2005). Another study suggested that p120 catenin interacts with p190 Rho GTPase activating protein (RhoGAP), locally inhibiting Rho in response to Rac activation (Wildenberg et al., 2006). p190 RhoGAP is activated by integrin adhesion and is thought to be a convergence point for signaling by integrins and syndecans (Bass et al., 2008). In epithelia and endothelia, in which both cell-cell and cell-matrix adhesions are required, p190 RhoGAP is likely a point of convergent signaling between integrins and cadherins.

Rho is transiently activated by the formation of new integrin adhesions (Bhadriraju et al., 2007; Ren et al., 1999), and this activation can have consequences for the adhesive functions of cadherins. There are several examples of Rho GTPases that act as signaling intermediaries between integrins and cadherins. The activities of Rho and Rac downstream of integrin signaling are thought to regulate the formation of adherens junctions in epithelial cells (Playford et al., 2008). Integrin signaling in colon cancer cells promotes cell-cell junction formation through activation of phosphatidylinositol 3-kinase (PI3K) and Rac1B (Chartier et al., 2006). In addition to these input-output pathways, Rho GTPases are also implicated in convergent signaling. For example, both integrin and cadherin adhesions have been shown to enhance cell proliferation by promoting the expression of cyclin D1 in a redundant manner through Rac (Fig. 1.2) (Fournier et al., 2008).

Rho activation is a node in the convergent signaling network initiated by cadherins and integrins that can exert drastically varied effects on adhesions depending on the downstream effectors involved (Fig. 1.2). Rho signaling through Dia reorganizes the actin cytoskeleton to stabilize adherens junctions, whereas Rho-kinase (ROCK) is

thought to disrupt cell-cell junctions by activating actomyosin contractility to excess (Sahai and Marshall, 2002). RhoA mediated activation of the effector ROCK is regulated by cell-matrix adhesion, cell shape and cytoskeletal tension. In fact, tension generated by cell spreading is required for activation of ROCK by RhoA (Bhadriraju et al., 2007). This suggests that a positive feedback loop exists, in which tension generated by cell-matrix adhesion stimulates activation of ROCK, which in turn enhances the formation and maturation of integrin-based adhesions. Regulation of cytoskeletal tension is also critical for accumulation of E-cadherin at cell-cell contacts. ROCK regulates the activity of the motor protein non-muscle myosin II downstream of initial E-cadherin ligation to stabilize newly formed cell-cell junctions (Shewan et al., 2005). Cdc42 limits Rho signaling to achieve the critical tension levels required to maintain cell-cell junctions, preventing excess tension that would likely dissociate these adhesions (Warner and Longmore, 2009).

Due to the complex spatiotemporal regulation of Rho GTPases, it is difficult to separate their roles in the initial establishment of adhesions from those in the signaling events downstream of cadherin and integrin engagement. Furthermore, because these proteins are involved in so many pathways, localization and timing become extremely important in dictating cellular responses to a given stimulus. Rac1 is localized to sites of cell-cell contact where it might have a role in mediating rapid changes in actin organization concurrent with the formation of new cell-cell junctions (Ehrlich et al., 2002). More recent work has shown that localization of both Rac and Rho to cell-cell contacts is essential for the formation and expansion of cadherin adhesions. The spatiotemporal localization of both the GTPases and their effectors suggests specific roles

in adhesion formation with Rac facilitating actin remodeling and Rho stimulating actomyosin contractility (Yamada and Nelson, 2007). The downstream effects of Rho GTPase activation can differ dramatically depending on the site of activation. Rac is required for epithelial wound healing and promotes cell migration when activated at cell-matrix contact sites, but promotes cell-cell adhesion and formation of adherens junctions when activated at cell-cell junctions (Liu et al., 2010; Van Aelst and Symons, 2002).

Network complexity increases when we consider the functions of other GTPases such as the Ras family member Rap1, which has been implicated in the transmission of signals between cell–cell and cell–matrix adhesions (Retta et al., 2006). It is known to activate integrins in various cell types, demonstrating a role for Rap1 in inside-out integrin signaling. Rap1 was also shown to be important for the formation and maintenance of cadherin adhesions (Watanabe et al., 2009). These findings place Rap1 upstream of both adhesion types. However, E-cadherin adhesion may also regulate Rap1 activity (Balzac et al., 2005). Disruption of E-cadherin adhesions results in a dramatic increase in Rap1 activity, which can then be down-regulated by re-forming cell–cell junctions. Although this finding suggests that Rap1 functions both upstream and downstream of cadherins, the same is not true for integrins. Rap1 activity is not dependent on the substrate onto which the cells are plated nor is it dependent on signaling through β1 integrin. Dissolution of cell–cell junctions does, however, result in an increase in focal adhesions, and this is abrogated by inhibition of Rap1 activity. This places Rap1 neatly between cadherin and integrin adhesions. It is not yet clear how Rap1 activity is affected by endogenous disruption of cadherin adhesion, such as through increased actomyosin-mediated tension. Additional data suggest that internalization and endocytic

trafficking of cadherins is required for Rap1 activation, although the precise mechanism of Rap1 regulation by cadherins is unknown.

Clearly, signaling through GTPases is a much used mechanism for intracellular communication and is influenced by both cell-cell and cell-ECM adhesions. Only recently have suitable tools been developed that enable GTPase activities to be visualized in time and space, thus revealing specific activation events mediating interactions between adhesions (Wang et al., 2010; Yamada and Nelson, 2007).

Tyrosine kinases

A number of tyrosine kinases are localized to cell-cell and cell-matrix adhesions (Giannone and Sheetz, 2006; McLachlan et al., 2007) where they function as prominent nodes in the adhesive network. Activation of Src family kinases frequently accompanies the formation of both cell-cell and cell-ECM adhesions. Src is recruited and activated upon E-cadherin ligation and this provides a positive feedback loop signaling through PI3K to promote the stability of cell-cell contacts (McLachlan et al., 2007). However, Src levels at cell-cell adhesions must be tightly regulated, as constitutively activated Src disrupts cell-cell contacts and alters cell morphology (Behrens et al., 1993). Integrin ligation also leads to Src activation and this has divergent downstream consequences, often involving Rho GTPases (Huveneers and Danen, 2009). In epithelial cells, constitutively activated Src at sites of integrin-matrix adhesion leads to peripheral accumulation of activated myosin, which is disruptive to cell-cell junctions (Avizienyte et al., 2004). However, moderate Src activation and regulation of actomyosin contractility by ROCK or myosin light chain kinase (MLCK) are necessary for the integrin-mediated

strengthening of E-cadherin adhesions (Martinez-Rico et al., 2010). Although cytoskeletal tension is important for the formation of both cell-cell and cell-matrix adhesions, excessive tension might serve to rip junctions apart or induce changes in protein conformation that lead to junctional instability.

The focal adhesion kinase (FAK or pp125FAK) is another non-receptor tyrosine kinase, which as a primary signaling partner of Src is implicated in many of the same signaling pathways (Playford and Schaller, 2004). Unlike Src, however, FAK contains a focal adhesion targeting (FAT) sequence consistent with its role as a downstream effector of integrin adhesion and signaling. For example, transforming growth factor-beta (TGF-β) inhibits epithelial to mesenchymal transition (EMT) in at least some colon cancer cells and stimulates increased expression of ECM leading to integrin engagement and activation of FAK (Wang et al., 2004). FAK then promotes E-cadherin expression and cell cohesion (Wang et al., 2004), but the mechanism by which this occurs remains unclear. Nonetheless, this is consistent with FAK knockdown studies reporting stimulation of EMT and inhibition of cadherin adhesion (Yano et al., 2004). Because FAK is normally associated with integrin adhesions there has been much speculation about its role in cell-cell junctions. Regulation of Rho GTPases is one possible mechanism of action, as FAK can inhibit the activity of Rho and constitutively active Rho mutants phenocopy FAK loss-of-function (Playford et al., 2008). Interestingly, FAK has also been shown to localize to cell-cell contacts although the significance, if any, of its localization at cell-cell adhesions is unclear (Crawford et al., 2003; Playford et al., 2008).

The non-receptor tyrosine kinase Fer is also reported to be involved in communication between cell-cell and cell-ECM adhesive contacts (Arregui et al., 2000). Fer can be activated upon engagement of either cadherins or integrins (El Sayegh et al., 2005; Sangrar et al., 2007). The association of Fer with the actin-organizing protein cortactin might help coordinate cellular response to various adhesive inputs. Cortactin is required for cell spreading on fibronectin and activation of cortactin by Fer promotes cell motility (Illés et al., 2006; Sangrar et al., 2007). Phosphorylation of cortactin by Src and/or Fer downstream of E-cadherin ligation enhances cell-cell adhesion (El Sayegh et al., 2005; Ren et al., 2009). This suggests that Fer signaling feeds back to cell-cell and cell-matrix adhesions by promoting cortactin-dependent reorganization of actin (Fig. 1.2).

A number of growth factor receptor tyrosine kinases are reported to regulate cadherin and integrin adhesive functions. For instance, vascular endothelial growth factor (VEGF) signaling through the VEGF receptor VEGFR2 both increases integrin-dependent migration and decreases stability of vascular endothelial (VE)-cadherin adhesions (Byzova et al., 2000; Carmeliet et al., 1999). Receptor tyrosine kinases can also enable lateral molecular associations between different types of adhesions. IGF-1R forms a ternary complex with E-cadherin and αv integrins at cell-cell contacts. The addition of IGF-1 causes the re-localization of αv integrin to focal contacts and an increase in cell-migration (Canonici et al., 2008). Thus, IGF-1R might sequester integrins at cell-cell contacts and inhibit migration in the absence of growth factor signaling.

Phosphatases

Given the central importance of kinases to many adhesion-dependent cell signaling pathways, it is crucial to also consider the role of phosphatases in the regulation of adhesive networks. There are a number of protein tyrosine phosphatases (PTP) that associate with cell-cell and cell-ECM adhesions such as PTP1B, which is found to co-localize with cytoplasmic tails of cadherins and with focal adhesions (Burridge et al., 2006; Sallee et al., 2006; Stoker, 2005). The catalytic activity of PTP1B is required for de-phosphorylation of β-catenin and association of N-cadherin with the actin cytoskeleton, both of which are crucial for the stability of cell-cell junctions (Sallee et al., 2006). PTP1B is also involved in signaling from integrin adhesions, likely through de-phosphorylation of the inhibitory tyrosine residue of Src, which leads to activation of Fak (Arregui et al., 2000). Outgrowth of neurites depends on both cell-cell and cell-matrix interactions and PTP1B has been shown to be required for this process, probably also through regulation of Src activity (Pathre et al., 2001). PTPμ is another member of the PTP family that is necessary for maintaining the integrity of cell-cell adhesions. In addition to its role in stabilizing cell-cell junctions through de-phosphorylation of junctional components, PTPμ might also recruit regulatory proteins to sites of cell-cell adhesion (Sallee et al., 2006). Expression of PTPμ in kidney epithelial cells is dependent on a complex between α3β1 integrin and tetraspanin that associates with E-cadherin on the lateral membranes of cells. An interesting feature of this lateral complex coupling is that a specific subset of un-ligated integrins appears to associate with and promote stability of cell-cell adhesions and that these are distinct from the subset of integrins involved in matrix adhesion (Chattopadhyay et al., 2003).

Scaffolding and adaptor proteins

The consequences of cadherin and integrin engagement can vary greatly depending upon the specific intracellular environment at the site of signal initiation. Scaffolding and adaptor proteins are crucial elements of adhesion dependent signaling cascades. They facilitate the localization of key downstream effectors, thereby increasing the probability of interactions between activated signaling components. Receptor for activated C kinase-1 (RACK1) is a scaffolding protein that binds the cytoplasmic tails of integrins and interacts with intracellular signaling components such as protein kinase C (PKC) (Besson et al., 2002). RACK1 is a critical component of the E-cadherin and α3β1 integrin-tetraspanin lateral signaling complex described above (Chattopadhyay et al., 2003). Binding to PTPμ might recruit RACK1 to cell-cell adhesions, serving to localize activated PKC or other effectors (Mourton et al., 2001). PKC has numerous roles in promoting cell-cell and cell-matrix adhesions (Larsson, 2006). Localization of active PKC by RACK1 might be key for specifying the types of adhesions that are affected by PKC signaling.

In general, adaptor proteins link signaling components but lack intrinsic enzymatic or kinase activities. Motifs such as the phosphotyrosine-binding Src homology 2 (SH2) domain allow adaptors to bring signaling proteins together and propagate signaling cascades initiated by a diverse array of stimuli. The SH2 domain-containing (Shc) adaptor protein forms a complex with growth factor receptor-bound protein 2 (Grb2) and the Son of Sevenless (SOS) family of guanine nucleotide exchange factors to activate Ras and subsequently mitogen-activated protein (MAP) kinases, a pathway that is activated through many inputs including integrin signaling and

mechanical force (Ravichandran, 2001). Shc has recently been shown to associate with both cell-cell and cell-matrix adhesions in response to flow across vascular endothelial cells (Liu et al., 2008). Phosphorylated Shc is recruited to cell-cell junctions at the onset of flow, particularly in areas of tissue where fluid flow shear stresses are high and result in inflammation. Previous work demonstrated the assembly of a VEGFR2-VE-cadherin complex in response to shear stress and it is now apparent that Shc interacts with components of this complex (Liu et al., 2008; Shay-Salit et al., 2002). Shc is also recruited to integrin adhesions in response to flow, a process that requires the presence of VE-cadherin. Phosphorylation of the MAPK family member ERK and activation of NF-κB are increased by flow in a Shc-dependent manner. Interestingly the activation of NF-κB, but not the activation of ERK, is dependent on ECM composition (Liu et al., 2008). These data suggest that Shc is a central mediator of flow-induced signaling events that include cadherin-dependent activation of signaling at cell-matrix junctions (Fig. 1.2).

There are several other classes of proteins that can act as adaptors even though they are not traditionally thought of as such. One example is the catenin family of proteins, of which some are involved in both cell-cell adhesion and cell signaling. Catenins are crucial for connecting cadherins to the cytoskeleton, although not necessarily through a direct physical link (Nelson, 2008). Catenins are required for the initiation of many signaling pathways downstream of cadherin adhesion including those that regulate Rho GTPase activities, actomyosin organization and contractility, and stability of cell-cell junctions (Perez-Moreno and Fuchs, 2006). Plakoglobin (Pkg) also known as γ-catenin, associates with both desmosomes and adherens junctions where it helps maintain tissue integrity through interactions with α-catenin or desmoplakin

(Acehan et al., 2008; Zhurinsky et al., 2000). By serving as a link between cadherin and either α-catenin or desmoplakin, Pkg connects cadherins to actin or intermediate filament networks, respectively. Pkg is reported to suppress motility of cell sheets and single keratinocytes on collagen (Yin et al., 2005). Although the mechanism for regulation of cell motility by Pkg is not clear, there is some evidence that Pkg works through long range mechanisms to promote fibronectin expression and inhibit Src function (Todorović et al., 2010; Yin et al., 2005). Pkg is a known target of Src kinase activity, thus it is possible that the presence of Pkg at cell-cell junctions might sequester Src away from cell-matrix adhesions where it typically promotes cell migration (Lee et al., 2010; Webb et al., 2004).

Cytoskeleton

One consequence of the signaling events and mechanical linkages that are initiated by both cell–cell and cell–matrix adhesions is the assembly and reorganization of cytoskeletal networks. Thus the regulation of cytoskeletal dynamics might be considered a consequence of convergent signaling. In turn, the cytoskeleton mediates both short-range and long-range physical interactions between adhesions throughout the cell. Linkage to the cytoskeleton provides structural integrity to adhesions and allows for cellular movement, maintenance of cell and tissue shape, and remodeling of the extracellular environment. Moreover, by coupling to molecular motors the cytoskeleton can exert forces that are then applied externally to the ECM and neighboring cells.

Actin filaments provide integral support to the cell by linking adhesive contacts on the cell surface to the interior. Actin is tethered by macromolecular complexes at

points of integrin contact with ECM, and this association can be visualized in vitro on planar substrates as focal adhesions. Cadherin adhesions direct the assembly of actin filaments near the cell cortex where they provide strength to lateral contacts between adjacent cells. A recent review article (Maruthamuthu et al., 2010), has detailed and summarized a plethora of reported connections between cell adhesion molecules and the actin cytoskeleton. The overall emerging picture is that – by acting as a force-bearing scaffold between sites of integrin and cadherin adhesion – the actin cytoskeleton provides a direct physical basis for adhesive network interactions.

Microtubule dynamic instability provides another mechanism for integrating the cytoskeleton with signaling pathways that are initiated by both cell–ECM and cell–cell adhesions. Microtubules are in a state of constant flux through processes of assembly and disassembly. Extension of microtubule plus ends into focal contacts promotes the dissolution of these adhesions (Ezratty et al., 2005). Association of microtubules with focal contacts promotes phosphorylation of kinases, including FAK, within the focal adhesion complex, inducing destabilization of protein–protein associations and resulting in the release of actin filaments from these contacts. Moreover, cadherins are reported to affect microtubule dynamics. In highly migratory and undifferentiated cells, the minus ends of microtubules are typically anchored in centrosomes. In terminally differentiated cells such as polarized epithelia, however, the minus ends of microtubules are instead stabilized by association with cadherin adhesions (Chausovsky et al., 2000; Meng et al., 2008). Likewise, plus ends of microtubules in these cells are stabilized by a linkage to the basal cortex through integrin adhesions (Hotta et al., 2010). Thus, microtubules that are

capable of regulating cell– ECM adhesions are also anchored and regulated by cadherins, providing another potential cytoskeleton-based mechanism for adhesive networking.

Intermediate filaments also associate directly with both integrin and cadherin adhesions. In contrast to actin filaments, intermediate filaments exhibit high tensile strength, extensibility, elasticity and flexibility (Fudge et al., 2003). Nonetheless, intermediate filaments are highly dynamic and capable of de-polymerization and polymerization anywhere along an existing filament (Colakoğlu and Brown, 2009; Godsel et al., 2008). Although most studies of intermediate filaments have focused on their association with highly stable adhesive junctions, such as desmosomes and hemidesmosomes, they are also found in association with more dynamic adhesions that involve classical cadherins (Kowalczyk et al., 1998; Leonard et al., 2008) and non-hemidesmosomal integrins (Bhattacharya et al., 2009; Tsuruta and Jones, 2003). Intermediate filaments lack filament polarity, and the distinct 'hubs' of filament organization and polymerization (Godsel et al., 2008) that are characteristic of the actin and microtubule cytoskeletons. Intermediate filament networks have yet to be implicated directly in functionally connecting different adhesions; however, their role in anchoring and stabilizing adhesive junctions suggests that they are important, particularly in cases where adhesive networks are subject to mechanical forces.

Different types of cytoskeletal network are further integrated through direct crosslinking by cytoskeletal scaffold proteins such as plectins, which contain binding sites for actin, microtubules and intermediate filaments (Sonnenberg and Liem, 2007). Moreover, motor proteins, such as myosin, kinesin and dynein, can be thought of as mobile crosslinkers that generate forces within and between cytoskeletal networks

(Chang and Goldman, 2004). As a consequence of these varied molecular crosslinks, cadherin and integrin adhesions are able to form and maintain physical connections that are not necessarily limited to a single cytoskeletal network.

1.10 Adhesive networks in mechanotransduction and multicellular processes

As signaling through adhesive networks proceeds, the impact on cellular functions is substantial. Many of the pathways discussed above were elucidated using immortalized tumorigenic cell lines, so the functional implications for normal tissues are not immediately apparent. However, other studies that focused on a variety of tissues, developmental systems and primary cells have provided considerable insight into the physiological roles of adhesive interactions. Nearly all major cellular functions are reported to be influenced by a combination of integrin and cadherin signaling events, including apoptosis (Fouquet et al., 1988; Kang et al., 2007), proliferation (Müller et al., 2008; Wildenberg et al., 2006), migration, and differentiation. Moreover, the coordinated initiation, strengthening and dissolution of cell–cell and cell–matrix adhesions are crucial for morphogenesis and, thus, the directing of both form and function.

Migration

In cancer metastasis and EMT, integrin and cadherin adhesions display an antagonistic relationship that determines whether cells will maintain associations with their neighbors or uncouple and initiate migration (Avizienyte et al., 2002; Guarino, 2007). For example, in ovarian carcinoma cells, down-regulation of E-cadherin through matrix metalloproteinase (MMP)-mediated proteolysis is initiated by integrin ligation to

collagen (Symowicz et al., 2007). This decreased cadherin-mediated cohesion allows the cells to disperse and migrate independently.

Although this scenario might best reflect the behavior of metastatic cancer cells and other instances of EMT, it is important to consider that normal intact tissues also undergo migratory processes. In collective cell migration, substrate traction is finely balanced with cell cohesion to maintain organization of the migratory tissue (Fig. 1.3A). In fact, cadherin adhesions in normal tissues provide instructive signals that regulate the polarity of cells and as a result, the direction of migration. As cells come in contact with one another, cadherin adhesions are formed, Cdc42 signaling is activated, and the centrosome reorients anteriorly relative to the cell nucleus (Desai et al., 2009; Dupin et al., 2009) indicating that a broad repolarization has occurred throughout the cell. Protrusive activity is suppressed locally near cadherin adhesions, and increased on opposing sides of the cell at sites of integrin-ECM adhesion (Borghi et al., 2010; Desai et al., 2009). Even highly migratory tissues such as some cranial neural crest cells maintain cell-cell adhesions while they move, although these adhesions are dynamic and cell contacts are transient. N-cadherin adhesions in neural crest cells are required for the subcellular localization of activated Rho GTPases in response to chemoattractants. Without N-cadherin the cells fail to migrate directionally or collectively (Theveneau et al., 2010). N-cadherin surface expression is regulated locally through signaling pathways initiated by β1 and β3 integrins (Monier-Gavelle and Duband, 1997). In Drosophila border cells, asymmetric protrusions initiated by localized Rac activation in a single border cell can alter migratory direction of an entire cluster of border cells (Wang et al., 2010). Border cell cohesion is stabilized by both β-integrin and Rac signaling through

the MAPK c-jun N-terminal kinase (JNK), and these signaling proteins are required for normal collective cell migration (Llense and Martín-Blanco, 2008; Wang et al., 2010).

Migration of whole tissues is a recurring feature of development and morphogenesis, and wound healing. Collectively migrating tissues use a mechanism of distributed traction whereby both leading edge cells and those that follow polarize and migrate in a directional manner (Fig. 1.3A) (Davidson et al., 2002; Farooqui and Fenteany, 2005). Substrate traction forces and intercellular tissue tension are developed as an intact tissue translocates. Trepat et al. (2009) reported that although leading cells generate the highest substrate traction, intercellular tension increases progressively as a function of distance from the leading edge. Moreover, tension on cadherin adhesions recruits scaffolding proteins, such as vinculin and α-catenin, to cell-cell adhesions where they mediate cytoskeletal reinforcement of the adhesions and the resultant strain-stiffening response (Chu et al., 2004; le Duc et al., 2010; Yonemura et al., 2010). However, an important question remains in tying these observations together: does tension on cadherin adhesions have ramifications for cell protrusive activity and polarity? We speculate that because cadherins are responsive to mechanical force, changes in the physical linkage of cadherins to cytoskeletal networks and the association with scaffolding proteins are likely to play an important role in the polarization of migratory cells and tissues.

Early embryonic morphogenesis

Several examples of adhesive networks can be illustrated by using early-embryonic models of tissue morphogenesis. During convergent extension, mesodermal cells

mediolaterally intercalate to form the notochord and drive axial elongation of the embryo (Fig. 1.3B). The cells are not able to complete this process in the absence of fibronectin, when α5β1-integrin is inhibited, or when cadherin adhesion is altered (Davidson et al., 2006; Marsden and DeSimone, 2003). Moreover, adhesion and signaling of α5β1-integrin can modulate cadherin adhesion, which is required for cell intercalation and cell-sorting behaviors (Marsden and DeSimone, 2003), although the mechanism of signaling between these adhesions remains unclear. Communication between adhesion receptors in this system is also bidirectional. Tension on cadherin adhesions induces integrin-dependent assembly of fibronectin fibrils (Fig. 1.3C) (Dzamba et al., 2009). Fibronectin fibril assembly is, in turn, required for normal morphogenetic movements in early embryogenesis, such as epiboly and mesendoderm migration (Rozario et al., 2009). Activation of the planar cell polarity pathway (PCP) – a non-canonical Wnt signaling cascade – is required for convergence and extension movements, and also promotes the assembly of the fibronectin matrix by regulating cadherin adhesion and tissue tension (Dzamba et al., 2009). Thus, PCP signaling is probably an important signaling pathway that links cadherin and integrin functions in the early embryo.

Differentiation

Differentiation of cells is influenced by cell adhesion receptors, which integrate several different adhesive inputs, including ECM composition, cell density and cell shape (Engler et al., 2006; McBeath et al., 2004; Messina et al., 2005; Rozario and DeSimone, 2010). Actomyosin-generated tension is applied through integrin adhesions and provides an instructive signal for the differentiation of mesenchymal stem cells into myoblasts

(Engler et al., 2006; Gao et al., 2010). Integrin-mediated activation of Rac impacts cell–cell adhesions through increasing N-cadherin expression, a process necessary for myogenesis (Gao et al., 2010). In myogenesis, cell–matrix adhesion signaling enhances cell–cell adhesions, but in some other cell types, cadherins and integrins antagonize each other to carry out a differentiation program. For example, in terminally differentiating keratinocytes, cadherins are required for tissue stratification, expression of keratinocyte specific genes and down-regulation of integrins – all crucial steps in the keratinocyte differentiation program (Hodivala and Watt, 1994; Watt, 2002). These types of coordinated interaction between cadherins and integrins alter cell signaling, and change tissue architecture to promote the differentiated phenotype.

Endothelial cell biology

Vascular endothelial cells comprise the inner layer of blood vessels and are exposed to three major types of mechanical stress: shear stress, cyclic strain and hydrostatic pressure (Fig. 1.3D). These cells are in tight cohesion with one another and with the underlying matrix, forming a semipermeable barrier against the pressurized bloodstream. Mechanical stress on this tissue is sensed and transduced, at least in part, by adhesion complexes. Shear stress induces alignment and elongation of cells in the direction of fluid flow, as well as expression of genes that result in an inflammatory response. VE-cadherin, platelet endothelial cell adhesion molecule (PECAM) and VEGFR2 form a complex in response to flow, and this complex signals through Shc to activate the integrin response to shear (Fig. 1.2) (Liu et al., 2008; Tzima et al., 2005). Cyclic strain induces proliferation in endothelial cells through a VE-cadherin– Rac1-

mediated pathway (Liu et al., 2007). Integrin signaling has been demonstrated to increase cyclin D1 in endothelial cells to promote proliferation (Schwartz and Assoian, 2001), and cell strain induces proliferation in some cell types through integrin signaling (Wilson et al., 1995). It remains to be determined, however, whether the proliferative effects of cyclic strain are mediated entirely by VE-cadherin or whether strain induction of endothelial proliferation also requires integrin-mediated cyclin D1 expression.

Proliferation can also be stimulated by signaling through αv-integrins in endothelial cells under hydrostatic pressure (Fig. 1.2) (Schwartz et al., 1999). However, the signal to proliferate is negatively balanced by the presence of VE-cadherin-mediated cell contacts (Ohashi et al., 2007), which are stabilized by physiological hydrostatic pressures (Muller-Marschhausen et al., 2008). The point at which VE-cadherin and αv-integrin signals converge to regulate proliferation induced through hydrostatic pressure is unknown. Furthermore, it is not clear how VE-cadherins negatively regulate proliferation in this context yet promote proliferation that is induced by cyclic strain. Clearly, different types of stress on cadherin adhesions stimulate unique signaling pathways that differentially affect integrin signaling. Endothelial cells in vivo are exposed to multiple stresses simultaneously. The mechanism by which cells integrate these disparate inputs and orchestrate a cellular response is an important question for future research.

1.11 Concluding thoughts on adhesive networks

This section has provided an overview of emerging mechanisms through which cadherin- and integrin-dependent adhesion and signaling functions intersect and interact. Although cell–cell and cell–ECM adhesive complexes have variable compositions and mediate

interactions at often topologically distinct positions in the cell, they share many structural similarities and signaling functions. Cadherins and integrins each coordinate responses to changes in the adhesive state through altered physical linkages with the cytoskeleton and by participating in bidirectional cell signaling events. Rather than thinking of cell–cell and cell– matrix adhesions in individual cells and tissues as operating largely in isolation, we argue that these complexes are part of a larger adhesive network wherein multiple types of cell adhesion necessarily interact. Much future effort in this area will continue to focus on elucidating the remaining signaling molecules, scaffolding and adapter proteins that comprise adhesive networks. However, the larger challenge is to understand how cell–cell and cell–ECM adhesion and signaling inputs are integrated to affect the responses of cells within contextually appropriate and dynamic microenvironments, such as those found within embryos, normal tissues and tumors.

1.12 Gastrulation movements and the mechanical environment of the embryo

Xenopus gastrulation provides several striking examples of collective cell movements and is an amenable experimental system for investigating polarized cell behaviors on both the cell and tissue scale. Gastrulation begins with the formation of apically constricted bottle cells and involution of presumptive mesoderm on the dorsal side of the embryo. The ventral mesoderm soon follows suit and dorsal and ventral mesoderm cells are joined by endoderm cells to form an annular ring of mesendoderm tissue migrating towards the animal pole along ECM assembled on the roof of the blastocoel (Fig. 1.4A). At the same time, cells of the blastocoel roof undergo radial

intercalation to form a tissue with fewer cell layers and a larger surface area. This thinning results in a spreading of the ectodermal sheet that serves to cover the external surface of the embryo with ectoderm. As gastrulation proceeds, convergent extension begins. This movement is primarily characterized by the mediolateral cell intercalation behaviors that drive the process. The dorsal mesoderm cells become bipolar in the mediolateral direction and intercalate between one another to form a longer and narrower tissue. This movement, in conjunction with radial intercalation of ectoderm cells, serves to extend the embryo along the anterior-posterior axis. Each of these behaviors depends on interactions between cells via cadherin-mediated cell-cell adhesions as well as mechanical or chemical signals from integrin-mediated adhesion to the Fn matrix (Lee and Gumbiner, 1995; Marsden and DeSimone, 2003, 2001; Papusheva and Heisenberg, 2010; Rozario and DeSimone, 2010; Rozario et al., 2009).

Although intercalation behaviors are dependent on both cadherin- and integrin-mediated adhesions, mesendoderm migration provides a more intuitive and experimentally tractable model for the study of collective migration (Davidson et al., 2002; Keller, 2005). The mesendoderm tissue displays an intriguing mode of motility. Each individual cell within the array sends out lamellipodial protrusions in the direction of travel. These cells are monopolar protrusive and migrate in a shingle-like arrangement where only the leading edge of each cell in the sheet contacts Fn. The trailing edge of each cell rests on the protruding edge of the cell behind it (Fig. 1.4B). Thus, not all of the cells in the tissue are in contact with the fibrillar Fn matrix at any given time, but they are all connected to their neighbors via cadherin based cell-cell adhesions.

Both Fn and α5β1 integrin are required for mesendoderm migration (Davidson et al., 2002; Marsden and DeSimone, 2003), and if attachment to the Fn substrate is disrupted the tissue "snaps back". The "snap-back" is anisotropic, meaning that the release of tension is greater in the x axis (direction of migration) that the y axis. This indicates the presence of tension within the tissue and implies that a force generation mechanism must be acting and that tension must be distributed to maintain tissue integrity. The transmission of force from one cell to the next is thought to be mediated by C-cadherin-mediated cell-cell adhesions. C-cadherin (also known as XB-, U-, or EP-cad), is expressed by all cells in the early *Xenopus* embryo and is responsible for "holding" the tissue together (Heasman et al., 1994; Kühl and Wedlich, 1996; Lee and Gumbiner, 1995). However, cell-cell adhesions are also required for polarized migration of mesendoderm cells; if the tissue is dissociated to single cells and plated on Fn, the cells become multipolar protrusive and migrate randomly (Winklbauer et al., 1992).

Are forces on cadherin- and integrin-based adhesions instructive cues guiding polarized cell behaviors? How do mesendoderm cells integrate physical and chemical signals from cell-cell and cell-ECM adhesions and translate them into collective cell migration? What are the components of this adhesive network that is guiding morphogenetic movements in the developing embryo? What proteins are involved in the transduction of mechanical stimuli into chemical signals? The work presented here comprises three distinct approaches to addressing these questions. In Chapter 2 we directly test the hypothesis that tension on cadherin adhesions can serve as a directional cue and identify several components of a mechanosensitive adhesion complex. Chapter 3 explores the functions of the integrin-associated protein FAK in early embryogenesis,

with a particular focus on directional migration of the mesendoderm. Chapter 4 details the initial stages of a mass spectrometry based screen designed to identify proteins that undergo conformational changes in response to tension on adhesion complexes. These studies each address a different aspect of the general question that is the focus of this dissertation: What mechanisms drive the self-organization of the collectively migrating *Xenopus* mesendoderm?

Figure 1.1

Different modes of adhesive interaction. (A) The term ‘adhesive crosstalk’ is used widely to highlight presumed functional interactions between two distinct types of adhesion (e.g. integrin and cadherin adhesions; blue and green dots, respectively). (B) Although often spatially distinct, integrin and cadherin adhesions activate many of the same signaling pathways and elicit similar cellular functions, supporting the notion that they should instead be considered as interdependent functional nodes in a larger adhesive network In some cellular contexts, cadherins and integrins are best perceived as functionally equivalent (teal nodes) with respect to output and network response. Modulation of one node influences adhesive function and signaling activities of adhesive nodes throughout the network. (C) Input–output signaling is used to describe long-range interactions between cadherins (monomers in blue) and integrins (heterodimers in green). Signaling from one adhesion receptor modulates the expression or activity of another adhesion type. The underlying mechanisms may involve changes in transcriptional activity or changes in signaling effector activity that regulate cell–cell and cell–matrix adhesions. (D) Lateral coupling of adhesion receptors allows for signaling in the absence of extracellular matrix or cell–cell adhesion. Macromolecular complexes are formed by association of cadherins with integrins, often through interaction with other trans-membrane proteins, such as tetraspanins (orange) or growth factor receptors (purple). Cytoplasmic adaptor or scaffolding proteins (pink oval), such as α-catenin together with cytoskeletal connections, can further support association of these molecular complexes. (E) Convergent signaling occurs when cadherins and integrins signal to common downstream effector molecules. These shared effectors include kinases, adaptor proteins and cytoskeletal components. Convergent signaling allows for cadherins and integrins to jointly affect cell physiology through redundant, additive or synergistic mechanisms. (F) All three modes shown in A–C may work in conjunction with one another. This figure was generated with Gregory Weber.

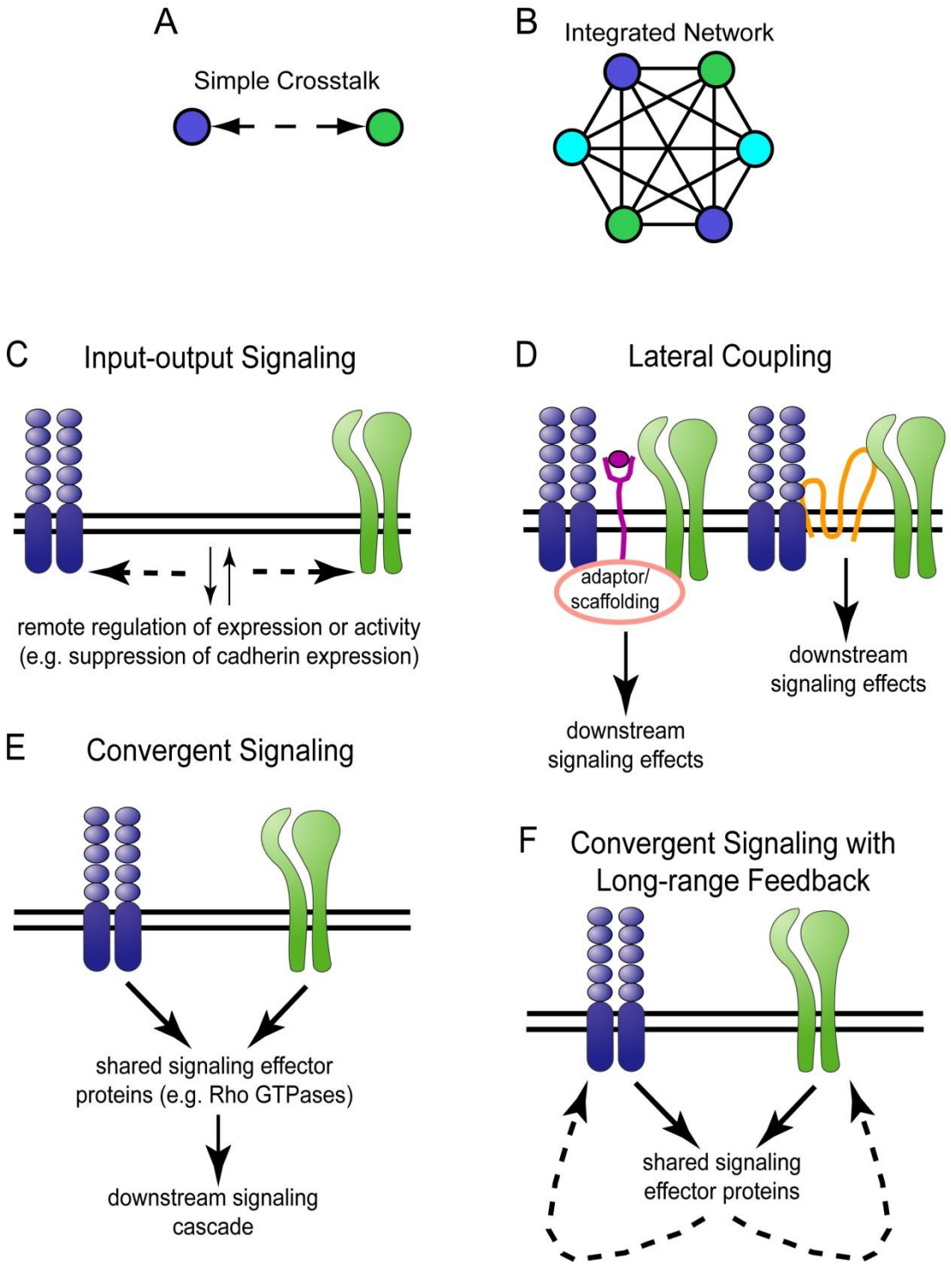
A
Simple Crosstalk
B
Integrated Network
C
Input-output Signaling
remote regulation of expression or activity
(e.g. suppression of cadherin expression)
D
Lateral Coupling
adaptor/
scaffolding
downstream
signaling effects
downstream
signaling effects
E
Convergent Signaling
shared signaling effector
proteins (e.g. Rho GTPases)
downstream signaling
cascade
F
Convergent Signaling with
Long-range Feedback
shared signaling
effector proteins

Figure 1.2

Molecular mechanisms for integration of adhesive signals. Activation of Rac by both cadherins (dark blue) and integrins (light green) up-regulates proliferation in an additive manner through an increase in the expression of cyclin D1 (orange arrows). Cyclic cell strain induces cadherin dependent activation of Rac and cyclin D1, but it has not yet been established how sensitive integrin-mediated promotion of proliferation is to cyclic strain. Cadherins and integrins antagonistically influence the activity of Rho GTPase and thus of Rho (purple arrows). Active Rho has dramatically different effects on cell adhesion depending on the downstream effector it binds. Rho signaling with Dia produces reorganization of actin in a manner that strengthens cell-cell adhesion, whereas signaling through ROCK enhances actin contractility, which in turn promotes cell-cell and cell-matrix adhesion. However, very high levels of Rho and ROCK mediated actin contractility are antagonistic to cell-cell junctions. Fer kinase is activated by cadherin and integrin adhesions and activated Fer phosphorylates the actin organizing protein cortactin (blue arrows). Reorganization of the actin cytoskeleton by cortactin can enhance either cell-cell adhesion or migration. Shear stress across endothelial cells leads to inflammation (green arrows). Shear stress induces the assembly of a VEGFR-VE-cadherin-Shc complex (vascular endothelial growth factor receptor shown in purple) and the activation of Shc, which then leads to activation of ERK and subsequently to inflammation. Activated Shc associates with integrins in a cadherin dependent manner and activates the NF-κB pathway, also resulting in inflammation. Solid lines represent direct interactions or effects, dashed lines indicate an indirect or unknown mechanism. The extracellular matrix is shown beneath the cells in blue and the actin cytoskeleton is represented by the pink lines in the cells.

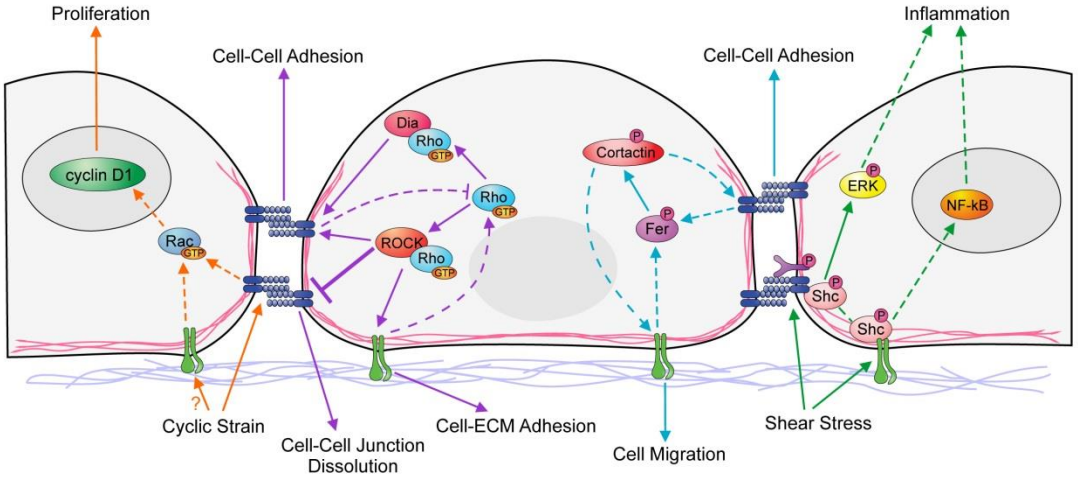
Proliferation
Cell-Cell Adhesion
Cell-Cell Adhesion
Inflammation
cyclin D1
Rac
GTP
Dia
Rho
GTP
Rho
GTP
ROCK
Rho
GTP
Cortactin
P
Fer
P
ERK
P
NF-kB
Shc
P
Shc
P
?
Cyclic Strain
Cell-Cell Junction
Dissolution
Cell-ECM Adhesion
Cell Migration
Shear Stress

Figure 1.3

Mechanical inputs modulate adhesive networks in complex tissue systems. (A) Collective migration involves traction forces through integrin-matrix adhesions to drive the tissue forward (green arrows). Extracellular matrix substratum illustrated in purple. The tissue advances against intercellular tissue tension (pink arrows) that is mediated by cadherins (pink rectangles). This intercellular tension is anisotropically distributed in the tissue and is greater within the tissue than at the leading edge. (B) Convergence and extension movements in gastrulation involve coordinated regulation of different adhesion types. Bidirectional protrusive activity (green arrows) mediated by PCP signaling and integrin-matrix adhesions enables sliding of cells past each other, which is a cadherin-dependent process (cadherin adhesions shown as pink rectangles). Intercalation behavior creates force in the anterior and posterior directions driving axial elongation. (C) Assembly of matrix (purple lines) in vivo can be regulated by force transduced through cadherin adhesions (pink rectangles). In multicellular tissues, cells pull on one another (pink arrows) via cadherin adhesions to increase local mechanical tension. It has been proposed that integrins translocate from sites of cell-cell contact across the free surface of the cell (green arrows) and promote matrix assembly. (D) Endothelial cells in vivo are simultaneously exposed to fluid flow shear stress, cyclic strain and hydrostatic compression (large open arrows), each representing a mechanical stress that applies force to cadherin and integrin adhesions (filled arrows, color matched to applicable force). Mechanical forces on cadherins and integrins initiate input-output and convergent type signaling across the adhesive network to regulate cell morphology and physiological responses such as cell proliferation. This figure was generated with Gregory Weber.

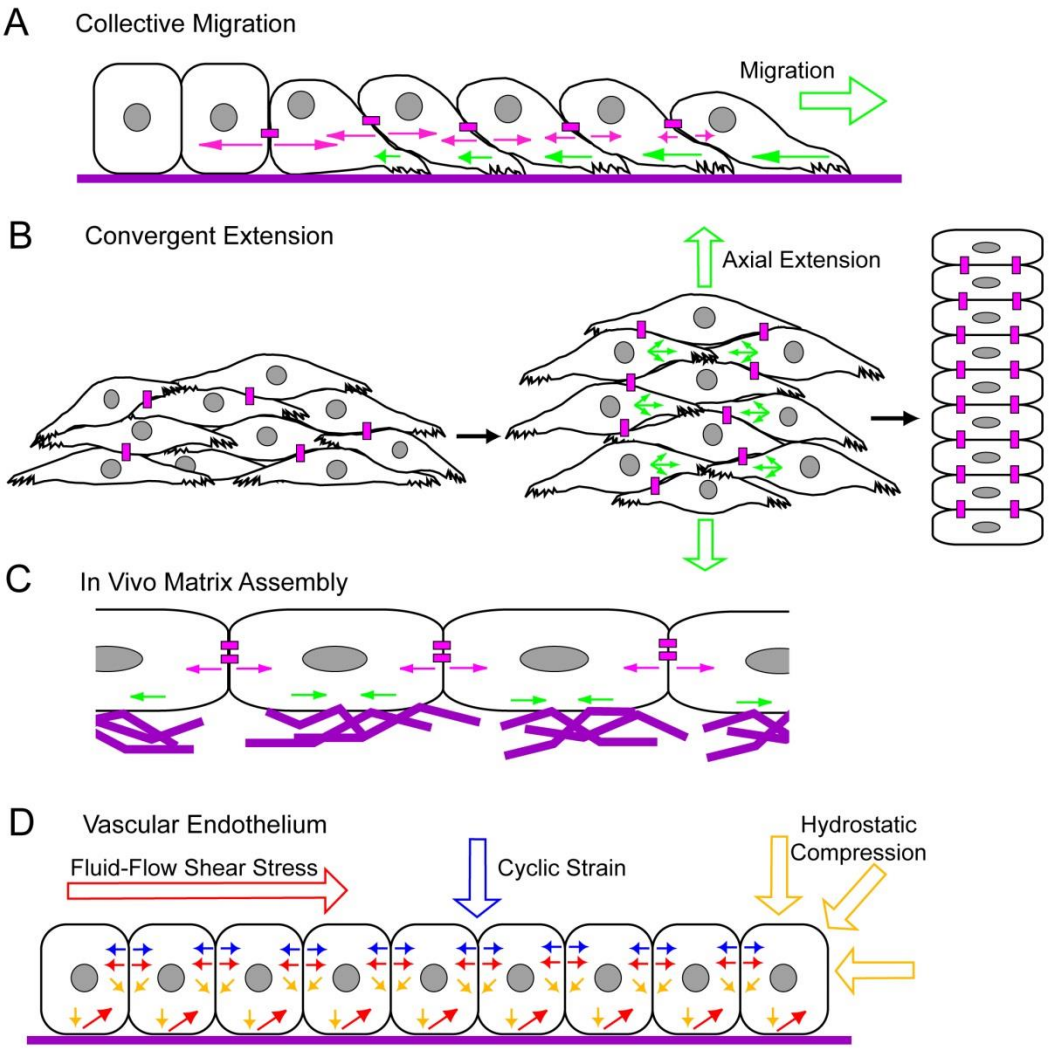
A
Collective Migration
Migration
B
Convergent Extension
Axial Extension
C
In Vivo Matrix Assembly
D
Vascular Endothelium
Fluid-Flow Shear Stress
Cyclic Strain
Hydrostatic
Compression

Figure 1.4

Organization of the migrating mesendoderm tissue. (A) Schematic of mesendoderm migration as viewed from the animal pole of the embryo with the blastocoel roof (and fibronectin matrix) removed. Mesendoderm tissue migrates toward the animal pole of the embryo as an annular ring, with each cell extending lamellipodial protrusions (green shading) in the direction of migration (blue arrows). (B) A cross sectional view taken at the dashed line in (A) Not all cells are in contact with the fibronectin matrix (purple), but those that are extend protrusions in the direction of migration (blue arrow). The rear of each cell rests on the top of the protrusion extended from the cell behind it creating a "shingled" arrangement of cells. Integrins (blue) interact with the fibronectin matrix to generate traction forces (blue arrow) that move the tissue forward. These traction forces are resisted and balanced by cadherin (red) adhesions that maintain tissue cohesion (red arrow).

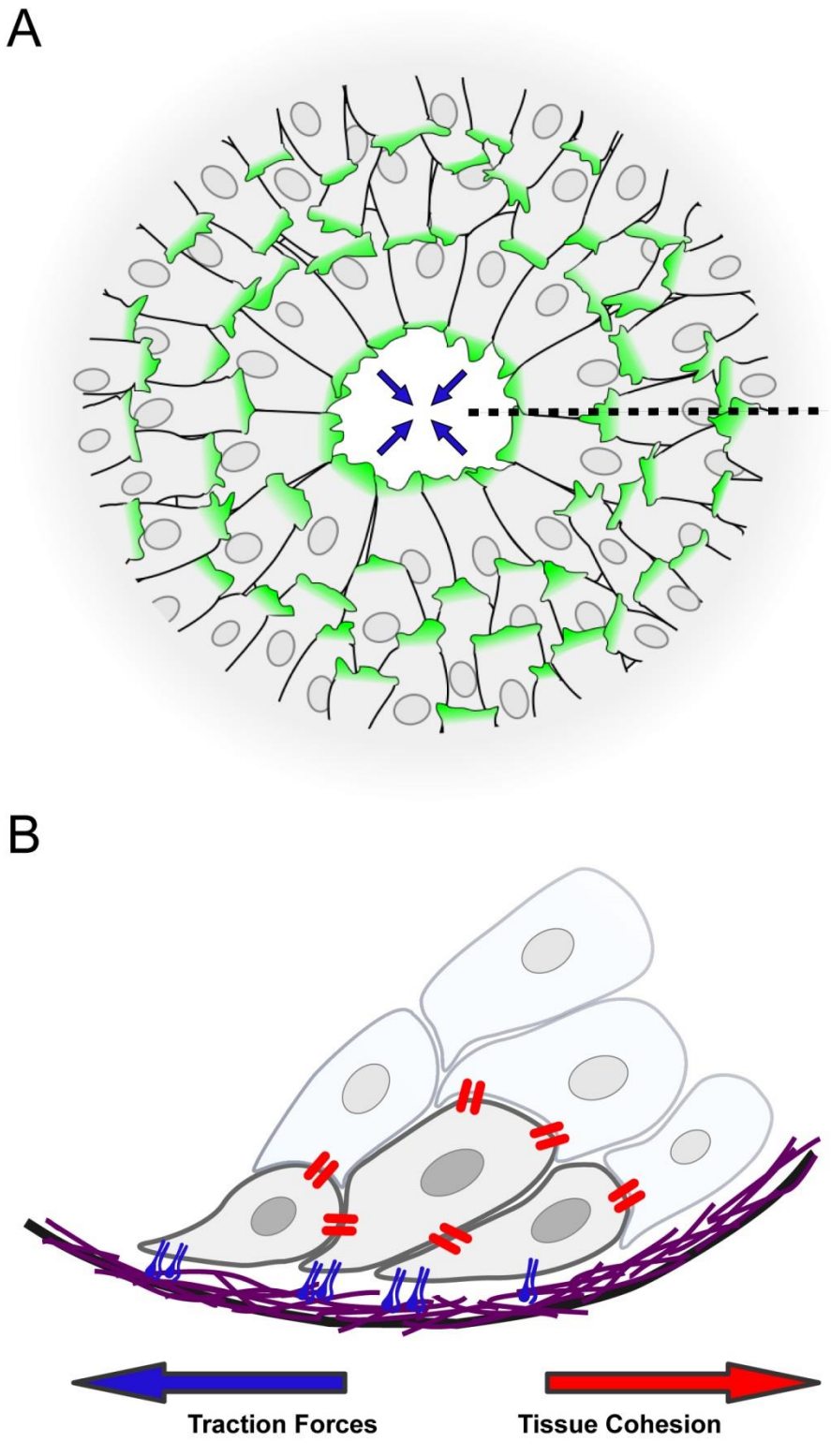
A
B
Traction Forces
Tissue Cohesion

Chapter 2

Plakoglobin and keratin are required for mechanosensitive self-organization of *Xenopus* mesendoderm

This chapter is based in part on previously published work: Weber GF, **Bjerke MA**, and DeSimone DW. 2012. A mechanosensitive cadherin-keratin complex directs protrusive behavior and collective cell migration. *Developmental Cell* 22:104-15

2.1 Abstract

Collective cell migration requires maintenance of adhesive contacts between adjacent cells, coordination of polarized cell protrusions, and generation of propulsive traction forces. We demonstrate that mechanical force applied locally to C-cadherins on single *Xenopus* mesendoderm cells is sufficient to induce the polarized cell protrusion and persistent migration typical of individual cells within a collectively migrating tissue. Local tension on cadherin adhesions induces reorganization of the keratin intermediate filament network toward these stressed sites. Plakoglobin, a member of the catenin family, is localized to cadherin adhesions under tension and is required for linkage of keratin to C-cadherins, mechanoresponsive polarized cell behavior and assembly of the keratin cytoskeleton at the rear of these cells. Local tugging forces on cadherins occur *in vivo* through interactions with neighboring cells as the tissue migrates and generates traction on the extracellular matrix. Cell-substrate traction forces are balanced by distribution of tension across cell-cell junctions and these forces result in coordinate changes in cell protrusive behavior. Thus, cadherin-dependent force-inducible regulation of cell polarity in single mesendoderm cells represents an emergent property of the collectively migrating tissue.

2.2 Introduction

Embryos undergo dramatic cell and tissue rearrangements throughout development that are required for sculpting the embryonic body plan. These underlying movements result in the generation of forces that are sensed both locally and globally by other cells and tissues in the embryo. Mechanotransduction is the cellular process responsible for converting these forces to chemical and electrical signals. Thus, physical force may serve to instruct and guide key aspects of development including gene expression, differentiation, cell polarity and morphogenesis (Mammoto and Ingber, 2010; Schwartz and DeSimone, 2008). Despite the likely importance of force and mechanotransduction to embryogenesis and development, relatively few specific examples of embryonic processes directed by mechanical inputs have been reported thus far.

Many diverse tissue types, including epithelial cell sheets (Farooqui and Fenteany, 2005), cords of metastatic cells (Wolf et al., 2007), neural crest cells (Theveneau et al., 2010), lateral line primordia (Haas and Gilmour, 2006) and mesendoderm of the *Xenopus* gastrula (Davidson et al., 2002), undergo collective cell migration and the morphological features of these events are remarkably conserved. Leading edge protrusions of each cell within the tissue are in contact with the extracellular matrix while the rear or "retracting" edge of each cell rests upon the leading edge of the cell behind it in a shingle-like arrangement (Figure 1.4B). Frog mesendoderm tissue migrates on fibronectin (Fn) matrix and, like other collectively migrating populations of cells, the fidelity of mesendoderm movement requires cell-cell contact. When cells from this tissue are dissociated from one another and plated on Fn they

become multi-polar, protrude randomly and migrate with erratic speed and direction (Nakatsuji and Johnson, 1982; Winklbauer et al., 1992). Chemotactic and haptotactic cues that may influence directional migration of intact mesendoderm are not sufficient to guide migration of single mesendoderm cells (Winklbauer, 1990; Winklbauer et al., 1992), further highlighting the importance of cell-cell contact in this process.

Collectively migrating tissues generate traction forces on the surface across which they migrate and advance against tensile forces distributed along cell-cell adhesive contacts. *Xenopus* mesendoderm explants migrate collectively on Fn substrates and perturbation of integrin-Fn adhesion causes a rapid uni-directional retraction of the cell sheet (Davidson et al., 2002). The retraction of the mesendoderm sheet occurs opposite the direction of mesendoderm migration and perpendicular to both the leading edge of the mesendoderm and the blastopore lip. The directional nature of tissue retraction under these conditions indicates that the intercellular tension in the mesendoderm tissue is asymmetric, being greatest in the axis of migration and weaker in the mediolateral axis. Recent studies of migrating MDCK cell sheets reveal a similar asymmetry of tension within the sheet, with greater forces applied to cell-cell contacts in the rows of cells behind those at the leading edge (Trepat et al., 2009). The implications of this force asymmetry for tissue morphogenesis are not known.

Classical cadherins enable cell-cell cohesion and allow development of migratory polarity in epithelial cell sheets *in vitro* (Desai et al., 2009; Dupin et al., 2009), however, the potential involvement of mechanical force on cadherin adhesions in these contexts has not been addressed. Cadherins have been reported to sense and respond to mechanical force by eliciting a strain-stiffening response (le Duc et al., 2010; Liu et al., 2010).

Integrins are well known to be involved in mechanotransduction (Moore et al., 2010; Schwartz and DeSimone, 2008), but only recently have cadherins also been implicated as important mediators of mechanical stimuli (le Duc et al., 2010; Yonemura et al., 2010). We hypothesize that asymmetries in tension on cadherins are an intrinsic consequence of tissues undergoing bulk movement or deformation and that these mechanical signals induce the establishment of cell protrusive polarity and directed migration.

Association of cadherins with the cytoskeleton provides both mechanical strength at points of adhesion and scaffolds for proteins involved in cell signaling. Binding of catenin family members, such as β-catenin or plakoglobin (Pkg; also known as γ-catenin), to the cytoplasmic tail of cadherins enables recruitment of cytoskeletal filaments to sites of cell-cell contact. Both β-catenin and Pkg can facilitate the association of classical cadherins with the actin cytoskeleton, likely through α-catenin and/or vinculin (Capaldo et al., 2014; Hirano et al., 1987). Pkg, unlike β-catenin, can also enable classical cadherin associations with intermediate filaments (IFs) through plakin family proteins (Kowalczyk et al., 1998; Leonard et al., 2008). While the linkage between cadherins and actin filaments has been studied extensively, the functional significance of IF-associated classical cadherin adhesions is not well understood. This study demonstrates that local forces applied to C-cadherins result in the Pkg-dependent recruitment of keratin IFs (KIFs), and that this mechanically responsive linkage is required for the directed protrusive behavior of individual cells within the collectively migrating mesendoderm.

2.3 Materials and Methods

Xenopus egg and embryo preparation

Embryos were obtained and cultured using standard methods and staged according to Nieuwkoop and Faber (1994). Embryos were dejellied in 2% cysteine and cultured at 16^{o}C in 0.1X Modified Barth's saline (MBS; 1X MBS: 88 mM NaCl, 1 mM KCl, 2.5 mM $NaHCO_3$, 0.35 mM $CaCl_2$, 0.5 mM $MgSO_4$, 5 mM HEPES pH 7.8).

RNA constructs, morpholinos, and microinjection

RNA was transcribed *in vitro* from plasmid DNA templates. Transcripts were injected in 5nl doses containing ~500 pg of RNA (250pg for mCherry-XCK1(8)) into one or two dorsal blastomeres at the two to four cell stage to target expression in mesendoderm. The following constructs were used in these studies: pCS2 C-cadherin-EGFP (B. Gumbiner, University of Virginia), pCS2 mtXPkg-GFP (plakoglobin-GFP) (M. Klymkowsky, University of Colorado) (Merriam et al., 1997), EGFP-XCK1(8) (V. Allan, University of Manchester) (Clarke and Allan, 2003), mCherry-XCK1(8), pCS2 XCK1(8)-myc (S. Wei, University of Virginia), pCS2 GAP43-EGFP (E. DeRobertis, University of California) and CS107 GFP-moesin (J. Wallingford, University of Texas). Antisense morpholino oligodeoxynucleotides used to inhibit translation were obtained from GeneTools (Philomath, OR). After titration for consistent phenotype and biochemical knockdown, all experiments were done with 40ng morpholino injected into each embryo. Injected embryos are commonly referred to as morphants. Sequences are as follows:

Control morpholino: 5'- CCTCTTACCTCAGTTACAATTTATA-3'
(stock sequence from GeneTools),

Pkg morpholino: 5'-TTTCCACTACGTCTCCCAAATCCAT-3'
(designed from Plakoglobin/γ-catenin/JUP sequence: NM_001090582.1)

XCK1(8) morpholino 1: 5'-TCGATCTGACGGACATGGTGGAGCT-3'
(designed from XCK1(8)/Krt8 sequence: NM_001087056.1)

Mesendoderm cell preparation

Glass coverslips were alkaline-ethanol washed and flamed prior to coating with fibronectin (Fn). Coverslips were coated with 200 µl of 2.5 µg/ml bovine plasma Fn (Calbiochem) overnight at 4^{o}C to yield a maximum coating density of 0.38 µg/cm^{2}. For poly-L-lysine (PLL) coating of coverslips, coverslips were coated with 200 µl of 0.1% poly-L-lysine solution (Sigma, P8920) overnight at 4^{o}C. Dorsal mesendoderm tissue was dissected from stage 10 *Xenopus* embryos and placed in Ca^{2+}/Mg^{2+}-free 1X MBS to dissociate the tissue to single mesendoderm cells. After approximately 20 minutes, cells dissociated from one another were transferred to 0.5X MBS containing Ca^{2+}/Mg^{2+} on Fn-coated coverslips. Mesendoderm cells were allowed 1 hour to attach and spread on the provided substrate before experimentation began.

Dorsal marginal zone explant preparation

DMZ explants were prepared according to Davidson et al., (2004). Briefly, stage 10 minus *Xenopus* gastrulae were placed in 0.5X MBS and lateral incisions were made to separate dorsal and ventral portions of the embryo. Vegetal cells were scraped away

using an eyebrow knife, leaving behind the mesendodermal, mesodermal and bottle cells. The explants were placed on Fn-coated coverslips and compressed from above with coverglasses supported and spaced with silicone grease. Explants were allowed 1 hour to attach and begin migrating before initiation of image acquisition.

Magnetic bead pull assays

Superparamagnetic beads (Spherotech, Libertyville, IL) were covalently coated with Protein G (Calbiochem), followed by affinity binding of C-cad.Fc protein (Barry Gumbiner, University of Virginia) (Chappuis-Flament, 2001). Coated beads were transferred to dishes of mesendoderm cells and positioned by pipette. After cells attached to beads, a magnetic tweezer was used to pull beads with 1100–1500 pN of force. For assessment of polarized protrusive behavior, force was applied to the cell-attached beads in a pulsatile manner (cycles of magnet on for 30 sec then off for 45 sec). See supplemental methods in Weber et al., (2012) for further details of the magnet and its use. For assessment of cytoskeletal linkage, a steady bead pull was used (magnet on without interruption). The actomyosin network was inhibited by treating cells with blebbistatin (100 µM, BioMol International) or cytochalasin D (10 µM, BioMol International) following attachment of cells to the Fn substrate and to C-cad.Fc coated beads but prior to application of force to the bound beads. The intermediate filament network was inhibited by treatment of the cells with acrylamide (5 mM, Bio-Rad) in the same manner.

Microscopy

Phase contrast images were acquired using a Zeiss Axiovert 35 and OpenLab software (Improvision/Perkin Elmer, Waltham, MA). Two different microscopes were used to acquire fluorescence and brightfield images, with the choice of equipment depending on sample thickness and fluorescence contrast. A Zeiss AxioObserver microscope equipped with structured light grid confocal system and Volocity software (Improvision/Perkin Elmer) was used for some single cell images. The majority of imaging was done using a Nikon C1 microscope equipped with a laser scanning confocal module. Image files were then compiled and viewed using Volocity software and ImageJ (http://rsb.info.nih.gov; National Institutes of Health).

Protrusion quantification

Cell protrusions in isolated mesendoderm cells are readily identified by a lack of yolk platelets, which remain constrained to the cell body. Protrusion angles were measured using the cell centroid as the vertex of the angle, the right hand side of the frame (i.e. magnet position) as 0^{o}, and the midline of the each protrusion as the final ray of the angle. Total protrusions from all cells were binned into 30^{o} ranges and plotted as rose diagrams using OriginPro software. Y-axis for all rose diagrams represents percent of total protrusions. For quantification of protrusions in cells comprising dorsal mesendoderm tissue, embryos were injected after fertilization with RNA encoding a membrane bound GFP (GAP43-GFP). Plasma membranes of cells comprising the tissue were then imaged by laser scanning confocal microscopy (see above for microscopy details). Acquired images were analyzed using ImageJ software to calculate the angles of

protrusions. First, a ray was drawn perpendicular to the leading edge of the tissue and intersecting the estimated centroid of the cell being measured. A second ray was drawn extending from the cell centroid through the middle of each protrusion on that cell. Angular measurements were grouped into bins of 30^{o}, where 180^{o} is equivalent to the direction of tissue movement, and plotted in rose diagram format using OriginPro software. Y-axis for all rose diagrams represents percent of total protrusions. Protrusive orientation data was analyzed using two statistical measures: Rayleigh test for randomness [p(rand)] and Mardia-Watson-Wheeler test [p(same)] for non-parametric two-sample comparison (Batschelet, 1981). Statistical analysis of protrusive orientation data was performed using PAST software (Hammer et al., 2001).

Immunofluorescence

Embryos and dissociated cells plated on Fn were fixed in Dent's fixative (80% methanol, 20% DMSO) or ice-cold 100% methanol. Samples were rehydrated via partial buffer changes with TBS. Embryos were blocked overnight with 10% goat serum, 1% BSA, and 0.15% Triton X-100, diluted in PBS. Overnight primary antibody incubation was followed by goat anti-mouse and rabbit IgG conjugated to Alexa-488, -555 or -647 fluorophores (Molecular Probes). Bisected embryos were dehydrated in methanol and cleared in benzyl benzoate/benzyl alcohol for microscopy.

Western blots

Whole *Xenopus* embryos were solubilized in lysis buffer (100 mM NaCl, 50 mM Tris-HCl pH 7.5, 1% Triton X-100, 2 mM PMSF (phenylmethylsulphonylfluoride), protease

inhibitor cocktail [Sigma]). Protein extracts were diluted in 2X Laemmli buffer (2% β-mercaptoethanol). One embryo-equivalent of protein per sample was resolved on a 7% SDS-PAGE gel and transferred to nitrocellulose for probing with antibodies.

Immunoprecipitation

Primary antibodies were pre-incubated with Protein G-agarose beads (Roche Diagnostics, Indianapolis, IN). Antibody-coupled beads were then incubated with lysates of gastrula stage embryos to immunoprecipitate C-cadherin, α5 integrin, or plakoglobin protein complexes respectively. Beads were pelleted by centrifugation at 12000xg and washed three times with lysis buffer (same recipe as used for Western Blot, described above). 2X reduced Laemmli buffer was added to beads to dissociate immunoprecipitated proteins and samples were loaded onto a 7% SDS-PAGE gel for separation.

Snap-back assays

Snap back assays were performed as previously described (Davidson et al., 2002). Preparation of purified mAbs against Xenopus Fn [4B12 (blocking) and 4H2 (control)] was previously described and characterized (Ramos et al., 1996). DMZ explants were placed onto a recombinant fragment of *Xenopus* Fn (GST 9.11) that contains both the synergy and RGD sites and on which DMZs migrate at the same rate as on plasma Fn (Davidson et al., 2002; Ramos and DeSimone, 1996). The mesendoderm explants were then allowed to migrate out, followed by addition of antibody to the culture media. Explants were imaged under brightfield illumination every 2 minutes for at least 30 min prior to and following the addition of the blocking (4B12) or control (4H2) antibodies.

Antibodies

Antibodies used in these studies include the following: 6B6 C-cadherin mAb and Xcad C-cadherin pAb (courtesy of Barry Gumbiner, University of Virginia), plakoglobin mAb (BD Biosciences, 610253), GFP mAb (Santa Cruz Biotechnology, sc-9996), myc mAb (Developmental Studies Hybridoma Bank (DSHB), 9E10), β-actin (Sigma, A3854), β-catenin pAb (Sigma, C2206), 881 α5 integrin pAb (Joos et al., 1995), P8D4 α5 integrin mAb (Benjamin Hoffstrom, Ph.D. Thesis, University of Virginia, 2002), XCK1(8) mAb (DSHB, 1h5) and fibronectin mAbs 4B12 and 4H2 (Ramos et al., 1996).

2.4 Results

Pulling on C-cadherin adhesions induces polarized protrusions

A magnetic tweezer was used to apply local pulling forces to cadherin adhesions in order to analyze the impact of this manipulation on cell polarity and migratory behavior (Fig. 2.1A). A key advantage of this approach over prior studies of cadherin involvement in migratory cell polarity (Borghi et al., 2010; Desai et al., 2009; Dupin et al., 2009) is the ability to distinguish between effects due only to cadherin engagement (bead attached/without pull) and those due to force on cadherin adhesions (bead pulled). C-cadherin (Cdh3) is the primary cadherin expressed in *Xenopus* gastrulae and is required for maintaining cell cohesion and tissue integrity (Heasman et al., 1994). Single paramagnetic beads coated with the extracellular domain of C-cadherin (C-cad.Fc) were placed alongside individual dissociated mesenoderm cells plated on Fn. Cells were

allowed 20 minutes to bind the beads and the attached beads were subsequently pulled in a pulsatile manner with the magnetic tweezer (Fig. 2.1A).

Application of mechanical force to C-cadherin adhesions restored the normal *in vivo* morphology of these migratory cells. When mesendoderm is dissociated to single cells they lose the characteristic monopolar protrusive behavior exhibited *in vivo* (Fig. 1.4) and become multipolar protrusive in random orientation (Fig. 2.1B). C-cad.Fc bead attachment alone had no effect on protrusive orientation [p(rand)=0.749] (Fig. 2.1C, E). When force was applied to the bead, protrusions became markedly biased opposite the direction of pull [p(rand)=0.002] (Fig. 2.1D, E). The cells then migrated persistently away from the direction of the applied force. Additionally, there was a reduction in the total number of protrusions from each cell upon bead pull (Fig. 2.1F), reflecting the monopolar protrusive behavior exhibited by mesendoderm cells *in vivo*. A pulling force of ~1.5 nN per 22.9 μm bead was sufficient to induce cell polarization. This force is about one order of magnitude less than the forces calculated between MDCK cell pairs on Fn substrate (Maruthamuthu et al., 2011). However, if it is assumed that a mesendoderm cell binds ¼ to ½ of the surface of a C-cad.Fc bead then 2-4 Pa of stress is being applied to mesendoderm cells in our bead pull assay, an amount comparable to the tugging stresses of 5 Pa reported for MDCK epithelial sheets (Trepat et al., 2009).

Because force was required to alter the polarity of protrusions, tension on the cell cortex is clearly a critical stimulus. However, it was unclear whether this response required signaling through cadherins or was a general consequence of pulling on the cell surface. The response to engagement and application of force to other adhesion molecules was also evaluated. Force application to the cell surface via beads coated with

poly-L-lysine (PLL), to syndecans via beads coated with the HepII domain of Fn, or integrins via beads coated with RGD-containing central cell binding domain of Fn were unable to induce the polarized protrusive behavior observed with C-cad.Fc beads (data not shown). These results indicate that the mechanical stimulation of monopolar protrusive activity and directional cell migration is specifically associated with signaling through C-cadherin adhesions.

It was also noted that individual mesendoderm cells were able to respond to repeated cycles of bead force application suggesting a significant degree of plasticity with regard to this mechanoresponsive behavior (data not shown). Force was applied to cadherin adhesions and then halted once monopolar protrusive behavior was induced. Cells rapidly reverted to multipolar protrusive behavior when force application ceased, typically within one or two minutes. Subsequent application of force re-induced monopolar protrusions away from the direction of the applied force. Similarly, single mesendoderm cells became monopolar protrusive when they formed adhesions with neighboring cells and reverted back to a multipolar state as these adhesions were broken (data not shown). Monopolar protrusive behavior was evident in >50% of cells within 5-10 minutes, but took as long as 20 minutes to develop in others. Once established, this protrusive behavior persisted until force on cadherin adhesion ceased or the cohesive bond was broken.

IFs are required for resistance to force on cadherin adhesions

Cadherins associate with cytoskeletal networks, including actin (Hirano et al., 1987) and intermediate filaments (IFs) (Kowalczyk et al., 1998; Leonard et al., 2008), to

provide both mechanical strength at points of adhesion and scaffolds for proteins involved in cell signaling. IFs in particular exhibit high tensile strength (Kreplak et al., 2008) and keratin intermediate filaments (KIFs) are well-known to impart mechanical resilience to cells (Coulombe et al., 1991). To determine which cytoskeletal network(s) were required for resistance to tension on cadherins, a modified bead pull assay was used. Steady force was applied to C-cad.Fc beads attached to mesendoderm cells for 10-20 min, rather than the pulsatile application of force used to induce polarized protrusive behavior. Prolonged application of force (>10 min) leads in most cases to detachment of the cell from the Fn substrate or, rarely, detachment of the bead from the cell (data not shown). Inhibition of actin-myosin contractility by treatment with blebbistatin had no effect on the bond between cell and substrate or on that between cell and bead (Fig. 2.2A). Inhibition of actin dynamics by cytochalasin D resulted in detachment of most treated cells (~80%) from the Fn substrate. The remaining fraction of cells released the bead. In contrast, disruption of the IF network by acrylamide caused a majority of cells (~70%) to release the C-cad.Fc coated bead when steady pull was applied. In some cases the cells detached from the substrate or detached from both the bead and the substrate. This suggests that IFs are the cytoskeletal element resisting tension on cadherin adhesions but does not rule out contributions from the actin network.

Keratin localization to stressed cadherin adhesions correlates with cell polarity

To investigate the relationship between cytoskeletal networks and cell polarity, the organization of actin and keratin filaments was examined in single (multipolar) cells and compared with filament organization in polarized cells. Actin filaments in single

mesendoderm cells were typically distributed in a fine mesh throughout the cell body or concentrated in lamellipodial protrusions (Fig. 2.2B). A very similar organization of actin filaments was evident in mesendoderm cells that were part of an intact tissue (Fig. 2.2C). In mesendoderm explants, actin was enriched in the protrusions at the leading edge of each cell. Actin filaments were broadly distributed throughout the cell and in some cells formed a ring around the cell cortex.

In contrast to actin filaments, the organization of KIFs in mesendoderm was tightly correlated with cell polarity and directed cell movements. KIFs in isolated cells were distributed randomly and lacked obvious orientation (Fig. 2.3A). However, when mesendoderm cells *in vitro* were in contact with their neighbors, KIFs were noted at discrete points along cell-cell interfaces (Fig. 2.3B). The correlation between cell protrusive polarity and reorganization of KIFs toward the points of cell-cell contact was particularly striking in small groups of live cells expressing EGFP-labeled keratin where KIFs aggregated near cell-cell contacts as cells formed protrusions in directions opposite these cell-cell boundaries (data not shown). Cells in live mesendoderm explants also had KIFs concentrated at the rear of each cell (Fig. 2.3C). Filaments were organized in a basket-like arrangement along the posterior-basolateral surface and were associated with the cell membrane at points of cell-cell contact. A similar organization of KIFs was evident in mesendoderm cells in sagittally bisected gastrula-stage embryos (Fig. 2.3D). An additional feature of keratin organization in whole tissues was the arrangement of KIFs into bundles perpendicular to the forward axis of migration but only in the row of cells that comprised the advancing front of the mesendoderm tissue (Fig. 2.3C). This KIF cabling parallel to the leading edge closely resembles what has been observed in

some epithelial cell sheets *in vitro* (Long et al., 2006). Binding of C-cad.Fc beads to mesendoderm cells had no effect on the localization of KIFs (Fig. 2.3E). When force was applied to these beads, however, KIFs were reorganized to the posterior of the cell proximal to the site of bead pull (Fig. 2.3E'). We conclude that mechanical forces applied to C-cadherin adhesions induce both directional protrusive behaviors and KIF reorganization toward the posterior of the newly polarized cell.

Keratin is required for force-induced polarized protrusive behaviors

To address whether KIFs are part of the molecular machinery that specifies polarity in these cells in response to a pulling force on C-cadherin, antisense morpholinos were used to knockdown expression of XCK1(8), also known as Krt8 (Fig. 2.4A). KIFs are obligate heteropolymers comprised of type I acidic and type II basic cytokeratin proteins. Early *Xenopus* gastrulae express multiple type I cytokeratins (Franz et al., 1983), but XCK1(8) is the only type II cytokeratin expressed at these stages of development (Franz and Franke, 1986). Intact XCK1(8) morphant embryos exogastrulated (Fig. 2.4B, C), a phenotype that closely parallels that reported in earlier studies targeting either keratin protein expression (Torpey et al., 1992) or filament assembly and organization (Klymkowsky et al., 1992) in *Xenopus*. As in other studies (Torpey et al., 1992), it was not possible to achieve complete knockdown of endogenous keratin due to maternal expression and slow turnover of keratin protein. The exogastrulation phenotype could be partially rescued by co-injection of morpholino (XCK MO-1) and an EGFP-tagged XCK1(8) transcript lacking the target sequence (Fig. 2.4B, C).

Dissociated mesendoderm cells from XCK1(8) morphant embryos were unresponsive to C-cad.Fc bead pull (Fig. 2.5A). This lack of response to bead pull was confirmed using a second morpholino (XCK MO-2) targeting a different sequence in the XCK1(8) mRNA (data not shown). Directed protrusive activity was also perturbed throughout intact mesendoderm explants derived from these embryos (Fig. 2.5B). Although keratin knockdown was incomplete, the severity of morphant phenotypes arising from partial keratin knockdown suggests that maintenance of normal XCK1(8) protein levels is critical for mechanoresponsive cellular behavior and normal gastrulation movements. Together these data demonstrate that KIFs are necessary for the induction of cell polarity and directed cell movements following application of force to C-cadherin adhesions.

Plakoglobin associates with C-cadherin at sites of tension and links KIFs to cell-cell junctions in intact tissue

Cadherins are linked to cytoskeletal networks through adhesion complexes that typically include members of the catenin family of proteins. Plakoglobin (Pkg; also known as γ-catenin) is known to associate with both desmosomal and classical cadherins. It is a component of adherens junctions (Knudsen and Wheelock, 1992) as well as the less-well understood classical cadherin complexes that associate with IFs (Kowalczyk et al., 1998; Leonard et al., 2008) (Fig. 2.6A). Co-immunoprecipitation analysis confirmed that Pkg was indeed associated with C-cadherin in *Xenopus* gastrulae (Fig. 2.6B).

Because Pkg is thought to be a possible linker between cadherin adhesions and KIFs and KIF organization was found to be mechanosensitive, we next examined

whether force on C-cadherin adhesions could induce the local recruitment of Pkg in normal cells. Discrete punctae of Pkg-GFP were observed at the plasma membrane in proximity with the C-cad.Fc bead when force was applied but not when the bead was merely attached (Fig. 2.7A, A'). After observing the force-dependent recruitment of Pkg to cell-cell contacts *in vitro*, the localization of Pkg was examined in intact mesendoderm tissues. In mesendoderm tissue explants, Pkg formed punctate plaques at cell boundaries and KIFs co-localized at these discrete locations (Fig. 2.7B, B'). These points of contact were found at the lateral and posterior contacts between mesendoderm cells. The force-dependent association of Pkg with C-cadherin and localization with KIFs in migrating tissue are consistent with a role for Pkg in mediating a mechanoresponsive linkage between C-cadherin and the KIF network.

Pkg is required for biochemical linkage between C-cadherin and KIFs

To explore the putative requirement for Pkg in the linkage of C-cadherin to KIFs, antisense morpholinos were used to knockdown expression of Pkg (Fig. 2.8A). Injection of Pkg MO into whole embryos reduced expression of Pkg protein by nearly 70% at gastrula stages. Co-immunoprecipitation analyses confirmed that EGFP-tagged XCK1(8), which is incorporated into endogenous KIFs (Clarke and Allan, 2003), was associated with C-cadherin obtained from control lysates (Fig. 2.9B, C). Knockdown of Pkg expression significantly reduced XCK1(8)-EGFP association with C-cadherin ($p<0.05$) (Fig. 2.9B, C). These data implicate Pkg as a key element of the mechanosensory apparatus involved in mediating C-cadherin force-induced cell polarity and KIF reorganization.

Pkg is important for force-induced polarized protrusive behaviors

As observed in the XCK1(8) knockdown experiments, inhibition of Pkg expression with antisense morpholinos resulted in failure of single mesendoderm cells to respond to C-cad.Fc bead pull by repolarizing (Fig. 2.10A). Pkg knockdown was also associated with an increase in the number of protrusions relative to control cells ($p<0.001$) and this increase was not affected by bead pull (Fig. 2.10B). Todorovic et al (2010) noted a similar increase in protrusive activity in Pkg-null keratinocytes, which they attributed to increased Rac activity.

Lamellipodial protrusions in the direction of tissue migration (180^{o}) are evident in both leading edge cells and following cells in normal intact mesendoderm (Fig. 1.4). In control explants, the angular variance of protrusions between leader cells and following cells was not statistically significant (Fig. 2.10C). In other words, both types of cells showed spatially well-oriented protrusion behaviors. Intact mesendoderm explants from Pkg knockdown embryos retained polarized protrusions in leader cells in the general direction of migration (Fig. 2.10D). However, protrusions of follower cells in Pkg morphant explants were significantly more broadly distributed than those of leader cells [$p(same)=0.001$]. These data indicate that Pkg has a role in regulating mesendoderm cell polarity but suggest that additional factors are involved in maintaining the polarized behaviors of cells in intact mesendoderm, particularly at the leading edge of the tissue.

Pkg is required for force-dependent reorganization of KIFs

We next investigated whether Pkg plays a role in linking KIFs to mechanically stimulated cadherins in the mesendoderm. Organization of KIFs was evaluated in cells from control or Pkg morphant embryos that were subjected to C-cad.Fc bead pull. The KIF cytoskeleton in both control and Pkg morphant cells was distributed broadly throughout the cytoplasm prior to the application of force to attached C-cad.Fc beads (Fig. 2.11A, B). In contrast to controls, KIFs in Pkg knockdown cells did not reorganize toward the direction of bead pull when force was applied (Fig. 2.11A', B').

Pkg was also required for normal KIF organization in intact mesendoderm tissues. EGFP-tagged XCK1(8) was expressed in embryos and time-lapse imaging of live mesendoderm explants was used to resolve KIF organization following knockdown of Pkg. In control explants, KIFs were located basally and associated with discrete points of cell-cell contact in the posterior half of each cell (Fig. 2.11C, E, arrowheads). A band of KIFs also spanned the anterior leading edge of cells perpendicular to the direction of tissue movement (Fig. 2.11C, E, arrow) as noted earlier (Fig. 2.3C). In Pkg morphant explants, KIFs were more broadly distributed and lacked clear points of association with cell-cell contacts (Fig. 2.11 D, F, arrowheads), however, the arrangement of KIFs along the anterior margins of the leading edge cells persisted (Fig. 2.11D, F, arrow). This suggests that Pkg-dependent and -independent mechanisms are involved in organizing these two distinct populations of filaments. Thus, the persistence of KIF cabling at the front of leading-edge cells in the absence of Pkg may contribute to the general maintenance of directed cell protrusions observed in tissue explants (Fig. 2.10D),

whereas keratin knockdown disrupts cell protrusion orientation in both leader and follower cells alike (Fig. 2.5B).

Traction on Fn is essential for organization of KIFs and localization of Pkg

When two dissociated cells on Fn formed a cell-cell adhesion *in vitro*, the cells polarized and moved in opposite directions but remained adherent while tugging on one another (Fig. 2.12A). As observed with C-cad.Fc bead pull, KIFs were recruited to the rear of these cells where force was being generated at the point of cell-cell contact as a consequence of traction forces on the Fn substrate (Fig. 2.12B). In contrast, cell pairs plated on PLL substrate are unable to generate substrate traction; they did not exhibit directed protrusive activity and failed to reorganize KIFs toward the cell-cell boundary (Fig. 2.12C).

To confirm and extend observations from the bead pull experiments, we visualized accumulation of C-cadherin and Pkg at cell-cell interfaces in cell pairs under conditions that permitted (i.e. Fn) or precluded (i.e. PLL) the generation of traction forces on the substrate. Pkg was observed along the cell-cell boundaries of cell pairs that were plated on Fn substrates and allowed to generate traction forces and protrude in opposing directions (Fig. 2.12D). In contrast, Pkg was not detected at cell-cell adhesions in cell pairs plated on PLL (Fig. 2.12E). C-cadherin was present at points of cell-cell contact regardless of whether cell pairs formed on Fn or PLL (Fig. 2.12F, G). Thus we conclude that the recruitment of Pkg to C-cadherin adhesions specifically requires tension on cell-cell junctions and that traction on Fn is required for the generation of this tension.

Pkg and keratin modulate mechanical properties of the mesendoderm tissue

KIFs are known to provide mechanical resilience to cells (Coulombe et al., 1991). Therefore, KIFs, and perhaps Pkg, are likely to be important for the mechanical properties of the migrating tissue. In light of the observation that perturbation of integrin-Fn adhesion causes migrating mesendoderm explants to recoil (Davidson et al., 2002), we used blocking antibodies to induce retraction of mesendoderm explants in order to probe the mechanical properties of the tissue. Over the course of 30 min following addition of a blocking antibody, retraction of Pkg and XCK1(8) morphant explants was similar to control explants (Fig. 2.13A). However, XCK1(8) morphant explants retracted significantly faster than either control or Pkg morphant tissues (Fig. 2.13B). A plot of the average velocity of retraction over time revealed a notable decrease in velocity of the initial recoil of Pkg morphant explants (Fig. 2.14A). This resulted in a significant decrease in the distance retracted at all time points up to, but not including, the end-point of the assay (Fig. 2.14B). The loss of the initial high velocity "snap" in Pkg morphant explants is suggestive of a reduction in tension within the tissue. In contrast, XCK1(8) morphants exhibited a prolonged initial recoil (Fig. 2.15A), which could be interpreted as an increase in tension. There was no difference at any time point in distance retracted by XCK1(8) explants compared with controls (Fig. 2.15B). These changes in the behavior of mesendoderm tissue following perturbation of integrin-Fn adhesion indicate that Pkg and keratin modulate the mechanical properties of the tissue but the specific effects are unclear and somewhat contrary.

2.5 Discussion

The identification of local force application on cadherins as an inductive signal for cell polarity offers some mechanistic insight into nearly 60 years of observations on the role of cell-cell contacts in directing cell migration (Abercrombie and Heaysman, 1953; Arboleda-Estudillo et al., 2010; Desai et al., 2009; Kolega, 1981). By applying tension to cadherin-based adhesions using a magnetic tweezer, a mechanical asymmetry was initiated in the cell that induced polarized protrusions and necessary tractions to resolve the imbalance of forces (Fig. 2.16A). A similar phenomenon was also observed in cell pairs (Fig. 2.16B) where forces at the cell-cell boundary are counterbalanced by traction forces biased away from the cell-cell interface (Liu et al., 2010; Maruthamuthu et al., 2011).

How then do forces on cell-cell contacts promote polarized protrusions in the *same* direction as in the mesendoderm or epithelial sheets where a morphological "shingling" of underlapping cells occurs? For each cell in the migrating sheet, force is greater on cell-cell contacts at the rear than on cell-cell contacts at the front (Trepat et al., 2009). In the leading edge cells, this asymmetry is obvious because cadherin adhesions themselves are isolated to the rear and lateral sides of each cell. In subsequent rows cadherin adhesions exist around the entire perimeter of each cell (Angres et al., 1991), but force on cadherin adhesions is greatest in the trailing ends rather than the leading edges of each cell in the collectively migrating array (Trepat et al., 2009). Thus, force on cell-cell adhesions is asymmetric even though the overall *presence* of cell-cell adhesions is symmetric. This is consistent with our conclusion that cadherin engagement alone is not sufficient to induce mesendoderm cell polarity and that force on the cadherin

adhesion is the key stimulus. We suggest that force imbalance between cadherin adhesions at the front and rear of each cell is an intrinsic property of the migratory cell sheet that stimulates directed cell protrusions.

If mesendoderm is migrating against an intercellular tension that builds within the tissue, then what balances the force in the opposing direction? As Trepat et al (2009) report, in simple epithelial culture models, opposite sides of a cell aggregate exert tractive stresses on the substrate in opposing direction (i.e., cells at margins of epithelial "islands" migrate radially away from the center of the cell aggregate) to balance intercellular stresses (Fig. 2.16C). In the case of the mesendoderm, however, this tissue is an integral part of a larger embryo comprised of multiple tissue types. Behind the migratory mesendoderm (i.e., in both the embryo and the tissue explants used in these studies) are the mesodermal cells, which in the dorsal region of the gastrula, intercalate mediolaterally and are oriented perpendicular to the movement of the mesendoderm (Keller, 2005). Thus, we speculate that the trailing mesoderm acts to "anchor" the mesendoderm by providing resistance to the cell-cell forces and migratory traction forces being generated within the latter (Fig. 2.16D). Interestingly, mesendoderm explants lacking these trailing mesoderm tissues fail to migrate directionally on Fn and instead spread radially in all directions (Winklbauer, 1990), as we would predict from our model.

Because cooperative migratory behaviors require cohesion amongst cells, we propose the term "cohesotaxis" to describe the guidance mechanism for this form of motility in which force imbalance on cell-cell adhesions is an implicit component. Examples of cohesotaxis would include cell groups with seemingly disparate phenotypes, such as cells that migrate away from one another (e.g., Fig. 2.12A) or that migrate

cooperatively in a unified direction in response to cohesive interactions [e.g., intact mesendoderm (Davidson et al., 2002), epithelial sheets (Farooqui and Fenteany, 2005), and *Drosophila* border cells (Prasad and Montell, 2007)].

Directed movement of the mesendoderm *in vivo* has been reported to require a gradient of ECM-bound PDGF deposited along the blastocoel roof on which the tissue migrates (Nagel et al., 2004). While such a chemotactic mechanism may contribute to directed motility, mesendoderm explants are still able to migrate directionally on isotropic Fn substrates lacking PDGF (Davidson et al., 2002; Winklbauer, 1990). Moreover, isolated single mesendoderm cells do not orient or migrate directionally on blastocoel roof explants or substrates conditioned with blastocoel roof matrix (Winklbauer, 1990; Winklbauer et al., 1992), which contain PDGF and any other factors that may be involved in chemotaxis (or haptotaxis) *in vivo*. We conclude that a chemotactic mechanism is alone insufficient to account for directed mesendoderm migration in the absence of cell cohesion. One possibility is that a gradient of PDGF is contributing to this process by modulating cadherin adhesion as in other systems (McDonald et al., 2003; Theisen et al., 2007; Yang et al., 2008).

A key step in the cellular response to tensile force stimulation is the recruitment of Pkg to C-cadherin adhesions under stress. Pkg is an adaptor protein that contains multiple armadillo repeats, which are involved in direct binding to classical and desmosomal cadherins, as well as the keratin-binding proteins desmoplakin and plakophilin (Bonné et al., 2003; Choi et al., 2009; Kowalczyk et al., 1997). Pkg and KIFs are associated with C-cadherin adhesions at discrete foci (Fig. 2.3B and 2.7B) and in response to increased mechanical tension (Fig. 2.3E’ and 2.7A’), suggesting the presence

and dynamic assembly-disassembly of nascent desmosome-like adhesions in a rapidly migrating tissue. C-cadherin in these cells is therefore likely to be involved in adherens junctions as well as in desmosome-like adhesive specializations, where the rapid molecular dynamics typical of classical cadherins and enhanced load-bearing typical of IF linkages may co-exist. Thus, Pkg is poised to function as a key physical link between the KIF cytoskeleton and classical cadherins such as C-cadherin. While current evidence supports this hypothesis an alternative possibility is that Pkg functions indirectly, perhaps by signaling changes in IF assembly and/or organization.

It is not yet clear how the localization and association of Pkg with cadherins and IFs is regulated by tension. One scenario is that Pkg continually associates with a subset of cadherins and these cadherins are recruited to sites of cell-cell tension. Alternately, Pkg may be diffusely localized throughout the cytoplasm or in association with IFs prior to application of tension and may associate with cadherins only when tension is applied. These interactions could be regulated by phosphorylation of Pkg and/or phosphorylation of cadherins and IFs (Busch et al., 2012; Miravet et al., 2003; Roura et al., 1999). Recruitment of cadherins or IFs might also rely on mechanical interactions such as changes in the organization of membrane domains or of the actin or microtubule networks (Delanoe-Ayari et al., 2004; Kölsch et al., 2009; Roberts et al., 2011; Ursell et al., 2009; Wöll et al., 2005).

Although KIF organization is disrupted in the cell body of Pkg morphant mesendoderm cells, trans-cellular cables of filaments persist at the leading edge of Pkg morphant explants (Fig. 2.11D, F). This finding indicates that the mechanism by which these cables are established and/or maintained is Pkg-independent. Members of another

linker protein family, the plakophilins, also interact with cadherins and with desmoplakin (Hatzfeld et al., 2000), to which KIFs bind directly (Kouklis et al., 1994). Plakophilins have been found to compete with plakoglobin for binding to desmoplakin (Bornslaeger et al., 2001) and could therefore constitute an additional element of the mechanosensitive complex. Preliminary studies do not indicate a requirement for plakophilin proteins in mesendoderm migration (data not shown), but plakophilins or other linker proteins could work redundantly with Pkg and contribute to KIF organization at the leading front. Alternately, KIFs could be linked to the actin cytoskeletal network either directly (Green et al., 1987) or through the cytoskeletal linker protein plectin (Jefferson et al., 2004). The continued presence of trans-cellular cabling could also explain the lesser degree to which knockdown of Pkg disrupted protrusive polarity in the mesendoderm tissue, relative to XCK1(8) knockdown. The KIF cables across the tissue front may serve to maintain the continuity of the leading edge and perhaps provide a polarity cue as well.

The finding that the organization of the KIF network is sensitive to mechanical stimuli and has a role in specifying migration polarity is remarkable. Long et al. (Long et al., 2006) previously observed that keratin-8 knockdown with siRNA inhibited directional migration of MCF-7, HeLa and Panc-1 epithelial cell sheets. This effect on migration was accompanied by irregular cell spreading and perturbation of cell-cell contacts that allowed cells to migrate individually in a randomized manner. Likewise, keratinocytes null for keratin-6 are more fragile than control cells and exhibit increased motility (Wong and Coulombe, 2003). While XCK1(8)-morphant mesendoderm remained a cohesive tissue, cell protrusive behavior and directional migration were

disrupted, suggesting that KIFs have a more specialized function than simple maintenance of tissue integrity.

The contribution of KIFs to cellular resilience is well established (Coulombe et al., 1991; Ramms et al., 2013) but it is not clear how the KIF network influences the mechanical properties of the mesendoderm tissue. Perturbation of integrin-Fn adhesion leads to immediate retraction of mesendoderm tissue, indicating a build-up of tension in the tissue during migration. The responses of Pkg and XCK1(8) morphant explants to addition of an antibody that inhibits adhesion to Fn are distinct from those of control explants. Pkg morphants initially recoil less than controls, perhaps due to a reduction in intercellular tension or to a loss of tissue elasticity (Fig. 2.14A). If tissue elasticity is indeed affected it suggests that the Pkg is a load bearing element. However, XCK1(8) morphant explants had a high initial retraction velocity, similar to that of controls (Fig. 2.15A). Furthermore, the high velocity retraction persisted twice as long in XCK1(8) morphants relative to control explants (Fig. 2.15A) and occurred sooner after addition of the blocking antibody (Fig. 2.13B). A tenuous connection between the XCK1(8) morphant mesendoderm and the Fn substrate could contribute to the decreased time to retraction and perhaps the prolonged initial recoil as well. Although we observed no clear defects in spreading of XCK1(8) morphant mesendoderm cells (Fig. 2.5B), this does not preclude the presence of subtle changes in adhesion strength or dynamics that could become evident when interaction with the Fn substrate is perturbed. KIFs can influence integrin-dependent adhesion in some cell types through PKCδ and focal adhesion kinase (FAK) (Bordeleau et al., 2010) or through Rho-mediated modulation of actin dynamics (Bordeleau et al., 2012). Therefore it becomes difficult to distinguish

strictly mechanical roles for KIFs from KIF mediated signaling events that may influence cellular stiffness or adhesion.

The functional interplay of mechanisms regulating both the adhesive and mechanical properties of cells in the mesendoderm is likely shared by other tissues undergoing collective forms of cell migration. In the case of wound healing, such changes may be achieved through differential expression of keratin pairs (Wong and Coulombe, 2003) with unique viscoelastic properties (Hofmann and Franke, 1997; Yamada et al., 2002). Stiffness of KIF networks can also be modulated by filament bundling (Yamada et al., 2002). IF function and organization are deeply integrated with the activities of many cell signaling pathways. Several extracellular ligands, including the bioactive lipid sphingosylphosphorylcholine (SPC), have been shown to induce migration of single cells, accompanied by collapse of the KIF network into a perinuclear-concentrated ring (Beil et al., 2003). Moreover, SPC-treated cells have a marked decrease in the elastic modulus, supporting the notion that IFs serve as tensile elements in living cells.

IFs are also reported to be regulated by Rho GTPases. Local activation of Rac1 promotes the disassembly of vimentin IFs, which induces lamellipodial protrusion in the "front" of the cell. Meanwhile assembled IFs are maintained at the "rear" (Helfand et al., 2011). Evidence from other recent studies show that Rac activity is negatively regulated by both Pkg (Todorović et al., 2010) and cadherin adhesion (Kitt and Nelson, 2011). We suggest that anterior-posterior orientation could be established by the stabilization of KIFs through the local inhibition of Rac by Pkg at sites of stressed cell-cell contacts while allowing KIF depolymerization and lamellipodial extension in the presumptive

front of the cell. Rac localization and activity are also regulated by integrin adhesions (Moissoglu and Schwartz, 2006). Integrin-associated signaling proteins such as FAK are required for recruitment of Rac1 to focal adhesions and Rac activity is greatly reduced in FAK null cells (Chang et al., 2007). Therefore, the observation that adhesion to Fn is essential for organization of KIFs and localization of Pkg to cell-cell junctions raises the question of whether this effect is dependent on signaling, mechanics or both. Traction on Fn may allow cells to generate tension on cadherin adhesions sufficient for the induction of polarized protrusive behavior but may also influence the localization and activation of Rac and thereby indirectly modulate the organization of IFs. The interactions between mechanical stimulation of cadherins, regulation of Rac activity, generation of polarized protrusive behavior and the organization and dynamics of IFs are an important line of future investigation.

The data presented here demonstrate the formation of polarized cellular protrusions in response to mechanical stimulation. However, the molecular components of the initiating mechanosensor(s) involved remain unclear. C-cadherin is one obvious candidate given that the observed morphological response requires specific application of force through cadherin adhesions. Signaling events proximal to the site of force application could involve direct conformational changes in C-cadherin or associated proteins that link C-cadherin to the cytoskeletal and/or signaling machinery within the cell. Alternatively, tugging on cadherin adhesions might increase the local accumulation of cadherins at the site of applied force. Indeed in some cells, the size of cadherin-based adhesions correlates with the magnitude of forces exerted by these adhesions (Ladoux et al., 2010; Liu et al., 2010). An accumulation of cadherin complexes at sites of local

mechanical stress could facilitate the recruitment Pkg and KIFs to these sites as well. This mechanism may not require immediate (e.g., milliseconds to seconds) activation of a "mechanosensor" complex per se, but rather a more gradual (e.g., seconds to minutes) cellular response to an initiating mechanical stimulus. Continued efforts and development of novel approaches will be needed to elucidate the pathways by which the mechanical stimuli generated during development are transmitted and transduced into the chemical signals required for the patterning and morphogenesis of embryos.

Figure 2.1

Force on cadherins induces monopolar protrusive behavior in mesendoderm cells. (A) Schematic of experimental strategy for magnetic bead pull assay (see materials and methods for details). (B) Still image from time-lapse movie of single multipolar mesendoderm cell plated on Fn. (C) Still image from time-lapse movie of isolated mesendoderm cell plated on Fn and with C-cadherin coated (C-cad.Fc) bead attached. (D) Still image of same cell as in (C), C-cad.Fc bead pulled by magnet at right (red magnet icon). A lamellipodium (arrow) forms opposite the direction of bead pull. (E) Quantitation of protrusion angles relative to cell centroid (center of rose diagram) and magnet at right (0^{o}). Y-axis for rose diagram represents percent of total protrusions. (F) Quantitation of protrusions per cell after bead attachment and pull. Data are represented as mean $\pm$ SEM. All scale bars, 50μm. (B-D) Elapsed time shown in minutes:seconds. These data were generated by Gregory Weber.

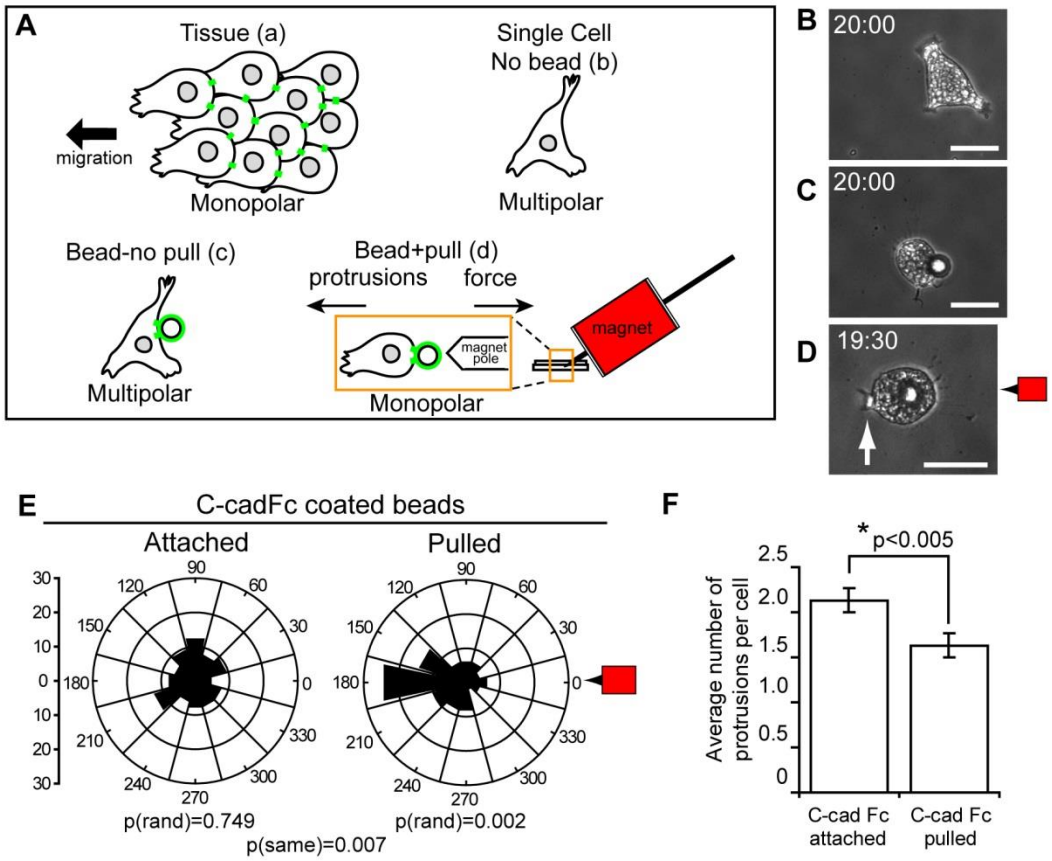
A
Tissue (a)
migration
Monopolar
Single Cell
No bead (b)
Multipolar
Bead-no pull (c)
Multipolar
Bead+pull (d)
protrusions
force
magnet
magnet pole
Monopolar
B
20:00
C
20:00
D
19:30
E
C-cadFc coated beads
Attached
Pulled
p(rand)=0.749
p(rand)=0.002
p(same)=0.007
F
* p<0.005
Average number of protrusions per cell
C-cad Fc attached
C-cad Fc pulled

Figure 2.2

Actin organization does not depend on cell context and disruption of actin does not result in release of C-cadherin coated bead but disruption of keratin does. (A) Quantification of cell responses to steady bead pull on C-cadherin coated beads, following addition of blebbistatin, cytochalasin or acrylamide to perturb the actin or intermediate filament cytoskeletal networks. (B) Single mesendoderm cell plated on Fn, labeled with Alexa555 dextran to show cell area (red) and expressing GFP-moesin to visualize actin filaments (green). Arrows denote lamellipodial protrusions. (C) Cells within explanted mesendoderm tissue plated on Fn, expressing GFP-moesin to visualize actin filaments. Arrows denote lamellipodial protrusions. Scale bars = 25μm. These data were generated by Gregory Weber.

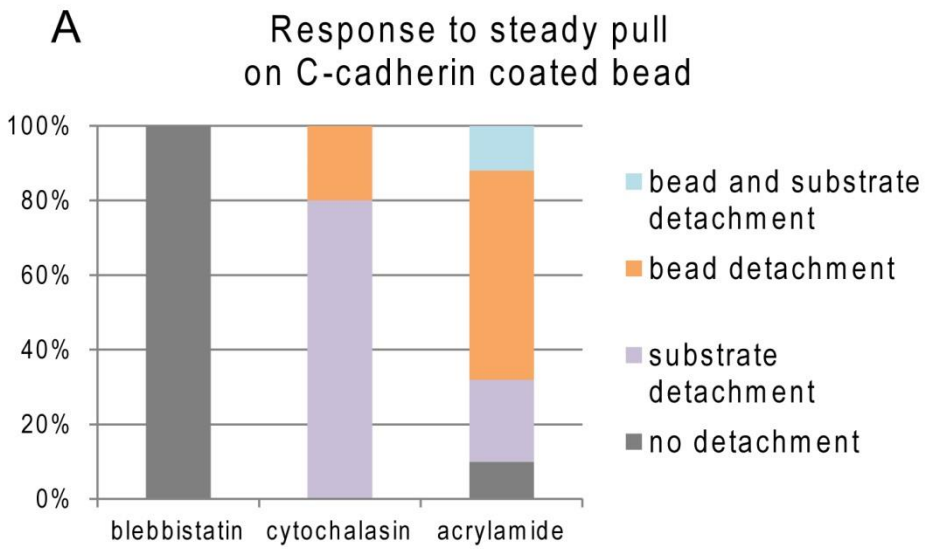
A
Response to steady pull
on C-cadherin coated bead
100%
80%
60%
40%
20%
0%
blebbistatin
cytochalasin
acrylamide
bead and substrate detachment
bead detachment
substrate detachment
no detachment

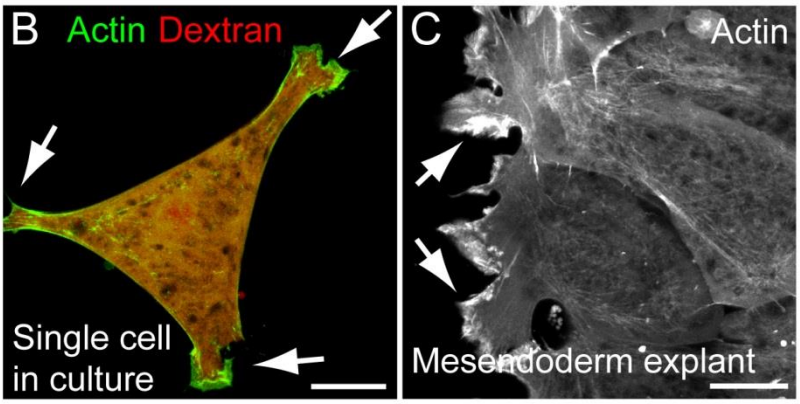
B Actin Dextran
Single cell
in culture
C Actin
Mesendoderm explant

Figure 2.3

Keratin organization is dynamic and responsive to tension on cadherins. (A) Single cell on Fn, labeled with Alexa555 dextran (red) and expressing EGFP-XCK1(8) to visualize keratin filaments (green). (B) Pair of fixed mesendoderm cells immunostained for C-cadherin (red) and XCK1(8) (green). Dashed line indicates cell-cell boundary. (C) Cell within mesendoderm tissue explant on Fn labeled with Alexa555 dextran (red) and expressing EGFP-XCK1(8) (green). (D) Sagittal perspective of mesendoderm cell in bisected embryo immunostained for C-cadherin (red) and XCK1(8) (green). Keratin filaments in posterior of polarized cells (arrowheads B-D) and along tissue leading edge (arrow in C). (E, E') Single mesendoderm cell on Fn labeled with Alexa555 dextran (red), expressing EGFP-XCK1(8) (green). C-cad.Fc bead (dashed circle) attached to cell (E), then pulled for 20 min (E'). Arrow denotes leading edge protrusion. Scale bars = 25μm. These data were generated in collaboration with Gregory Weber and Bette Dzamba.

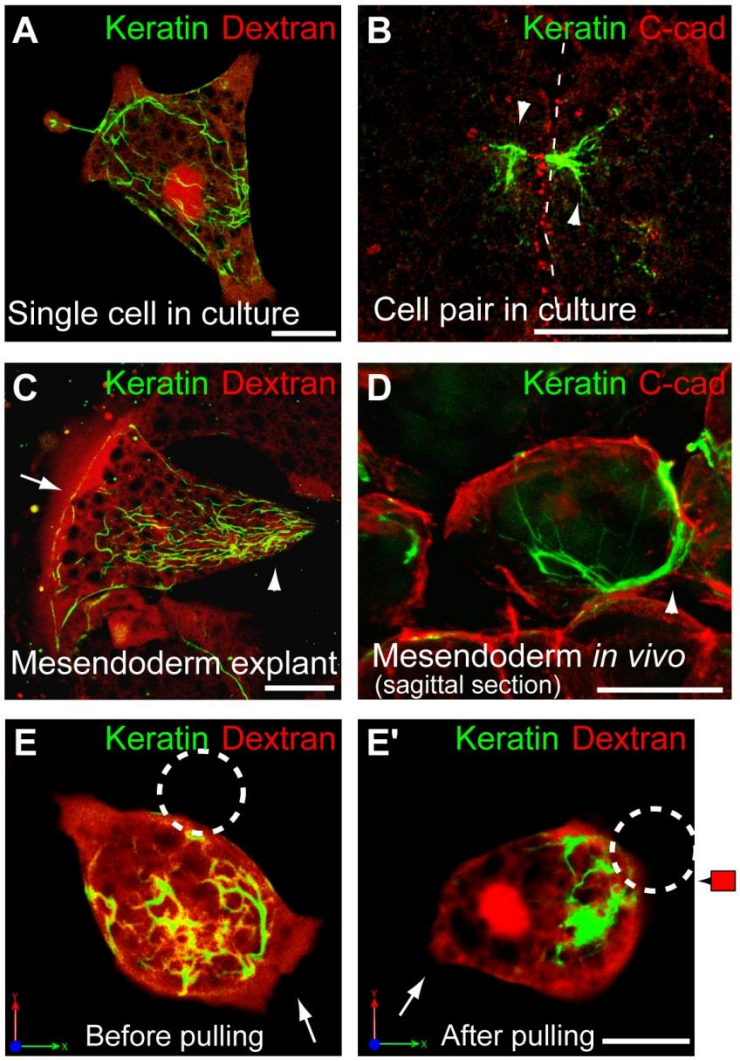
A
Keratin Dextran
Single cell in culture
B
Keratin C-cad
Cell pair in culture
C
Keratin Dextran
Mesendoderm explant
D
Keratin C-cad
Mesendoderm *in vivo*
(sagittal section)
E
Keratin Dextran
Before pulling
E'
Keratin Dextran
After pulling

Figure 2.4

XCK morpholino knocks down XCK protein expression and the morphant phenotype can be rescued by injection of RNA not targeted by the morpholino. (A) Immunoblot of lysates from embryos expressing XCK1(8)-myc and injected with Control MO or MOs targeting XCK1(8). (B) Exogastrulation phenotype induced by injection of XCK1(8) MO (compare left and middle panels) is rescued by co-injection with EGFP-XCK1(8), which is not targeted by the MO (right panel). (C) Quantification of embryos with blastopore phenotype at stage 12. Data are mean ± SEM, N=7. These data were generated in collaboration with Gregory Weber.

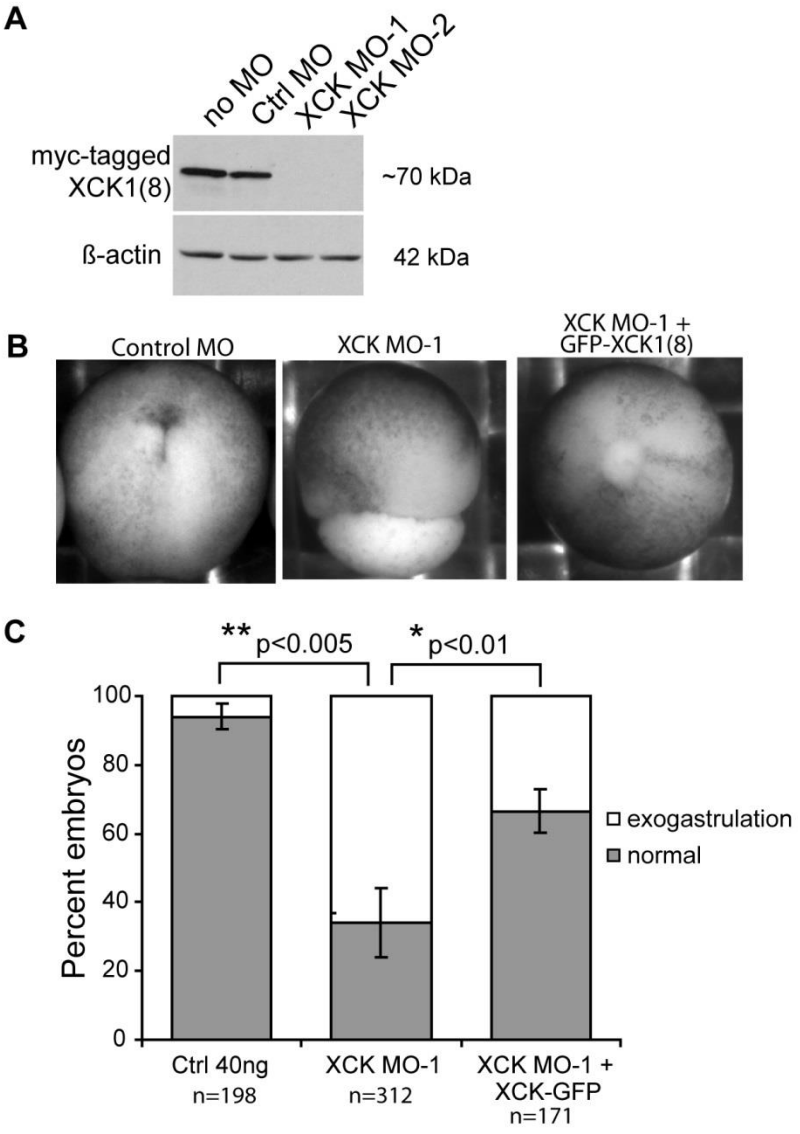
A
no MO
Ctrl MO
XCK MO-1
XCK MO-2
myc-tagged XCK1(8)
~70 kDa
ß-actin
42 kDa
B
Control MO
XCK MO-1
XCK MO-1 + GFP-XCK1(8)
C
** p<0.005
* p<0.01
Percent embryos
100
80
60
40
20
0
exogastrulation
normal
Ctrl 40ng
n=198
XCK MO-1
n=312
XCK MO-1 + XCK-GFP
n=171

Figure 2.5

Keratin is essential for force-induced protrusive polarity and tissue polarity. (A) Quantitation of protrusion angles from XCK1(8) morphant cells with C-cad.Fc beads attached and following bead pull. (B) GAP43-EGFP labels plasma membranes in intact mesendoderm explants prepared from control morphant (left) and XCK1(8) morphant embryos (right). Green arrowheads indicate protrusions in the direction of tissue movement and red arrowheads mark protrusions in any other direction. Scale bar = 25μm. These data were generated by Gregory Weber.

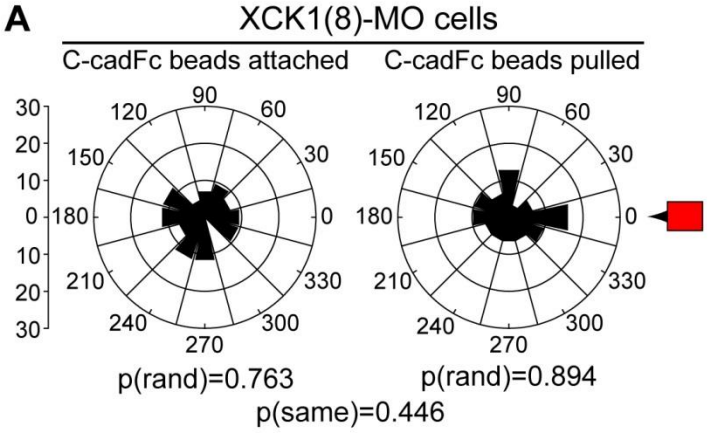
A
XCK1(8)-MO cells
C-cadFc beads attached
C-cadFc beads pulled
30
20
10
0
10
20
30
90
120
60
150
30
180
0
210
330
240
300
270
p(rand)=0.763
p(rand)=0.894
p(same)=0.446

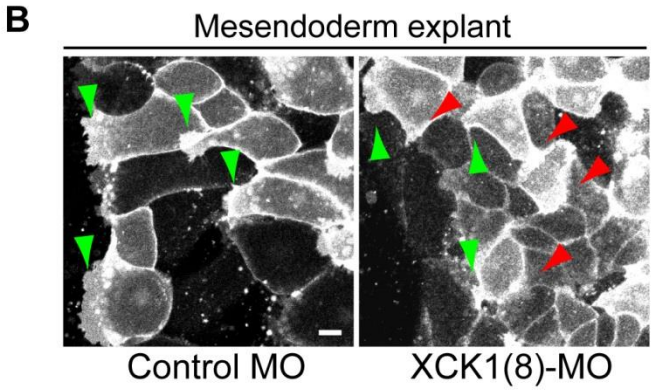
B
Mesendoderm explant
Control MO
XCK1(8)-MO

Figure 2.6

Plakoglobin associates biochemically with C-cadherin. (A) Schematic cartoon of proposed linkages between classical cadherins and the intermediate filament and actin cytoskeletal networks. (B) C-cadherin and Pkg were immunoprecipitated from whole embryo lysates and immunoblotted as indicated. α5 integrin immunoprecipitates served as negative controls. These data were generated in collaboration with Gregory Weber.

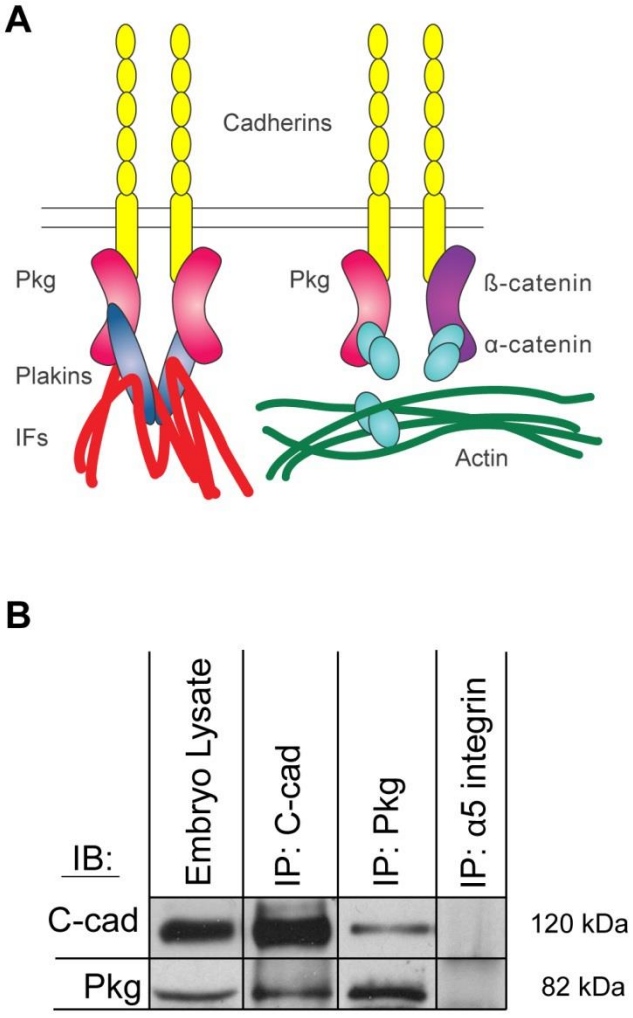
A
Cadherins
Pkg
Pkg
ß-catenin
α-catenin
Plakins
IFs
Actin
B
IB:
Embryo Lysate
IP: C-cad
IP: Pkg
IP: α5 integrin
C-cad
Pkg
120 kDa
82 kDa

Figure 2.7

Pkg localizes to cadherins in cells under tension and co-localizes with XCK in mesendoderm tissue. (A, A') 3D rendered side view of a normal cell injected with Alexa555 dextran (red) and expressing Pkg-GFP (green) before (A) and after (A') C-cad.Fc bead pull. Location of bead indicated by dashed circle. (B) Mesendoderm cells in explanted mesendoderm tissue expressing Pkg-GFP (red), mCherry-XCK1(8) (green), and labeled with Alexa647-dextran (gray). Image is a collapsed 2μm Z-stack of the posterior-lateral region of two adjacent cells in a mesendoderm explant. (C) Zoomed in view of area inside white box in (B). (C'-C''') Zoomed in views of area inside box in (C), separated into single channels. Scale bars = 15μm. These data were generated in collaboration with Gregory Weber.

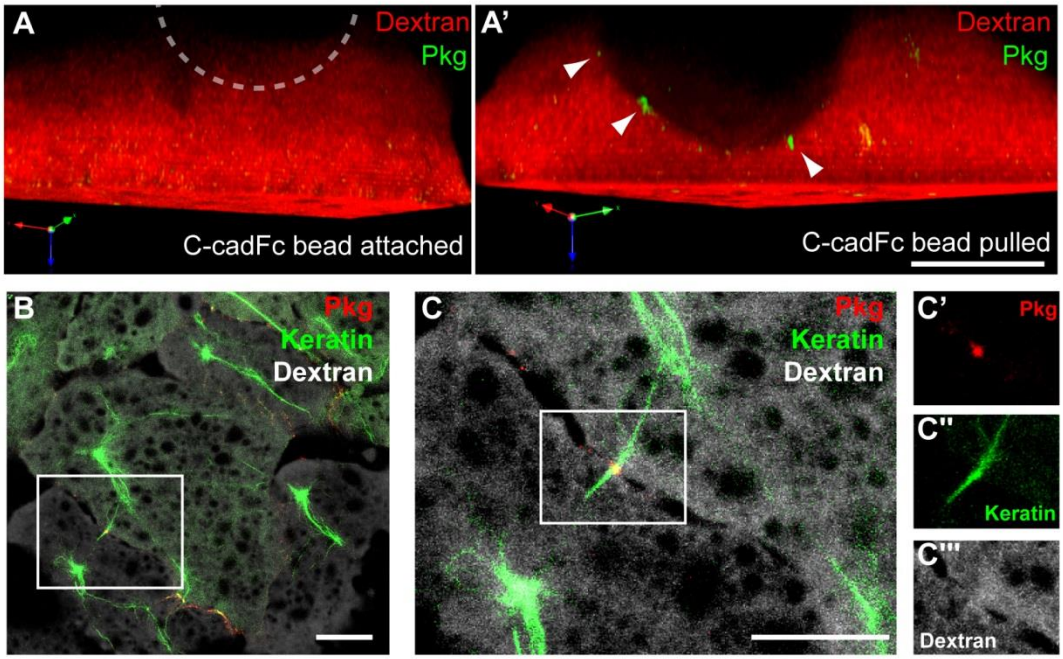
A
Dextran
Pkg
C-cadFc bead attached
A'
Dextran
Pkg
C-cadFc bead pulled
B
Pkg
Keratin
Dextran
C
Pkg
Keratin
Dextran
C'
Pkg
C''
Keratin
C'''
Dextran

Figure 2.8

Pkg morpholino knocks down Pkg protein expression. (A) Lysates of *Xenopus* embryos injected with 40ng Control MO or Pkg MO and immunoblotted for plakoglobin and β-actin. (B) Quantification of Pkg expression levels in gastrula stage embryos, normalized to β-actin and shown relative to control embryos. Data are mean ± SEM, N=4.

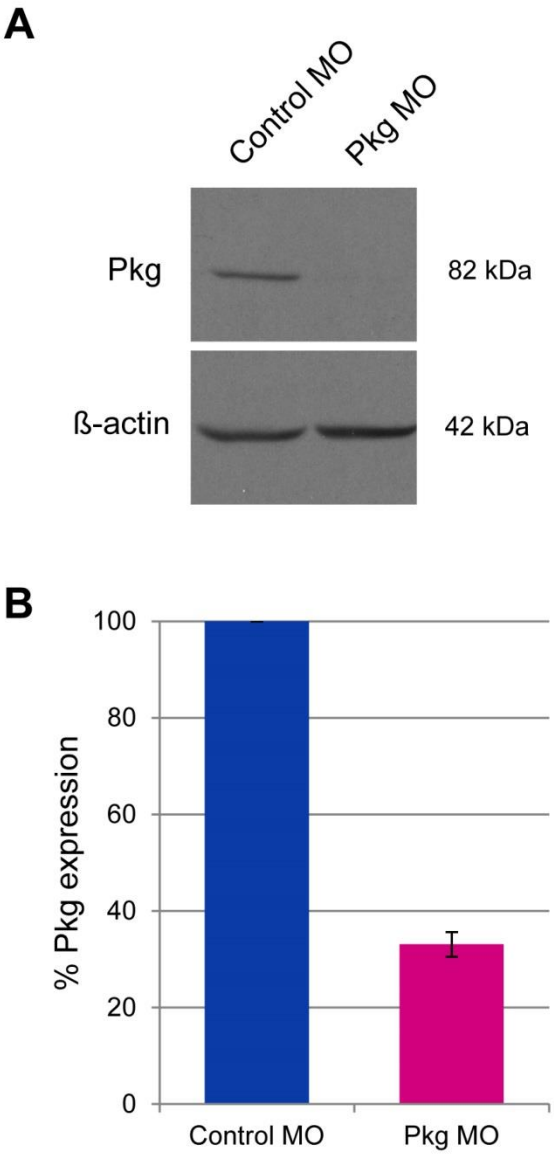
A
Control MO
Pkg MO
Pkg
82 kDa
ß-actin
42 kDa
B
100
80
60
40
20
0
% Pkg expression
Control MO
Pkg MO

Figure 2.9

Knockdown of Pkg diminishes association of XCK with C-cadherin. (A-C) Embryos were injected with XCK1(8)-EGFP, with or without Pkg MO. (A) Immunoblots of embryo lysates show expression levels of XCK1(8)-EGFP and endogenous Pkg with or without Pkg MO. (B) C-cadherin immunoprecipitates immunoblotted for XCK1(8)-EGFP and C-cadherin with or without Pkg MO. (C) Data are mean ± SEM, N=3. These data were generated by Gregory Weber.

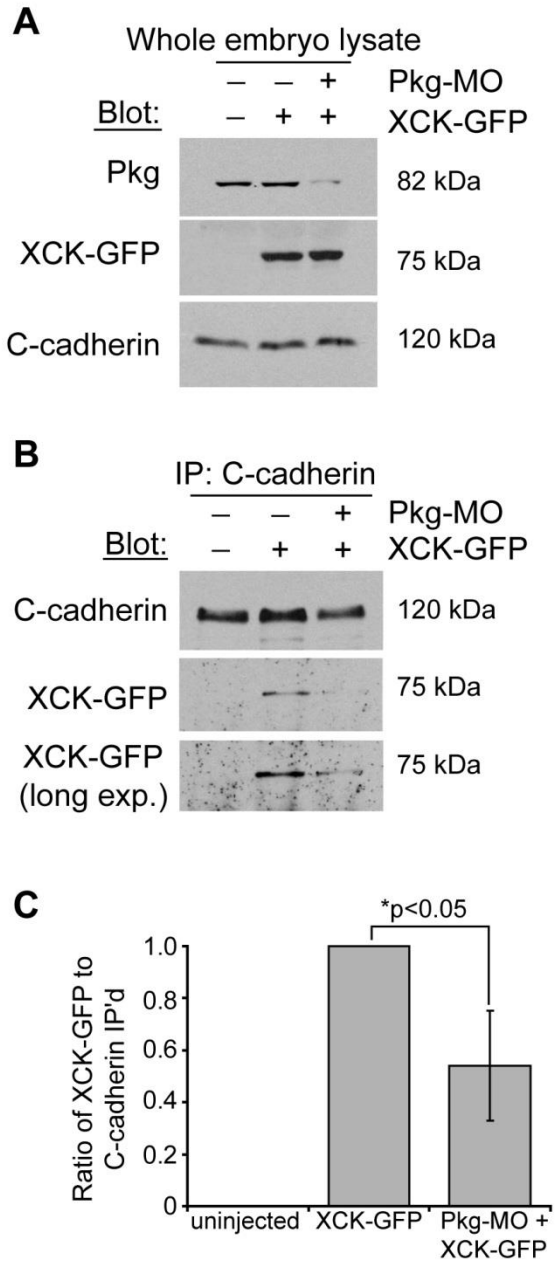
A
Whole embryo lysate
– – + Pkg-MO
Blot: – + + XCK-GFP
Pkg
82 kDa
XCK-GFP
75 kDa
C-cadherin
120 kDa
B
IP: C-cadherin
– – + Pkg-MO
Blot: – + + XCK-GFP
C-cadherin
120 kDa
XCK-GFP
75 kDa
XCK-GFP (long exp.)
75 kDa
C
*p<0.05
Ratio of XCK-GFP to C-cadherin IP'd
1.0
0.8
0.6
0.4
0.2
0
uninjected
XCK-GFP
Pkg-MO + XCK-GFP

Figure 2.10

Pkg is important for force-induced protrusive polarity and tissue polarity. (A) Quantitation of protrusion angles from Pkg morphant mesendoderm cells with C-cad.Fc beads attached and following bead pull. (B) Quantitation of protrusion number per cell in normal and Pkg morphant mesendoderm cells. Data are mean ± SEM. (C, D) Quantitation of protrusion angles, where 180^{o} equals direction of tissue migration, in Control morphant explants (C) and Pkg morphant explants (D). Leading cells = row 1, following cells = rows 2-4. In panels at right, GAP43-EGFP labels plasma membrane of mesendoderm explants from control and Pkg morphant embryos. Green arrowheads indicate protrusions in the expected direction of tissue movement and red arrowheads mark protrusions in any other direction. Scale bars = 25μm. These data were generated in collaboration with Gregory Weber.

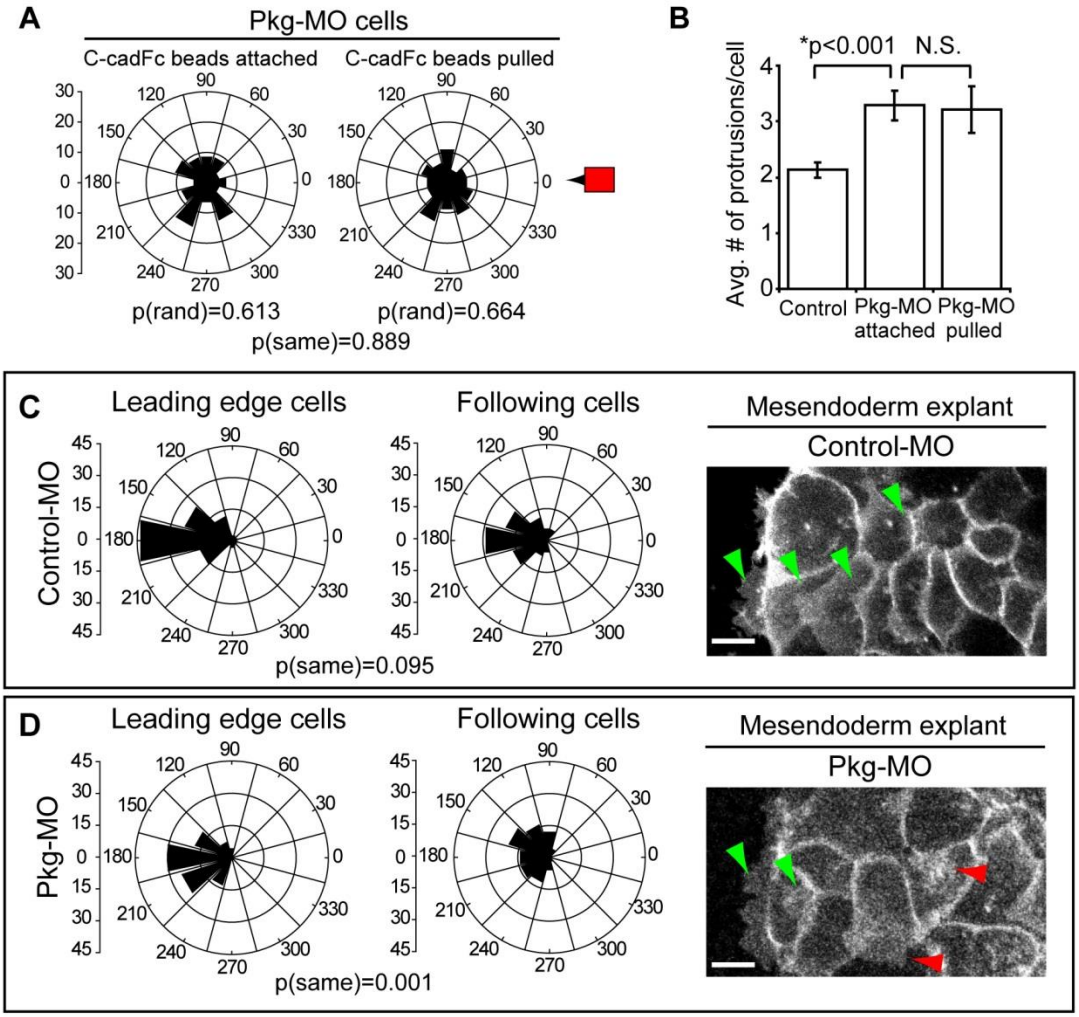
A
Pkg-MO cells
C-cadFc beads attached
C-cadFc beads pulled
p(rand)=0.613
p(rand)=0.664
p(same)=0.889
B
*p<0.001 N.S.
Avg. # of protrusions/cell
Control
Pkg-MO attached
Pkg-MO pulled
C
Leading edge cells
Following cells
Mesendoderm explant
Control-MO
Control-MO
p(same)=0.095
D
Leading edge cells
Following cells
Mesendoderm explant
Pkg-MO
Pkg-MO
p(same)=0.001

Figure 2.11

Pkg is required for organization of keratin in posterior of cells under tension. (A, B) Single cells labeled with Alexa dextran and expressing EGFP-XCK1(8) (green), plated on Fn. (A, A') is a control cell (blue dextran) and (B, B') is a Pkg morphant cell (magenta dextran). C-cad.Fc bead (circle) bound (A, B), then pulled (A', B'). (C) Control morphant (blue dextran) and (D) Pkg morphant (magenta dextran) mesendoderm tissue explants expressing EGFP-XCK1(8) (green). (E) Image from (C) is displayed as separate color channels for Alexa647 dextran (left) and EGFP-XCK1(8) (right). (F) Image from (D) is displayed as separate color channels for Alexa555 dextran (left) and EGFP-XCK1(8) (right). Some minor spectral bleedthrough is observed from the EGFP-XCK1(8) into the channel for detection of Alexa555 dextran, but not the inverse. These data were generated in collaboration with Gregory Weber.

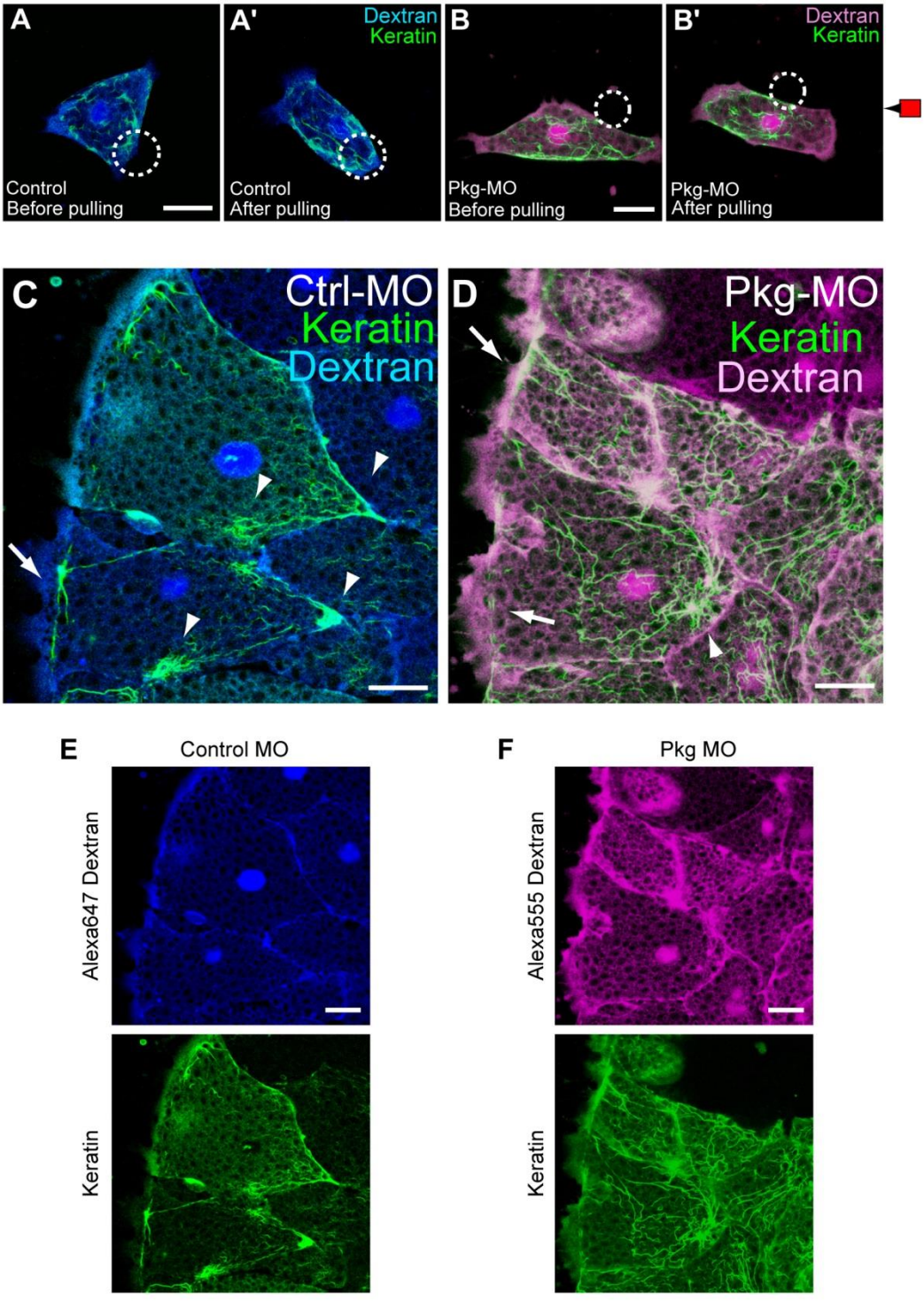
A
Control
Before pulling
A'
Dextran
Keratin
Control
After pulling
B
Pkg-MO
Before pulling
B'
Dextran
Keratin
Pkg-MO
After pulling
C
Ctrl-MO
Keratin
Dextran
D
Pkg-MO
Keratin
Dextran
E
Control MO
Alexa647 Dextran
Keratin
F
Pkg MO
Alexa555 Dextran
Keratin

Figure 2.12

Cells must generate traction force on Fn for organization of XCK and Pkg at cell-cell junctions. (A) Brightfield image of cell pair on Fn, polarized in opposing directions (double arrow). (B, C) Cell pairs expressing EGFP-XCK1(8), plated on Fn (B) or PLL (C). Dashed line indicates cell-cell boundary. Cell borders outlined by dotted line in (B). Cells expressing either Pkg-GFP (D, E) or C-cadherin-GFP (F, G), plated on either Fn (D, F) or PLL (E, G) and allowed to form cohesive pairs. Arrowheads indicate plane of cell-cell boundaries. Scale bars (A-C) = 25μm, scale bars (D-G) = 15μm. These data were generated in collaboration with Gregory Weber.

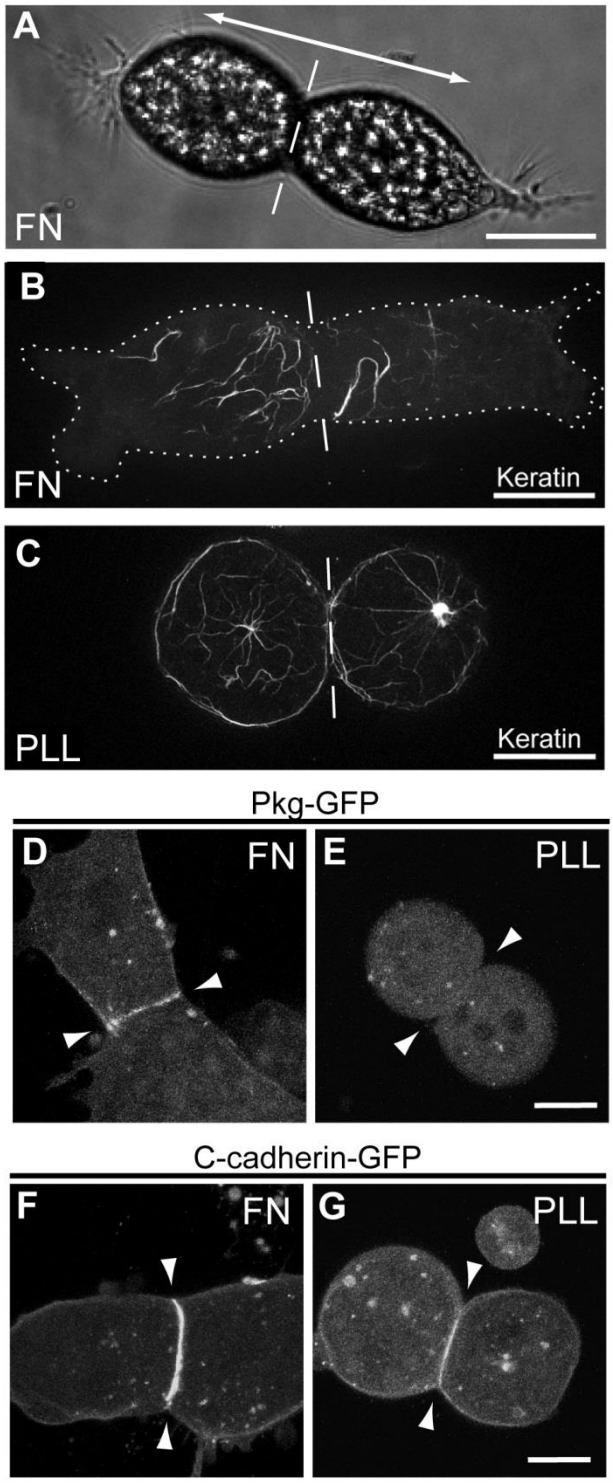
A
FN
B
FN
Keratin
C
PLL
Keratin
Pkg-GFP
D
FN
E
PLL
C-cadherin-GFP
F
FN
G
PLL

Figure 2.13

Keratin and Pkg morphant explants retract a similar distance to control explants but keratin morphant explants snap back sooner after inhibition of cell-ECM adhesion. (A) Quantification of leading edge retraction distance in mesendoderm explants dissected from Control, Pkg, or XCK1(8) morphant embryos, plated on Fn, then treated with antibody to block cell-ECM interactions. Distance measured from the point of farthest migration. (B) Quantification of time elapsed between addition of blocking antibody and the first retraction of the leading edge of the mesendoderm explant. Data are mean ± SEM, N=9, 7, and 4 for Control, Pkg and XCK1(8) morphants respectively.

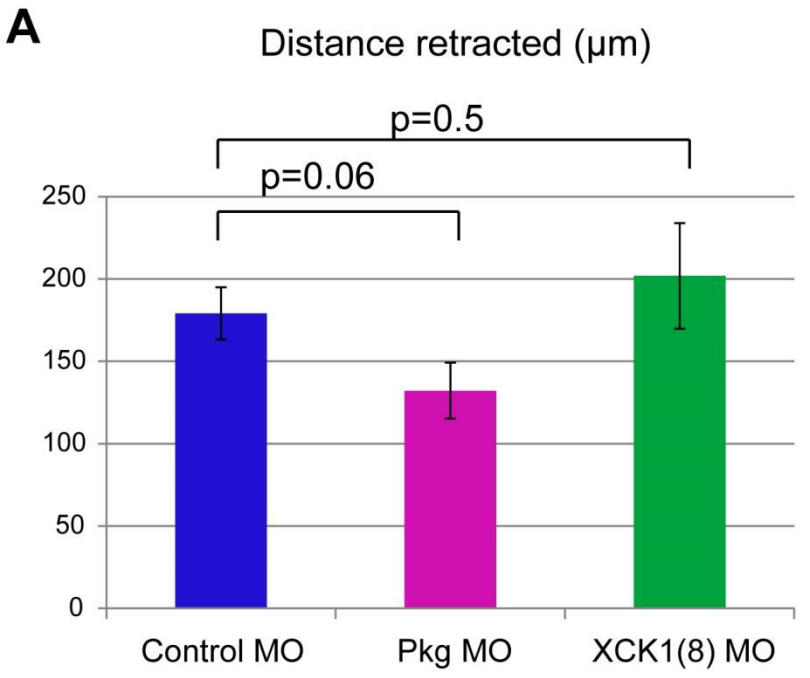
A
Distance retracted (μm)
p=0.5
p=0.06
250
200
150
100
50
0
Control MO
Pkg MO
XCK1(8) MO

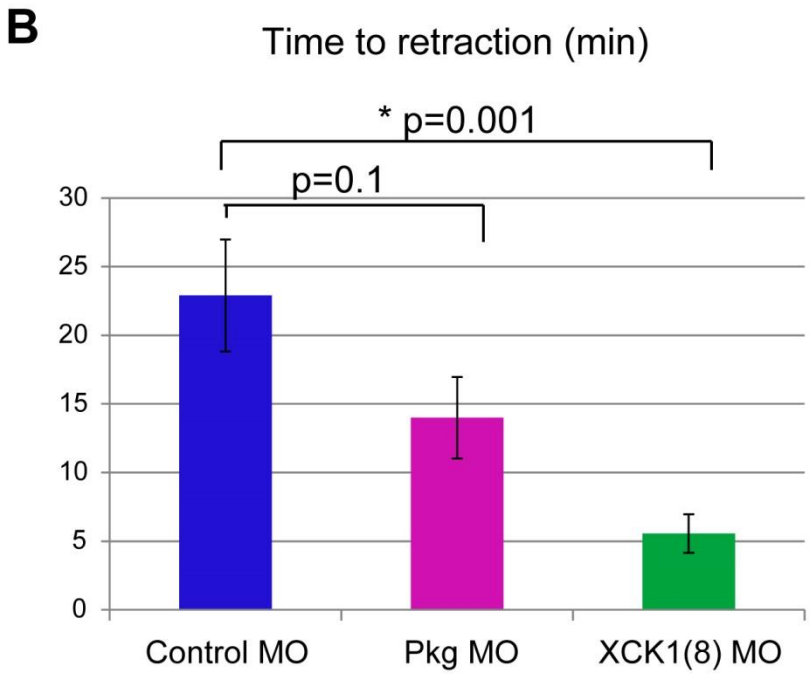
B
Time to retraction (min)
* p=0.001
p=0.1
30
25
20
15
10
5
0
Control MO
Pkg MO
XCK1(8) MO

Figure 2.14

Pkg morphant explants snap back more slowly than controls. (A) Quantification of average velocity of leading edge retraction over time following addition of blocking antibody to mesendoderm explants on Fn, data are inverted so that a positive velocity represents retraction. (B) Quantification of the average distance of leading edge retraction from the time of addition of blocking antibody to mesendoderm explants cut from Control or Pkg morphant embryos and plated on Fn. Data are mean ± SEM, N= 9, 7 for Control and Pkg morphants respectively. Time points at which Pkg morphants were significantly different from controls are indicated by *, $p < 0.03$.

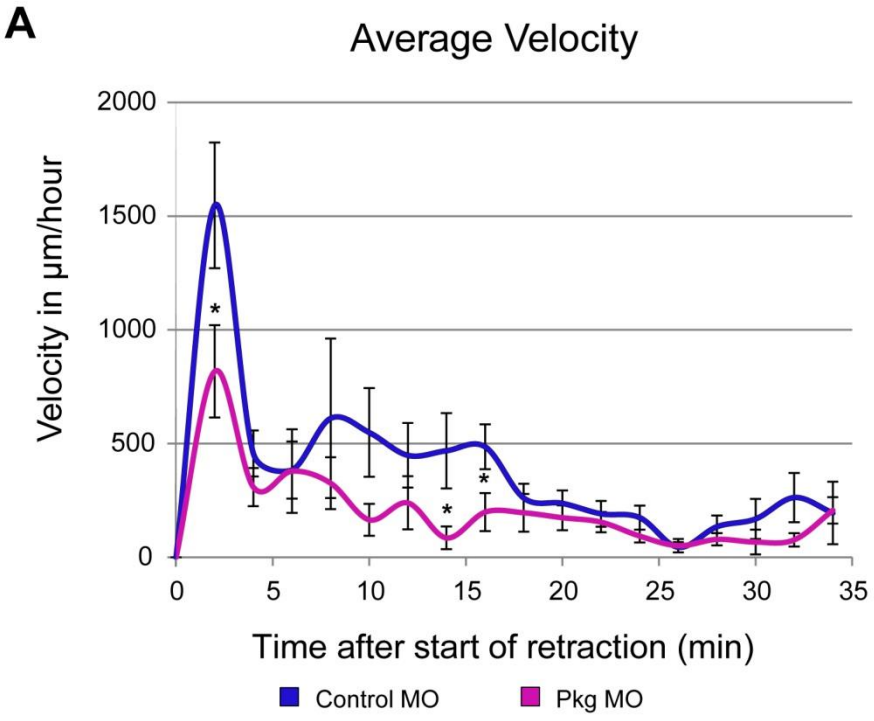
A
Average Velocity
Velocity in µm/hour
2000
1500
1000
500
0
0
5
10
15
20
25
30
35
Time after start of retraction (min)
Control MO
Pkg MO

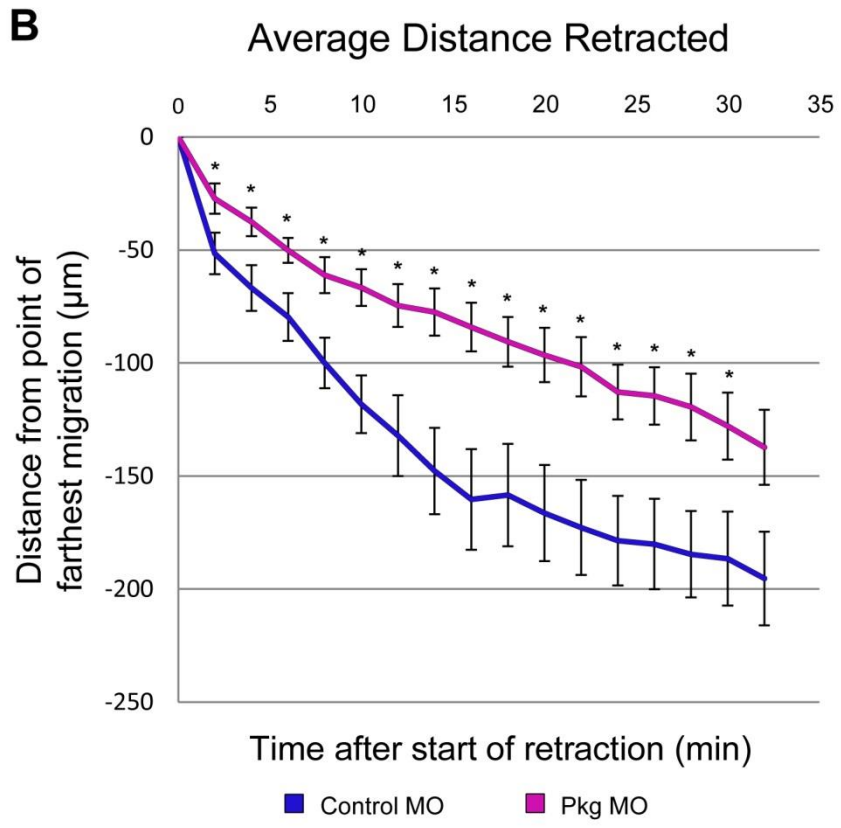
B
Average Distance Retracted
Distance from point of farthest migration (µm)
0
-50
-100
-150
-200
-250
0
5
10
15
20
25
30
35
Time after start of retraction (min)
Control MO
Pkg MO

Figure 2.15

Keratin morphant explants exhibit a longer period of high velocity retraction than do controls. (A) Quantification of average velocity of leading edge retraction over time following addition of blocking antibody to mesendoderm explants on Fn, data are inverted so that a positive velocity represents retraction. (B) Quantification of the average distance of leading edge retraction from the time of addition of blocking antibody to mesendoderm explants cut from Control or XCK1(8) morphant embryos and plated on Fn. Data are mean ± SEM, N= 9, 4 for Control and XCK1(8) morphants respectively. Time points at which XCK1(8) morphants were significantly different from controls are indicated by *, $p < 0.05$.

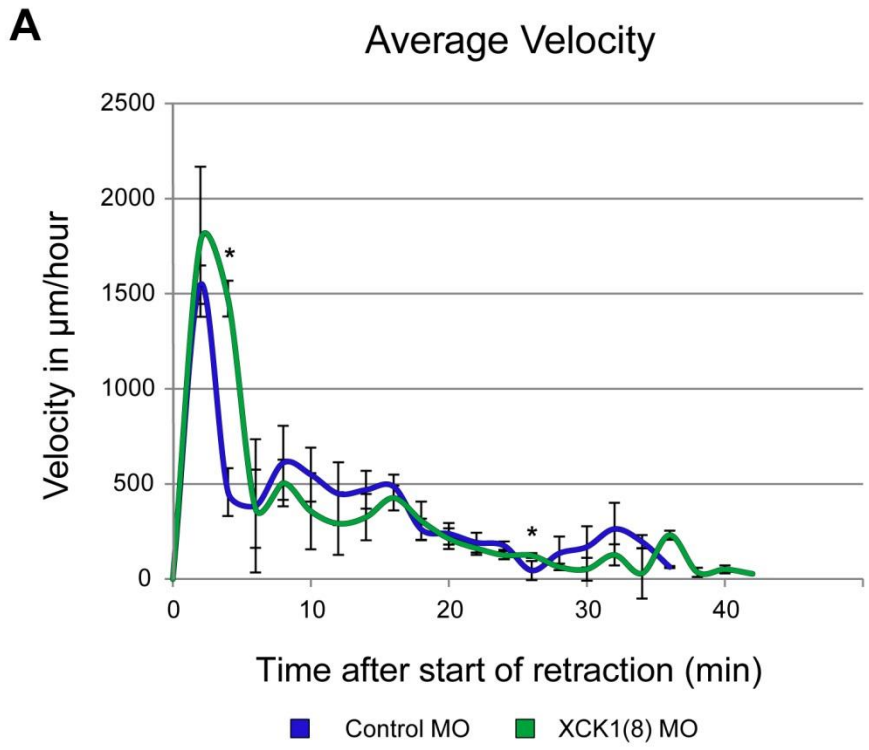
A
Average Velocity
Velocity in µm/hour
2500
2000
1500
1000
500
0
0
10
20
30
40
*
*
Time after start of retraction (min)
Control MO
XCK1(8) MO

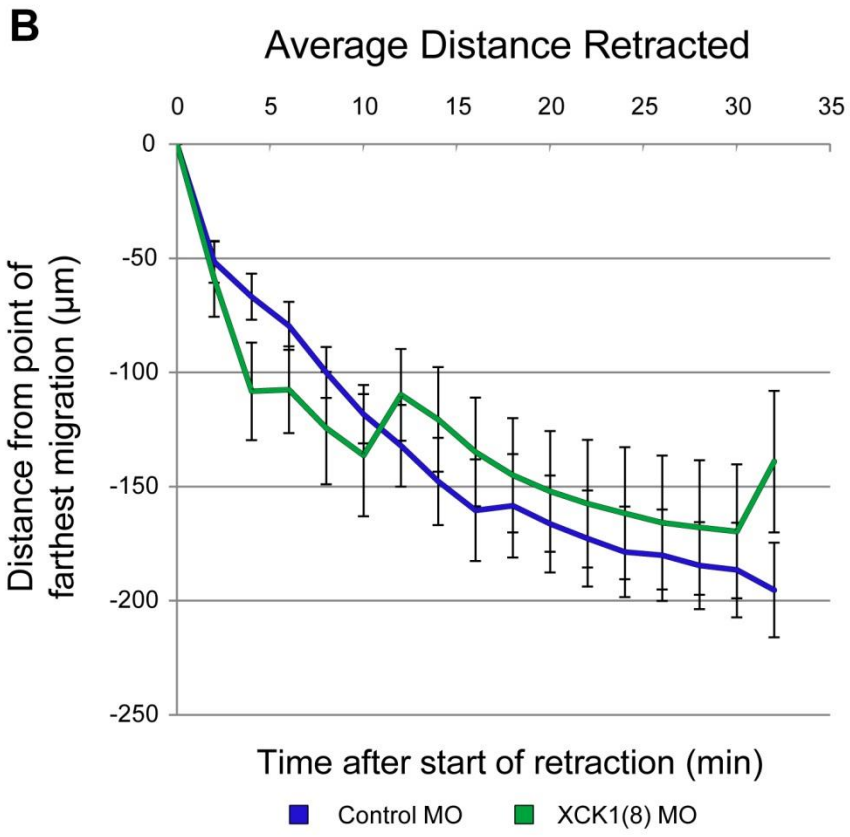
B
Average Distance Retracted
Distance from point of farthest migration (µm)
0
5
10
15
20
25
30
35
0
-50
-100
-150
-200
-250
Time after start of retraction (min)
Control MO
XCK1(8) MO

Figure 2.16

Model for force-induced regulation of cell migration polarity. (A) Applying tensile force on cadherins (F_C, pink arrows) in a single cell with a C-cad.Fc bead and magnetic tweezer mimics forces normally applied by neighboring cells in a multicelled array and induces a protrusion opposite the direction of applied force. When velocity is constant, net traction forces (T, green arrows) exerted by the cell are necessarily equal to the force used to pull the bead (F_B). (B) Two cells that form a stable cell-cell contact polarize in opposite directions. Traction force that each cell exerts on the substrate (T) is balanced by an equivalent force at the cell-cell interface (F_C) to maintain cohesion. (C) In a cell sheet, stresses on cell-cell adhesions (F_C) increase within the sheet and balance the traction stresses (T) exerted by several rows of cells at the periphery of the sheet. Tractions at opposite margins of the cell sheet are opposed but equal, and the stress is borne between the tractive ends of the aggregate by intercellular adhesions (after Trepat et al., 2009). (D) Mesendoderm, like epithelial cell sheets *in vitro*, migrates via a distributed traction mechanism (Davidson et al., 2002). The traction forces that each cell exerts on the substrate must be balanced by the cell-cell adhesions that keep a cell part of a cohesive tissue. For the leader population of cells, this means that traction force (T_1) equals the force on the posterior cell-cell adhesion (F_{C1}). In follower cells that have cell-cell contacts at both front and back, the difference between forces on the rearward cell-cell adhesion and forces on the forward cell-cell adhesion ($\Delta F_{Row\ x}$) is balanced by traction forces (T_x) (example shown for row 4). In this model, the trailing mesoderm provides resistance to the cell-cell tension being generated by the advancing mesendoderm. Diagrams generated by Gregory Weber.

A Bead pull

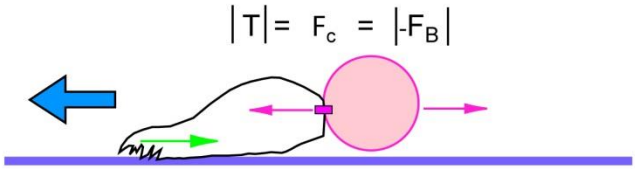

B Cell pair

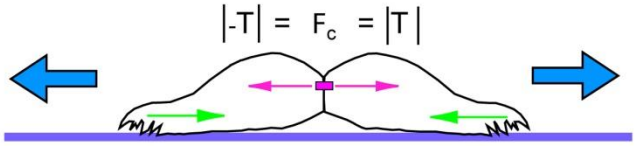

C Cell colony/aggregate

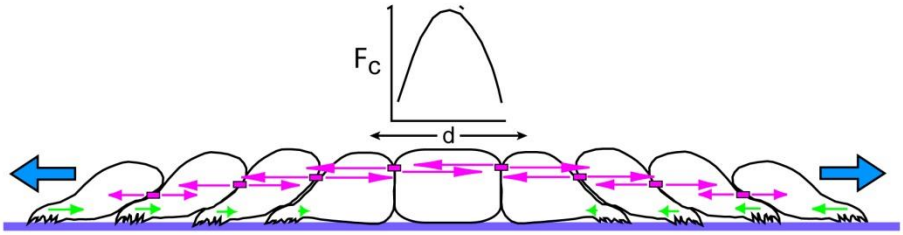

D Tissue *in vivo*

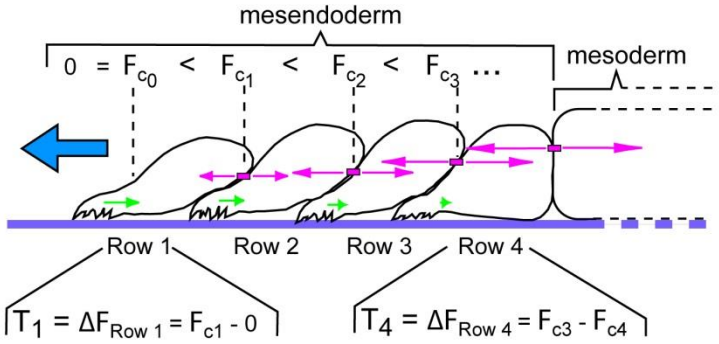

Chapter 3

FAK is required for tension-dependent organization of collective cell movements in *Xenopus* mesendoderm

This chapter is based on work submitted but not yet accepted for publication

3.1 Abstract

Collective cell movements are integral to biological processes such as embryonic development and wound healing and also have a prominent role in some metastatic cancers. In migrating *Xenopus* mesendoderm, traction forces are generated by cells through integrin-based adhesions and tension transmitted across cadherin adhesions. This is accompanied by assembly of a mechanoresponsive cadherin adhesion complex containing keratin intermediate filaments and the catenin-family member plakoglobin. We demonstrate that focal adhesion kinase (FAK), a major component of integrin adhesion complexes, is required for normal morphogenesis at gastrulation, closure of the anterior neural tube, axial elongation and somitogenesis. Depletion of zygotically expressed FAK results in disruption of mesendoderm tissue polarity similar to that observed when expression of keratin or plakoglobin is inhibited. Both individual and collective migrations of mesendoderm cells from FAK depleted embryos are slowed, cell protrusions are disordered, and cell spreading and traction forces are decreased. Additionally, keratin filaments fail to organize at the rear of cells in the tissue and association of plakoglobin with cadherin is diminished. These findings suggest that FAK is required for the tension-dependent assembly of the cadherin adhesion complex that guides collective mesendoderm migration, perhaps by modulating the dynamic balance of substrate traction forces and cell cohesion needed to establish cell polarity.

3.2 Introduction

The morphogenetic events of early embryonic development are comprised of a series of complex cell and tissue movements. These movements include mesendoderm migration, epiboly and convergent extension, each of which relies on tight temporal and spatial control of chemical and mechanical signals over multiple length scales (Keller et al., 2000; Shook and Keller, 2003; Winklbauer, 2009). Developing embryos can be considered morphogenetic machines, generating and responding to a variety of forces including compression, traction, tension, and flow (Wozniak and Chen, 2009). In recent years there has been a growing appreciation for the importance of the mechanical properties of the developing embryo, particularly in the case of tension-dependent signaling through adhesion receptors (Keller, 2012; Schwartz and DeSimone, 2008).

Xenopus mesendoderm provides a striking example of cells migrating cooperatively as a cohesive unit. Mesendoderm cells move collectively at gastrulation across a fibrillar fibronectin (Fn) matrix lining the roof of the blastocoel cavity (Winklbauer, 2009), generating traction forces on the substrate as they proceed (Davidson et al., 2002). Cohesion of the mesendoderm tissue is maintained by cadherin-based cell-cell contacts across which tensile forces are distributed (Davidson et al., 2002; Lee and Gumbiner, 1995). Tension on C-cadherin is sufficient to direct polarized protrusive activity, assembly of junctional complexes containing catenin-family proteins, and rearrangement of the keratin intermediate filament cytoskeleton (Weber et al., 2012). These responses are dependent on adhesion of mesendoderm cells to a Fn substrate. The interaction of cells with the Fn matrix through integrin adhesion complexes is also

essential for other morphogenetic movements during gastrulation, including epiboly and convergent extension (Davidson et al., 2006, 2002; Marsden and DeSimone, 2003, 2001).

Focal adhesion kinase (FAK) is a non-receptor tyrosine kinase that is a central component of integrin adhesion complexes. FAK was originally identified as a highly phosphorylated protein that localizes to integrin adhesion complexes (Hanks et al., 1992; Schaller et al., 1992) and is activated by adhesion to extracellular matrix (ECM) and clustering of integrins (Calalb et al., 1995). The kinase activity of FAK is regulated via phosphorylation of conserved tyrosine residues in response to adhesion, growth factor signaling and other extracellular stimuli (Mitra et al., 2005). Signaling by FAK through downstream effector proteins influences cell survival, growth, adhesion and motility (Parsons, 2003). FAK is essential for the normal adhesion and migration of many cell types both in vitro and in vivo (Ilić et al., 1995; Mitra et al., 2005). Cell culture studies have also demonstrated that FAK expression and activity impact the organization and polarity of cells undergoing directed migration (Gu et al., 1999; Lim et al., 2010; Owen et al., 2007; Schober et al., 2007; Tomar et al., 2009; Wang et al., 2001), however, the mechanism of these actions is not well understood.

While FAK is typically localized to integrin adhesions, it has been reported in some cases to be enriched at cell-cell contacts (Crawford et al., 2003; Playford et al., 2008), suggesting a potential role in integrin-cadherin crosstalk. It has been demonstrated that FAK can influence the stability of cell-cell adhesions indirectly by stimulating expression of E-cadherin (Wang et al., 2004) or by modulating Rho activity (Playford et al., 2008). FAK is also thought to regulate assembly and disassembly of integrin adhesion complexes (Mitra et al., 2005) and to be critical for sensing and

regulating changes in integrin-dependent adhesion forces (Dumbauld et al., 2010; Schober et al., 2007; Wang et al., 2001). Therefore, FAK is likely to be an essential element of an adhesive network that integrates chemical and mechanical cues to regulate collective movements in developing embryos and tissues (Weber et al., 2011).

Several loss-of-function studies have implicated FAK in the normal development of *Xenopus* and other vertebrate models (Crawford et al., 2003; Doherty et al., 2010; Fonar et al., 2011; Furuta et al., 1995; Henry et al., 2001; Ilić et al., 1995; Kragtorp and Miller, 2006; Petridou et al., 2013, 2012; Stylianou and Skourides, 2009). Although most studies have focused on late stages of development, targeted disruption of the FAK gene in mice revealed defects in gastrulation and morphogenesis of mesodermal derivatives (Furuta et al., 1995). FAK knockout embryos show no obvious defects in mesoderm differentiation and are able to initiate gastrulation but they fail to separate the three germ layers and do not survive beyond the end of neurulation. In *Xenopus* embryos, FAK expression increases during gastrulation (Hens and DeSimone, 1995) and is enriched in the mesoderm, mesendoderm, and ectoderm (Petridou et al., 2012). Recent investigations using dominant negative constructs (Kragtorp and Miller, 2006; Petridou et al., 2013; Stylianou and Skourides, 2009) or antisense inhibition of FAK expression (Fonar et al., 2011) have implicated FAK in neurulation, axial elongation and somitogenesis. However, these studies include a number of discrepant observations, perhaps reflecting variations in the approaches and assays used and/or the developmental stages investigated. Although there is some indication that FAK is important for normal migration of mesendoderm cells (Stylianou and Skourides, 2009), little is known about

specific FAK functions at gastrulation or the role of FAK in responding to and regulating mechanical signals during this process.

In the current study we investigate the contributions of FAK to morphogenetic movements in early stage embryos and, in particular, the role of FAK in the tension-dependent organization of collectively migrating mesendoderm. Detailed analyses of single cell behaviors are essential to understanding the emergent properties of a tissue undergoing collective movements, for example, the mediolateral intercalation of cells that drives convergent extension and axial elongation (Keller, 2002). The *Xenopus* embryo is particularly advantageous for analyses of complex behaviors of cells and tissues. Mesendoderm explanted from the embryo recapitulates the in vivo behavior of the developing tissue and is amenable to imaging and manipulation (Davidson et al., 2002). We use explants in combination with biochemical and biophysical techniques to establish the role of FAK in the collective migration of the mesendoderm tissue during gastrulation.

3.3 Materials and Methods

Xenopus embryos and animal caps

Xenopus laevis embryos were obtained using standard methods, cultured in 0.1X Modified Barth's Saline (MBS; Sive, Grainger, & Harland, 2000) and staged according to Neiuwkoop and Faber (1994). Animal cap extension assays were performed as

previously described (Symes and Smith, 1987) except with 5ng/mL recombinant activin (R&D Systems) as the inducing signal.

Morpholinos

The antisense morpholino oligodeoxynucleotide (MO) used to inhibit translation of FAK mRNA was obtained from GeneTools (Philomath, OR). The FAK MO (5'-CAGGTAAGCCGCAGCCATAGCCTTG-3') corresponds to a region that includes the translation start site and is complementary to the published *X. laevis* and *X. tropicalis* cDNA sequences for FAK (NM_001090597.1 and CR926269.1). FAK MO contains 2 mismatches with the putative pseudoallele of FAK in *X. laevis* (NM_001091540.1). The standard GeneTools Control MO sequence (5' CCTCTTACCTCAGTTACAATTTATA 3') was used in all control experiments. Morpholinos were injected into 1 or 2-cell stage embryos at a final concentration of 20-25ng per embryo. Alexa-dextrans (Invitrogen) were co-injected with morpholinos to allow sorting of MO injected embryos (morphants) and to facilitate tracking of cell movements and analyses of cell shape.

RNA constructs

For expression of fluorescently-tagged proteins and of FAK constructs, RNA was transcribed *in vitro* from plasmid DNA templates. The following constructs were used in this study: pCS2 GAP43-EGFP (E. DeRobertis, University of California), pCS107 GFP-moesin (J. Wallingford, University of Texas), EGFP-XCK1(8) (V. Allan, University of Manchester; Clarke and Allan, 2003), pCS2 xFAK (subcloned using fragments B1 and F1 from Hens and Desimone, 1995), and pCS2 cFAK (J.T. Parsons, University of

Virginia). Constructs used for imaging mesendoderm explants (GAP43-EGFP, GFP-moesin, and EGFP-XCK1(8)) were injected into the marginal zone region of one or both dorsal blastomeres at the 4-cell stage with a final concentration of 500-700pg of RNA per embryo. xFAK and cFAK were injected animally into both blastomeres at the 2-cell stage with a final concentration of 200pg of RNA per embryo.

Microscopy and image analysis

Embryos and explants were photographed on a Zeiss SteREO Lumar.V12 stereomicroscope using a Zeiss AxioCam MRm camera. Widefield fluorescence images were collected using a Zeiss AxioObserver inverted microscope, Zeiss PlanApo/20x/0.8 and PlanApo/40x/1.0/Ph3 objectives, Retiga Exi camera (QImaging) and Volocity software (Improvision/PerkinElmer). Structured illumination images were collected on the Zeiss AxioObserver using an OptiGrid system (Qioptic). Confocal images were taken on a Nikon C1 confocal microscope with a Nikon PlanApo/60×/1.40 objective. Image analysis was performed using Volocity, ImageJ (http://rsb.info.nih.gov; National Institutes of Health) and Fiji (http://fiji.sc/Fiji; Schindelin et al., 2012) software packages.

Fixation and immunofluorescence

For imaging of internal structures and staining of animal caps, embryos were fixed in 3.7% formaldehyde overnight at 4°C. Embryos were washed in 1X Tris-HCl buffered saline + 0.1% Tween20 (TBS-tween) and sectioned or bisected on a clay-bottomed dish using a scalpel blade. Bisected gastrulae were imaged using a

stereomicroscope, tailbud sections were imaged using a confocal microscope. Animal caps were cut from fixed stage 11 embryos and incubated overnight at 4°C with an antibody directed against Fn (4H2; Ramos et al., 1996), diluted 1:300 in TBS-tween. Caps were washed in TBS-tween and incubated with an Alexa-tagged secondary antibody (Invitrogen) then washed again and mounted in 50% glycerol/TBS. Caps were imaged by structured illumination as described above.

Mesendoderm explant preparation

Glass coverslips were washed in alkaline-ethanol solution and flamed, and then affixed using epoxy to the bottom of 35mm plastic dishes previously drilled with a lathe. Coverslips were coated with 200µL of 2.5µg/mL bovine plasma Fn (Calbiochem) overnight at 4°C to yield a coating density of 0.39µg/cm^2. Coverslips were blocked with 5% bovine serum albumin then washed with 0.5X MBS. Dorsal marginal zone explants were prepared as previously described (Davidson et al., 2004b, 2002). Explants were placed on the Fn coated coverglass, lightly compressed under glass fragments supported by silicone grease, and allowed 1 hour to adhere and begin to migrate prior to imaging.

Protrusion quantification

Migrating explants expressing GAP43-EGFP were imaged using a Nikon C1 confocal microscope. Six x 1µm z-slices covering the portion of the cells in immediate contact with the Fn substrate were acquired every 30 seconds for 5-10 minutes. The last frame of each time-lapse series was used for all analyses, with the earlier time points used to exclude retracting cell extensions from analysis. Yolk-free areas were designated as

lamellipodial protrusions and fine filopodial extensions were excluded. Protrusion angles were measured using ImageJ as described previously (Weber et al., 2012) and rose diagrams were plotted in OriginPro 7.5 (OriginLab).

Quantification of cell spreading and migration

Mesendoderm tissue was excised from stage 10-11 embryos and dissociated in 1X Ca^{2+}/Mg^{2+}-free MBS for 40 minutes. Cells were then plated at a sub-confluent density into 0.5X MBS on a coverslip coated overnight at 4°C with 0.39µg/cm^2 bovine plasma Fn and blocked with 5% bovine serum albumin. Cells were given 1 hour to attach and spread and were imaged using brightfield or widefield fluorescence illumination on an inverted microscope. For migration studies, Volocity imaging software was used to acquire time-lapse images every 30 seconds for 10-20 minutes. Movements of single cells were tracked using automated identification of cell centroids. Cells in explants were outlined manually but centroid identification and tracking was automated. Average velocity was calculated by dividing final displacement by total elapsed time. Persistence was calculated by dividing total cell path length by final displacement. ImageJ was used for counting spread cells and calculating circularity. Cells were outlined manually and circularity calculated using the Shape Descriptors function.

Quantification of traction forces

Fn-coated, DiI labeled, #12 microfabricated post array detectors (mPADs) were obtained from Christopher Chen's lab (Yang et al., 2011). Before use, mPADs were recoated with bovine plasma Fn overnight, then blocked with 5% bovine serum albumin

and washed with 0.5X MBS. Isolated mesendoderm cells were plated on prepared mPADs at sub-confluent density. A single-plane confocal image was acquired for each attached cell, capturing both the dextran-labeled cells and the top of the fluorescent microposts. Deflection measurements and force calculations were carried out in Matlab (MathWorks) using a program provided by Mark Breckenridge and the Chen lab.

Western blots and co-immunoprecipitation

For Western blotting, 10 embryos per condition were solubilized in 200µL lysis buffer: 100 mM NaCl, 50 mM Tris-HCl pH 7.5, 1% NP-40, 2 mM PMSF (phenylmethylsulphonylfluoride), and protease inhibitor cocktail (Sigma P2714). Phosphatase inhibitors were added as needed for pTyr (1mM sodium orthovanadate and 0.2mM H_2O_2) or pSer/Thr (1mM EDTA, 1mM EGTA, 1mM β-glycerophosphate, and 2.5mM $Na_4P_2O_7$). Yolk was removed by spinning samples for 5 min at 3,000rcf at 4ºC and moving supernatant (sample) to new tube. Protein extracts were diluted in 2X reducing Laemmli buffer (5% β-mercaptoethanol), separated by SDS-PAGE (8 or 10%) then blotted onto nitrocellulose. Blots were probed with antibodies directed against FAK (2A7; Upstate, 05-182, used 1:500) (4.47; Millipore, 05-537, used 1:1000), Fn (4H2; Ramos et al., 1996, used 1:333), $pFAK^{Y397}$ (Life Technologies, 44624G, used 1:1000), $pFAK^{Y861}$ (Life Technologies, 44626G, used 1:1000), pMLC (Sigma, M6068, used 1:1000) or β-actin (Sigma, A3854, used 1:25,000) followed by appropriate HRP-conjugated secondary antibodies and ECL detection.

For co-immunoprecipitation, 10 embryos per condition were solubilized in 100 µL lysis buffer: 100mM NaCl, 50mM Tris-HCl pH 7.5, 1% Triton X-100, 2mM PMSF,

1mM EDTA, 1mM EGTA, 1mM β-glycerophosphate, 2.5mM $Na_4P_2O_7$, 1mM sodium orthovanadate and 0.2mM H_2O_2. Yolk was removed by spinning samples for 5 min at 3,000rcf at 4ºC then moving supernatant (sample) to new tube. 1 embryo equivalent was removed for western blot and the remaining sample brought up to 500µL in lysis buffer. Target proteins were immunoprecipitated overnight at 4ºC using 50µL protein-G agarose beads per sample (Roche) that were pre-incubated with antibodies against plakoglobin (BD Biosciences, 610253, 4µg/500µL) or β-catenin (Sigma, C2206, 4µg/500µL) at 4ºC for 1 hour. The precipitates were diluted in 2X reducing Laemmli buffer and separated by SDS-PAGE (8%) then immunoblotted with an antibody against C-cadherin (6B6, supernatant used 1:6 in TBST; Brieher, 1994; courtesy of Barry Gumbiner).

Statistical analyses

Assembly of data and statistical analyses were performed with Microsoft Excel and PAST (http://folk.uio.no/ohammer/past; Hammer et al., 2001). For pairwise comparisons in which the data were consistent with a Gaussian distribution (as determined by the Shapiro-Wilk test), an F-test was used to check for equal variance followed by either a t-test or an unequal variance t-test. Non-parametric tests were used for datasets in which an assumption of Gaussian distribution was not valid. Levene's test was used to test for equal variance, followed by either a Mann-Whitney test (for datasets consistent with an assumption of equal variance) or a Kolmogorov-Smirnov test (for datasets with unequal variance). Circular statistics were used for analyses of protrusion direction, either Rayleigh's test for randomness of distribution or the Mardia-Watson-Wheeler test for the comparison of two sample groups. Correlation analyses were

performed using Kendall's tau test. In each case where multiple analyses of the same data were performed, the Holm-Bonferroni correction was applied to ensure that the type I error rate was not inflated; this did not affect the significance of any comparisons.

3.4 Results

Focal adhesion kinase is required for normal blastopore closure and axial elongation

We designed an antisense morpholino oligodeoxynucleotide (MO) to block translation of *Xenopus* focal adhesion kinase (FAK) mRNA in order to investigate the functions of FAK in early morphogenetic movements. Although previous studies using different sets of morpholinos targeted to FAK reported no effects on gastrulation (Doherty et al., 2010; Fonar et al., 2011), those sequences were shown to knock down FAK expression by only 30-50% at gastrulation (Doherty et al., 2010; Petridou et al., 2012). Injection of the FAK MO selected for this study effectively inhibited translation of co-injected xFAK transcript (Fig. 3.1A) and resulted in >70% reduction in endogenous FAK protein expression by gastrula stages (Fig. 3.1B, C). Remnant FAK expression in gastrula stage morphant embryos was equivalent to the level of protein present at 1-cell stage (Fig. 3.1D), suggesting that the FAK remaining in morphant gastrulae is due to the persistence of maternal FAK protein translated during oogenesis.

In FAK morphant embryos, the appearance of the dorsal blastopore lip was delayed by about 90 minutes relative to age matched control embryos (data not shown). Closure of the blastopore (Fig. 3.2, arrowheads) was also delayed in FAK morphant

embryos. Significant lethality was evident during gastrulation with approximately 60% of embryos surviving to tailbud stages. The majority of surviving embryos failed to form normal anterior structures including eye anlagen, otic vesicles, and pharyngeal grooves, while other embryos failed to close portions of the neural tube, particularly at the anterior end (Fig. 3.3A-C). Onset of axial elongation was delayed in FAK morphant embryos (Fig. 3.3C, D) and morphants remained truncated along the anterior-posterior axis, relative to controls, with a pronounced curve toward the dorsal aspect (Fig. 3.3E). Additional tailbud stage defects included disorganization of the neural tube, the presence of cells within the neurocoel, lack of vacuolation of cells in the notochord, failure to extend the notochord to the posterior of the embryo, and malformed gut epithelia (Fig. 3.4A-B'). We also noted failures in the alignment and elongation of somites in FAK morphants (Fig. 3.4C, D). None of the FAK morphant embryos survived to tadpole stages. Control embryos were indistinguishable from uninjected embryos throughout development (data not shown). FAK protein levels and the gross morphological phenotypes of FAK morphants were partially rescued by co-expression of the chicken ortholog of FAK (cFAK) (Fig. 3.5A-C). The sequence of cFAK is sufficiently dissimilar to that of xFAK in the region targeted by the MO that its translation is not inhibited by FAK MO. These rescue experiments indicate that the observed phenotypes are due to the specific knockdown of FAK.

Animal cap extension assays were performed to further investigate the defect in axial elongation. When animal cap ectoderm is dissected from control embryos at stage 8, it forms a ball of cells that elongates in response to treatment with the mesoderm inducing factor activin (Symes and Smith, 1987) and has thus been used as a model of

convergence and extension movements (e.g. Ninomiya et al., 2004). Animal caps obtained from FAK morphant embryos did not respond to activin treatment by extending, rather they remained globular and formed multiple small protuberances (Fig. 3.6A, B), indicating that normal FAK expression is required for these movements.

Phenotypes of FAK morphant embryos were similar to those of Fn morphants (Davidson et al., 2006) which in turn resemble embryos unable to deposit Fn matrix following injection of function blocking antibodies (Marsden and DeSimone, 2003). However, Fn protein levels and assembly of Fn matrix on the blastocoel roof appeared normal in FAK morphant embryos (Fig. 3.7A-C). A previous study found that pFAK^{Y397} is highly enriched in the animal cap cells that assemble the Fn matrix (Petridou et al., 2012). Phosphorylation of FAK at the auto-phosphorylation site Tyr397 is commonly used as a readout for FAK kinase activity (Schlaepfer et al., 1999). Interestingly, we found that the FAK protein that remains in FAK morphant embryos was phosphorylated on Tyr397 at only a slightly lower level than non-morphant controls (Fig. 3.7D). In contrast, FAK phosphorylated by Src at Tyr861 is normally enriched in mesoderm and mesendoderm (Petridou et al., 2012) and was greatly attenuated in FAK morphant embryos (Fig. 3.7E). These data suggest that the residual level of pFAK^{Y397} in morphant embryos (Fig. 3.7D) is sufficient to support assembly of Fn matrix along the blastocoel roof (Fig. 3.7B) where pFAK^{Y397} is normally enriched (Petridou et al., 2012). Therefore, it is unlikely that the defects in gastrulation movements observed in FAK morphants are due to lack of Fn matrix assembly along the blastocoel roof.

Mesendoderm from FAK morphant embryos migrates more slowly and with less persistence

Bisection of fixed embryos at various time points throughout gastrulation was used to reveal the morphology and progression of mesendoderm tissue in vivo. In control embryos, mesendoderm migration begins with the formation of a ridge of tissue on the dorsal side of the embryo at the margin between involuting mesoderm and the endodermal mass (Fig. 3.8A, Control MO, red arrowhead). Ventral and lateral mesendoderm cells follow suit, forming a ring or cup of tissue moving cohesively toward the animal pole (Davidson et al., 2002). In contrast, formation of the dorsal mesendoderm ridge was delayed in FAK morphants, with both dorsal and ventral tissue simultaneously initiating translocation across the blastocoel roof (Fig. 3.8A, FAK MO, red arrowheads). The progression of the mesendoderm tissue toward the animal pole of FAK morphant embryos lagged behind that of Control MO injected embryos by 1.5-2 hours and the leading edge of the tissue was uneven. The appearance and elongation of Brachet's cleft (Fig. 3.8A, arrow, Bc) was delayed in FAK morphants, consistent with a delay in advancement of the mesendoderm tissue. Thinning of the marginal tissue was also disrupted in FAK morphants (Fig. 3.8A, brackets in middle panels) but there was no effect on radial intercalation in the blastocoel roof (Fig. 3.8A, arrow, bcr), which appeared to thin normally.

To better observe the behavior of cells within the mesendoderm we utilized explants comprised of tissue excised from the dorsal marginal region of the embryo. These explants were placed in a simple salt solution (i.e. MBS) on Fn coated coverslips, a technique commonly used to recapitulate "ex vivo" the organization and behavior of

mesendoderm tissue as it would normally occur in the intact embryo (Davidson et al., 2004b, 2002). We found that the average velocity (displacement/time) of mesendoderm cells in explants taken from FAK morphant embryos was reduced, resulting in a decreased rate of tissue advancement relative to controls (Fig. 3.8B). Similarly, single mesendoderm cells from dissociated FAK morphant tissue had a lower average velocity than control cells. Both single cells and explanted tissues from FAK morphant embryos moved less persistently than controls (Fig. 3.8C). Single mesendoderm cells from control embryos moved in apparently random directions and with low persistence, calculated as displacement divided by path length. Cells in explants from control embryos migrated collectively and with a high degree of directionality and persistence. However, no significant increase in persistence of cells was observed in tissue explanted from FAK morphant embryos compared with single FAK morphant cells. These data indicate that FAK is required for persistent migration of mesendoderm cells and, in contrast to control cells, the influence of neighboring cells is not sufficient for establishment of persistent migration. The meandering behavior exhibited by FAK morphant cells likely contributes to the decreased rate of mesendoderm tissue advancement observed in both explants and intact embryos.

FAK contributes to regulation of protrusion number and protrusive polarity

We analyzed protrusive activity in mesendoderm explants expressing membrane localized EGFP in order to determine whether the meandering behavior of FAK morphant cells reflects changes in directional polarity during collective migration. Yolk free extensions from the cell body were designated as protrusions and the directions and

total numbers of these protrusions were measured for cells in the first four rows of the migrating explants. Retracting edges, identified by time-lapse imaging, and fine filopodia-like extensions were excluded from the quantification. Most cells within control explants displayed monopolar protrusive behavior, extending one or two lamellipodial protrusions toward the contiguous leading edge of the migrating tissue (Fig. 3.9A). Cells in tissue explanted from FAK morphant embryos frequently extended protrusions in directions other than the expected direction of tissue migration, in addition to protrusions in the expected direction (Fig. 3.9B). Uneven progression of the leading edge was also evident in FAK morphant explants. To determine directionality, the angle of each protrusion was measured relative to a line running through the cell centroid and parallel to the direction of migration. The predicted direction of tissue advancement was defined as 180°. Angles from the entire population of control or FAK morphant cells were binned into twelve 30° increments and the percent of angles in each bin calculated. As previously reported (Weber et al., 2012), cells in control explants extend the majority of their protrusions toward 180° (±15°) with no protrusions extended greater than 90° away from the direction of tissue migration (Fig. 3.9C). The directional distribution of protrusions in FAK morphant explants was significantly broadened, with a small but significant number of protrusions extending more than 90° from the expected direction of migration (90°-270°). Quantification of protrusion number in explants revealed that control cells extended an average of 1.71 protrusions per cell while FAK morphant cells had a significantly higher average of 1.96 protrusions per cell (Fig. 3.9D).

Additional analyses of protrusive behavior were performed by grouping cells according to distribution of their protrusions. In FAK morphant explants, we observed a

significant decrease in the percent of cells only extending protrusions within 45° of the expected direction of tissue migration (set as 180º) (Fig. 3.9E). 9% of FAK morphant cells extended protrusions only in the direction opposite the leading edge, quantified as any direction greater than 75° off axis (105º-255º) (Fig. 3.9F). This is in contrast to control cells that did not extend any protrusions toward the rear of the explant, with only two protrusions near 90° (out of a total of 100 counted protrusions). 29% of cells in FAK morphant explants had off-axis protrusions (105º-255º) in addition to at least one protrusion in the predicted direction (225º-135º), a significant difference from the protrusive behavior observed in control cells (Fig. 3.9G). Taken together with the increase in number of protrusions per cell, these data suggest that FAK is important for limiting off-axis protrusions from mesendoderm cells in the intact tissue.

Actin organization is altered in FAK morphants

While quantifying the number and polarity of protrusions extended by FAK morphant mesendoderm cells we noted a marked difference in the morphology of these protrusions. In FAK morphant explants, an abundance of filopodia-like extensions were evident in addition to a significant increase in the average number of lamellipodial protrusions per cell. Because actin organization is integral to protrusion morphology, we investigated whether changes in protrusions were accompanied by changes in actin organization. Expression of a GFP tagged version of the actin binding protein moesin was used to visualize the actin filament network in control and FAK morphant cells. Cells in control explants extended broad lamellipodial protrusions across the leading edge with smaller lamellipodial extensions in the cells in following rows (Fig. 3.10A, green

arrowheads). These lamellipodia were filled with a dense meshwork of actin amongst fine bundles of filaments. While broad lamellipodia were occasionally observed in FAK morphant explants, these cells typically had narrower and more dynamic protrusions which contained actin spikes and generally lacked the dense actin network present in protrusions of control cells (Fig. 3.10B, yellow arrowheads). This finding suggests that FAK is important for the organization of the lamellipodia, or perhaps the dynamics of the actin network in protrusions.

Actin filaments in the body of control cells were typically distributed around the cell cortex and organized in a fine mesh throughout the cytoplasm, with slight enrichment at the midpoint or rear of some cells (Fig. 3.10C, green arrowheads). A cortical distribution of actin filaments was observed in the body of most cells in FAK morphant explants; however, there was an increased prevalence of stress fibers spanning the cells (Fig. 3.10D, yellow arrowheads). FAK morphant cells were also frequently observed to have numerous filopodia-like protrusions along their lateral edges where they contact neighboring cells, perhaps indicative of changes in cell-cell adhesion (Fig. 3.10E). Although actin organization was abnormal in FAK morphant cells no change was detected in phosphorylation of myosin light chain, suggesting that actomyosin contractility was unaltered (Fig. 3.11A, B). In summary, actin organization in the cell bodies and protrusions of cells in FAK morphant explants differed significantly from controls. FAK morphant cells retained the ability to extend protrusions and form cell-cell junctions, albeit in abnormal forms in both cases.

FAK is required for organization of the keratin filament network

Expression and organization of keratin is integral to protrusive polarity in collectively migrating mesendoderm cells (Weber et al., 2012). Because cell polarity was disrupted in FAK morphant mesendoderm tissue we investigated whether keratin organization might also be disrupted in these cells. Expression of EGFP labeled keratin (EGFP-XCK1 (8)) was used to visualize the organization of the keratin filament network in live FAK morphant explants. In control tissues, keratin filaments are typically most prominent at the rear of each cell where they often form a basket-like arrangement (Fig. 3.12A, green arrowheads). In embryos and in mature mesendoderm explants (those that have been migrating for one hour or more), keratin filaments also form a cable along leading edge cells, just behind and dorsal to the lamellipodia as well as between cells (Fig. 3.12B, green arrowheads). This organization was severely disrupted in explants from FAK morphant embryos; filaments were distributed throughout each cell and often biased toward the front of leading edge cells (Fig. 3.12C, yellow arrowheads). Furthermore, the cable-like connections behind the lamellipodia and between cells were absent under these conditions (Fig. 3.12D, yellow arrowheads). The degree of disrupted filament organization in each cell appeared to be correlated with alterations in cell spreading and polarity. In well-spread cells with forward facing lamellipodia we observed rearward, basket-like localization of keratin filaments, while in less well polarized cells we observed random localization or an increase in filaments at the cell front. Many cells with round morphology were evident in FAK morphant explants (Fig. 3.12D, dashed yellow line). The keratin filaments in these cells were organized in a wagon-wheel arrangement similar to that observed in pairs of cells plated

on poly-L-lysine substrates that do not support generation of traction forces (Weber et al., 2012). Both the rearward localization and cabling of keratin filaments were rescued by co-expression of cFAK (Fig. 3.12E, F, green arrowheads). These findings indicate that FAK is essential for organization of the keratin filament network in collectively migrating mesendoderm cells.

Spreading and cell traction on fibronectin is reduced in FAK morphants

FAK morphant cells in intact explants appeared less well spread and less adherent to Fn than cells in control explants. Furthermore, the wagon-wheel arrangement of keratin filaments observed both in cells in FAK morphant explants (Fig. 3.12D) and in cell groups on poly-L-lysine (Weber et al., 2012) suggested that generation of traction force on the substrate might be affected by loss of FAK. To quantify the effects of diminished FAK expression on cell spreading we plated isolated mesendoderm cells from both control and FAK morphant embryos on Fn coated coverglass (Fig. 3.13A) and tallied the percent of cells spread (Fig. 3.13B). FAK morphant mesendoderm cells attached to the substrate but were about 30% less likely to be fully spread.

We then measured traction forces generated by isolated control and FAK morphant mesendoderm cells on Fn coated micropost arrays (Yang et al., 2011). FAK morphant cells generated significantly less total traction force per cell, but there was no significant change in the force per post (Fig. 3.13C, D). Thus, there is less total traction being applied by FAK morphant cells because they have proportionally less contact with the substrate. Calculation of the circularity of control and FAK morphant cells using the same images as those from which traction data were gleaned revealed a significant

increase in roundness in FAK morphant cells, indicating a decrease in the degree of spreading (Fig. 3.14A, B). Indeed, the two measures were strongly correlated; well-spread cells tended to exert more force on the Fn substrate than poorly-spread cells (Fig. 3.14C, D). There was a statistically significant correlation between circularity and total cell force for both control cells and FAK morphant cells (Control MO; $p = 0.038$, FAK MO: $p = 0.0009$). We conclude that FAK is a critical component of the traction machinery in mesendoderm cells, and disruption of FAK function leads to alterations in the mechanical properties and morphology of mesendoderm tissue.

FAK is important for association of plakoglobin with cadherin

Previous work in this system has demonstrated the importance of anisotropic tension in the recruitment of plakoglobin (also known as γ-catenin) and keratin to cell-cell contacts (Weber et al., 2012). In light of these findings, and our observations of diminished traction and disrupted organization of keratin filaments in FAK morphant cells, we hypothesized that loss of FAK would have a negative effect on assembly of the plakoglobin-containing adhesion complex. We investigated the assembly of these complexes, specifically the linkage between C-cadherin and plakoglobin, by performing co-immunoprecipitation analyses. We used association of C-cadherin with β-catenin as a control for changes in assembly of adherens junctions. During early gastrulation (stage 10), when the mesendoderm is just beginning to migrate, there was a reduction in the association of plakoglobin with C-cadherin in FAK morphant embryos relative to controls (Fig. 3.15A, B). However, at the end of gastrulation (stage 12) there was no longer a significant difference in the association of plakoglobin with C-cadherin in FAK

morphant embryos relative to controls. Loss of FAK expression had no effect on the association of β-catenin with C-cadherin at either time point (Fig. 3.15A, C). These results are consistent with a role for FAK in regulation of the tension-dependent recruitment of plakoglobin to cell-cell junctions during the establishment of polarity in migrating mesendoderm.

3.5 Discussion

This study supports a critical role for FAK in the morphogenetic movements of early development including mesendoderm migration, neural tube closure and axial elongation. Furthermore, we show that FAK is required for normal subcellular organization of keratin intermediate filaments and for assembly of a cadherin-plakoglobin adhesion complex. Both of these events were reported previously to be dependent on cell-cell tension and essential for guidance of collective mesendoderm migration (Weber et al., 2012). The data presented here suggest that FAK is essential for development of tension in the mesendoderm and therefore acts upstream of keratin and plakoglobin to guide migratory polarity of the tissue in vivo.

FAK function in vertebrate development

A requirement for FAK in the normal development of mesodermal derivatives, such as the notochord and somites, is shared among several vertebrate species including mouse, zebrafish, and *Xenopus* (Crawford et al., 2003; Furuta et al., 1995; Henry et al., 2001; Hens and DeSimone, 1995; Kragtorp and Miller, 2006). We report here that FAK

is also essential for gastrulation movements in *Xenopus*, particularly for the coordination of collective migration of mesendoderm. This finding is consistent with a study using the dominant negative FAK splice variant FRNK (FAK-related non-kinase) in which blastopore closure and mesendoderm migration are both slowed or disrupted (Stylianou and Skourides, 2009), although underlying cell behaviors were not reported. Evidence indicates that FAK also plays a critical role in closure of the neural tube and in axial elongation, but with some variations noted in the presence and degree of phenotypes resulting from different experimental perturbations. For example, injection with FAK MO (Fig. 3.3C and Fonar et al., 2011) or transcript encoding FRNK (Stylianou and Skourides, 2009) leads to defects in closure of the neural tube. However, injection of the dominant negative FAK construct FF, which lacks the kinase domain and is thought to act by displacing endogenous FAK, has no apparent effect on neural tube closure (Petridou et al., 2013). Interestingly, injection of FAK MO (Fig. 3.3E and Fonar et al., 2011) or expression of FF (Petridou et al., 2013) severely disrupts axial elongation, but FRNK expression has no notable effect on embryo length (Stylianou and Skourides, 2009). Despite some differences, these data together indicate that normal zygotic FAK expression is important for the morphogenetic events of gastrulation, neurulation, axial elongation and somitogenesis.

FAK morphant phenotypes are not due to disruption of Fn matrix

The defects in mesoderm development evident in FAK null mice (Furuta et al., 1995) are similar to both Fn (Georges-Labouesse et al., 1996) and integrin α5 nulls (Yang et al., 1993), suggesting a general role for cell-ECM interactions in this tissue. Indeed, loss of

Fn in zebrafish (Jülich et al., 2005) or *Xenopus* (Davidson et al., 2006) leads to defects in blastopore closure, axial elongation and somitogenesis that are similar to those in FAK morphant embryos. The assembly of the Fn matrix in *Xenopus* embryos has been reported to regulate the rate of mesendoderm migration (Rozario et al., 2009). Could loss of Fn matrix account for the defects observed in the migration of mesendoderm in FAK morphant embryos? Previous work using FAK null cells in culture (Ilić et al., 2004) or expression of exogenous FRNK in *Xenopus* (Kragtorp and Miller, 2006) suggested that FAK may be an important factor in the assembly of Fn fibrils. Moreover, the progressive assembly of matrix during *Xenopus* gastrulation is dependent on tissue tension in the ectodermal cells of the blastocoel roof (Dzamba et al., 2009), so any changes in cell and tissue stresses at this stage might be expected to alter matrix assembly. However, we find no disruption of Fn matrix in FAK morphant embryos (Fig. 3.7B), nor was any significant disruption reported previously in embryos injected with FF (Petridou et al., 2013). We conclude that the fraction of $pFAK^{Y397}$ present in FAK morphant embryos (Fig. 3.7D) is sufficient for assembly of Fn matrix on the blastocoel roof. These results suggest that defects in the migration of FAK deficient mesendoderm do not result from a reduction in Fn matrix assembly on the blastocoel roof. Thus, they are likely to be a function of "tissue autonomous" changes in migratory capacity of the mesendoderm.

FAK is necessary for directed migration and protrusive activity

Our findings demonstrate that FAK is critical for directional migration of mesendoderm cells both in isolation and in intact tissue. Single FAK morphant mesendoderm cells migrate more slowly and erratically than control cells and cell

spreading is decreased (Fig. 3.8, Fig. 3.13). The persistence of collectively migrating FAK morphant cells is also decreased and protrusive polarity severely disrupted. Furthermore, maintenance of cell-cell contacts and tissue geometry are alone not sufficient to generate directed migration in the absence of FAK. Control cells in explanted tissue have significantly greater directional persistence than isolated cells. In contrast, FAK morphant cells do not exhibit an increase in directional persistence in an explant. The decreased persistence of FAK morphant cells may help explain the reduced migration rate reported following perturbation of FAK in *Xenopus* mesendoderm and other cell types (Petridou et al., 2013; Schlaepfer et al., 2004; Stylianou and Skourides, 2009).

Decreased directional persistence could be explained by changes in the stability of protrusions. We observed an increase in the number of lamellipodial protrusions in FAK morphant mesendoderm (Fig. 3.9D), consistent with previous observations of cultured fibroblasts and macrophages (Owen et al., 2007; Tilghman et al., 2005). However, the broad lamellipodia evident in control mesendoderm cells are rarely observed in FAK morphant cells (Fig. 3.9A, B) or FAK null fibroblasts (Tilghman et al., 2005). Instead, FAK morphant cells exhibit multiple smaller protrusions with aberrant morphologies, suggesting that FAK is important for stabilization of broad lamellipodial protrusions at the leading edge of migrating cells. FAK has also been shown to facilitate the turnover of integrin adhesion complexes, and this is thought to be a key function of FAK in cell migration (Ilić et al., 1995; Owen et al., 2007; Ren et al., 2000; Schober et al., 2007). The off-axis protrusions observed in FAK morphant mesendoderm could therefore be the result of failure to disassemble adhesions and retract mis-directed protrusions. Thus,

FAK may be acting at the leading edge to stabilize polarized protrusions and also at the lateral and trailing edges to tune polarity by facilitating turnover of adhesions in off-axis protrusions.

In addition to the increase in lamellipodial protrusions, we observed a marked increase in filopodia-like protrusions in FAK morphant tissues. The general morphology of these filopodial protrusions are similar to those observed in other FAK null cells (Ilić et al., 1995; Tilghman et al., 2005). The abundance of filopodia-like protrusions or microspikes is reminiscent of changes in Cdc42 signaling (Hall, 1998). It is well known that Rho family GTPases, including Rho, Rac, and Cdc42, are integral to regulation of adhesion and migration (Nobes and Hall, 1999). Both increases and decreases in Rho, Rac, or Cdc42 activity can have a dramatic impact on actin organization and the morphology of protrusions, and there have been several studies linking FAK to modulation of Rho GTPase signaling (Chang et al., 2007; Chen et al., 2002; Fabry et al., 2011; Lim et al., 2008; Myers et al., 2012; Ren et al., 2000; Tomar et al., 2009). Thus, modulation of Rho, Rac, or Cdc42 activity is a potential mechanism by which FAK may regulate protrusive morphology in the mesendoderm tissue and perhaps actin organization as well.

Reduced traction and spreading of FAK morphant cells disrupts actin and keratin organization

Assembly and organization of the keratin filament network are thought to be dependent on actin (Kölsch et al., 2009; Wöll et al., 2005). Therefore, the changes in keratin organization in FAK morphant cells could be a result of alterations in the actin

cytoskeleton. In control cells, actin filaments fill lamellipodial protrusions and form a fine cortical mesh while keratin filaments are biased toward the rear of each cell. FAK morphant cells have an increase in actin microspikes in protrusions and the appearance of actin stress fibers throughout the cell body. We also observe dense cortical actin bundles and other aberrant actin structures in rounded FAK morphant cells (data not shown), similar to the typical phenotype of FAK null fibroblasts (Fabry et al., 2011; Ilić et al., 1995; Serrels et al., 2007; Sieg et al., 1999). However, we find that in spread and polarized cells, a minority of the FAK morphant population, there is a more modest change in actin organization (Fig. 3.10). This suggests that large changes in actin organization often noted in the absence of FAK are not directly associated with cell polarity but more likely are related to cell spreading. In FAK morphant cells, changes in actin are accompanied by a seemingly random organization of keratin filaments in each cell and the absence of keratin cabling along the leading edge of the tissue. Disruptions of the actin filament network are less severe than those of the keratin network and thus unlikely to account for the major alterations observed in keratin filament organization.

How might FAK affect the organization of keratin filaments, if not via changes in the actin network? We noted a marked similarity between the appearance of keratin filaments in many of the FAK morphant cells and in control cells plated on poly-L-lysine. Mesendoderm cells attach tightly to poly-L-lysine substrates but fail to generate significant traction forces under these conditions. The cells do not spread and the keratin filaments exhibit a “wagon wheel” arrangement (Weber et al., 2012). This same arrangement is observed in FAK morphant cells, which also spread poorly (Fig. 3.12C and 3.13A) and exert less traction force on Fn substrates (Fig. 3.13C). The decrease in

traction force per cell is correlated with reduced spreading (Fig. 3.14) as previously reported for FAK null fibroblasts (Fabry et al., 2011). Both traction on Fn and tugging forces on cadherin adhesions contribute to the normal spatial organization of keratin filaments within mesendoderm cells (Weber et al., 2012). In addition integrin α5β1 is required for the development of anisotropic tension in the mesendoderm (Davidson et al., 2002). Therefore, FAK may be regulating keratin organization indirectly by facilitating the generation of the traction forces on Fn required for spreading and for development of anisotropic tension by integrins within the migrating tissue.

We reported previously that coordinated protrusive activity in the mesendoderm is dependent on tugging forces on cadherins, recruitment of plakoglobin (γ-catenin), and reorganization of keratin filaments (Weber et al., 2012). Interestingly, the disruption of tissue polarity in FAK morphant embryos is similar to that observed in keratin morphants. However, both keratin organization and tissue polarity are more severely affected by depletion of FAK than by loss of plakoglobin. Protrusive polarity is significantly disrupted in both leading and following cells in FAK morphant tissue, in contrast to the subtle changes in directional distribution of protrusions in plakoglobin morphant tissue. Moreover, plakoglobin morphant mesendoderm maintains a continuous leading edge with keratin cables running perpendicular to the direction of travel while FAK morphant mesendoderm has a discontinuous leading edge and lacks these cables. Loss of directionally persistent migration could cause the discontinuity of the leading edge observed in both in FAK morphant mesendoderm (Fig. 3.9B) and in FAK null fibroblasts (Tilghman et al., 2005) and may result in an inability to form trans-cellular cabling. If supra-cellular organization of keratin or other cytoskeletal elements serves to

maintain or reinforce tissue polarity, the lack of such structures in FAK morphants would account for the increased disruption of tissue polarity relative to plakoglobin morphants, particularly at the leading edge.

FAK is required for efficient assembly of a mechanoresponsive cadherin adhesion complex

One intriguing finding is the decreased association of plakoglobin with C-cadherin in FAK morphant embryos during a stage of development when establishment of tissue polarity is occurring (Fig. 3.15). One possible explanation for the effect of FAK on plakoglobin-cadherin association is a change in cellular contractility. FAK is thought to modulate actomyosin contractility via Rho and Rho-kinase (Fabry et al., 2011; Playford et al., 2008; Ren et al., 2000; Schober et al., 2007). Changes in cellular contractility downstream of Rho family GTPases affect stability of cadherin adhesions (Braga and Yap, 2005; Liu et al., 2010; Playford et al., 2008; Yamada and Nelson, 2007), traction forces on Fn (Beningo et al., 2006), and organization of the actin cytoskeleton (Burridge and Wennerberg, 2004; Hall, 1998). FAK is also thought to be required for altering the dynamics and force generation of integrin adhesion complexes in response to changes in contractility (Dumbauld et al., 2010; Schober et al., 2007). We observed no change in phosphorylation of myosin light chain in FAK morphants, but it is possible that FAK is regulating cellular contractility or responses to tension via another signaling pathway.

What other factors might explain the role of FAK in assembly of the mechanoresponsive cadherin complex? We noted a decrease in association of plakoglobin with C-cadherin that is dependent on developmental stage; by the end of

gastrulation there is no difference between FAK morphants and controls (Fig. 3.15). Therefore, the decrease in association of plakoglobin with C-cadherin might be explained by the delay observed in development of FAK morphant embryos. However, FAK knockdown has no effect on association of β-catenin with C-cadherin, an interaction previously reported to increase at the onset of gastrulation (Schneider et al., 1993). This indicates that general delays in development are unlikely to be the cause of any differences in plakoglobin-cadherin association. We speculate that delays and defects in FAK morphant mesendoderm migration per se reflect a decrease in anisotropic mechanical stimulation of cadherin adhesions and thereby inefficient assembly of the cadherin-plakoglobin-keratin complex that is required for coordination of migration (Weber et al., 2012).

In summary, these data suggest that FAK has an essential role in governing the organization of morphogenetic movements during early development. FAK may be working to maintain a balance of forces between substrate tractions (via integrins) and cell-cell cohesion (via cadherins) that is critical for self-organization and directionality of migrating mesendoderm. Loss of this organization in vivo results in defects in the development of the anterior and dorsal structures to which the mesendoderm contributes. It is clear that coordination of collective cell migration depends on both cadherin and integrin adhesion complexes, though the specific mechanisms of interaction between these adhesions have yet to be fully elucidated. A key area of interest is the mechanism by which signals are transduced between the mechanoresponsive cadherin adhesions at the rear and lateral sides of the cell and the integrin-based adhesions at the front of the cell. How mechanical signals are transduced by cells also remains poorly understood.

Recent work suggests this could occur through force-induced conformational changes (Johnson et al., 2007; Sawada et al., 2006), particularly in proteins associated with adhesions (e.g. Yonemura et al., 2010). Emerging methodologies (Borghi et al., 2012; Eyckmans et al., 2011; Grashoff et al., 2010; Legant et al., 2010; Machacek et al., 2009) will allow these questions to be addressed with the high degree of spatial and temporal resolution required for understanding of the complex and dynamic signals likely to be involved. Further studies will be needed to enhance our understanding of the adhesive networks that transduce chemical and mechanical signals important in the collective cell movements essential for development.

Figure 3.1

FAK morpholino knocks down FAK protein expression in *X. laevis*. (A) Quantification of expression of endogenous and exogenous (*Xenopus* FAK (xFAK), 200pg injected transcript) FAK protein, β-actin was used as a loading control (N=3). Data are mean ± SEM. (B) Representative Western blot of FAK expression levels in gastrula stage embryos injected with 25ng of Control or FAK morpholino (MO), β-actin was used as a loading control. (C) Quantification of FAK protein levels in gastrula stage embryos, normalized to β-actin and shown relative to control embryos (N=10). Data are mean ± SEM. (D) Quantification of FAK expression at gastrula stage in FAK morphant embryos, compared with the amount present in control embryos at 1-cell, 8-cell, gastrula and neurula stages. FAK expression was normalized to β-actin and shown relative to expression in control embryos at gastrula stage (N=3). Data are mean ± SEM.

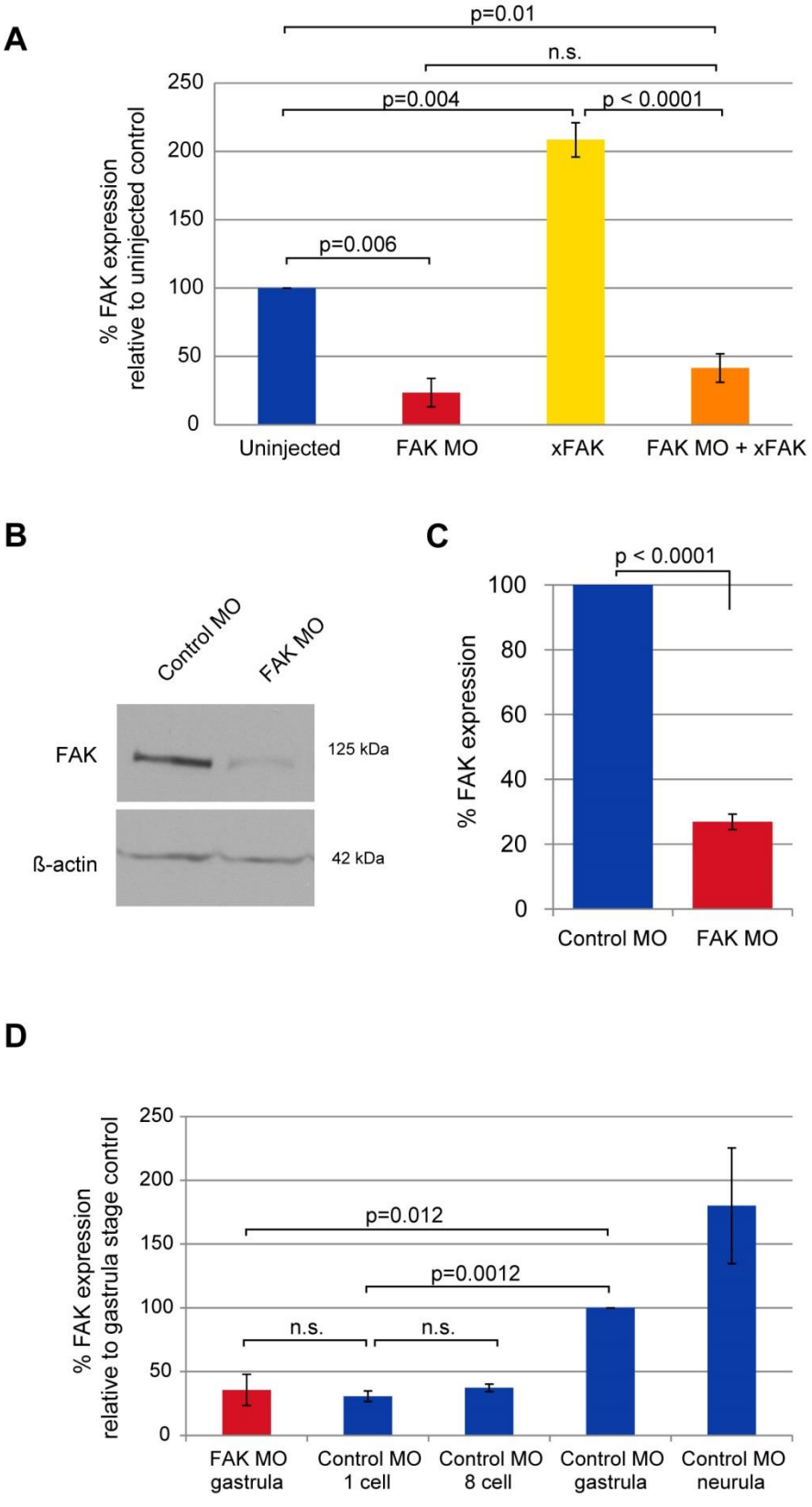
A
p=0.01
n.s.
p=0.004
p < 0.0001
p=0.006
% FAK expression relative to uninjected control
250
200
150
100
50
0
Uninjected
FAK MO
xFAK
FAK MO + xFAK
B
Control MO
FAK MO
FAK
125 kDa
ß-actin
42 kDa
C
p < 0.0001
% FAK expression
100
80
60
40
20
0
Control MO
FAK MO
D
% FAK expression relative to gastrula stage control
250
200
150
100
50
0
p=0.012
p=0.0012
n.s.
n.s.
FAK MO gastrula
Control MO 1 cell
Control MO 8 cell
Control MO gastrula
Control MO neurula

Figure 3.2

FAK knockdown inhibits blastopore closure. Time matched views of representative Control and FAK MO injected embryos. Vegetal views, arrowheads indicate blastopore lip, red arrowhead=dorsal. Stages given for control embryos.

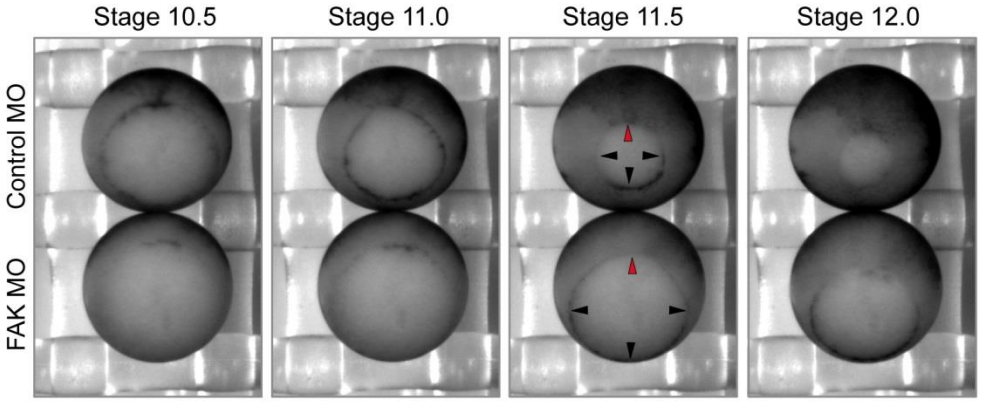
Stage 10.5
Stage 11.0
Stage 11.5
Stage 12.0
Control MO
FAK MO

Figure 3.3

FAK morphants have defects in neurulation, formation of anterior structures and axial elongation. (A, B) Representative images of collapsed 10μm z-stacks through transverse sections of fixed tailbud stage embryos injected with Control or FAK MO and fluorescent dextrans to show cell shape (blue), yolk auto-fluorescence also captured for contrast (green). (A) Anterior section of control tailbud, arrows denote eye anlagen (e), diencephalon (d) and foregut (f). (B) Anterior section of FAK morphant tailbud. Arrows denote lack of clear eye anlagen (e) and poor organization of the neuro- and gastro-epithelia (d, e). (C) Dorso-anterior view at late neurula (stage 22, red dashed line marks open neural tube). (D) Dorso-lateral view at early tailbud (stage 25). (E) Lateral view at late tailbud (stage 32). Stages given for control embryos, a=anterior, p=posterior.

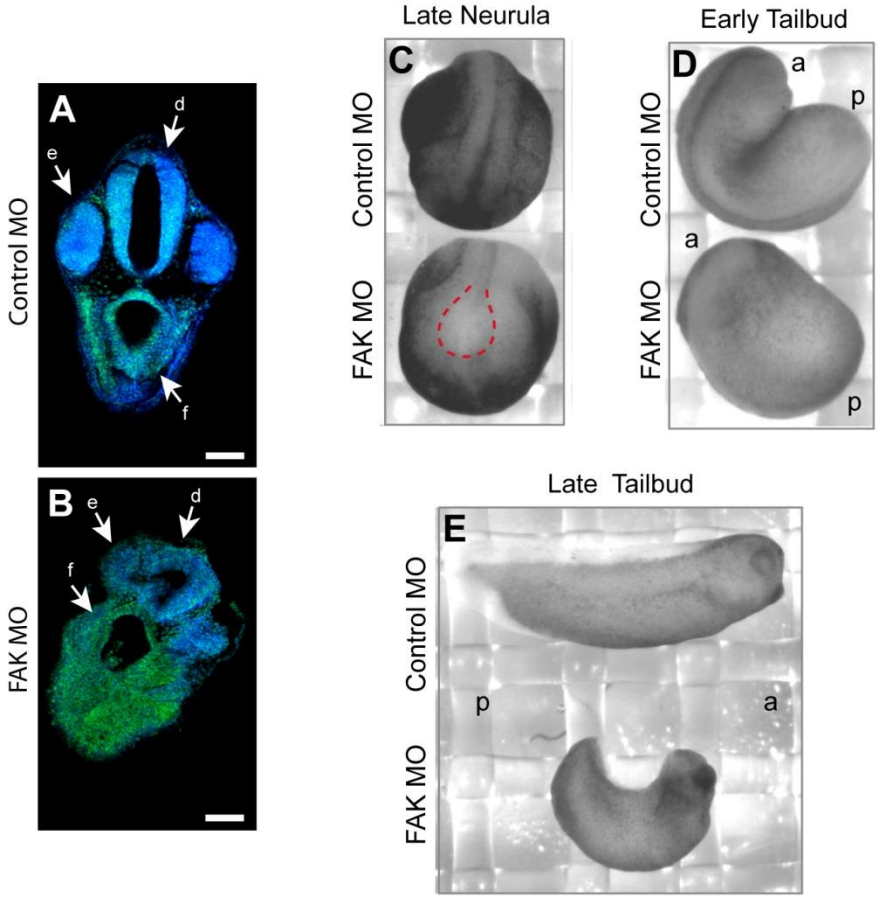
Late Neurula
Early Tailbud
Late Tailbud
Control MO
FAK MO
A
B
C
D
E
d
e
f
a
p

Figure 3.4

FAK morphants have defects in notochord, gut and somites. (A-B') Representative images of collapsed 10µm z-stacks through transverse sections of fixed tailbud stage embryos injected with Control or FAK MO and fluorescent dextrans to show cell shape (blue), yolk auto-fluorescence also captured for contrast (green). (A, A') Mid-body (A) and posterior (A') sections of control tailbuds, arrows denote neural tube (nt), somites (s), notochord (n), midgut (m) and hindgut (h). (B, B') Mid-body (B) and posterior (B') sections of FAK morphant tailbuds, arrows denote cell-filled neural tube (nt), poorly defined somites (s), shortened and un-vacuolated notochord(n), and disorganization of the yolk rich endoderm cells fated to give rise to the gut (m, h). (C, D) Representative collapsed 10µm z-stacks images of sagittal sections of control (C) and FAK morphant (D) tailbud stage embryos, co-injected with fluorescent dextrans to label cells and show structure of the somites. Anterior is at the top of both images. Scale bars = 100µm.

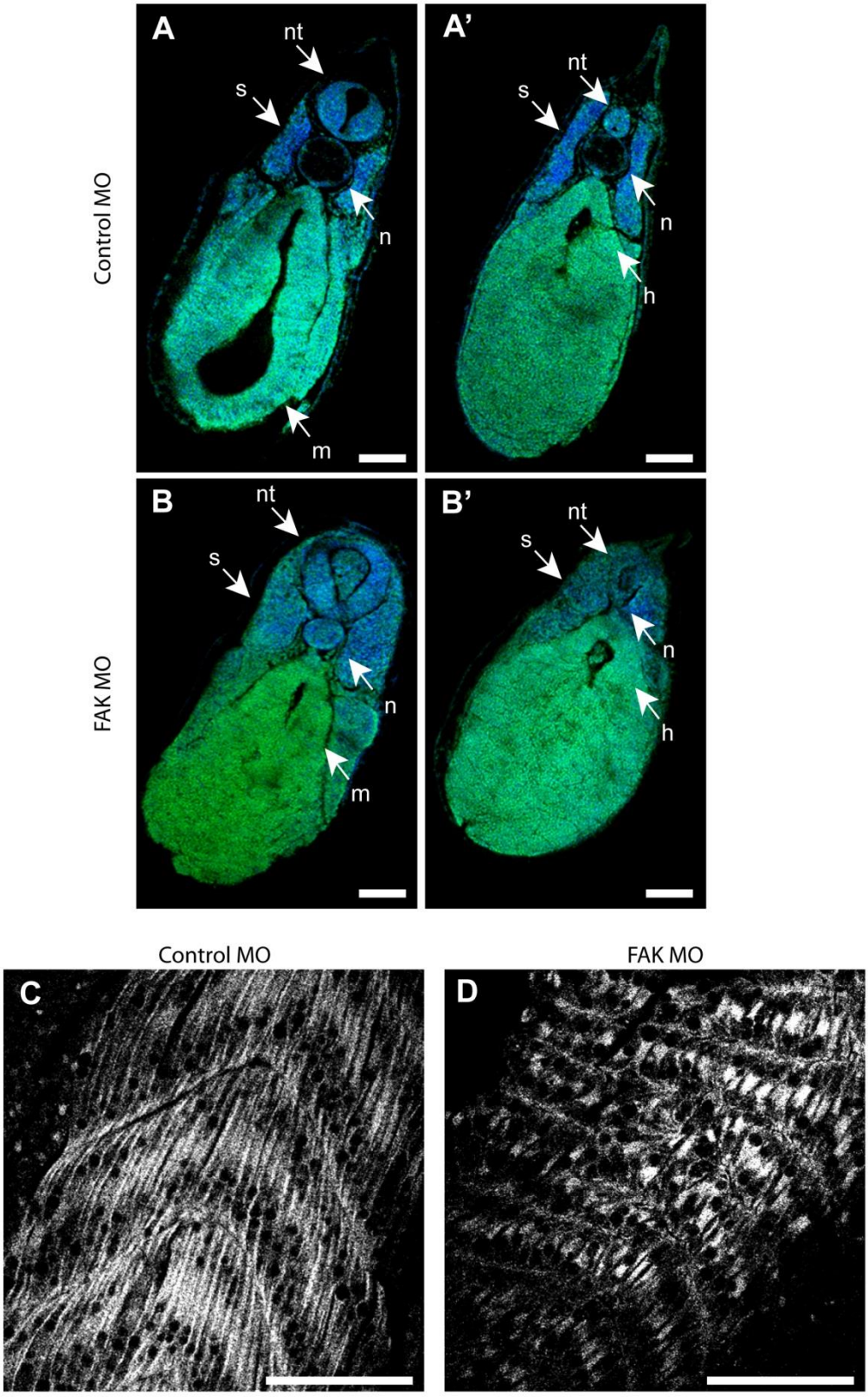
A
nt
s
n
m
A'
nt
s
n
h
Control MO
B
nt
s
n
m
B'
nt
s
n
h
FAK MO
Control MO
FAK MO
C
D

Figure 3.5

FAK protein expression and FAK morphant phenotypes are rescued by injection of cFAK RNA. (A) Representative Western blot analysis of FAK protein expression in embryos co-injected with FAK MO and the chicken (*Gallus gallus*) ortholog of FAK (cFAK, 200pg injected transcript), which is not targeted by FAK MO. Quantification is for blot shown. Expression levels were normalized to β-actin and calculated relative to uninjected controls. (B) Representative images and quantification of gastrulation phenotype (blastopore closure) in Control and FAK MO injected embryos compared with embryos co-injected with FAK MO and cFAK (N=7, Control MO n=371, FAK MO n=513, FAK MO + cFAK RNA n=327). Embryos were counted as having defects if their development was more than 1 hour behind that of control embryos, if there was failure to form or close the blastopore, or if the embryos died during gastrulation. The example given for "FAK MO + cFAK" was counted as rescued (a mild phenotype and not included in count of embryos with defects). (C) Representative images and quantification of tailbud phenotype (axial elongation and formation of anterior structures) in Control and FAK MO injected embryos compared with embryos co-injected with FAK MO and cFAK (N=4, Control MO n=225, FAK MO n=183, FAK MO + cFAK RNA n=217). Embryos were counted as having defects if they failed to form eye anlagen, had a distinctly shortened anterior-posterior axis or failed to close the neural tube. The example given for "FAK MO + cFAK" was counted as rescued (a mild phenotype and not included in count of embryos with defects). Data in B and C are mean ± SEM.

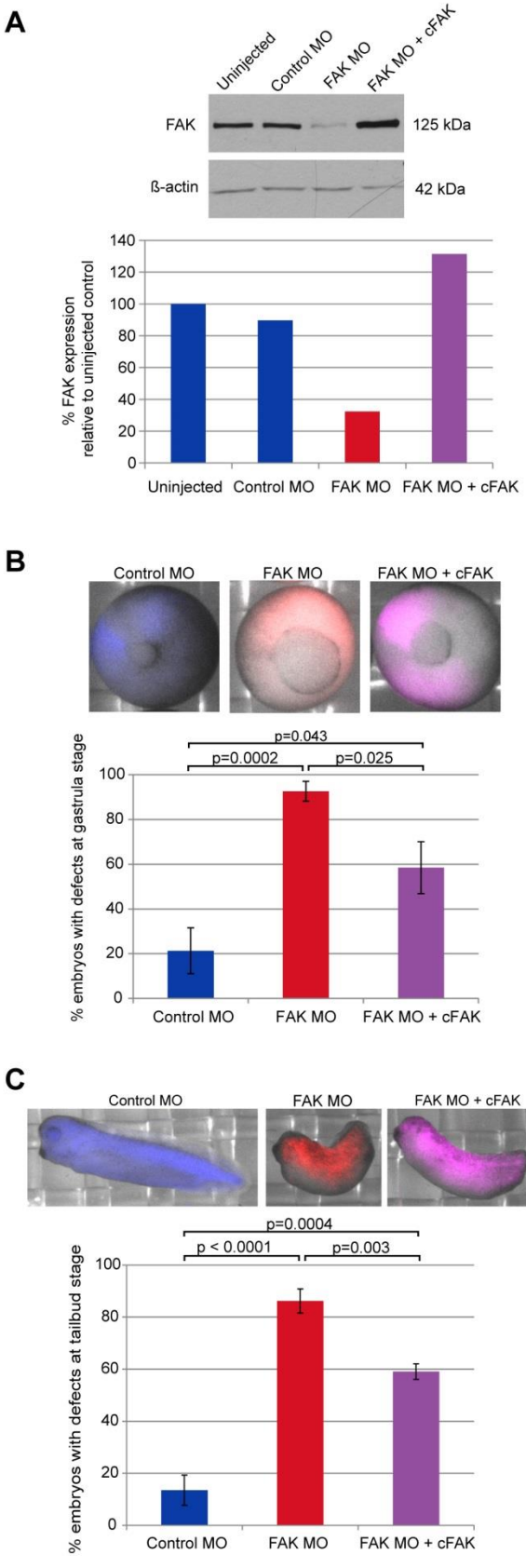
A
Uninjected
Control MO
FAK MO
FAK MO + cFAK
FAK
125 kDa
ß-actin
42 kDa
% FAK expression relative to uninjected control
140
120
100
80
60
40
20
0
Uninjected
Control MO
FAK MO
FAK MO + cFAK
B
Control MO
FAK MO
FAK MO + cFAK
p=0.043
p=0.0002
p=0.025
% embryos with defects at gastrula stage
100
80
60
40
20
0
Control MO
FAK MO
FAK MO + cFAK
C
Control MO
FAK MO
FAK MO + cFAK
p=0.0004
p < 0.0001
p=0.003
% embryos with defects at tailbud stage
100
80
60
40
20
0
Control MO
FAK MO
FAK MO + cFAK

Figure 3.6

FAK morphant animal cap explants do not extend upon treatment with activin. (A, B) Animal cap extension assay. Animal caps dissected from Control and FAK MO injected embryos (A) without (-) and (B) with (+) activin treatment (N=4, n=40/condition).

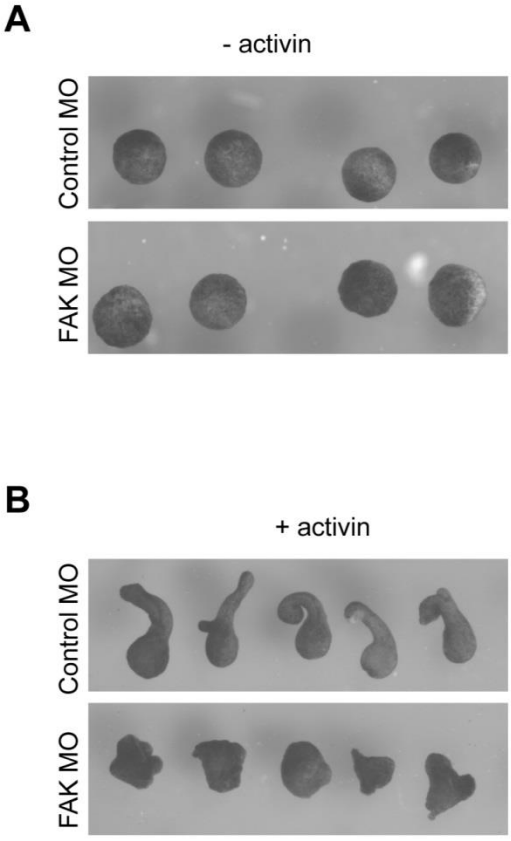
A
- activin
Control MO
FAK MO
B
+ activin
Control MO
FAK MO

Figure 3.7

Fn expression and matrix assembly are not affected by loss of FAK expression. (A, B) Examples of single-plane structured-illumination images of fixed animal caps from control (A) or FAK morphant (B) embryos, stained for Fn. (C) Western blot analysis of Fn expression in control and FAK morphant embryos, blot was also probed with antibodies against FAK and β-actin to control for FAK knockdown and gel loading respectively. (D, E) Western blot analysis of levels of phosphorylation of FAK on tyrosine 397 (D) (N=4) or tyrosine 861 (E) (N=3), β-actin was used as a loading control. The same lysates were also blotted for FAK to control for FAK expression levels; β-actin was used as a loading control. Scale bars = 100μm.

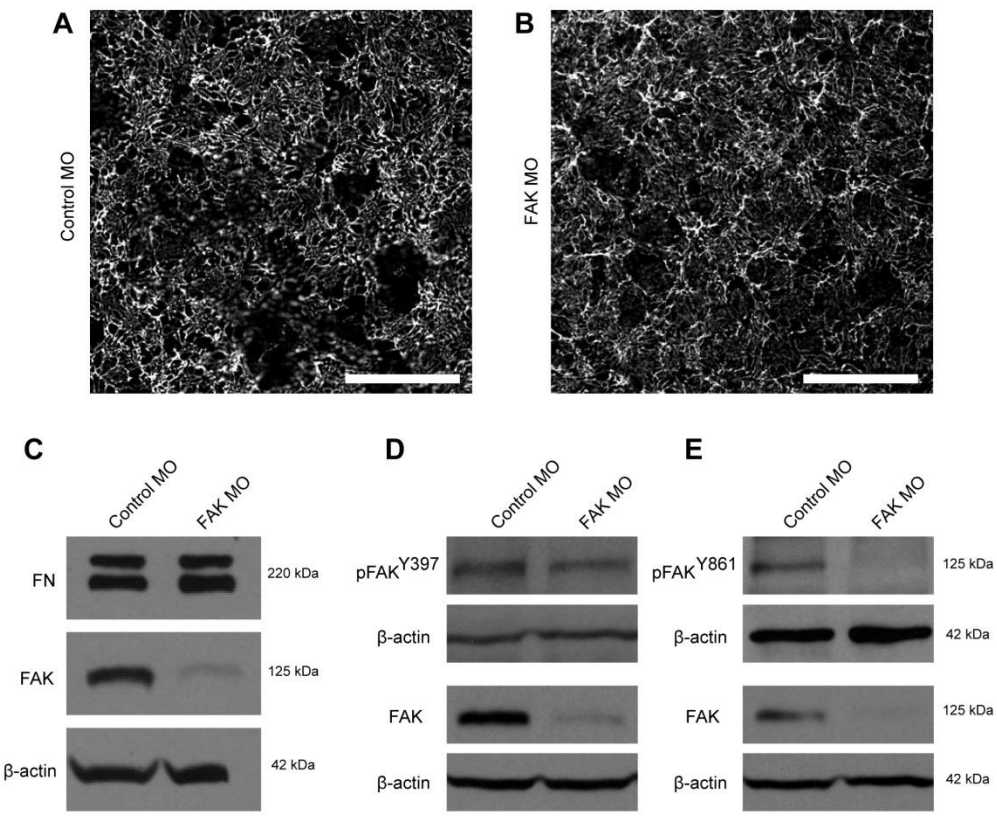
A
Control MO
B
FAK MO
C
Control MO
FAK MO
FN
220 kDa
FAK
125 kDa
β-actin
42 kDa
D
Control MO
FAK MO
pFAKY397
β-actin
FAK
β-actin
E
Control MO
FAK MO
pFAKY861
125 kDa
β-actin
42 kDa
FAK
125 kDa
β-actin
42 kDa

Figure 3.8

FAK morphant mesendoderm cells migrate slowly and lack persistence. (A) Sagittal views of representative Control or FAK MO injected embryos from the same clutch that were fixed and bisected at time matched stages during gastrulation. Arrowheads indicate position of the mesendoderm mantle, red arrowheads mark the first displacement between the mesendoderm and the blastocoel roof (bcr), black brackets mark the thickness of the marginal tissue, Bc=Brachet's cleft, d=dorsal, v=ventral. (B, C) Quantification of average velocity (B, displacement/time) and persistence (C, displacement/path length) of single mesendoderm cells (N=3, Control MO n= 32, FAK MO n=65) or cells in mesendoderm explants (N=3, Control MO n=19, FAK MO n=23). Data are mean ±SEM. *$p<0.05$, **$p<0.01$, ***$p<0.001$.

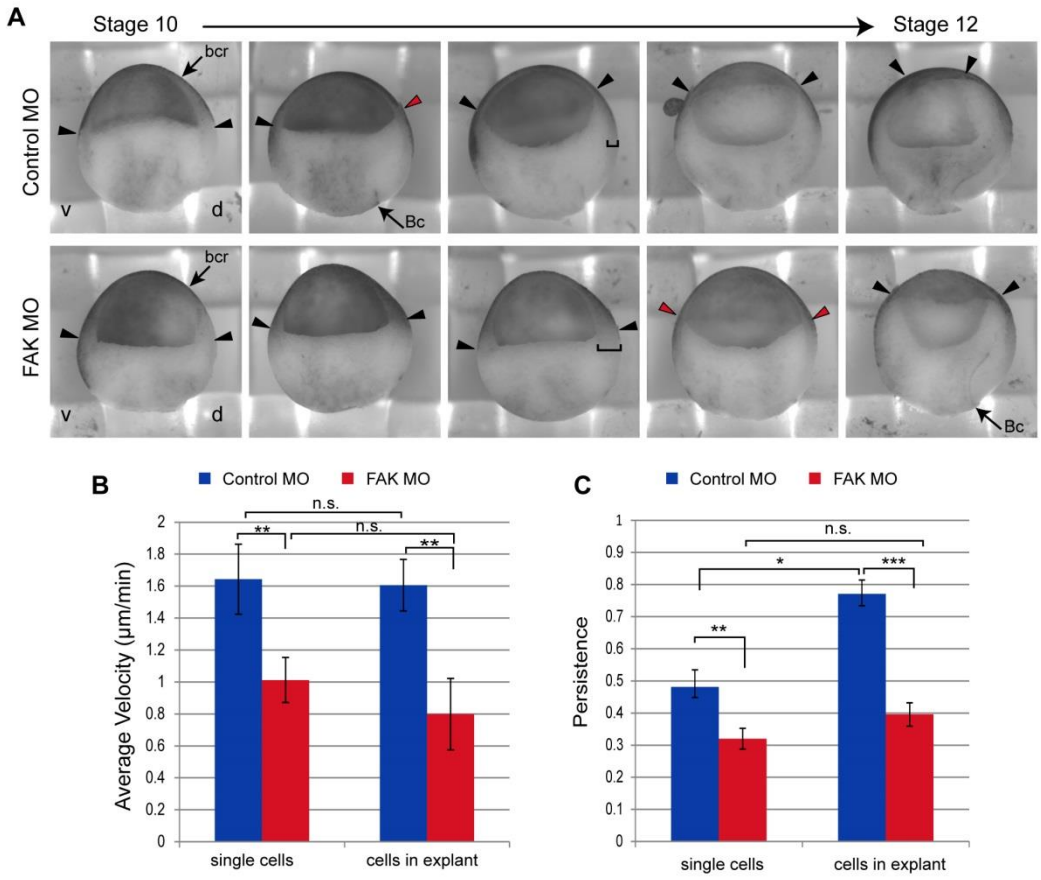
A
Stage 10
Stage 12
Control MO
FAK MO
bcr
Bc
v
d
B
Control MO
FAK MO
Average Velocity (µm/min)
n.s.
**
n.s.
**
single cells
cells in explant
C
Control MO
FAK MO
Persistence
n.s.
*
***
**
single cells
cells in explant

Figure 3.9

FAK is essential for normal polarity of migrating mesendoderm. (A and B) Representative collapsed 5µm z-stack images of live cells in control (A) and FAK morphant (B) mesendoderm explants expressing GAP-43-EGFP to label membranes. Green arrowheads highlight protrusions in the expected direction of tissue movement and yellow arrowheads mark protrusions in any other direction. (C) Quantification of protrusion angles of mesendoderm cells in explants from control (N=4, n=100) and FAK morphant (N=4, n=210) embryos, relative to cell centroids (center of rose diagram). 180° is defined as the predicted direction of normal tissue movement and marked in dark green. Mis-directed protrusions at 90° or 270° are marked in yellow and those at 0° are marked in red. Y axis for the rose diagrams represents percent of protrusions in each directional bin. Protrusions were quantified in both leading (row 1) and following (rows 2-4) cells. Significance was evaluated using circular statistical tests for randomness of distribution (Rayleigh's test, p(random)) and similarity of distribution (Mardia-Watson-Wheeler, p(same)). (D-G) Additional quantification of the data set shown in (C) Data are mean ± SEM. (D) Quantification of protrusions per cell in control and FAK morphant mesendoderm explants. (E-G) Quantification of percent of control or FAK morphant cells in mesendoderm explants with protrusions in the area defined in the cartoon beneath each graph, color coded to match graphs in (C). (E) Percent of cells with protrusions **only** within 45° of the direction of tissue migration. (F) Percent of cells with **only** protrusions deviating 75° or more from the direction of travel. (G) Percent of cells with at least one protrusion in the direction of travel and also one or more greater than 75° away from the expected direction of tissue migration. Scale bars = 25µm.

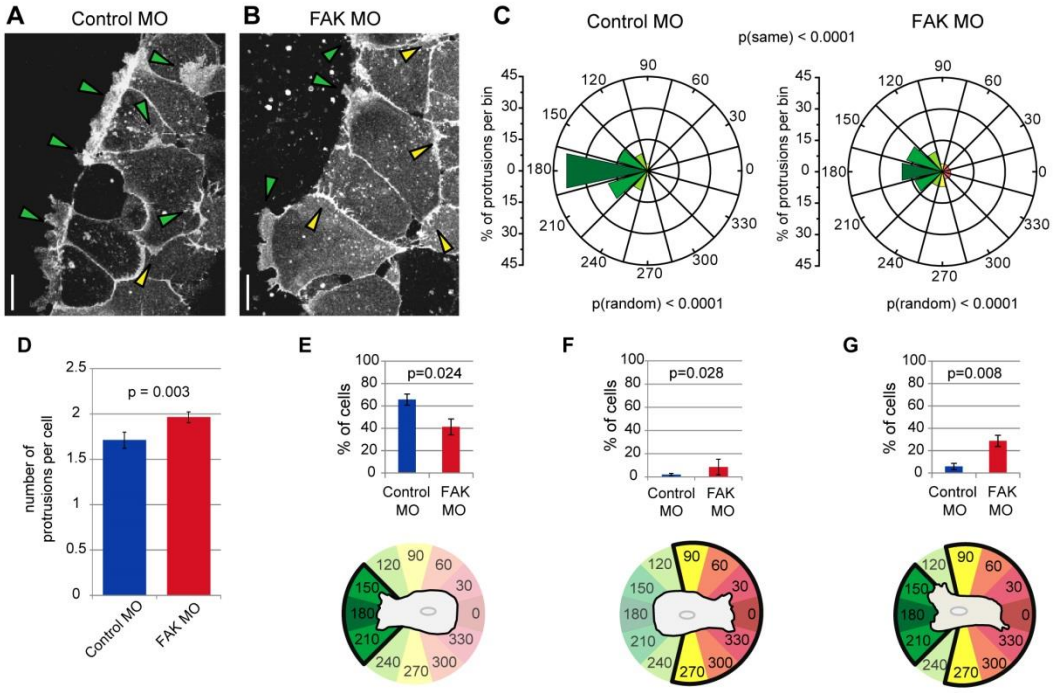
A
Control MO
B
FAK MO
C
Control MO
p(same) < 0.0001
FAK MO
% of protrusions per bin
p(random) < 0.0001
p(random) < 0.0001
D
p = 0.003
number of protrusions per cell
Control MO
FAK MO
E
p=0.024
% of cells
Control MO
FAK MO
F
p=0.028
% of cells
Control MO
FAK MO
G
p=0.008
% of cells
Control MO
FAK MO

Figure 3.10

Actin organization is altered in FAK morphant cells. (A-E) Representative confocal images of live cells in mesendoderm explants expressing GFP-moesin to label the actin filament network. (A) Single plane confocal images of actin at the leading edges of cells in the first row (left) and following rows (right) of control mesendoderm explants. Green arrowheads indicate actin rich protrusions. (B) Single plane confocal images of actin on the leading edges of cells in the first row (left) and following rows (right) of FAK morphant mesendoderm explants. Yellow arrowheads indicate actin microspikes. (C) Collapsed 7.5µm z-stack image of actin in a cell on the leading edge cell of a control explant. Greed arrowheads indicate cortical actin. (D) Collapsed 7.5µm z-stack image of actin in a cell on the leading edge of a FAK morphant explant. Green arrowhead indicates cortical actin; yellow arrowheads indicate actin stress fibers. (E) Collapsed 5.5µm z-stack images of cell-cell junctions in following rows of control (top) and FAK morphant (bottom) explants. Dashed lines mark the boundary between cells. Scale bars = 10µm (A, B, E) or 25µm (C, D).

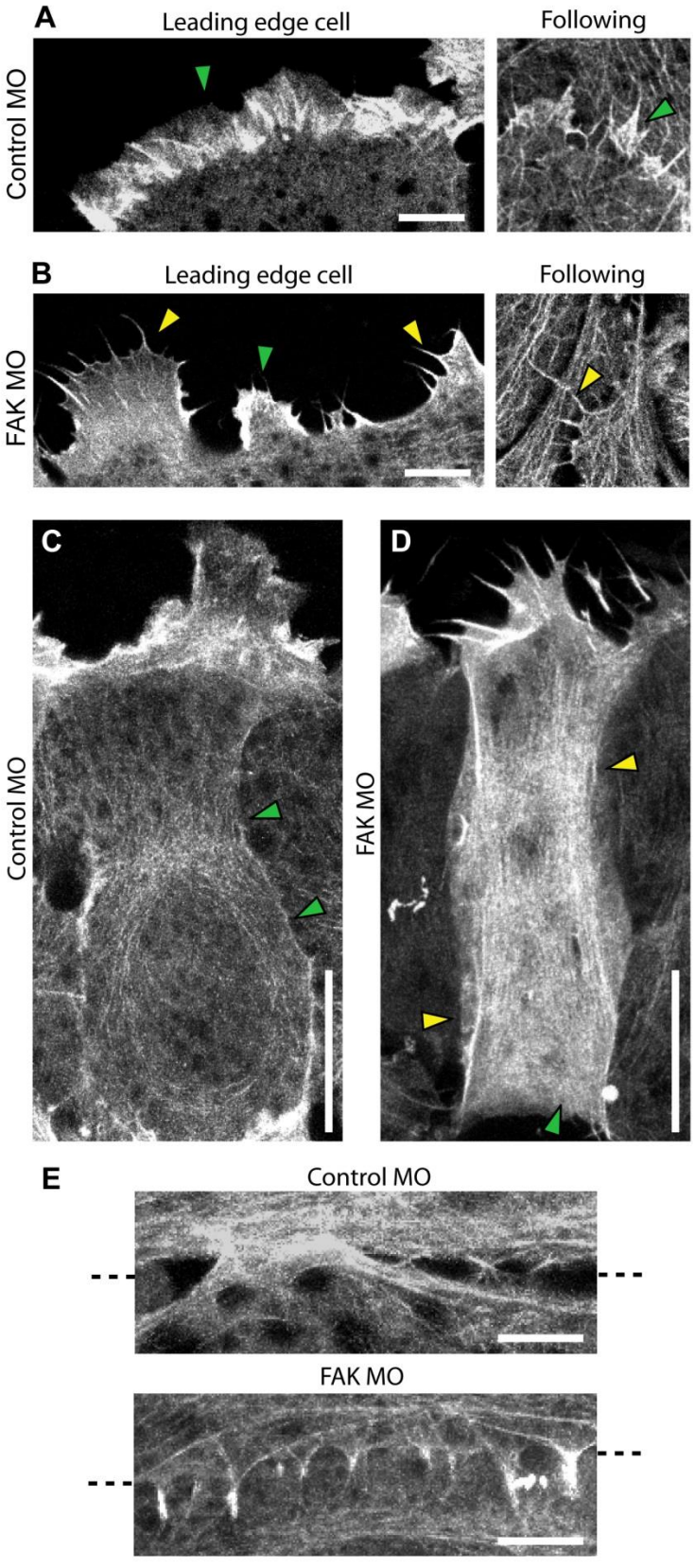
A
Leading edge cell
Following
Control MO
B
Leading edge cell
Following
FAK MO
C
D
Control MO
FAK MO
E
Control MO
FAK MO

Figure 3.11

Phosphorylation of myosin light chain (MLC) is not altered in FAK morphants. (A) Representative image of Western blot of whole embryo lysates probed with an antibody against pMLC, β-actin was used as a loading control. (B) Quantification of pMLC levels in control and FAK morphant embryos (N=3). Data are mean ± SEM.

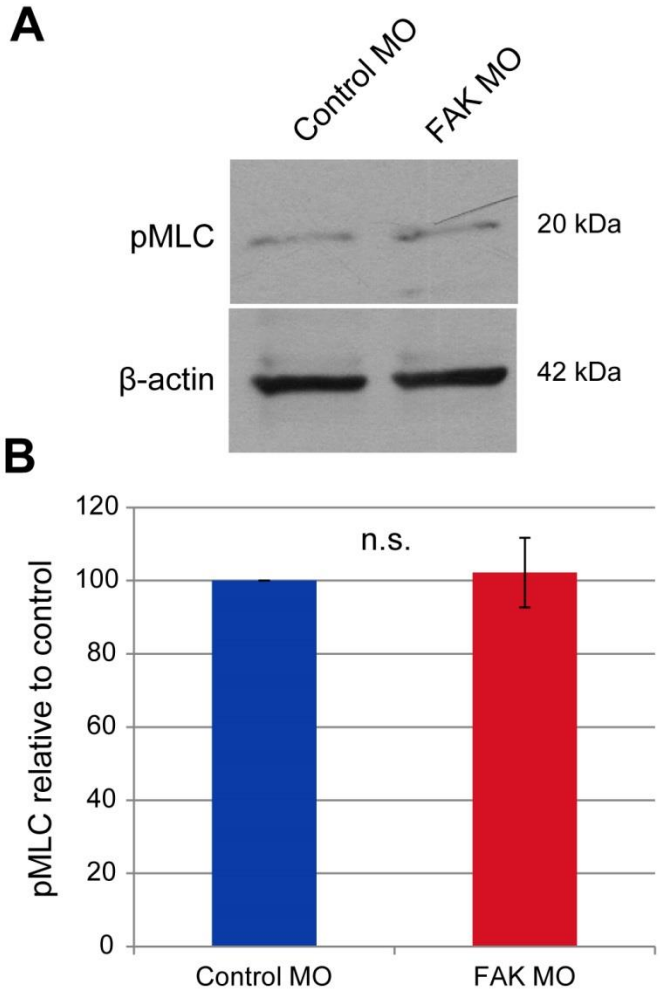
A
Control MO
FAK MO
pMLC
20 kDa
β-actin
42 kDa
B
pMLC relative to control
120
100
80
60
40
20
0
n.s.
Control MO
FAK MO

Figure 3.12

FAK is required for organization of the keratin filament network. (A-F) Representative collapsed 10µm z-stack images of live cells in mesendoderm explants expressing EGFP-XCK1 (8) to label the keratin filament network. (A, B) Keratin filaments in leading edge cells in control explants. Green arrowheads indicate basket like arrangement of filaments in the rear of each cell and cabling across the leading edge cells. (C, D) Keratin filaments in leading edge cells in FAK morphant explants. Yellow arrowheads indicate mis-localized filaments and loss of cabling, yellow dashed line in (D) denotes cell outline. (E, F) Keratin filaments in leading edge cells in explants co-injected with FAK MO and cFAK RNA, which is not targeted by the morpholino. Green arrowheads indicate basket-like arrangement of filaments and cabling across leading edge cells. Scale bars = 50µm.

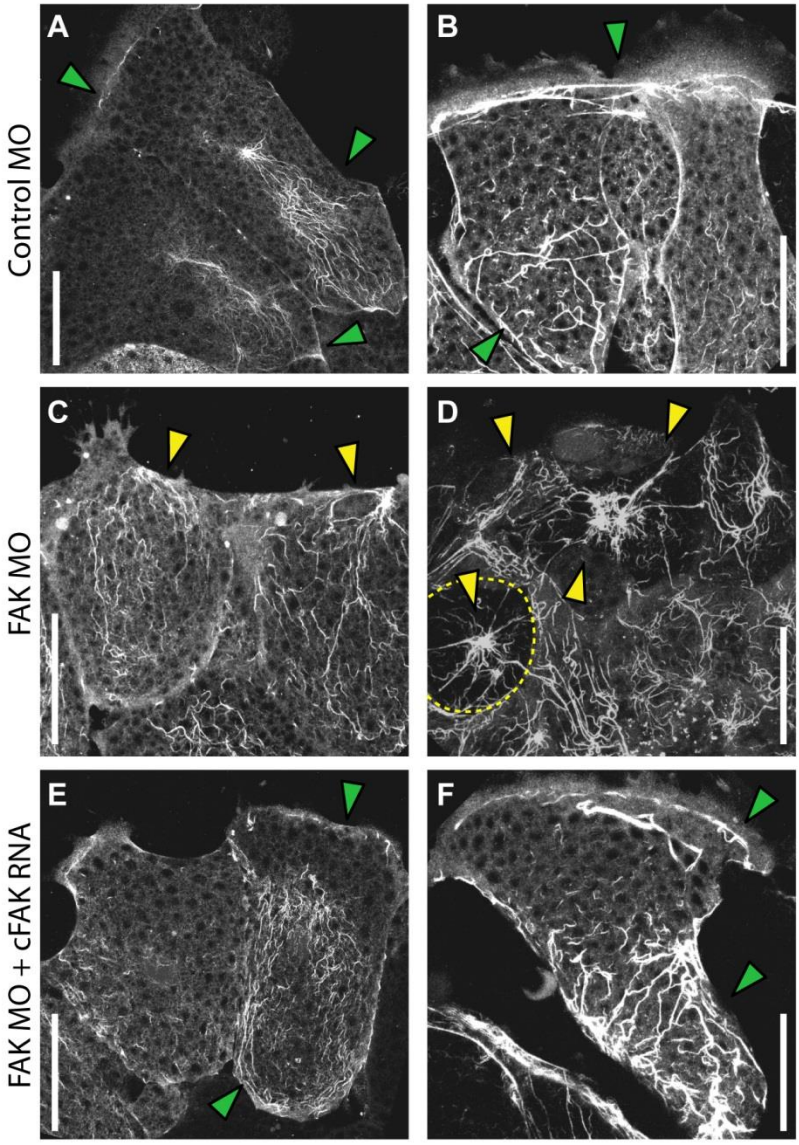
A
B
Control MO
C
D
FAK MO
E
F
FAK MO + cFAK RNA

Figure 3.13

Spreading and cell traction are reduced in FAK morphant mesendoderm cells. (A) Representative image of control (blue) and FAK morphant (red) mesendoderm cells plated on Fn coated coverglass. Cells labeled with fluorescently tagged dextran to show cell shape and mark control vs. FAK morphant cells. (B) Quantification of percent of mesendoderm cells spread on Fn coated coverglass (N=3, Control MO n=88, FAK MO n=97). Data are mean ± SEM (C) Quantification of average force per cell exerted by mesendoderm cells on Fn coated micropost arrays (N=4, Control MO n=74, FAK MO n=56). (D) Quantification of average force per micropost exerted by mesendoderm cells on Fn coated micropost arrays. Data in (C, D) are shown in box-whisker plots, bold line indicates mean, box delimits 25^{th}-75^{th} percentile and whiskers mark minimum and maximum values, statistical outliers are marked as dots. Scale bar = 200µm

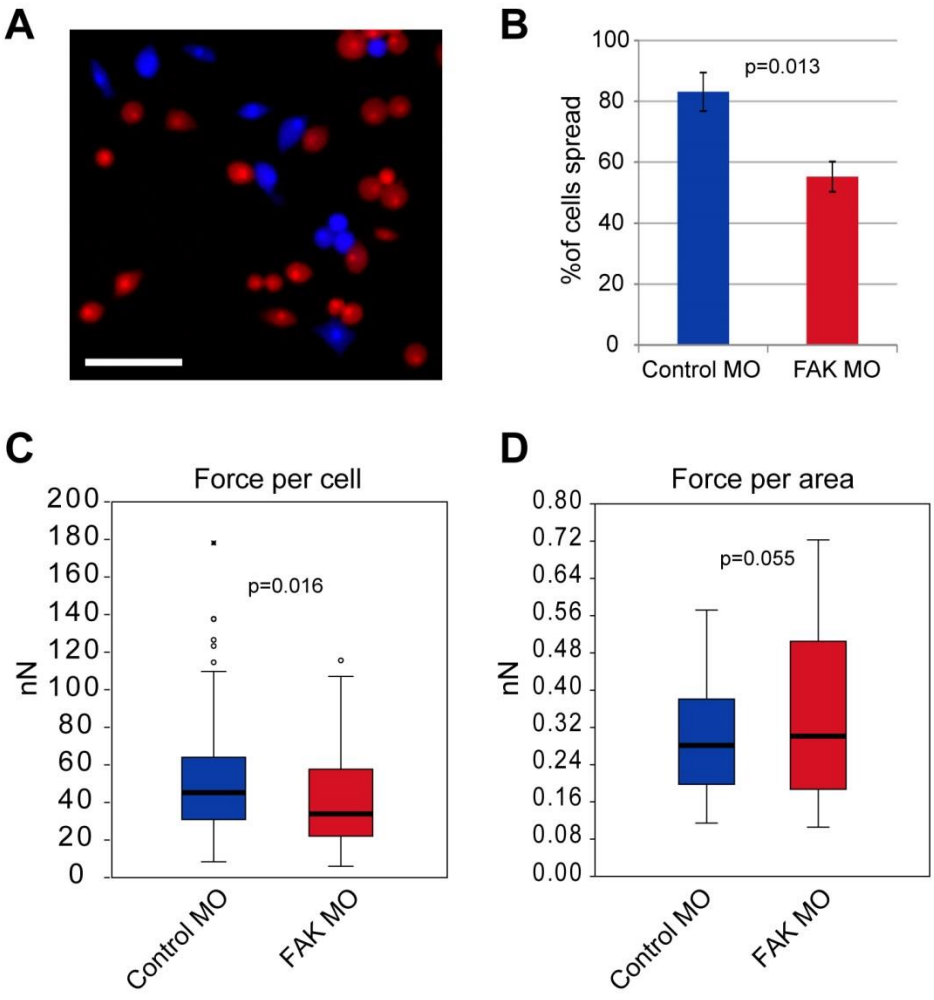
A
B
100
80
60
40
20
0
%of cells spread
p=0.013
Control MO
FAK MO
C
Force per cell
200
180
160
140
120
100
80
60
40
20
0
nN
p=0.016
Control MO
FAK MO
D
Force per area
0.80
0.72
0.64
0.56
0.48
0.40
0.32
0.24
0.16
0.08
0.00
nN
p=0.055
Control MO
FAK MO

Figure 3.14

Knockdown of FAK increases cell roundness and there is a significant correlation between decreased cell force and increased circularity. (A) Quantification of circularity of cells quantified in Figure 3.13 C, D. Data are shown in box-whisker plots, bold line indicates mean, box delimits 25^{th}-75^{th} percentile and whiskers mark minimum and maximum values (N=4, Control MO n=74, FAK MO n=56). (B) Examples of cells from (A) illustrating the circularity values indicated in top right corner of each panel. Cells labeled with fluorescently tagged dextran to show cell shape, microposts are shown in green. (C, D) Scatter plots of total cell force (y-axis, see Fig. 6C) and circularity (x-axis, see Fig. 6D) of mesendoderm cells isolated from control (C) and FAK morphant (D) embryos and plated on Fn coated micropost arrays. Correlation was analyzed using Kendall's tau test, the test statistic (τ) and p value are given. Scale bars = 50μm.

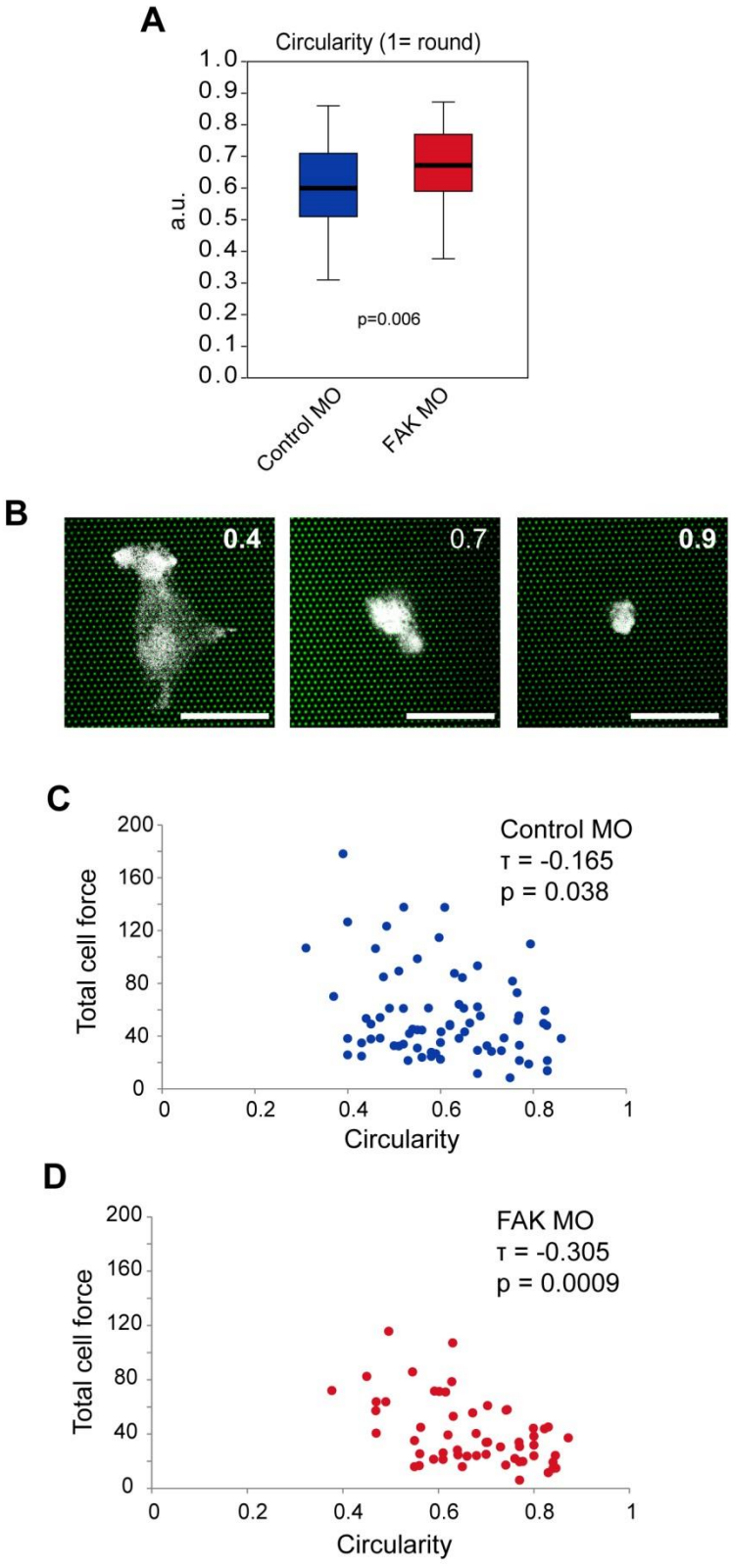
A
Circularity (1= round)
a.u.
1.0
0.9
0.8
0.7
0.6
0.5
0.4
0.3
0.2
0.1
0.0
p=0.006
Control MO
FAK MO
B
0.4
0.7
0.9
C
Total cell force
200
160
120
80
40
0
0
0.2
0.4
0.6
0.8
1
Circularity
Control MO
τ = -0.165
p = 0.038
D
Total cell force
Circularity
FAK MO
τ = -0.305
p = 0.0009

Figure 3.15

Association of plakoglobin with C-cadherin is disrupted in early FAK morphant gastrulae. (A) Representative Western blot of plakoglobin or β-catenin immunoprecipitates from whole embryo lysates of control or FAK morphant embryos, probed with an antibody directed against C-cadherin. (B) Quantification of C-cadherin association with plakoglobin in early (stage 10) and late (stage 12) gastrulae injected with Control or FAK MOs. (C) Quantification of C-cadherin association with β-catenin in early (stage 10) and late (stage 12) gastrulae injected with Control or FAK MOs. Embryos from the same clutch were used for both plakoglobin and β-catenin co-immunoprecipitation at early and late stages of gastrulation (N=3). Blots were re-probed with antibodies directed against plakoglobin or β-catenin respectively and scans of these blots were used to normalize scans of C-cadherin blots, all values are shown relative to early control gastrulae. Data are mean ± SEM. **p=0.003.

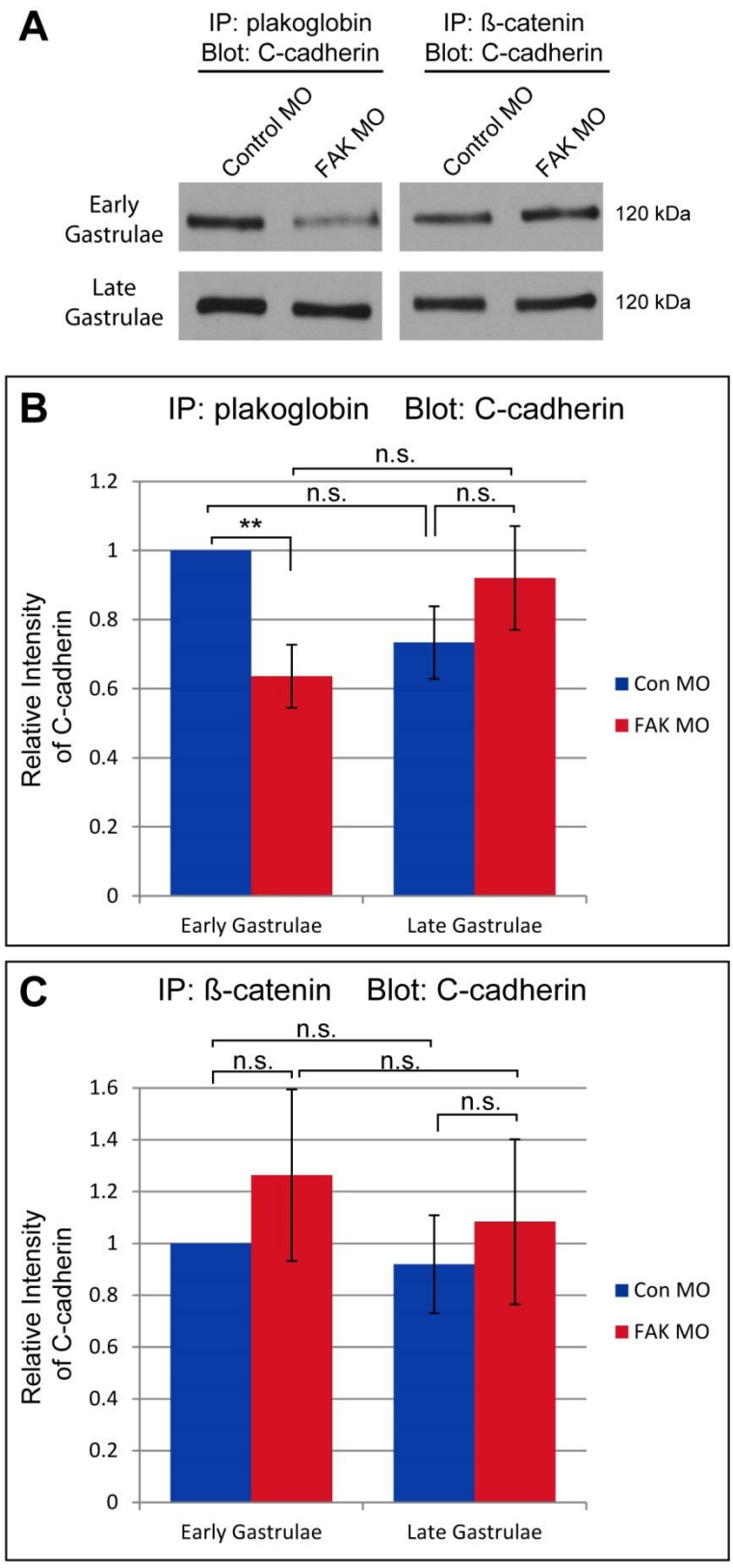
A
IP: plakoglobin
Blot: C-cadherin
IP: ß-catenin
Blot: C-cadherin
Control MO
FAK MO
Control MO
FAK MO
Early Gastrulae
Late Gastrulae
120 kDa
120 kDa
B
IP: plakoglobin Blot: C-cadherin
Relative Intensity of C-cadherin
n.s.
n.s.
n.s.
**
Con MO
FAK MO
Early Gastrulae
Late Gastrulae
C
IP: ß-catenin Blot: C-cadherin
Relative Intensity of C-cadherin
n.s.
n.s.
n.s.
n.s.
Con MO
FAK MO
Early Gastrulae
Late Gastrulae

Chapter 4

Identification of mechanically sensitive proteins in *Xenopus* mesendoderm

This chapter is composed of unpublished data

4.1 Abstract

The overall goal of this project was to use state-of-the-art biochemical and proteomic approaches coupled with *Xenopus* embryo explant preparations to discover proteins that may change conformation directly in response to varying mechanical stress at sites of cell-cell and cell-ECM contact. Mechanical stimuli have emerged as key regulators of the morphogenesis and patterning of developing embryos, but the mechanisms by which forces are generated and sensed are not well understood. A number of hypotheses have been proposed to explain the molecular mechanism of mechanotransduction, one of which entails force-induced unfolding and/or relaxation of proteins in response to changing mechanical stimuli. Cysteine-shotgun mass spectrometry (CS-MS) was adapted to enable the identification of proteins that undergo conformational changes in response to force on the adhesion complexes of *Xenopus* mesendoderm cells. Several proteins have been identified thus far, primarily enzymes associated with cellular metabolism. This suggests that tension across adhesion complexes can modulate energy production in the cell, perhaps providing fuel for high energy processes like actin assembly and contractility. However, these effects are likely to be downstream effects of signaling cascades initiated by the proteins that are sensing and responding directly to force. Thus, complementary strategies were devised to narrow the focus to proteins most proximal to the adhesions under tension. These studies set the stage for a continuing investigation into the components and mechanisms of adhesion-dependent mechanotransduction.

4.2 Introduction

How cells within tissues sense and respond to physical forces is one of the major outstanding questions in cell and developmental biology. The cell and tissue rearrangements underlying morphogenesis result in the generation of tension, pressure, shear and other forces that are sensed both locally and globally by cells and tissues in the embryo (Ricca et al., 2013; Wozniak and Chen, 2009). It has long been suggested that the forces generated during development may play key roles in embryogenesis (Mammoto and Ingber, 2010; Rozario and DeSimone, 2010; Wozniak and Chen, 2009). There are now several compelling examples of how "mechanochemical" signals can influence diverse developmental processes that include gene expression (Farge, 2003), asymmetric cell division (Kozlowski et al., 2007), and cell and tissue shape (Lecuit and Lenne, 2007; Rauzi et al., 2008).

When cells are subjected to extrinsic forces arising from associations with neighboring cells or the extracellular matrix (ECM), the major load-bearing elements involved are the cadherin and integrin-dependent adhesive complexes arrayed at their cell surfaces (Leckband et al., 2011; Ross et al., 2013; Schwartz and DeSimone, 2008). These adhesion molecules not only resist and distribute mechanical forces through junctional and cytoskeletal linkages but are also involved in signal transduction in response to mechanical stimuli. Their activities are responsible for adhesive strengthening in reaction to applied stress, and the ability of cells to sense changes in the rigidity of their microenvironments (Chan and Odde, 2008; Geiger et al., 2009; Jiang et al., 2006; Kostic and Sheetz, 2006; Riveline et al., 2001; Tzima et al., 2005; Wang et al., 2001). Cell and tissue responses to mechanical forces are also underlying factors in varied pathologies

that include hypertension and atherosclerosis, tumorigenesis and metastasis, bone degeneration, and deafness (Jaalouk and Lammerding, 2009; Orr et al., 2006; Papachroni et al., 2009)(Jaalouk and Lammerding, 2009). Despite the importance of mechanotransduction to development, normal physiology and disease, the molecular mechanisms involved remain poorly understood.

One of the specific questions surrounding mechanotransduction concerns the mechanism(s) by which cells sense and transduce local stresses via adhesive specializations and the cytoskeleton (Bershadsky et al., 2006). The primary hypothesis tested here posits that mechanosensation in the developing embryo involves force-dependent changes in the conformations of proteins involved in cell adhesion and related signaling events. Conformational change is now considered an important regulator of protein interactions at sites of adhesion (Moore et al., 2010). Some key adhesion components, including vinculin and talin, are known to undergo conformational changes that regulate their activity (Chen et al., 2005; Gingras et al., 2006). While a small number of proteins have been shown to undergo force dependent conformational change (Sawada et al., 2006; Smith et al., 2007), observations with clear physiological significance are limited. Most studies on protein unfolding have been performed in vitro using single molecule atomic force microscopy (AFM), fluorescence resonance energy transfer (FRET), or other high-tech approaches (Forman and Clarke, 2007). Thus, approaches are needed that not only test rigorously the overall hypothesis, but simultaneously make a significant impact on this important new field by identifying classes of proteins subject to conformational changes occurring under physiologically relevant conditions.

The development of new techniques to visualize and identify force-induced unfolding of proteins in live cells has provided a new angle of attack for the exploration of mechanosensory pathways. Cysteine (Cys) is a mildly hydrophobic amino acid that is commonly sequestered from the intracellular milieu by tertiary and quaternary protein structures. Changes in protein conformation, however, may lead to exposure of some or all of the highly reactive thiol groups of these buried Cys residues. Non-toxic, membrane-permeable, thiol-reactive, fluorescent dyes can then be used to bind covalently to these exposed thiols. Cysteine-shotgun mass spectrometry (CS-MS) protocol published by Johnson et al. (2007) takes advantage of these reagents to detect changes in Cys accessibility and infer conformational change. In brief, cysteine residues accessible to the cytosol are labeled in stressed and non-stressed cells, proteins from labeled cells are separated by SDS-PAGE to identify changes in fluorescent dye intensity, and selected bands are analyzed by mass spectrometry.

The technique can be used with or without application of exogenous force to label proteins that have unfolded, re-folded or undergone some other type of modification that alters Cys accessibility. For example, differences in Cys-labeling may result from altered protein-protein interactions or changes in post-translational modifications such as glycosylation. Cys residues are commonly found in the active sites of various enzymes and phosphatases that utilize ATP. Thus, changes in the activity of these proteins might also yield changes in exposure of reactive Cys residues to the intracellular milieu. The CS-MS technique enables identification of proteins with differential Cys-labeling and also provides precise information about which Cys residues have been modified. Proof-of-concept studies have demonstrated the efficacy of this approach using a variety of cell

types in culture (Engler et al., 2008; Johnson et al., 2007). This chapter describes the development of CS-MS to screen for conformational changes in proteins obtained from an embryonic tissue known to be mechanosensitive.

Collective cell migration is a morphogenetic process important in development, regeneration, tissue repair and some metastatic cancers, but the mechanisms by which collective cell movements are guided and regulated are not fully understood. The mesendoderm of *Xenopus laevis* gastrula stage embryos undergoes a collective cell migration event that requires both cell-cell cohesion and adhesion to a fibronectin (Fn) substrate in order to move directionally. Recent studies support the hypothesis that mechanical forces are essential elements in the signaling network guiding the morphogenesis of the developing *Xenopus* embryo. The assembly of Fn fibrils in vivo was recently shown to be an integrin-dependent process that requires a cadherin-dependent build-up of cell surface tension in the blastocoel roof (Dzamba et al., 2009). This unexpected result highlights not only the importance of tension but also cadherin and integrin crosstalk (Weber et al., 2011). Moreover, the collective cell migration of mesendoderm along the blastocoel roof is guided by anisotropic tension on cadherin adhesions (Chapter 2) (Weber et al., 2012). Thus, the mesendoderm provides a compelling system for detailed investigation of a robust mechanosensitive response required for the collective behaviors of cells within a tissue. This study aims to shed new light on this process by identifying candidate proteins that may then be tested for direct functional involvement in mechanosensation.

4.3 Materials and Methods

Xenopus egg and embryo preparation

Embryos were obtained and cultured using standard methods and staged according to Nieuwkoop and Faber (1994). Embryos were dejellied in 2% cysteine and cultured at 16^{o}C in 0.1X Modified Barth's saline (MBS; 1X MBS: 88 mM NaCl, 1 mM KCl, 2.5 mM $NaHCO_3$, 0.35 mM $CaCl_2$, 0.5 mM $MgSO_4$, 5 mM HEPES pH 7.8).

Substrate preparation

For live cell imaging on glass substrates, glass coverslips were alkaline-ethanol washed and flamed prior to coating with fibronectin (Fn). Coverslips were coated with 200 µl of 2.5 µg/ml bovine plasma Fn (Calbiochem) overnight at 4^{o}C to yield a maximum coating density of 0.38 µg/cm^2. The following day the dishes were blocked with 5% BSA for 20 minutes then washed and filled with 0.5X MBS.

For live cell imaging on substrates of differing stiffness, polydimethylsiloxane (PDMS) (Sylgard, Dow Corning) substrates were prepared by spreading a 100 µm layer of premixed base and cure Sylgard solutions onto glass coverslips and curing at 85° overnight. The elastic properties of the substrates were varied by altering the ratio of the base and cure components of the PDMS solution. The elastic properties of the cured PDMS substrates were measured using standard stress-strain experiments as previously described (Dzamba et al., 2009). The PDMS substrates were coated with 200 µL of 20 µg/mL Fn in 0.5X MBS at 4°C overnight. The following day the substrates were blocked with 5% BSA for 20 minutes then washed and covered with 0.5X MBS.

For cell stretch experiments, silicone sheeting (0.010", NRV, Gloss/Gloss, 40D, 12"x 12", SMI Manufacturing) was cut into 3"x4" pieces and mounted into uniaxial stretch devices (courtesy of the Skalak Lab). 2 mL of 2 μg/mL Fn in 0.5X MBS was placed in the center of each mounted sheet and spread across about 6 cm^2 of the surface by carefully overlaying a piece of parafilm to yield a maximum coating density of 0.66 $\mu g/cm^2$. Mounted sheets were incubated overnight at 4^oC. Alternately, 2mL of 2 μg/mL C-cad.Fc in Ca^{2+}/Mg^{2+}-free 0.5X MBS was placed on each mounted sheet and treated in the same fashion. The following day the mounted sheets were blocked with 5% BSA for 20 minutes then washed and covered with 0.5X MBS.

For basal adhesion extraction experiments, 35mm plastic dishes were coated with 2mL of 2μg/mL C-cad.Fc in Ca^{2+}/Mg^{2+}-free 0.5X MBS to yield a final coating concentration of $0.4\mu g/cm^2$. Dishes were incubated overnight at 4°C, blocked with 5% BSA for 20 minutes at RT and washed and filled with 0.5X MBS.

Mesendoderm cell preparation

360° rings of mesendoderm tissue were dissected from stage 11 *Xenopus* embryos and placed in Ca^{2+}/Mg^{2+}-free 1X MBS to dissociate the tissue to single mesendoderm cells. After approximately 30 minutes, cells dissociated from one another were transferred to 0.5X MBS containing Ca^{2+}/Mg^{2+} on Fn- or C-cad.Fc coated substrates. Mesendoderm cells were allowed 1 hour to attach and spread on the provided substrate before experimentation began unless otherwise noted.

Cysteine labeling with monobromobimane

Cysteine residues (those accessible to the cytosol) were labeled in live mesendoderm cells using the Cys-reactive dye monobromobimane (mBBr) (Molecular Probes/Invitrogen). mBBr is a membrane permeable dye that fluoresces (394/490 nm Ex/Em) upon reaction with cysteines or other reactive sulfhydryl groups. Adherent mesendoderm cells were treated with 200-400 µM mBBr in 0.5X HEPES-free MBS (HF-MBS; 1X HF-MBS: 88 mM NaCl, 1 mM KCl, 2.5 mM $NaHCO_3$, 0.35 mM $CaCl_2$, 0.5 mM $MgSO_4$, 0.5 mM $Ca(NO_3)_2$, 5 mM TrisHCl pH 7.6) for 10-30 minutes as noted in the text. The cells were then treated with 3-5 washes of a solution containing an excess of beta-mercaptoethanol (7mM in 0.5X HF-MBS) to quench and remove unreacted mBBr. The quenching solution was then replaced with 0.5X HF-MBS. All steps following addition of mBBr took place in a dark room and/or with foil covering to prevent photo-bleaching of the dye.

Microscopy

A Zeiss AxioObserver microscope equipped with Volocity software (Improvision/Perkin Elmer) was used for live fluorescent and brightfield imaging of isolated mesendoderm cells. Images of mBBr labeled cells were collected using widefield illumination and a CFP filter set (436/480 nm Ex/Em). Confocal microscopy was performed using a Nikon C1 microscope equipped with a laser scanning confocal module. Image files were compiled and viewed using Volocity software and ImageJ (http://rsb.info.nih.gov; National Institutes of Health).

Cell stretch

Hand operated uniaxial stretch devices (courtesy of the Skalak Lab) were used to apply force to integrin adhesions or to cadherin adhesions. Silicone sheeting was mounted onto the device and coated with either Fn or C-cad.Fc, (see *Substrate preparation*). 1 mL of 0.5X MBS was placed in the blocked and washed well of each coated stretch device. 200µL of isolated mesendoderm cells (see *Mesendoderm cell preparation*) were pipetted from the dissociation dish and spread evenly across the coated substrates. For cells plated on Fn, care was taken to disperse the cells and minimize cell-cell contacts. Cells were kept at RT for 45-60 min to allow them time to attach and spread. Uniaxial strain was applied to the cells by turning the center knob until stopped by the limit screws. This resulted in 16% strain in the direction of applied stretch and -3% strain in the perpendicular direction. Strain was calculated by spreading fluorescent microspheres (1µm diameter, Invitrogen) over the surface of a mounted silicone sheet and collecting an image of the bead positions, then applying stretch and measuring the displacement of the spheres at multiple locations. Cells were stretched either after pre-incubation with mBBr or immediately following addition of mBBr as noted in the text.

Cell lysis

All steps took place in dark room and/or with aluminum foil covering. Following dye labeling, quenching and washout, all liquid was removed from the culture dishes or stretch devices to which the cells were adherent. This was immediately replaced with 150-400µL of lysis buffer (100mM NaCl, 50mM Tris pH 7.5, 1% Triton X-100, 2mM PMSF, 1x Protease Inhibitor Cocktail (Sigma)) and the dishes placed on ice for 2-5

minutes. The cells in lysis buffer were pipetted vigorously to remove bound material from the dishes or stretchers and to complete lysis. Lysates were pipetted into chilled microfuge tubes and placed on ice. Unreacted cysteine residues were alkylated by addition of 100mM [final] iodoacetamide (IAM, MP Biomedicals). Samples were spun down at 14,000 rpm at 4°C for 20 min. The supernatant was then removed and placed in new, chilled microfuge tubes. Lysates were stored at -80°C or run on gel immediately.

SDS-PAGE

All steps involving protein samples labeled with mBBr took place in the dark and/or with aluminum foil covering. Polyacrylamide gels were prepared in advance and soaked overnight in ddH_2O or were purchased pre-cast (Bio-Rad). The gels used were either 8% acrylamide or a 4-20% gradient as indicated in figure legends. Alternate gel concentrations and compositions, including bis-tris gels, were tested but did not result in any notable improvements in separation of labeled proteins. For mBBr labeled samples, 6X sample buffer (1.2g SDS (sodium dodecyl sulfate), 0.01% bromophenol blue, 4.7ml glycerol, 1.2ml Tris 0.5M pH6.8, 2.1ml ddH_2O) was added 1:6 to lysates prepared as described above. Samples were boiled for 3 min and spun down for 1 min at 3,000rpm. For other samples, standard 2X Laemmli buffer was added 1:2 to lysates and samples boiled for 5 min. 40uL of sample (or size marker) was loaded into each well of prepared polyacrylamide gels and the gels run at 85-100V until the dye fronts reached the lower edge of the gels.

In-gel analysis by fluorescence

All steps took place in the dark and/or with aluminum foil covering except during imaging and all solutions were filtered prior to use. Polyacrylamide gels were removed from their casings and placed immediately into a solution of 12% trichloroacetic acid (TCA) in ddH_2O to fix proteins. Gels were washed gently on a belly-dancer style rocker overnight at RT. Gels were then carefully moved to new dishes and washed in a solution of 50% methanol and 10% acetic acid for at least 2 hours at RT. Gels were then illuminated with a long wave UV lamp (365nm) and imaged using a standard ethidium bromide filter (580nm). Excitation and emission optima for mBBr are 394/490nm. Although not ideal, the illumination and filters used were sufficient for imaging and analysis of labeled protein bands.

Coomassie staining

After imaging of mBBr labeled bands, separated proteins were labeled with Coomassie blue. Gels were incubated in filtered Coomassie stain (0.1% (w/v) Coomassie blue R350, 20% (v/v) methanol, and 10% (v/v) acetic acid) for at least 1 hour but most typically overnight at RT. Coomassie stain was replaced with several washes of Destain I solution (40% methanol, 7% acetic acid) then incubated in Destain I until background staining was very light. The solution was then replaced with Destain II (5% methanol, 7% acetic acid) and folded up Kimwipes were placed in the corner of each dish, not touching the gel. Gels were incubated in Destain II with regular changes of solution and new Kimwipes until background was clear. After scanning, gels were stored in ddH_2O or 5% acetic acid at 4°C.

Mass spectrometry

Selected bands with significantly differing dye intensities in the stretched and unstretched (control) samples were subjected to mass spectrometry utilizing the services of the UVA School of Medicine Mass Spectrometry Core as well as the kind assistance of Dr. Alban Gaultier. Proteins in isolated gel fragments were digested with trypsin or chymotrypsin and subjected to LC-MS/MS analysis as previously described (Johnson et al., 2007). Mass spectrometry data was compared with the database of *Xenopus* protein sequences using SEQUEST and manual annotation.

Mitochondrial labeling

Mesendoderm cells were isolated and plated in 0.5X HF-MBS onto Fn coated glass as described above. Cells were allowed to attach and spread for 1 hour at RT. MitoTracker Red (Life Technologies) was diluted in dimethylsulfoxide (DMSO) to a working concentration of 50ng/µL. MitoTracker Red was then added to the spread cells at a final concentration of 75mM, with an equal volume of the diluent (DMSO) added to another dish of cells as a control. Cells were incubated with MitoTracker Red or DMSO in the dark at RT for 45 min. Labeling solution was removed and replaced twice with 0.5X MBS. Cells were imaged using confocal microscopy.

Basal adhesion extraction

Cells from 10 360° mesendoderm pieces were isolated and plated on C-cadherin coated glass prepared as described above. Cells were allowed to attach and spread for at least 45 min, then nearly all liquid was removed from each dish and replaced with 200µL of

extraction buffer (50mM NaCl, 0.5% Triton X-100, 10mM pH 6.8 PIPES buffer, 2.5mM $MgCl_2$, 1mM EGTA, 0.3M sucrose, 1mM sodium orthovanadate, 0.2mM H_2O_2, 1x Protease Inhibitor Cocktail (Sigma)). Dishes were incubated on ice or 14°C cold stage for 2-5 min. Extraction buffer was gently pipetted into microfuge tubes and kept on ice. 200µL lysis buffer (100mM NaCl, 1% Triton X-100, 50mM pH 7.5 Tris-HCl, 2mM PMSF, 5mM EDTA, 1mM sodium orthovanadate, 0.2mM H_2O_2, 1x Protease Inhibitor Cocktail (Sigma)) was immediately added to each dish. Buffer was pipetted vigorously and dishes scraped to remove cells from plates. Lysates were spun at 14,000 rpm for 20 min at 4°C, supernatants removed to fresh microfuge tubes and all samples frozen at -80°C or immediately prepared for SDS-PAGE. To determine efficacy of basal adhesion extraction, blots were probed with 4 different antibodies: 6B6 C-cadherin mAb (courtesy of Barry Gumbiner, University of Virginia), glyceraldehyde 3-phosphate dehydrogenase pAb (GAPDH; ProteinTech, 10494-1-AP), β-catenin pAb (Sigma, C2206), and HRP-β-actin mAb (Sigma, A3854), followed by the appropriate HRP labeled secondary antibody. Blots were cut at the 75 kDa marker immediately after transfer and each half probed with a different antibody. Blots were the stripped by incubation with OneMinute Western Blot Stripping Buffer (GM Biosciences) for 3 min then re-probed with the remaining antibodies.

Biotin-HPDP and Immunoprecipitation

Cells from 20 360° mesendoderm pieces were isolated and plated on Fn coated stretch devices as described above. Cells were allowed to attach and spread for at least 45 min, then nearly all liquid was removed from the dish and replaced with a solution of 1mM N-

[6-(Biotinamido)hexyl]-3-(2-pyridyldithio)propionamide (Biotin-HPDP; Soltec Ventures) dissolved in dimethylformamide (DMF) then diluted in HF-MBS. Stretch was applied to the cells as described above, with at least one device remaining unstretched as a control. Stretched and unstretched cells were incubated in Biotin-HPDP for 20 min at RT then washed gently with HF-MBS and lysed with a standard lysis buffer (100mM NaCl, 50mM Tris pH 7.5, 1% Triton X-100, 2mM PMSF, 1x Protease Inhibitor Cocktail (Sigma)). Lysates were brought up to a volume of 500uL in lysis buffer and subjected to one of the following two purification schemes:

1) Lysates were incubated with 50µL Protein G-agaorose beads (Roche Diagnostics, Indianapolis, IN). 4µL of an antibody against Pkg (BD Biosciences, 610253) was pre-incubated with an additional 50 µL aliquot of Protein G-agarose beads. Samples were spun down to remove Protein G beads and the supernatant applied to the antibody-coupled beads to immunoprecipitate plakoglobin protein complexes. Samples were incubated with antibody-coupled beads overnight at 4°C. Beads were pelleted by centrifugation and washed three times with lysis buffer. 2X **non-reducing** Laemmli buffer was added to beads and samples boiled for 5 min to dissociate immunoprecipitated proteins. Samples were loaded onto an 8% SDS-PAGE gel for separation, transferred to nitrocellulose and probed with HRP-conjugated neutravidin.

2) Lysates were incubated with Streptavidin-agarose overnight at 4°C. Beads were pelleted by centrifugation and washed three times with lysis buffer. 2X **reducing** Laemmli buffer was added to beads and samples boiled for 5 min to dissociate immunoprecipitated proteins. Samples were loaded onto an 8% SDS-PAGE gel for

separation, transferred to nitrocellulose then probed with an antibody directed against Pkg (BD Biosciences, 610253) and an HRP-conjugated secondary antibody.

4.4 Results

Experimental strategy

The initial stages of this study were designed to establish baseline parameters for labeling embryonic cells with a Cys-reactive dye, investigate changes in dye-labeling of proteins following force application, and optimize mass-spectrometry and related bioinformatic analyses. The overall experimental strategy was similar to that described by Johnson et al (2007). Briefly, cells were treated with a fluorescent Cys-reactive dye to label thiol groups exposed to the intracellular milieu following application of stress to cadherin or integrin adhesions (Fig. 4.1A). Labeled proteins were separated by SDS-PAGE, differential labeling was identified by changes in fluorescence intensity, selected bands were subjected to tandem mass spectrometry and the sequence data was analyzed using standard bioinformatic approaches (Fig. 4.1B).

Initial experiments focused on dye labeling with and without the application of stretch to dissociated mesendoderm cells adherent to glass, polydimethylsiloxane (PDMS) or elastic silicone substrates coated with adhesion proteins. To confirm the presence of reactive Cys residues and examine subcellular localization of labeled thiols, cells were plated on Fn-coated coverglasses or PDMS. Cells were allowed to attach and spread prior to the addition of a cell membrane-permeable, Cys-reactive fluorophore

monobromobimane (mBBr) (structure shown in Fig. 4.1A). Dye was then washed out and unreacted dye promptly quenched using an excess of β-mercaptoethanol (β-Me), followed by imaging of the labeled cells. To exert stress on cells via adhesive contacts, a hand-operated stretch device was used to reproducibly stretch an elastic silicone sheet along one axis (16% in direction of stretch and -3% in the perpendicular axis) (Fig. 4.1C). A uniaxial stretch device was used because this more closely mimics the anisotropic distribution of forces in intact mesendoderm tissue (Davidson et al., 2002). Isolated mesendoderm cells were seeded onto elastic sheets coated with either Fn or C-cad.Fc (Chappuis-Flament, 2001). The useable area of the sheet was 6-8 cm^2, accommodating cells from ~10-20 dissociated mesendoderm explants. The thiol-reactive dye mBBr was added and the cells were subjected to uniaxial strain in the presence of the dye. After stretch the dye was washed out, unreacted dye quenched with β-Me, and the cells lysed using a modified RIPA buffer. The lysates were then treated with iodoacetamide (IAM) to alkylate any unreacted cysteine residues. Dye concentrations were determined empirically to maximize signal and ensure health of the cells. Proteins were separated using 1D SDS-PAGE and fluorescent intensities of the bands in the stretched and unstretched (control) samples compared by densitometric analysis. The gels were also stained with Coomassie blue for normalization of protein loading. The intensities of selected bands were quantified and compared between stretched and control lanes (Fig. 4.1D). Bands with differing dye intensities in the stretched and control samples were subjected to mass spectrometry to identify the labeled proteins and sites of labeling.

mBBr prominently labels cell edges and labeling is more intense in cells on stiff substrates relative to soft substrates

Reaction of mBBr with thiol groups such as those on Cys residues results in fluorescence of the compound which can be used to visualize the subcellular localization of the reactive residues. Single mesendoderm cells on Fn-coated glass were most prominently labeled around the cell edges with a notable absence of fluorescence in protrusions (Fig. 4.2A, A'). In groups of mesendoderm cells under wide-field illumination, fluorescence intensity was high both at cell edges and at cell-cell junctions near the outside of the cluster (Fig. 4.2B, B'). Most of the mBBr labeling in each cell is likely to be on glutathione peptides throughout the cytoplasm (Mbemba et al., 1985). However, the area of intense mBBr labeling along cell edges is consistent with the location of actomyosin filaments (Fig. 2.2, 3.10). Myosin molecules in the "tensed" or active state have been shown to have greater exposure of Cys^{90} between the head and rod domains of the protein and increased labeling of that site with thiol-reactive dyes (Johnson et al., 2007). Thus an accumulation of active myosins could account for the intensity of mBBr labeling along cell edges. The low intensity of mBBr fluorescence in cell protrusions might be explained by the relatively small volume of these thin structures in comparison with the large volume of the cell body. Interestingly, the intensity of mBBr fluorescence was greater on stiff Fn-coated PDMS gels (Fig. 4.2C, D) than on softer ones (Fig. 4.2E, F). These data suggest that mBBr labeling is more intense when cells are under higher tension.

mBBr labeling of mitochondrial aconitase increases when tension is applied to cells adherent to Fn

To identify proteins that are differentially labeled when cells are under tension, cells were plated on Fn-coated stretch devices, labeled with mBBr, stretched, lysed and separated by SDS-PAGE (as shown in Fig. 4.1B). The intensity of mBBr labeled protein in each band (Fig. 4.3A) was normalized to the total amount of protein labeled with Coomassie stain in each band (Fig. 4.3B). Aligned line scans of each lane of the gel revealed peaks and valleys in the normalized ratio of mBBr intensity in stretched samples relative to control samples (Fig. 4.3C). Several bands (Fig. 4.3A, B, C, arrowheads) were differentially labeled in repeated experiments (Fig. 4.3D). One of these bands (#6, red arrowhead, red bar) was selected for further analysis using mass spectrometry. Lysates from labeled stretch and control samples were run out on SDS-PAGE gels in duplicate and the selected band excised. The excised samples were subjected to in-gel digestion with the enzymes trypsin or chymotrypsin. Peptides were identified and mBBr labeling quantified by liquid chromatography-coupled tandem mass spectrometry (LC-MS/MS).

Analysis of the mass spectrometry data yielded three peptides that were differentially labeled by mBBr in stretched and control samples (Fig. 4.4A, B). The differentially labeled peptides all corresponded to two variants of mitochondrial aconitase, a citric acid cycle enzyme. One of the differentially labeled peptides was common between the two variants. Cys-labeling of the common peptide was increased by 20% in stretched cells relative to control cells. Labeling of each of the unique peptides was increased by greater than 50% in samples from stretched cells. Overall sequence coverage of this high abundance protein was very good, comprising peptides

corresponding to >40% of the protein sequence (Fig. 4.5A, B, yellow highlighting). However, there were several Cys residues in each aconitase variant that were not represented among the peptides identified by mass spectrometry (blue highlighting). Additionally, some peptides were represented only once or a few times among the identified peptides. Therefore, additional mass spectrometry runs would be required to verify that the two differentially labeled Cys residues are the only Cys residues in aconitase that are exposed in response to force on integrin adhesions. These two differentially labeled residues are located outside of the iron-sulfur (Fe-S) cluster binding region that is known to be essential for the enzymatic activity of aconitase (Lauble and Stout, 1995). Rather, both residues reside in the region identified as the "swivel" domain. Aconitase is thought to undergo a conformational change upon activation but it is not clear whether these two Cys residues are likely to be exposed in the "active" or the "inactive" state. The identification of mitochondrial aconitase as a target of mechanically sensitive signaling pathways suggests that cellular metabolism may be altered in response to mechanical stimuli, but this effect is likely to be a result of downstream signaling events rather than direct physical linkage.

Proteins related to cellular "housekeeping" are differentially labeled by mBBr when tension is applied to C-cadherin adhesions

There are three broad categories of proteins that could be identified using variations on the dye labeling protocol described above: (1) proteins that are directly load bearing, (2) those involved in proximal signaling events, and (3) those undergoing conformational change as a downstream consequence of the various signaling pathways

initially activated by mechanical stimuli. The CS-MS method is predicted to identify proteins in all three categories. Mechanotransduction is rapid and occurs on a scale of microseconds-seconds (Na et al., 2008). Thus, the initial 10-15 min time frame used for dye-labeling following stretch (e.g. Fig. 4.3) was certainly sufficient to allow long-range intracellular responses. However, these conditions do not permit discernment of long-range responses versus those more proximal in time and space to the applied force. One way to bias attention to these more proximal events is to decrease the post-stretch labeling time to 1 minute or less by loading the cells with the Cys-reactive dye prior to stretch. A practical technical limit of 15 seconds from time of stretch to lysis was established empirically. Although this limits the analysis to those proteins that increase (rather than decrease) in labeling intensity upon stretch, it has the advantage of narrowing the results to differentially labeled proteins in categories 1 and 2.

Pre-labeling, stretch and immediate lysis of cells plated on C-cad.Fc-coated substrates yielded ladders of mBBr labeled bands similar to, but less intense than, the bands observed following the longer term labeling of cells on Fn (Fig. 4.6A). After normalizing the intensity of mBBr labeling (Fig. 4.6A) to the intensity of Coomassie staining (Fig. 4.6B), two bands had consistently increased mBBr labeling in stretched samples across multiple experiments (Fig. 4.6C). These bands were excised, digested with trypsin and subjected to LC-MS/MS as before. Analysis of the mass spectrometry data yielded mBBr labeled peptides corresponding to 5 different proteins (Fig. 4.7A). For each protein, only one mBBr labeled peptide was identified and not all labeled peptides were differentially labeled in stretched samples relative to controls (Fig. 4.7B). The labeled proteins all serve general “housekeeping” functions in the cell: glycolysis

[glyceraldehyde-3-phosphate dehydrogenase (GAPDH), enolase], the citric acid cycle [malate dehydrogenase], protein synthesis [elongation factor], and de-ubiquitination [ubiquitin c-terminal hydrolase]. The proteins that were not differentially labeled in stretched samples relative to controls were excluded from further analysis.

Cell motility and resistance to mechanical stress require cytoskeletal remodeling (Huveneers and de Rooij, 2013; Pollard and Borisy, 2003) which is generally quite dependent on ATP (Bugyi and Carlier, 2010). Therefore it is reasonable to expect that exogenous or endogenous application of tension to cell adhesions could trigger changes in the amount and location of energy production within cells. Differential labeling of Cys residues on both aconitase and malate dehydrogenase suggests that changes in the activity of the citric acid cycle are triggered by tension across adhesions. Furthermore, two enzymes in the glycolysis pathway had increased mBBr labeling in stretched samples. These data support the hypothesis that cellular metabolism is sensitive to mechanical stimuli. To address this hypothesis we examined the size, shape, and localization of mitochondria in single cells and cells pairs. These measures can serve as readouts of metabolic activity (Friedman and Nunnari, 2014; Galloway and Yoon, 2012). Labeling of adherent mesendoderm cells with MitoTracker revealed punctate and squiggle shaped mitochondria throughout the cell body and protrusions (Fig. 4.8A, B). No changes in mitochondrial shape or localization were observed in cell pairs relative to single cells (Fig. 4.8C, D). Further analysis of mitochondrial activity using dyes sensitive to changes in electrical potential of the mitochondrial membrane will be required in order to ascertain whether tension (or cell-cell contact) alter metabolic activity in mesendoderm cells.

Overall, these findings confirm that conformation-dependent changes in Cys reactivity upon application of force to mesendoderm cells can be detected. The CS-MS assay applied to whole cells represents an unbiased approach likely to yield numerous unexpected players in adhesive mechanotransduction, and this preliminary finding highlights the broad range of proteins and pathways that may be identified. However, these results also highlight potential limitations of the CS-MS approach. First, CS-MS analyses of total protein in stretched cells will favor the identification of the most abundant cellular proteins, which are unlikely to include many targets of greatest initial interest (i.e., those proteins involved in sensing and responding to mechanical forces applied at sites of cell adhesion). Second, even if the CS-MS approach provides clear evidence of a change in the ratio of conformational states of a given protein as a downstream indirect consequence of a mechanical stimulus (e.g., as in the case of aconitase), although potentially interesting, this knowledge is unlikely to shed new light on the question of how mechanical signals are being sensed.

Alternate approaches

In order to focus on the signaling events proximal to mechanical stimulation of adhesions, a basal extraction was performed to isolate only those proteins that were physically associated with adhesion complexes. The general strategy was to lyse cells in place on the adherent substrate to remove apicolateral membrane, cytoplasm, nucleus, mitochondria and other organelles but leave behind the basal membrane, with embedded adhesion molecules, the cortical cytoskeleton and associated proteins. Conditions and protocols for basal extraction have been established successfully by Martin Schwartz's

lab and others (Taddei et al., 2002) in order to enrich for adhesive and cortical proteins. Preliminary tests were performed using mesendoderm cells plated on C-cad.Fc coated dishes. In each test, C-cadherin was retained in the final lysate from the basal adhesion extraction (BAE) protocol (Fig. 4.9, green box) but the cytosolic protein GAPDH was nearly absent (Fig. 4.9, red box). Linker proteins such as β-catenin and cytoskeletal elements such as actin might be expected to be present in the cytosolic and/or nuclear fractions as well as in physical association with the cadherin adhesion complex. The amounts of β-catenin and β-actin present in the BAE samples were highly variable between experiments (Fig. 4.9, yellow boxes). The presence or absence of other known adhesion-associated proteins (e.g. plakoglobin, α-catenin) and cytosolic or nuclear proteins (e.g. ran, histone H1) must be assessed to determine the efficacy of this protocol. However, these data suggest that this approach enriches for proteins most likely to be involved in sensing and responding to an applied force.

Biochemical purifications typically require many steps and long incubation times and the sensitivity of mBBr fluorescence to light exposure makes handling of Cys-labeled samples difficult. To avoid this pitfall, an alternate thiol-reactive reagent was used to test the feasibility of purification or immunoprecipitation in conjunction with Cys-labeling and application of stretch to adherent cells. N-[6-(Biotinamido)hexyl]-3-(2-pyridyldithio)propionamide (Biotin-HPDP) is a membrane-permeable biotin derivative that reacts reversibly with exposed thiol groups. Biotin-HPDP does not bind covalently to Cys residues and therefore cannot be used to identify labeled peptides by mass spectrometry. However, it is not sensitive to light and binds strongly to streptavidin/neutravidin, which may be used to purify labeled peptides when conjugated

to agarose beads or to probe western blots when conjugated to horseradish peroxidase (HRP) (Fig. 4.10A).

Samples from Biotin-HPDP labeled cells were initially purified using Streptavidin-agarose beads and proteins separated by SDS-PAGE. No differences were observed between control and stretch samples when separated proteins were stained with Coomassie blue (data not shown). Probing of the blotted samples with antibodies directed against Pkg (Fig. 4.10B, B') or C-cadherin (data not shown) revealed minimal labeled sample in either control or stretch samples. Very little Pkg was evident in the supernatant (supe) not bound to the beads, perhaps indicating that the samples were not sufficiently concentrated or that the sample was subject to degradation during purification. This specific approach has a number of limitations including the lack of a definite positive control for proteins known to have differential labeling of Cys residues in response to stretch, although GAPDH could serve this function (Fig. 4.7). Furthermore, the separation of proteins by 1D SDS-PAGE may be insufficient for visualization of differences in the presence or intensity of proteins in Coomassie- or silver-stained gels.

Another alternate approach is "targeted" immunoprecipitation (IP) in conjunction with Cys-labeling. Pull down experiments allow the focus of initial attention to be on promising candidates, based on what we already know about mechanosensitivity of the mesendoderm (Chapter 2) (Weber et al., 2012). For example, IPs of plakoglobin (Pkg)-containing protein complexes before and after stretch and Cys-labeling are of primary interest because we have determined independently that Pkg is a key component of the cadherin-dependent response in the mesendoderm (Fig. 2.10, 2.11). Samples from

Biotin-HPDP labeled cells were immunoprecipitated with agarose beads conjugated to an antibody directed against Pkg, proteins separated by SDS-PAGE and blots probed with HRP-neutravidin. Several bands were evident in the immunoprecipitated samples but there was no band evident at the expected size for Pkg and there were no visible differences between control and stretch samples (Fig. 4.10C, C'). These results suggest that Pkg itself does not undergo a conformational change in response to tension on cadherin adhesions, or at least not one that results in exposure of an otherwise shielded Cys residue. Further investigation is needed to determine whether there are any significant but subtle changes in thiol-labeling of Pkg-associated proteins in response to stretch, but these data provide proof of concept for the isolation of Cys-labeled adhesion complexes by IP.

4.5 Discussion

The data presented here represent the initial stages of an ongoing investigation into the mechanisms by which intrinsic mechanical stimuli are transduced into the cellular signals that guide morphogenesis. The molecular basis of mechanotransduction is challenging to unravel as it is likely there is more than one protein that is responsible for sensing and transducing force in a given system. No one yet knows how large or complicated mechanically sensitive adhesion complexes might be; just a few proteins or numbering in the tens or even hundreds. In response to application of forces, adhesion complexes generate signals that then feed into common cellular signaling pathways

(Jaalouk and Lammerding, 2009; Wozniak and Chen, 2009), creating a vast network of proteins involved in the cellular response to mechanical stimuli.

Limitations and optimization of CS-MS

Adaptation of Cys-shotgun mass spectrometry (CS-MS) to the study of force-induced conformational change in a physiological model of collective cell migration has provided a powerful new tool for investigating mechanisms of mechanotransduction. While it is true that CS-MS cannot detect all proteins undergoing conformational change (i.e., those proteins lacking cysteines altogether or that lack cysteines in conformationally sensitive domains), the initial results from this study and those from the Discher lab (Engler et al., 2008; Johnson et al., 2007) suggest that CS-MS is likely to yield many candidates worthy of further evaluation and analysis. A query of the sequences of 70 adhesion-related and cytoskeletal proteins revealed that more than half of these proteins contain 10 or more Cys residues. Only 1 protein lacked cysteines altogether. It is currently not possible to estimate the fraction of these cysteines that will become exposed or hidden in response to a change in mechanical force. However, the broad distribution of cysteines in these proteins increases the likelihood that the CS-MS approach can successfully detect a change in the conformations of many proteins.

Although the CS-MS assay can detect proteins that undergo conformational change in response to applied mechanical forces, it cannot necessarily distinguish proximal signaling events from downstream events. As discussed earlier, mechanically sensitive proteins can be grouped into three broad categories: directly load bearing, proximal signal transducers and downstream signal transducers and targets. In the initial

tests of the CS-MS protocol, the proteins identified all serve what might be classified as cellular “housekeeping” functions (e.g. mitochondrial aconitase) and would likely be classified as downstream targets of mechanically stimulated signaling. One explanation for the failure to identify proximal signaling components is the low abundance of such proteins relative to the proteins involved in metabolism and other core cellular housekeeping functions. Mass spectrometry analysis is limited by the peak capacity of the instrumentation, which is the number of compounds that can be distinguished with a reasonable degree of certainty (de Hoffmann and Stroobant, 2007). In a complex mixture of proteins there is a high statistical probability that more than one peptide product will be eluted from the liquid chromatography column into the mass spectrometer at the same time. Although proteins are separated by gel-electrophoresis prior to proteolytic digestion, these samples still contain many proteins. The final result is then skewed toward the most abundant proteins and there is a low probability of identifying labeled peptides from low abundance proteins (Gygi et al., 2000).

Further optimization of the dye labeling, sample preparation and mass-spec protocols will allow increased sequence coverage and identification of modifications in lower abundance proteins. Recent improvements in analysis of 2D electrophoresis, new peptide separation schemes and the use of tagged proteins and peptides may all be useful in honing the CS-MS technique to best assess conformational changes in low abundance proteins (Aebersold and Mann, 2003; Rabilloud et al., 2010). Another challenge is the selection of proteins to act as positive and negative controls. Proteins such as non-muscle myosin IIa and Fn have been shown to undergo conformational changes detectable by Cys-reactive dye labeling in response to force (Johnson et al., 2007; Little et al., 2009)

and could be used as positive controls in future experiments. We have also identified proteins (based on high coverage by mass-spec) that could serve as negative controls in further analyses. These include proteins with cysteines that are either consistently dye-labeled (e.g., elongation factor 2, EF-2) (Fig. 4.7) or unlabeled (e.g., large ribosomal protein P0) (data not shown) regardless of stretch conditions.

Biochemical fractionation and targeted immunoprecipitation

Pull downs of protein complexes with known mechanosensitivity (e.g. Fig. 4.10) may be useful for increasing coverage of lower abundance proteins by mass-spec (Malovannaya et al., 2010). Various tagging schemes such as tandem affinity purification (TAP) or localization and purification (LAP) tags have been used successfully to purify protein complexes for mass spectrometry (Cheeseman and Desai, 2005; Cheeseman et al., 2004; Rigaut et al., 1999). Although lacking the advantages of an unbiased "shotgun" approach, IP or tag based experiments could provide direct evidence of force-dependent recruitment of proteins to the complex or conformational changes resulting from forces applied to specific adhesions. However, if a protein is only recruited to a complex that is stressed, it may dissociate from the complex once the cell is lysed and thus could be missed by IP. While such a protein would not be identified as a member of the complex in this case, it would likely still be identified as mechanically responsive in a more unbiased CS-MS screen. Chemical crosslinking could be used to ameliorate this problem by stabilizing labile protein complexes during the biochemical separation and purification steps leading up to mass spectrometry analysis (Rappsilber, 2011).

Proteins represented in the "shotgun" assay but with poor sequence coverage would also be good subjects for a targeted approach in cases where antibodies suitable for IP are available. This would maintain the broad appeal of an initially unbiased approach but would help confirm differential Cys-labeling of candidate proteins by improving sequence coverage. Analysis of mass spectrometry data from complex mixtures could be supplemented by the use of an MS-BLAST program that performs cross-species comparisons to maximize the identification of peptides (Liska et al., 2004). Clearly, analyzing candidate bands arising from all of these various conditions by mass-spectrometry would be impractical and prohibitively expensive. However, the use of fluorescent Cys-reactive dyes or Biotin-HPDP allows analysis of changes in Cys-labeling by simple densitometric scans of samples run out on 1D gels. These straightforward assays enable the prioritization of the most promising approaches and samples for further analysis by mass spectrometry.

Mechanical regulation of cellular metabolism

Although no direct or proximal mechanotransducers were identified in the initial stages of this study, the data indicate that cellular energy production may be regulated by mechanical stimuli. The protein aconitase is known to undergo a conformational change related to its activity (Lauble and Stout, 1995). Both of the differentially labeled Cys residues detected reside in the so-called "swivel" domain of aconitase and may be exposed upon a change in activation state. We initially dismissed aconitase as a "housekeeping" enzyme not especially relevant to the proximal events of mechanotransduction. However, mechanical force might in fact trigger interesting

changes in metabolism or other core cellular functions, even though a direct link between force and an enzyme like aconitase is unlikely. Interestingly, aconitase activity can be inhibited by nitric oxide (NO), a second messenger known to be regulated by mechanical stimuli (Harrison et al., 2006; McGarry et al., 2008; Tórtora et al., 2007).

If metabolic activity is altered in mesendoderm cells in response to force applied to adhesion complexes, how might these changes be confirmed? The morphology and localization of mitochondria are known to be related to the energy usage of a cell (Friedman and Nunnari, 2014; Galloway and Yoon, 2012). Fusion and fission events are correlated with changes in metabolic activity and fission is thought to be important for transport of mitochondria to parts of the cell where ATP is needed. Inhibition of fusion and fission events has been shown to impair migration of epithelial tumor cells (S. P. Desai et al., 2013). Although pairs of mesendoderm cells display protrusive polarity and cytoskeletal organization that is distinct from that observed in single cells (Fig. 2.3, 2.12), preliminary analysis reveals no obvious alterations in the localization or shape of mitochondria in cell-pairs compared with single cells (Fig. 4.8). A recent study indicated that mitochondrial fission events may be regulated by mechanical stimuli, specifically cellular contractility (Korobova et al., 2014). Therefore, further investigation into mitochondrial shape and localization may be warranted to determine whether fusion or fission events are an intermediate in the pathway linking tension on cell adhesions and changes in metabolic activity.

Metabolic activity can be assessed more directly through the use of fluorescent dyes that are sensitive to mitochondrial membrane potential (e.g. tetramethylrhodamine), or by measuring the cellular levels of ATP or other metabolites. Of course, the most

critical aspect of such an analysis is the correlation of metabolic activity with force. One way to do this is to combine live imaging of tetramethylrhodamine labeled cells with traction force microscopy. This would facilitate the correlation of local mitochondrial activity with the spatial distribution of traction forces exerted by a migrating mesendoderm cell. An alternate method is to monitor mitochondrial activity or the presence of metabolites in cells that are being stretched or subject to the bead pull assay described previously (Chapter 2) (Weber et al., 2012).

Future directions

The question of what to do with a catalog of mechanosensitive candidate proteins, and in what order, is of considerable importance but also very difficult to predict. Proteins of interest for further study could be prioritized based on whether they were already known to be involved in cadherin or integrin linkages to the actin and intermediate filament cytoskeletons. Their role in mechanotransduction would be investigated initially through the use of antisense morpholinos to knock down expression of each candidate protein in embryos. The cell pull assays described in Weber et al. (Fig. 2.1) (Weber et al., 2012) could then be used to ask whether mesendoderm cells remain mechanoresponsive in the absence of the candidate protein. Any proteins implicated as mechanically important in this system would be subject to structure-function and biophysical analyses to confirm stress induced conformational changes, identify the domains affected and the functional significance of these changes (e.g., interactions with other proteins, activation of kinase activity). A more direct but technically challenging approach is to identify candidate proteins that could be engineered to signal where and

when a physiologically relevant protein undergoes a conformational change in response to forces generated by cells or explanted tissues. For example, FRET biosensors have recently been used to investigate force induced conformational changes in vinculin in living cells (Grashoff et al., 2010). Although it is now only in the early stages, the final goal of this continuing study is to produce a list of proteins unfolded in response to physiologically relevant forces and to establish possible pathways for translation of the observed unfolding into polarization and collective cell migration.

Figure 4.1

Schematic of experimental strategy. (A) Force is hypothesized to induced conformational changes that may alter the exposure of hydrophobic cysteine residues to the cytosolic environment. Thiol reactive dyes such as monobromobimane (shown) form a covalent bond with exposed cysteines and fluoresce upon reaction. (B) Flowchart of the experimental strategy used for application of force to the adhesive complexes of mesendoderm cells, labeling of exposed cysteines and either live cell imaging or identification of labeled peptides. (C) Stretch device used for application of tension to the integrin or cadherin adhesions of mesendoderm cells. Stretch is applied by turning the black knob on the right until stopped by set screws. This results in a nearly uniaxial strain of the silastic membrane of along the x-axis (16%) as well as a small decrease (3%) in strain along the y-axis. (D) Equation for calculation of mBBr fluorescence intensity (F) normalized to Coomassie blue staining (C, inverted intensity) in stretched (S) and unstretched (U) samples. B = selected band, T = total intensity of the lane (to normalize for variations in labeling of all proteins by mBBr or Coomassie blue).

A

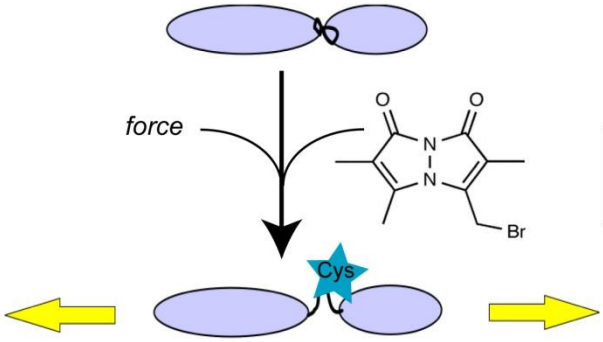

B

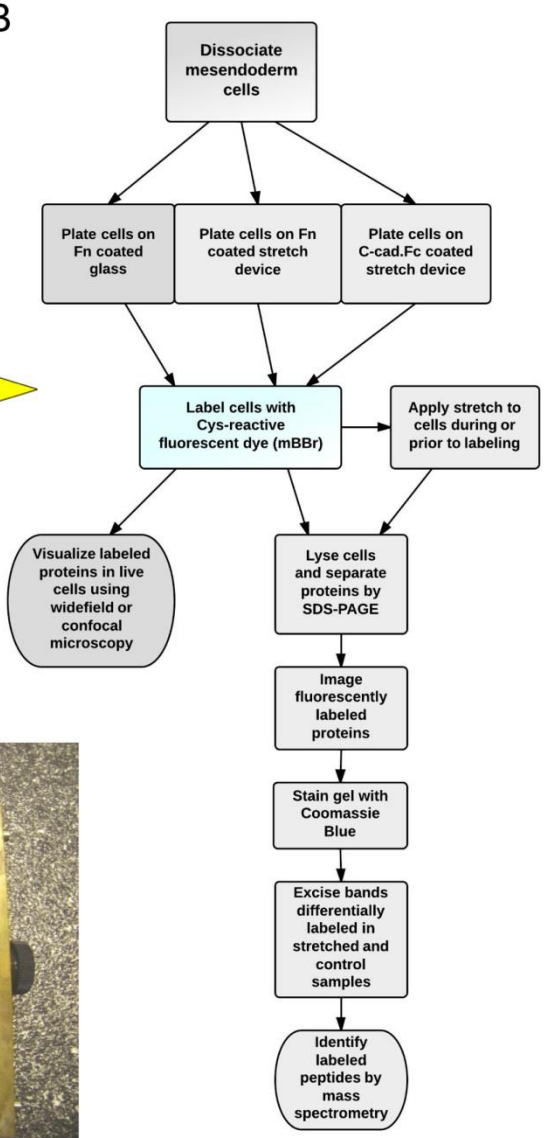

C

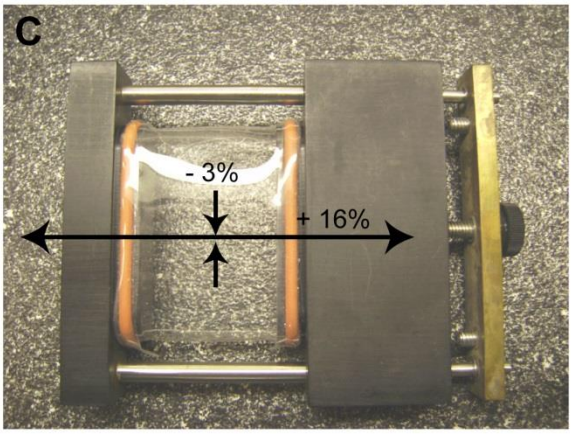

D

$$\frac{S_{BF}}{S_{BC}} \Big/ \frac{S_{TF}}{S_{TC}} = S \qquad \frac{U_{BF}}{U_{BC}} \Big/ \frac{U_{TF}}{U_{TC}} = U$$

Figure 4.2

A thiol reactive dye preferentially labels edges of mesendoderm cells and cells on stiff substrates. (A-B') Mesendoderm cells spread on Fn coated glass and labeled for 10 min with 200mM mBBr. Images of live cells were acquired with wide-field illumination following quenching and wash-out of unreacted dye. (A, B) Brightfield images of mBBr labeled single cell (A) or cell cluster (B). (A', B') Pseudo-colored images of fluorescence intensity in the mBBr labeled cells shown in (A, B). White arrowheads denote cell edges and cell-cell contacts, black arrowheads denote protrusions. (C-F) Pseudo-colored fluorescent images of mesendoderm cells plated on stiff (C, D) or soft (E, F) Fn coated PDMS substrates and labeled for 10 min with 200mM mBBr. Scale bars = 50 μm.

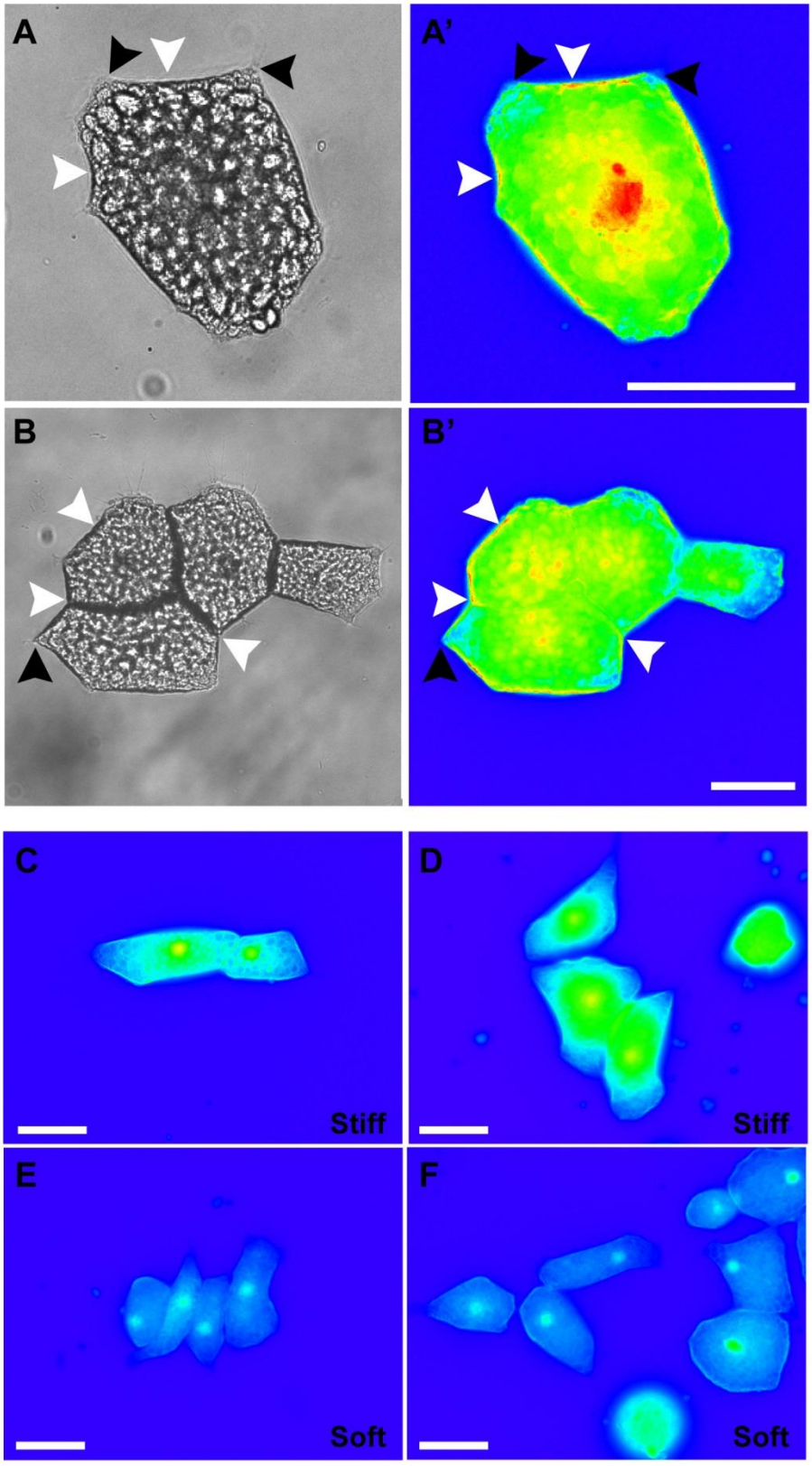
A
A'
B
B'
C
Stiff
D
Stiff
E
Soft
F
Soft

Figure 4.3

Proteins in lysates from stretched and unstretched mesendoderm cells on fibronectin are differentially labeled with a thiol reactive dye. (A, B) 4-20% gradient SDS PAGE gel loaded with lysates from mesendoderm cells plated on Fn coated stretch devices and labeled with mBBr. (A) Image of gel illuminated at 394 nm (pseudo-colored). (B) Image of Coomassie stained gel from (A) (image inverted). (C) Densitometric profile of percent change in fluorescence intensity derived from a single representative SDS PAGE gel shown in (A, B). (D) Data compiled from multiple experiments and gels, highlighting the bands showing most change in stretched versus unstretched conditions and greatest reproducibility. Arrowheads in (A-C) indicate 6 gel regions (numbered 1-6) showing reproducible changes, red arrowhead and bar mark the band selected for analysis by mass spectrometry. Data are mean ±SEM, N=3.

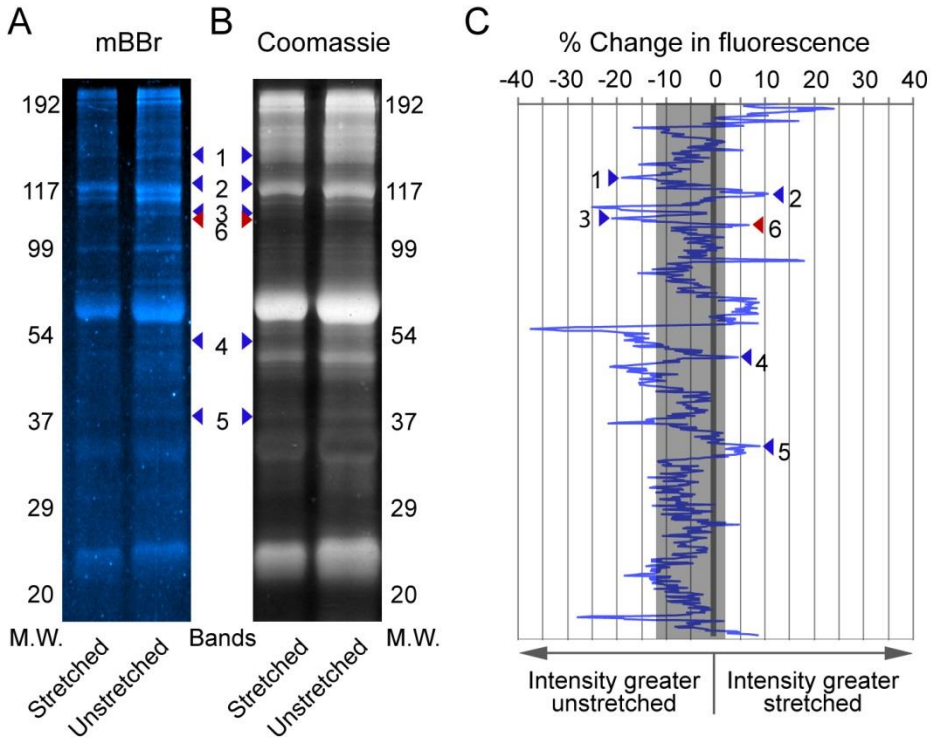
A
mBBr
B
Coomassie
C
% Change in fluorescence
192
117
99
54
37
29
20
M.W.
Stretched
Unstretched
Bands
1
2
3
6
4
5
-40 -30 -20 -10 0 10 20 30 40
Intensity greater unstretched
Intensity greater stretched

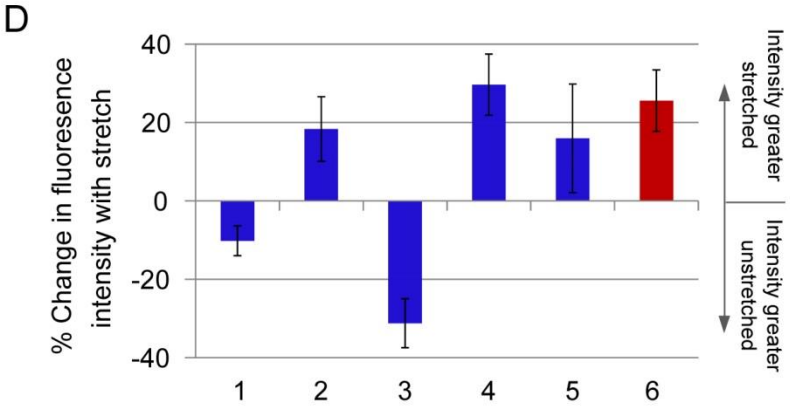
D
% Change in fluoresence intensity with stretch
40
20
0
-20
-40
1
2
3
4
5
6
Intensity greater stretched
Intensity greater unstretched

Figure 4.4

Cysteine residues in mitochondrial aconitase proteins are differentially labeled in stretched and unstretched samples. (A) Ratio of mBBr labeled peptides to IAM labeled peptides identified by CS-MS of control (unstretched) and stretched mesendoderm cells on Fn coated stretch devices. Peptides shown are those that were found to be differentially labeled in control and stretch conditions and are segments of two variants of the mitochondrial aconitase protein. (B) Ratios of stretched versus control samples, from the data shown in (A).

A

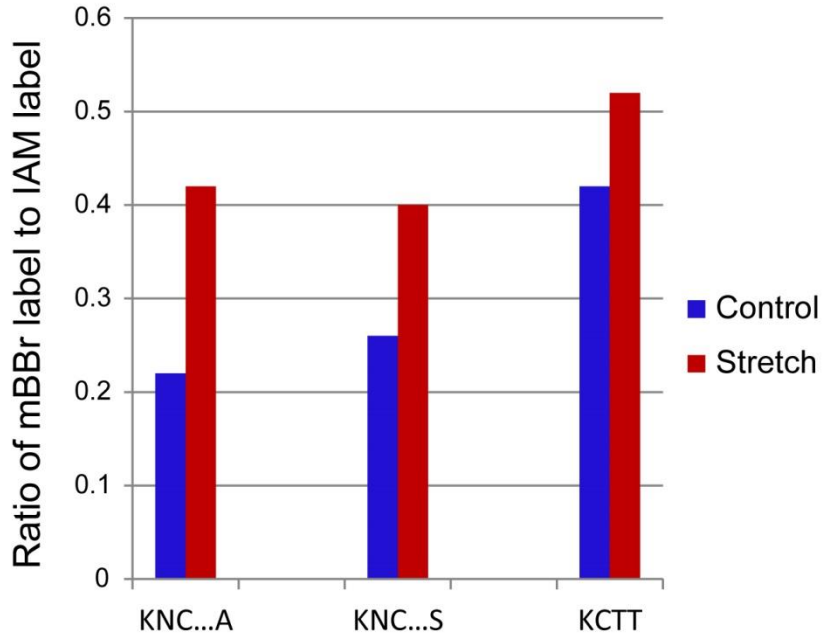

B

Aconitase peptides	Stretch : Control
KN<u>C</u>VNQEYG<u>A</u>VPDTARY	1.91
KN<u>C</u>VNQEYG<u>S</u>VPDTARY	1.54
K<u>C</u>TTDHISAAGPWLKF	1.21

Figure 4.5

Sequence coverage of the two isoforms of mitochondrial aconitase. (A-B) Complete protein sequence of the two variants of the *Xenopus laevis* mitochondrial aconitase (A) LOC398139 aconitase and (B) aconitase 2, annotated to show peptides identified by mass spectrometry and other key features. Yellow highlighting indicates peptide sequence identified in the mass spectrometry analysis, blue highlighting indicates cysteine residues in sequence not represented in the mass spectrometry results, green highlighting indicates cysteine residues labeled with IAM, red highlighting indicates cysteine residues labeled with mBBr, red text indicates the cysteine residues that are critical for binding of the iron-sulfur cluster that is essential for the activity of aconitase, underlining marks the "swivel domain" of the aconitase protein.

A

>gi|46329514|gb|AAH68910.1| LOC398139 protein [Xenopus laevis]
MASYCLLASRLQQVLGHGARRYHVSSVLCQRAKVAMSHFEANEYVNYEKLDKNINIVRKRLDRPLTLSEK
IVYGHIDDPVSQEIVRGKTYLRLRPDRVAMQDATAQMAMLQFISSGLARVAVPSTIHCDHLIEAQLGGEK
DLKRAKDINQEVYNFLATAAAKYGVGFWKPGSGIIHQIILENYAFPGVLLIGTDSHTPNGGGLGGICIGV
GGADAVDVMAGIPWELKCPNVIGVKLTGQLSGWTSPKDVILKVAGILTVKGGTGAIVEYHGPGVDSISCT
GMATICNMGAEIGATTSVFPYNHRMKKYLDKTGRSEIASLTDEFKSNLVPDEGCEYDQLIEINLDELKPH
INGPFTPDLANPVSEVGAVAEQKGWPLDIRVGLIGSCTNSSYEDMGRAAAVARQALDHGLKCKSQFTITP
GSEQIRATIERDGYAAVLRDVGGVVLANACGPCIGQWDRKDIKKGEKNTIVTSYNRNFTGRNDANPETHA
FVTSPEIVTALSIAGTLKFDPERDFLTGADGKKFKLQPPDADELPKSSFDPGQDTYQHPPKDGNSLQVEV
SPTSQRLQLLEPFDKWDGKDLENMQILIKVKGKCTTDHISAAGPWLKFRGHLDNISNNLLIGAINIENNK
ANSAKNCVNQEYGSVPDTARYYKAHGIKWVVIGDENYGEGSSREHAALEPRHLGGRAIITKSFARIHETN
LKKQGLLPLTFSDPADYDRIHPEDKITLAGLKDLAPGKPVKCIITHQNGSQETILLNHTFNETQIEWFQA
GSALNRMKELQK

B

>gi|147904130|ref|NP_001086263.1| MGC84375 protein [Xenopus laevis]
MASYCQLASRLQQALGHGARRYHISSVLCQRAKVAMSHFEANEYINYEKLDKNINIVRKRLDRPLTLSEK
IVYGHIDDPVTQEIVRGKTYLRLRPDRVAMQDATAQMAMLQFISSGLPKVAVPSTIHCDHLIEAQLGGDK
DLKRAKDINEEVYNFLATAAAKYGVGFWKPGSGIIHQIILENYAFPGVLLIGTDSHTPNGGGLGGICIGV
GGADAVDVMAGIPWELKCPKVIGVKLTGQLSGWTSPKDVILKVAGVLTVKGGTGAIVEYHGPGVDSISCT
GMATICNMGAEIGATTSVFPYNHRMKTYLDKTGRSEIASLTDEFKSHLVPDEGCEYDQLIEINLDELKPH
INGPFTPDLANPVSEVGAVAEQKGWPLDIRVGLIGSCTNSSYEDMGRAAAVAKQALAHGLKCKSLFTITP
GSEQIRATIERDGYAAVLRDVGGVVLANACGPCIGQWDRKDIKKGEKNTIVTSYNRNFTGRNDANPETHA
FVTSPEIVTALSIAGTLKFDPERDFLTGADGKKFKLQPPDADELPKSSFDPGQDTYQHPPIDGSSLNVDV
SPTSQRLQLLEPFDKWDGKDLENMQILIKVKGKCTTDHISAAGPWLKFRGHLDNISNNLLIGAINIENNK
VNSAKNCVNQEYGAVPDTARYYKAHGIKWVVIGDENYGEGSSREHAALEPRHLGGRAIITKSFARIHETN
LKKQGLLPLTFSDPADYDKIHPEDKITLAGLKDLAPGKPVKCIITHQNGSQETIILNHTFNETQLQWFQA
GSALNRMKELQK

Legend

Peptides found by MS
Cys residues not found
Cys residues with IAM
Cys residues with mBBr
Key cys for Fe-S binding
Aconitase swivel domain

Figure 4.6

Proteins in lysates from stretched and unstretched mesendoderm cells on C-cadherin are differentially labeled with a thiol reactive dye. (A, B) 8% SDS PAGE gel loaded with lysates from mesendoderm cells plated on C-cad.Fc coated stretch devices and labeled with mBBr. (A) Image of gel illuminated at 394 nm. (B) Image of Coomassie stained gel. (C) Data compiled from multiple experiments and gels, highlighting bands showing most change between control and stretched samples and greatest reproducibility. Arrowheads in (A, B) indicate gel regions showing reproducible changes, only the regions shown here (1 and 5) were selected for analysis by mass spectrometry. Data are mean ±SEM, N=3. * indicates $p<0.05$

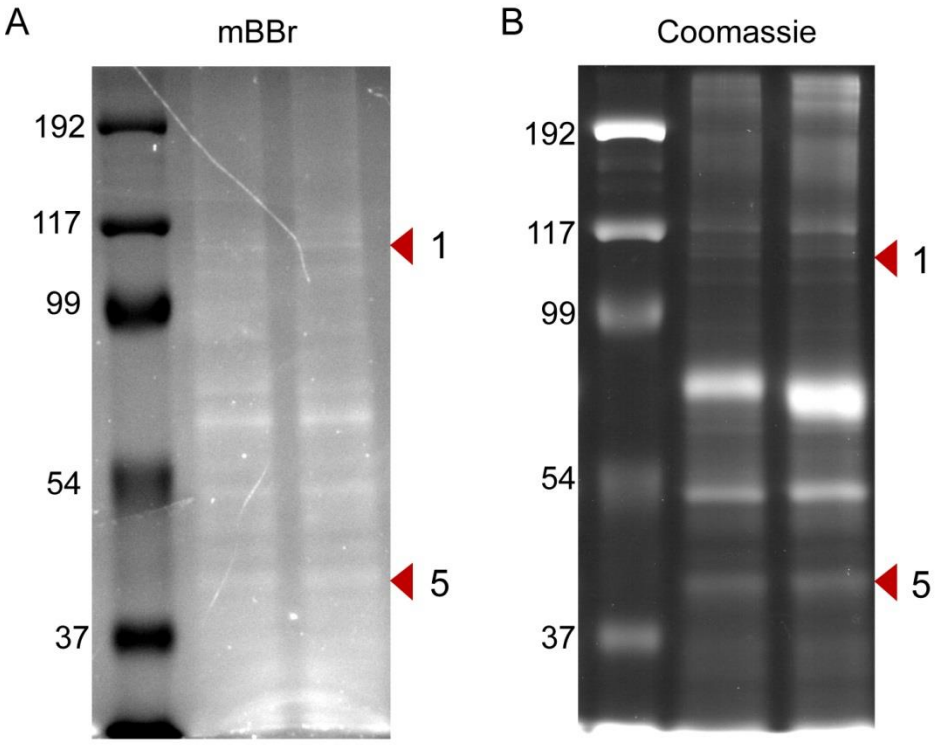
A
mBBr
192
117
99
54
37
1
5
B
Coomassie
192
117
99
54
37
1
5

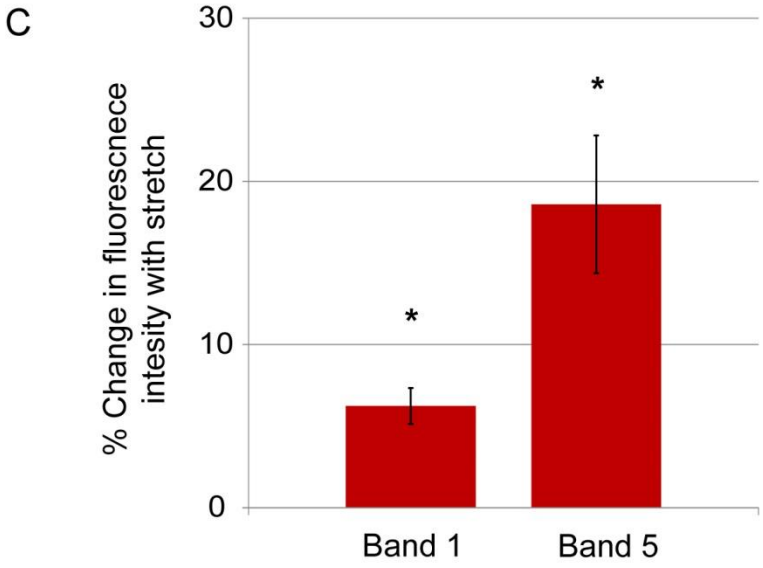
C
% Change in fluorescnece intesity with stretch
30
20
10
0
*
*
Band 1
Band 5

Figure 4.7

Differentially labeled proteins are primarily related to cellular metabolism. (A) Table of data from mass spectrometry analysis of the bands highlighted in Figure 4.6. Peptides were identified by CS-MS of mesendoderm cells on C-cad.Fc coated stretch devices. Red text indicates labeled cysteine residues. Control refers to unstretched samples. mBBr/IAM indicates the number of peptides labeled with mBBr/number labeled with IAM. IAM Cys is the number of distinct cysteine residues in each protein found to be labeled with IAM. mBBr Cys refers to the number of distinct cysteine residues in each protein found to be labeled with mBBr. Total Cys is the total number of cysteine residues in each protein. % coverage is the percent of protein sequence represented by all of the peptides identified by mass spectrometry. (B) Ratios of mBBr/IAM labeling on peptides from stretched vs control (unstretched) samples. For each protein the ratio is for the mBBr labeled peptide shown in (A), data are gleaned from values shown in (A).

A

Protein	Labeled peptide	Control mBBr/IAM	Stretch mBBr/IAM	IAM Cys	mBBr Cys	Total Cys	% Coverage
Malate dehydrogenase	IVEGLCINDFSR	2/6	4/8	3	1	5	56.51
GAPDH	LTGMAFRVPVPNVSVVDLTCR	1/16	1/14	3	1	5	48.96
elongation factor 2	NMSVIAHVDHGKSTLTDSLVCK	4/0	4/0	0	1	5	9.07
enolase 1a	GNPTVEVDLYTCK	0/1	1/1	3	1	7	22.95
ubiquitin c-term hydrolase	YCEGEIR	0/0	2/0	0	1	5	12.99

B

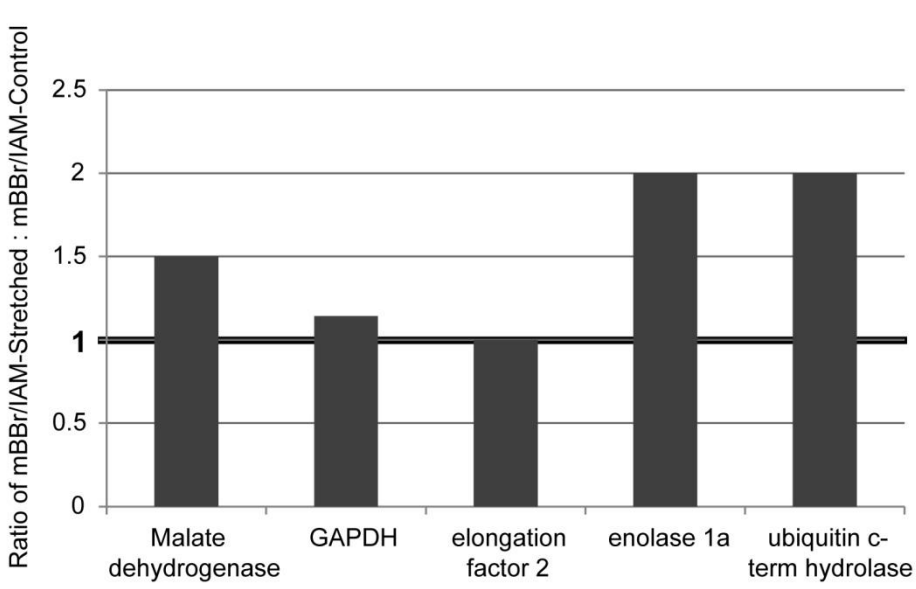

Figure 4.8

Mitochondria are spread throughout the cell body and protrusions of mesendoderm cells. (A-D) Single confocal images of mesendoderm cells plated on Fn coated glass and labeled with MitoTracker Red. (A, B) Single mesendoderm cells. (C, D) Pairs of mesendoderm cells. Arrows denote protrusions, dashed lines indicate cell-cell boundaries. Scale bars = 50 μm.

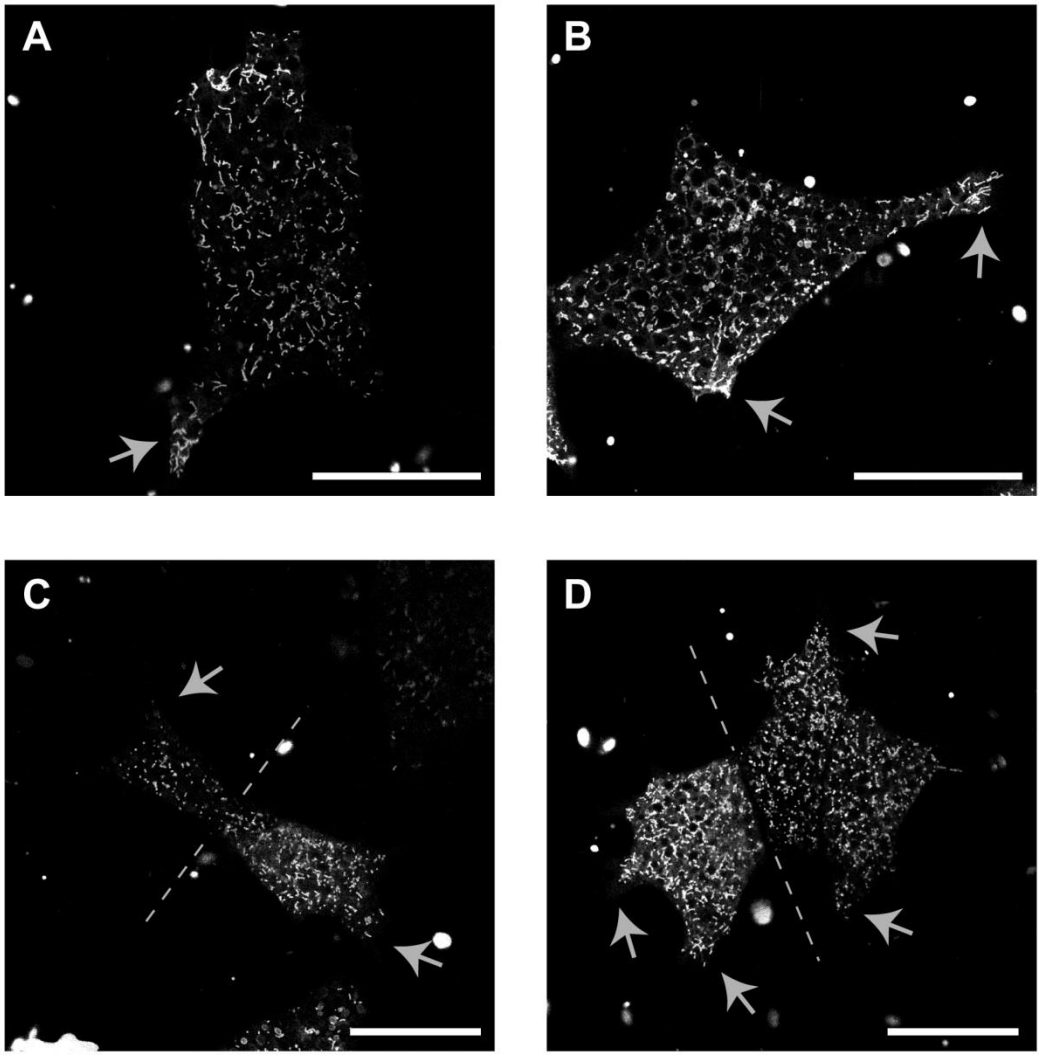
A
B
C
D

Figure 4.9

A multi-step lysis protocol separates adhesion associated proteins from cytosolic proteins. Western blot of two sets of cell lysates prepared from mesendoderm cells on a C-cad.Fc coated substrate, using the standard (control) or basal adhesion extraction (BAE) protocols (see 4.3 Materials and Methods). Blot was cut at 75 kDa marker and probed first for either C-cadherin or GAPDH then stripped and re-probed for either β-catenin or β-actin. Green box indicates a protein that should remain in BAE samples, red box indicates a protein that should be eliminated from BAE samples, and yellow boxes indicate proteins that may be bound to the adhesion complex and therefore remain in the BAE samples or may be lost or diminished in the BAE samples.

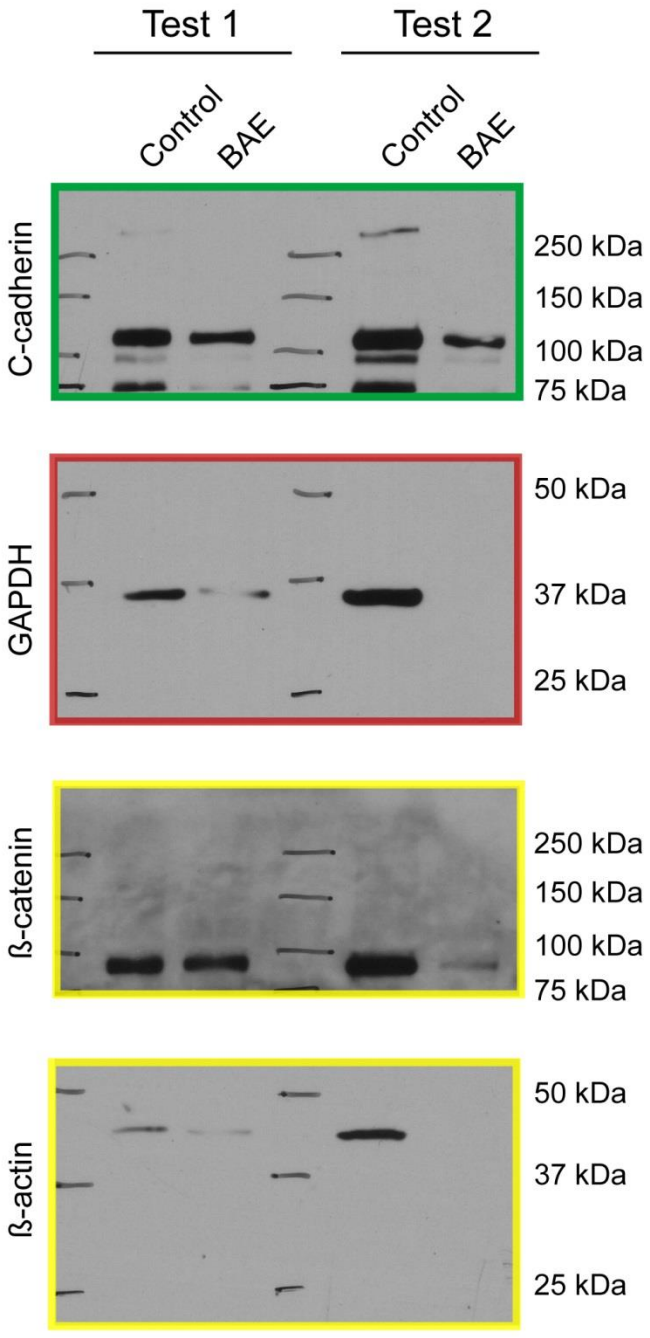
Test 1
Test 2
Control
BAE
Control
BAE
C-cadherin
250 kDa
150 kDa
100 kDa
75 kDa
GAPDH
50 kDa
37 kDa
25 kDa
ß-catenin
250 kDa
150 kDa
100 kDa
75 kDa
ß-actin
50 kDa
37 kDa
25 kDa

Figure 4.10

A thiol-reactive biotin conjugate could serve as an alternate to thiol-reactive dyes for biochemical purification of mechanically sensitive proteins. (A) Flowchart of the experimental strategy used for labeling of mesendoderm cells with Biotin-HPDP, separation of labeled proteins and analysis of differences in labeling in control (unstretched) and stretched samples. (B, B') Short (B) and long (B') exposures of a blot of samples prepared as shown in (A). Labeled proteins were precipitated with streptavidin and the blot probed with an antibody directed against Pkg. (C, C') Short (C) and long (C') exposures of blot of samples prepared as shown in (A). Labeled proteins were immunoprecipitated with an antibody directed against Pkg and the blot probed with HRP-neutravidin to detect Biotin labeled proteins that co-precipitate with Pkg.

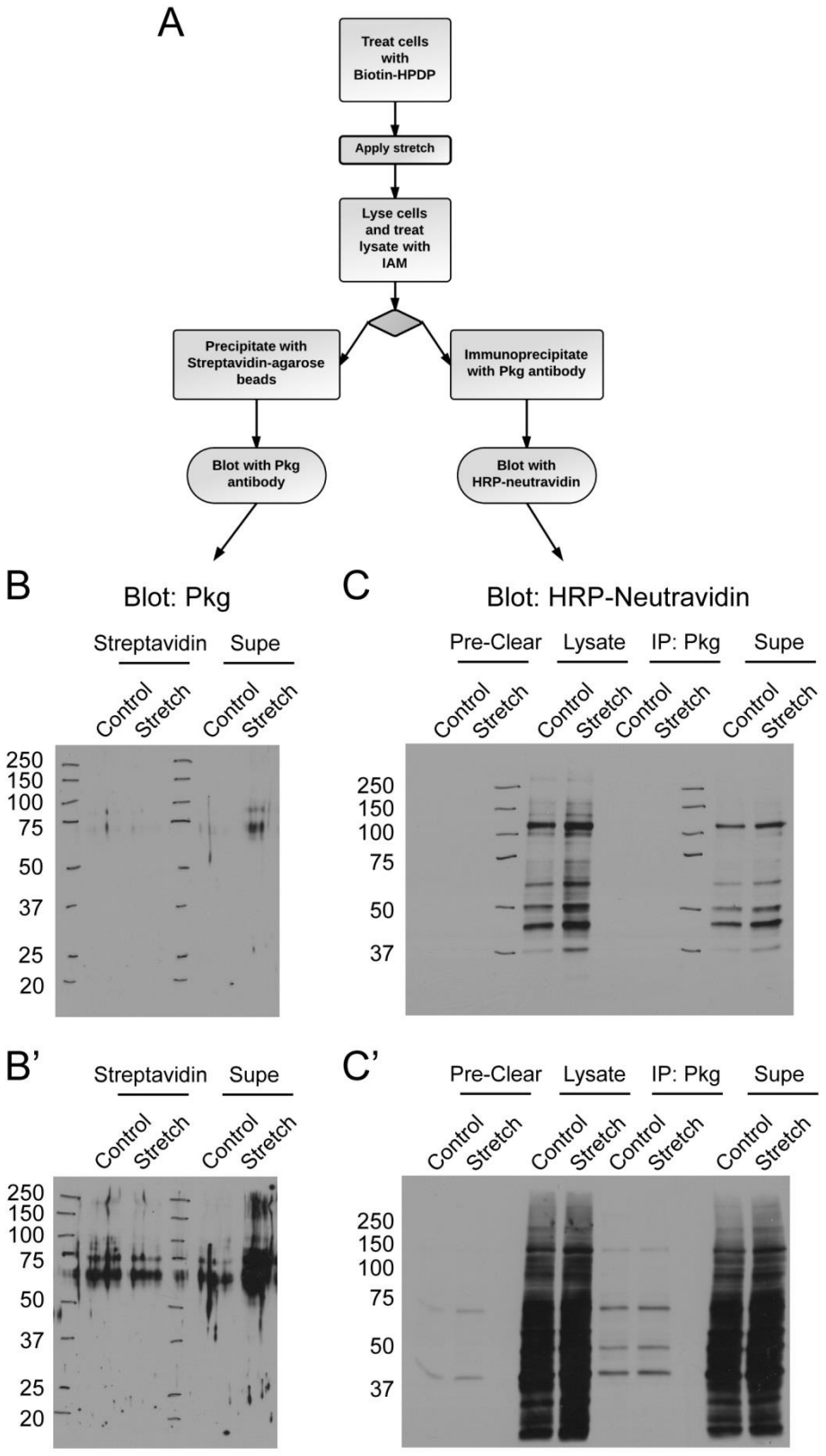
A
Treat cells with Biotin-HPDP
Apply stretch
Lyse cells and treat lysate with IAM
Precipitate with Streptavidin-agarose beads
Immunoprecipitate with Pkg antibody
Blot with Pkg antibody
Blot with HRP-neutravidin
B
Blot: Pkg
Streptavidin
Supe
Control
Stretch
250
150
100
75
50
37
25
20
C
Blot: HRP-Neutravidin
Pre-Clear
Lysate
IP: Pkg
Supe
B'
C'

Appendices

The following pages contain data that were not included in any manuscript but have bearing on the interpretation of the data presented in Chapters 2 and 3. The first figure details controls performed to ensure the even spread of morpholinos throughout injected embryos. The next figures relate to the effects FAK knockdown may have on cell-cell interactions and cadherin-based adhesion, the subcellular localization of FAK in mesendoderm cells, and a potential association between FAK and C-cadherin. The final two figures also supplement the conclusions from Chapter 3, showing the subcellular localization of fluorescently labeled Pkg and the co-expression of labeled actin and keratin within migrating FAK morphant mesendoderm tissues. Each legend includes the details of the experiment(s) and a description of the results. Discussion of these data is incorporated into the overall conclusions presented in Chapter 5.

Figure A.1

Co-injection of fluorescently-tagged dextrans serves as a reliable marker for the spread of morpholinos through embryos. (A-E) 20ng of Fluorescein-tagged β-catenin MO (Fluor β-catenin MO), FAK MO, or Control MO was co-injected with Alexa 555 dextran (final dilution 1:8) into embryos at stage 1, except in (C) where only half of the embryos were co-injected with dextran. (A-C) Embryos were imaged with the Zeiss SteREO Lumar.V12 at stage 10, views are of the ventral surface. (A) The distribution of dextran throughout the embryo was similar for each condition indicating that the sequence of the MO does not affect the spread of the co-injected dextran. (B) The distribution and intensity of the fluorescent signal from Alexa 555 dextran is equal to that of the signal from Fluor β-catenin MO, indicating similar diffusion throughout embryos. (C) The distribution and intensity of the fluorescent signal from Fluor β-catenin MO is not affected by co-injection with Alexa 555 dextran. (D, E) Explants and cells were allowed to attach and migrate for 60 minutes then imaged on a confocal microscope (see methods in Chapter 2 for details). (D) Dorsal marginal zone explants were cut from stage 10 minus embryos and plated on fibronectin (Fn) coated coverglass as previously described (see materials and methods in Chapter 2 or 3 or Davidson et al., 2004, 2002). (E) 20ng of Fluor β-catenin MO was co-injected with Alexa 555 dextran into embryos at stage 1. Mesendoderm cells were dissected from stage 11 embryos, dissociated in 1X Ca^{2+}/Mg^{2+}-free MBS and plated on Fn coated coverglass (see Chapter 2 or 3). As in whole embryos, the distribution and intensity of fluorescent signals in mesendoderm cells was identical for Alexa 555 dextran and Fluor β-catenin MO. N = 1, n = 50 embryos/condition. Scale bars = 50μm

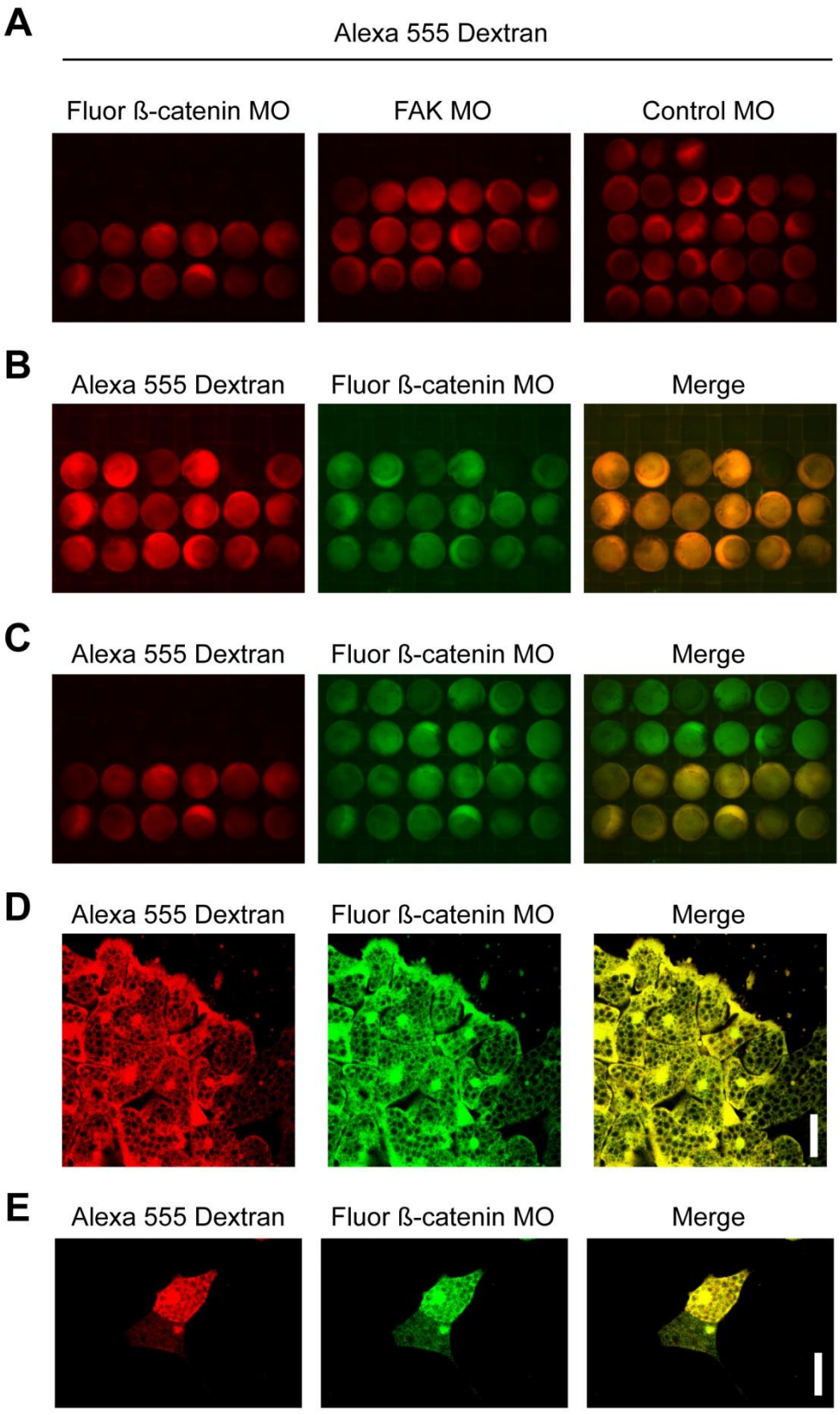
A
Alexa 555 Dextran
Fluor ß-catenin MO
FAK MO
Control MO
B
Alexa 555 Dextran
Fluor ß-catenin MO
Merge
C
Alexa 555 Dextran
Fluor ß-catenin MO
Merge
D
Alexa 555 Dextran
Fluor ß-catenin MO
Merge
E
Alexa 555 Dextran
Fluor ß-catenin MO
Merge

Figure A.2

FAK morphant cells segregate from control cells in aggregates of mesendoderm cells. A cell aggregation assay was used to test for differences in cell-cell adhesion when FAK was knocked-down. (A-C) Embryos were injected with Control or FAK MO and MOs were mixed with either Alexa 488 or Alexa 555 tagged dextrans to differentiate between control and FAK morphant cells. Mesendoderm cells were dissected from stage 11 embryos and dissociated in Ca^{2+}/Mg^{2+}-free MBS. Dissociated cells (2-4 mesendoderms per condition) were placed together in agarose coated dishes and incubated 6-8 hours at RT with gentle swirling of the dishes until solid aggregates formed. Aggregates were fixed in 3.7% formaldehyde overnight, bisected, cleared in benzyl benzoate: benzyl acetate and imaged on a confocal microscope. Images are collapsed z-stacks of 20 x 0.5µm slices. (A, B) Interior surfaces of bisected aggregates. (A) Control aggregates (Con MO mixed with Con MO, or FAK MO mixed with FAK MO) display little cell sorting behavior. (B) Aggregates made from Con MO cells and FAK MO cells together. Aggregates were made with each possible combination of dextran and MO then pseudo-colored for ease of visualization. Some sorting is evident in nearly all cases with FAK MO cells (red) moving to the interior of the aggregates. (C) Exterior surfaces of bisected aggregates made from Con MO and FAK MO cells together. The exterior surfaces are nearly exclusively composed of Con MO cells (green) that have sorted to the outside. These data show a change in cell sorting behavior that is suggestive of changes in cell-cell adhesion in FAK morphants. However, changes in cell sorting could be influenced by changes in cortical tension or deposition of Fn by the cells during the aggregation process. Scale bars = 100µm. N = 3, n = 12 (controls) 24 (mixed aggregates).

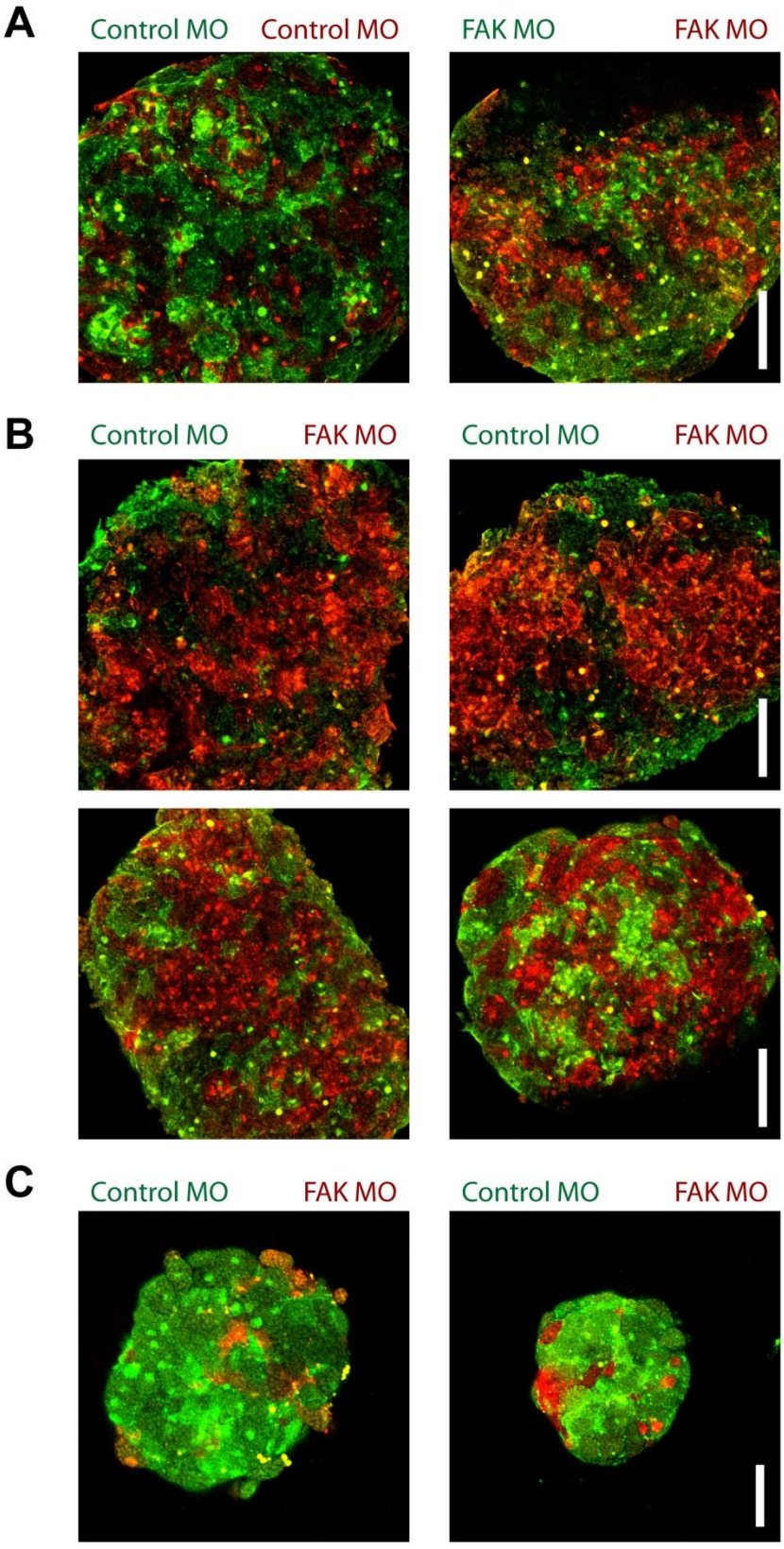
A
Control MO
Control MO
FAK MO
FAK MO
B
Control MO
FAK MO
Control MO
FAK MO
C
Control MO
FAK MO
Control MO
FAK MO

Figure A.3

FAK morphant mesendoderm cells spread and attach to C-cadherin substrates slightly better than control cells. (A) An attachment assay (short adhesion time) was used to probe for changes in adhesiveness of cells to a cadherin substrate upon depletion of FAK. Control or FAK MOs were co-injected with fluorescent dextrans to differentiate between control and FAK morphant cells. Mesendoderm cells were dissected from stage 11 embryos, dissociated, then plated in marked circles on a plastic dish coated with varying concentrations of C-cad.Fc. Cells were imaged using a Zeiss SteREO Lumar.V12 microscope, the elapsed time for image acquisition was 20 min after which time the dish was gently swirled to move unattached cells to the middle and all unattached cells removed. There is a trend toward increased attachment of FAK morphant cells at all C-cad.Fc concentrations tested but only the highest concentration showed a statistically significant difference. N = 3, n = 12 fields of cells. (B) Cell spreading on C-cad.Fc was used as an alternate measure of adhesion to cadherin. Cells were prepared in the same manner as above before plating on a glass coverslip coated with 5µg/mL C-cad.Fc and allowed to attach and spread before imaging with a Zeiss AxioObserver inverted microscope. Cell areas were quantified using Volocity and ImageJ. FAK morphant cells are significantly more spread on a cadherin coated substrate than are control cells. However, as with the aggregation assay, spreading is an imperfect measure of adhesion and the results are subject to alternate interpretations. Increased cell spreading could reflect changes in the mechanical properties of the cells (stiffness, contractility) rather than cell-adhesion per se. Data are mean ± SEM. N =1 (representative experiment, similar results obtained with different C-cad.Fc coating concentrations), n= 48 (FAK MO cells) 50 (Con MO cells).

A

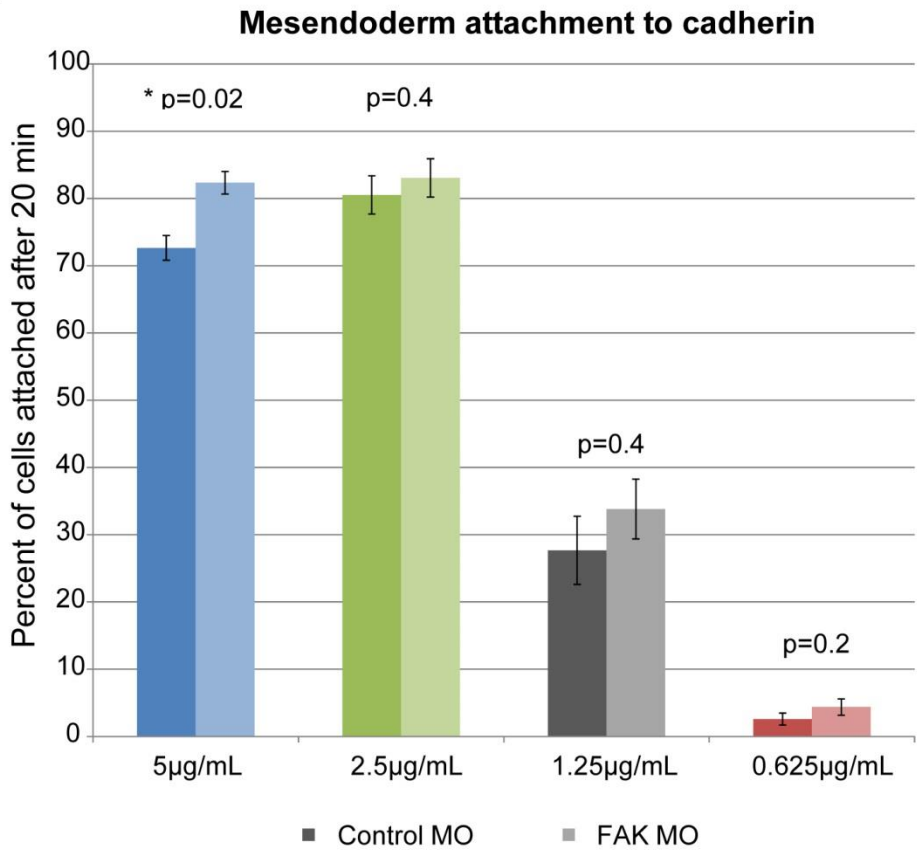
Mesendoderm attachment to cadherin
Percent of cells attached after 20 min
100
90
80
70
60
50
40
30
20
10
0
* p=0.02
p=0.4
p=0.4
p=0.2
5µg/mL
2.5µg/mL
1.25µg/mL
0.625µg/mL
Control MO
FAK MO

B

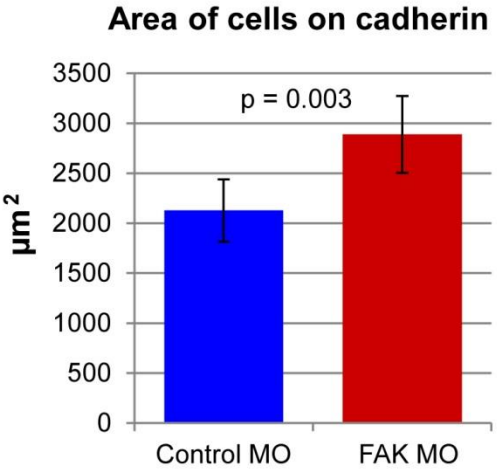
Area of cells on cadherin
µm 2
3500
3000
2500
2000
1500
1000
500
0
p = 0.003
Control MO
FAK MO

Figure A.4

Total levels of C-cadherin protein are unchanged in FAK morphant embryos. Changes in interactions of cells with each other and with cadherin coated substrates could be due to changes in expression levels of cadherins. To examine cadherin levels in FAK morphant cells, whole embryos lysates were prepared from control and FAK morphant embryos at stage 11 using standard lysis buffer. Lysates were separated by SDS-PAGE (8% gel), transferred to nitrocellulose and probed with antibodies directed against C-cadherin (6B6), FAK (2A7) and β-actin (see materials and methods in Chapter 3 for details on Morpholinos and Western blots). No change in total cadherin protein levels was apparent (C-cadherin is the only cadherin expressed at this stage), but surface levels of cadherin could change without altering the total level of cadherin protein. This concern may be addressed in the future using biotinylation of surface proteins followed by lysis and western blot. N=3, 10 embryos per condition, 1 embryo-equivalent per lane, representative image shown.

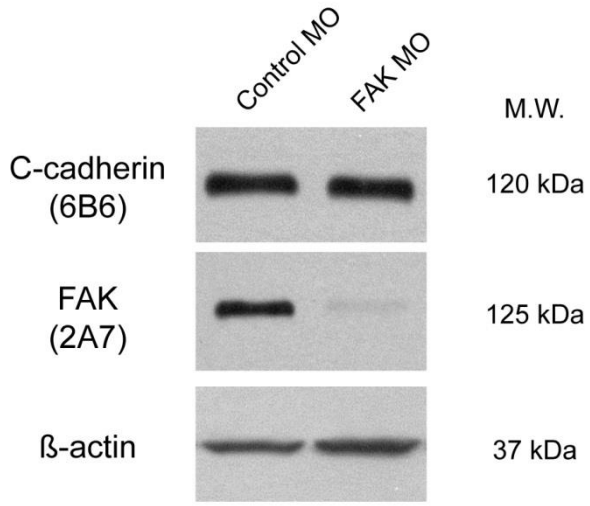
Control MO
FAK MO
M.W.
C-cadherin
(6B6)
120 kDa
FAK
(2A7)
125 kDa
ß-actin
37 kDa

Figure A.5

FAK is localized primarily to focal contacts but is also present in filopodia-like extensions. (A-D) Representative images of EGFP-FAK expressed in migrating mesendoderm explants. 400pg EGFP-FAK RNA mixed with Alexa 555 dextran (pseudo-colored blue) was injected into the dorsal marginal region of each of the two dorsal blastomeres at 4-cell stage. Mesendoderm explants were dissected at stage 10 and plated on Fn coated glass-bottom dishes for at least 60 min prior to image acquisition (see methods in Chapter 2 or 3 for details). Time lapse images were acquired using a confocal microscope, single z-slices from selected time-points are shown. The green channel (EGFP-FAK) is shown individually on the left, merged channels (green = EGFP-FAK, blue = dextran) are shown on the right. (A, B) Images of one explant at two different times (and different scales). Although expression levels of EGFP-FAK vary among cells, FAK is typically localized to focal contacts in the lamellipodia of leading and following cells (A, B, arrowheads) and is also sometimes visible in focal contacts along the basal surface of cells near the leading edge (B, arrowhead). (C, D) Images of one cell at two different times and two different z-planes, both more than 3µm above the basal surface where cells are in contact with the Fn substrate. Higher magnification views are shown on the far right. (C) FAK punctae are visible in finger-like cell-cell contacts at the trailing edge of a cell in the following rows of a migrating explant. (D) A FAK puncta is also visible in a filopodial extension making contact with a neighboring cell. These data suggest that FAK may be present at nascent cell contacts in addition to the expected localization to focal contacts. N = 4. Scale bars = 25µm (A-D), 15µm (higher mag images in C, D).

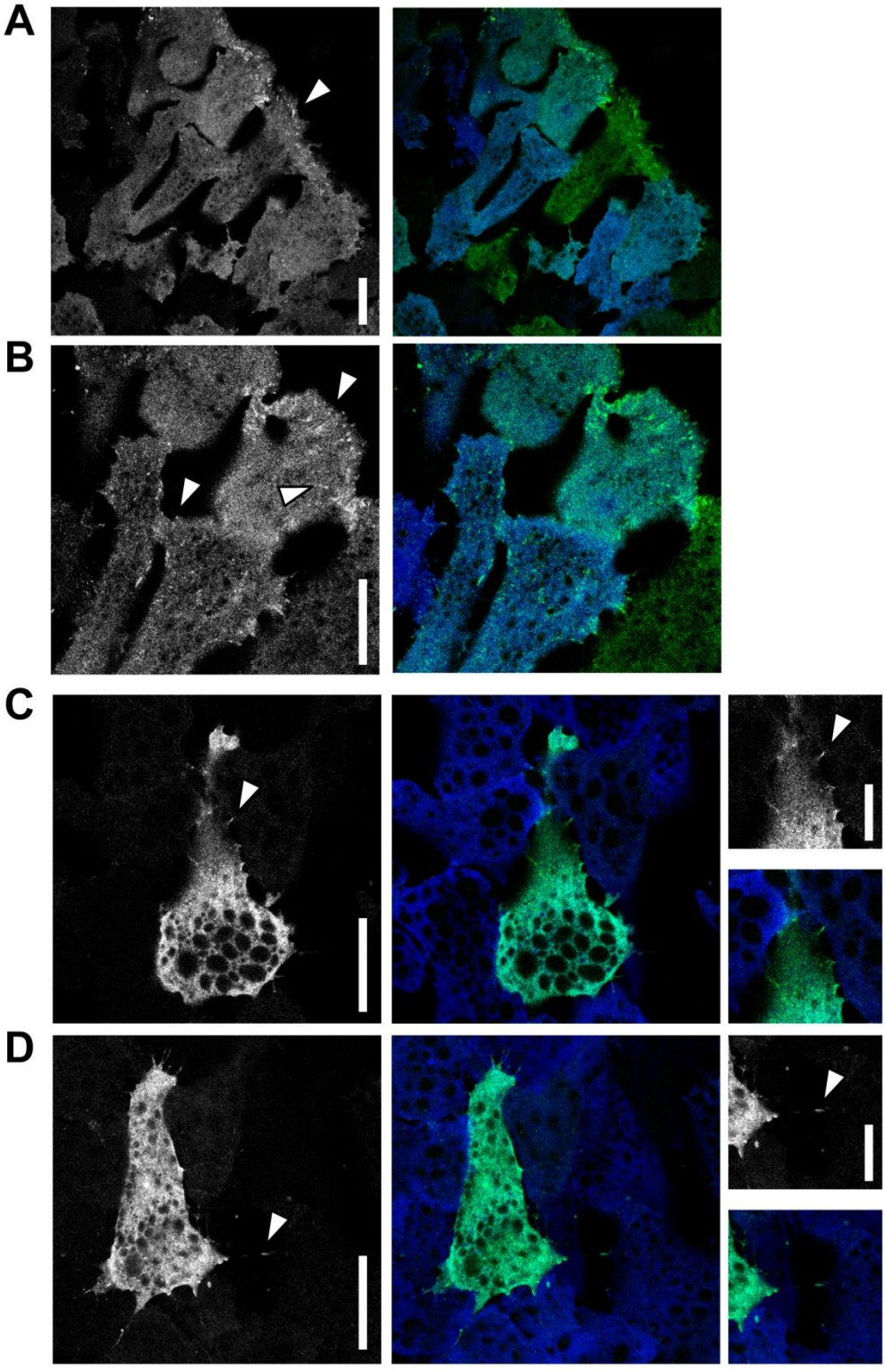
A
B
C
D

Figure A.6

C-cadherin may co-immunoprecipitate with FAK. If FAK is altering cadherin adhesion and is present at nascent cell-cell contacts, perhaps it is biochemically associated with cadherins? (A, B) Co-immunoprecipitation analyses were performed, IP of FAK from lysates of stage 11 embryos was followed by SDS-PAGE, transfer of proteins to nitrocellulose and probing of the blot with antibody directed against C-cadherin (6B6). (A) Lysates were prepared using a standard IP buffer (see materials and methods in Chapter 3, in this instance made with only pTyr phosphatase inhibitors). Co-IP of C-cadherin with Pkg was used as a positive control. FAK was IP'd using the 2A7 antibody (note: requires sodium orthovanadate in lysis buffer even though it is not supposed to be phospho-specific). After probing the blot with 6B6, one band was evident but it was smaller than expected. However, it did correspond to one of the bands observed in the Pkg IP. N = 1. (B) An alternate antibody (4.47) was used to IP FAK. The IP, SDS-PAGE, and western blot were performed in tandem with lysates made with embryos from two different clutches of eggs (clutch A and B). Once again a smaller-than-expected band was observed. These results suggest that FAK may be associated with a fragment of C-cadherin. The fragment does not appear to be a product of degradation due to the IP protocol because it is not more or less evident in samples that were treated identically to the IP samples (fresh) relative to samples that were kept at -80°C (frozen). Because the fragment is present in both IP samples in (A), it could represent a natural degradation product or splice variant. The identity of this fragment could be explored using an antibody specific to the intracellular tail of C-cadherin (6B6 recognizes the extracellular region). Alternately, the result could be due to a lack of specificity of the 6B6 antibody. Alternate antibodies directed against C-cadherin could be used to probe the blot. Ideally the Co-IP could also be done in the inverse direction (IP: C-cadherin, Blot: FAK). N =3, representative image shown.

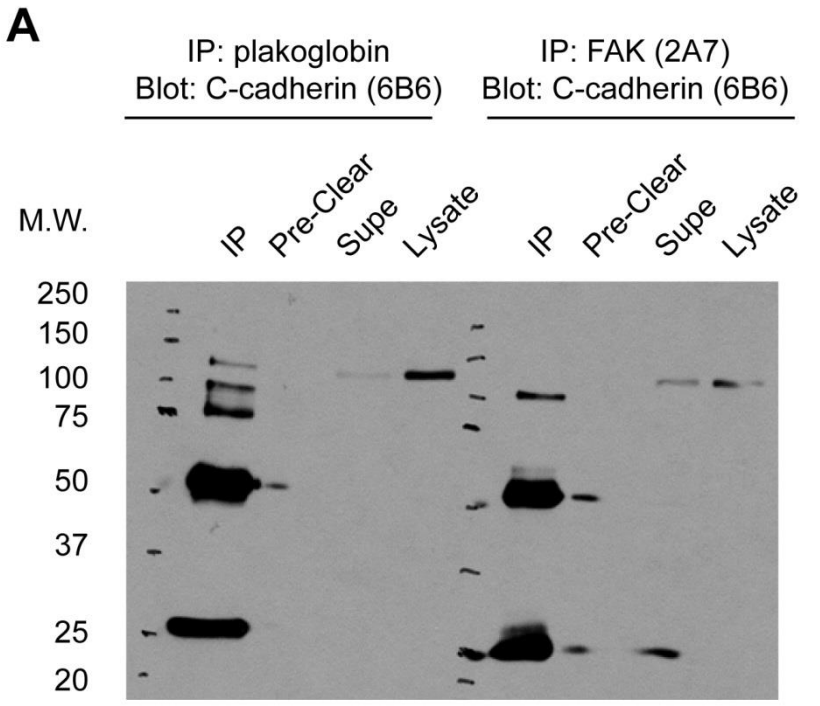
A
IP: plakoglobin
Blot: C-cadherin (6B6)
IP: FAK (2A7)
Blot: C-cadherin (6B6)
M.W.
IP
Pre-Clear
Supe
Lysate
IP
Pre-Clear
Supe
Lysate
250
150
100
75
50
37
25
20

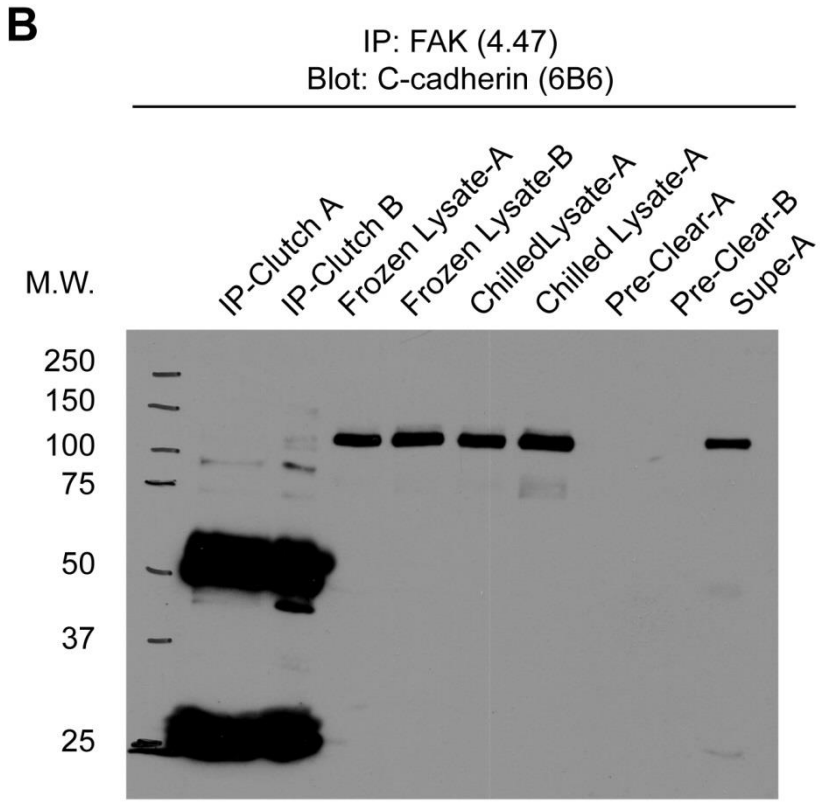
B
IP: FAK (4.47)
Blot: C-cadherin (6B6)
M.W.
IP-Clutch A
IP-Clutch B
Frozen Lysate-A
Frozen Lysate-B
ChilledLysate-A
Chilled Lysate-A
Pre-Clear-A
Pre-Clear-B
Supe-A
250
150
100
75
50
37
25

Figure A.7

EGFP-plakoglobin is localized to cell-cell contacts in Control and FAK MO injected mesendoderm explants. The biochemical analyses presented in Fig. 3.15 suggest that association of Pkg with C-cadherin is diminished in FAK morphant embryos. To confirm this result and visualize the localization of Pkg to cell-cell junctions in control and FAK morphant mesendoderm, EGFP-plakoglobin was expressed and its localization assessed in mesendoderm explants. (A-B) Control or FAK MO was injected into 1-cell stage embryos, followed by injection of 250pg EGFP-plakoglobin RNA into the marginal region of 1 dorsal blastomere at 4-cell stage. Mesendoderm explants were dissected from stage 10 embryos and plated on Fn coated cover-glasses, then imaged using a confocal microscope (see materials and methods in Chapter 2 for details). Images are collapsed z-stacks of 10 x 0.5µm slices. (A) Pkg is normally localized in punctae or in continuous segments along cell-cell boundaries and appears to be especially prevalent at junctions near the leading edge (arrowhead) (see also Fig. 2.7B). (B) In FAK morphant tissue, Pkg is present at cell-cell junctions but appears to be somewhat more punctate. The subtle phenotype in the FAK morphant tissue and the confounding factors of exogenous expression (e.g. variability in expression levels, perturbation of normal function by over-expression) make interpretation of these data difficult. Assessment of the localization of Pkg and C-cadherin by immunostaining of fixed embryos or mesendoderm explants is needed but has presented a number of technical difficulties relating to antibody compatibility. Scale bars = 50µm. N = 2, representative images shown.

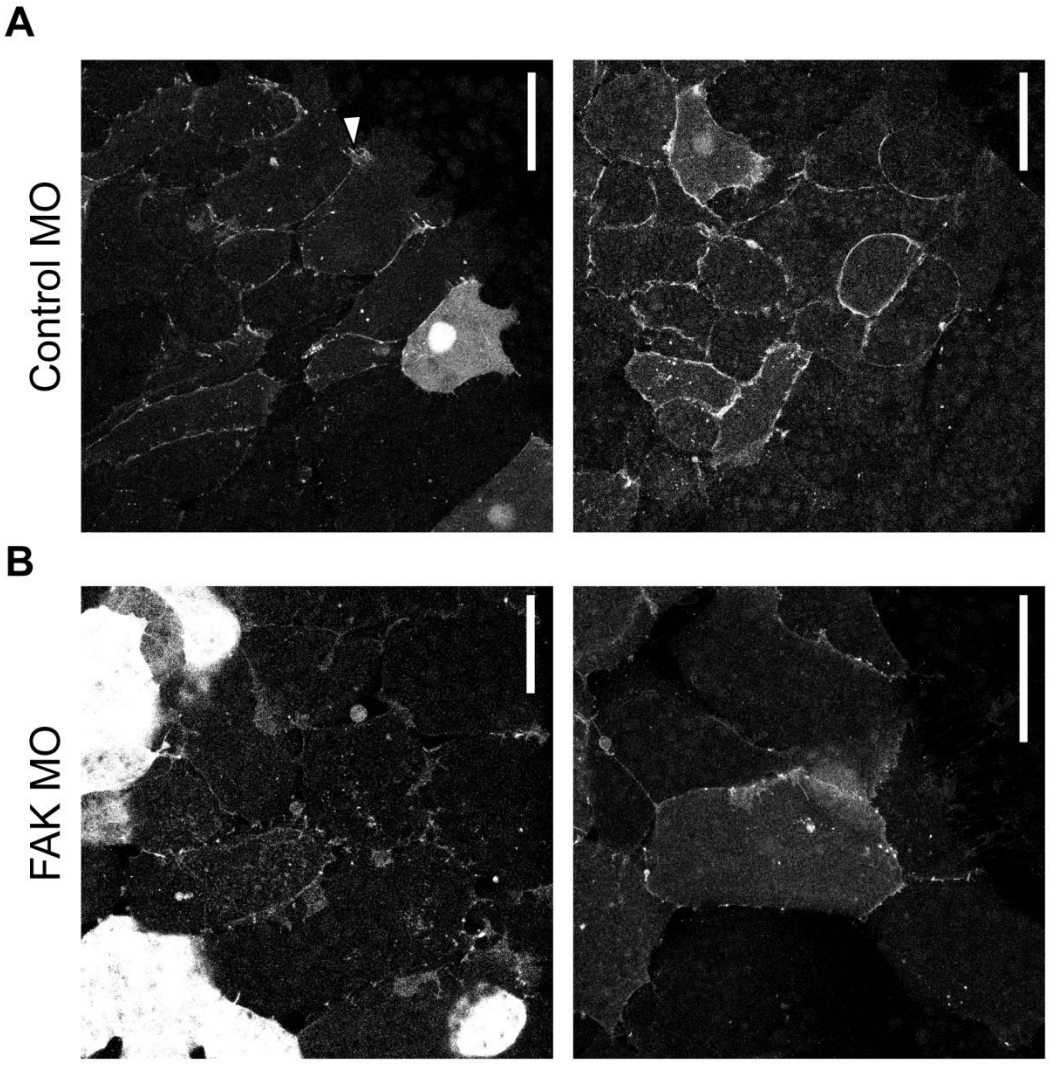
A
Control MO
B
FAK MO

Figure A.8

Minimal co-patterning of actin and keratin filament networks in Control and FAK MO injected mesendoderm explants. Is disruption of the keratin filament network in FAK morphant mesendoderm related to disruption of actin filaments? To address this question, fluorescently tagged actin and keratin proteins were co-expressed and imaged in migrating mesendoderm explants. (A, B) Control or FAK MO was injected at 1-cell stage followed by injection of a mix of 500pg GFP-moesin and 250pg mCherryXCK1(8) RNA into the marginal region of 1 blastomere at 4-cell stage. Mesendoderm explants were dissected from stage 10 embryos and plated on Fn coated coverglasses, then imaged using a confocal microscope (see materials and methods in Chapter 2 for details). Images are collapsed z-stacks of 10 x 0.5µm. (A) Actin filaments in control explants were prominent in protrusions at the leading edge of each cell and assembled into a fine cortical network around each cell body. Keratin filaments were typically localized to the rear of each cell (see also Fig. 3.10C, 3.12A-B). (B) In FAK morphant mesendoderm, actin was enriched in protrusions and also distributed around the cortex of the cell. Some stress fibers were also apparent. Keratin filaments were distributed randomly within each cell and sometimes appeared to be clumped at the cell center rather than forming a network of elongated filaments (see also Fig. 3.10D, 3.12C-D). No notable co-patterning was observed between filament systems. Although there are likely to be interactions between the actin and keratin filament networks, keratin disruption does not appear to be a direct effect of grossly altered actin filament organization. Scale bars = 25µm. N=5, representative images are shown.

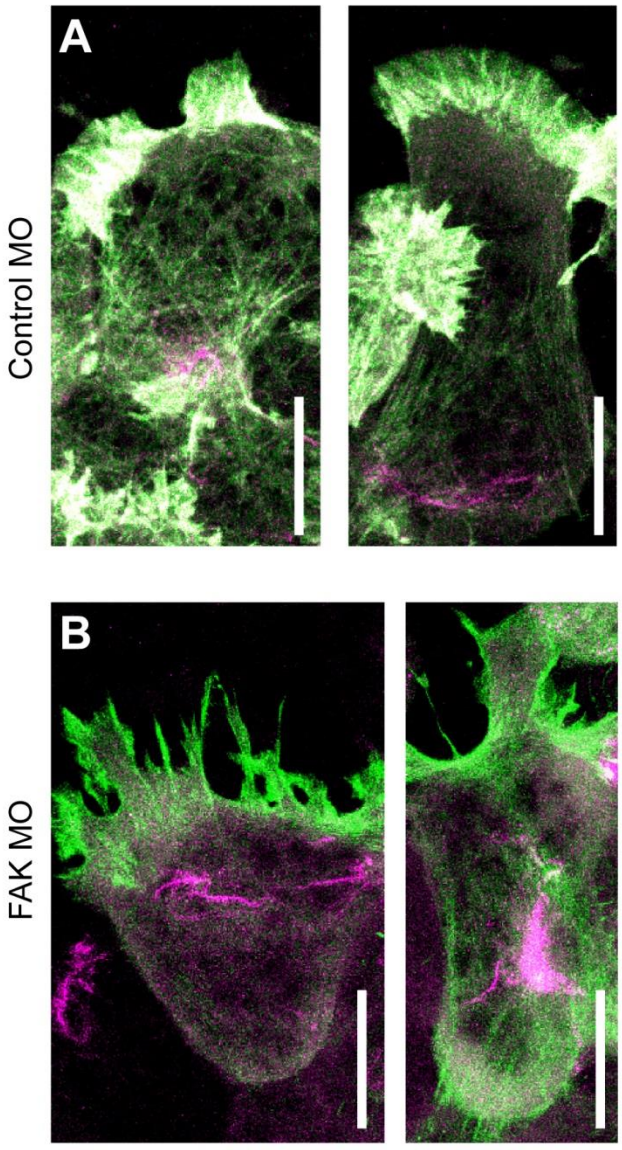
A
Control MO
B
FAK MO

Chapter 5

Conclusions and Perspectives

5.1 Overview

The studies presented in this dissertation were designed with the aim of contributing a global and integrative view of the mechanisms by which cells sense and respond to mechanical signals generated during the course of embryonic development. Three distinct approaches were utilized to investigate how signaling through adhesive networks guides the morphogenesis of *Xenopus* mesendoderm. First, we tested the hypothesis that intercellular tissue tension acts as an instructive cue for directional migration of the mesendoderm tissue. We confirmed this hypothesis and identified three components (cadherin, plakoglobin, and keratin) of the mechanosensitive signaling complex required for directional migration. We found that forces on cadherins and traction on Fn are each required for polarized localization of plakoglobin and keratin.

Next, I investigated the functions of the integrin-associated protein FAK during gastrulation, neurulation, and axial elongation. I placed a particular emphasis on the role of FAK in the organization and migration of mesendoderm cells in an effort to understand the contributions of cell-ECM interactions to coordinated movement of the mesendoderm tissue. I found that FAK is required for normal cell spreading and for persistent migration of mesendoderm cells, as has been established in other cell types. Interestingly, coordination of protrusive polarity, subcellular organization of keratin filaments and interaction of cadherin with plakoglobin are all perturbed by depletion of FAK. These data suggest that the interactions of mesendoderm cells with the Fn substrate on which they migrate and with neighboring cells through cadherin adhesions are both critical for the mechanically sensitive organization of the mesendoderm tissue (Fig 5.1).

Finally, I sought to identify proteins directly involved in sensing mechanical cues and the transduction of mechanical stimuli into chemical signals. To do this I adapted cysteine shotgun mass spectrometry (CS-MS) for the study of mechanically induced signaling in *Xenopus* mesendoderm and used this technique to find proteins that undergo conformational changes in response to tension on adhesions. Although I did not identify proteins likely to be directly acted upon by mechanical stimuli, I did find that several proteins involved in the citric acid cycle and glycolysis undergo conformational change in response to tension on cell-cell or cell-ECM adhesions. These results confirm that CS-MS can be used to detect mechanically sensitive proteins in the mesendoderm and suggest that cellular metabolism may be regulated by the mechanical environment of a cell.

Together these data highlight the combinatorial effects of chemical and mechanical signals on adhesion, migration and morphogenesis. Although this study only addresses mesendoderm migration in *Xenopus*, similar factors are in play in other morphogenetic or pathologic migration events. Directionality of mesendoderm migration is mediated by cell-cell contacts in zebrafish (Dumortier et al., 2012), intercellular tension orients cells in epithelial and endothelial cells sheets (Reffay et al., 2011; Tambe et al., 2011), physical interactions work in concert with chemical cues to guide neural crest cell migration in *Xenopus* (Theveneau et al., 2010) and migration of the lateral line primordium in zebrafish (Donà et al., 2013; Haas and Gilmour, 2006). Common themes are also emerging for the mechanisms by which these guidance signals are sensed and transduced. However, there are many details yet to be clarified in order to bring the big picture into focus.

5.2 Cohesotaxis

The migration of the mesendoderm tissue during gastrulation of the *Xenopus* embryo nicely illustrates many of the concepts discussed in Chapter 1, particularly the importance of cell-cell contacts for morphogenesis. In this tissue, cell-cell contacts are required for the cohesion of the tissue which itself serves as a guidance signal. We have named this phenomenon "cohesotaxis" and defined it as the guidance of cell migration by differences in intercellular forces. It has been proposed that this sensation of mechanical gradients by cells in a tissue may be akin to the sensation of chemical gradients (Roca-Cusachs et al., 2013). Cells must not only detect a force but must also be sensitive to differences between forces on one side of the cell versus another. Trepat and colleagues have identified a slightly different type of organizational signal that is also dependent on anisotropic force distribution within a group of cells. They use the term "plithotaxis" to describe the movement of cells to align themselves with the maximum principle intercellular stress such that perpendicular intercellular tension is maximized and parallel or shear tension is minimized (Tambe et al., 2011). Plithotaxis differs from cohesotaxis in that the former depends only on directional anisotropy (i.e. force is larger in x than in y) while the latter also requires a difference in forces on what is to be the front versus the rear of a cell.

An important commonality between these two mechanisms of mechanotaxis is that simple contact between cells is not enough; rather the cells must be mechanically coupled in order to transmit guidance signals to one another and throughout the tissue. The generation of gradients of intercellular tension is highly dependent on both the mechanical coupling amongst cells and the physical interactions of cells with their

substrate. Traction forces exerted by cells on the substrate as they spread and migrate are balanced by the cohesive forces between cells in a cell group or tissue (Fig. 1.3A, 1.4B) (Maruthamuthu et al., 2011; Tambe et al., 2011; Trepat et al., 2009). In a tissue that is migrating into free space (e.g. mesendoderm moving across the blastocoel roof or wound healing) the movement of the leading cells could generate anisotropic forces that are greater in the axis of migration. Thereafter, plithotaxis and cohesotaxis may both contribute to the alignment of cells along the axis of migration, reorganization of cytoskeletal networks and development of protrusive polarity in following cells. The ensuing directional migration of following cells would then increase the efficiency of collective movement. If any of these processes is disrupted, the migration of the tissue may yet proceed albeit more slowly or in a less organized manner. Leading cells could simply tow following cells into the open space. Individual migrations of cells lacking mechanical coupling to their neighbors may still be spatially constrained by said neighbors and thus migrate directionally. However, in either of these potential scenarios the physical interactions among cells remain paramount in the guidance of collective movement.

5.3 Additional influences from cell-cell contacts

While it has become quite clear that we must take into account the mechanical influences of cell-cell contacts in a migrating tissue, there are many different types of cell-cell interactions that we should also consider. Close apposition of cells through cadherin-mediated cell-cell adhesion permits the formation of gap junctions and the

interactions of membrane bound signaling components like Notch/Delta and the ephrin/Eph family.

Gap junctions

The potential for transmission of small molecules and second messengers through gap junctions is of particular interest given the observation of calcium waves in the converging and extending *Xenopus* mesoderm, during gastrulation in zebrafish and in wounded cell monolayers (Gilland et al., 1999; Sammak et al., 1997; Wallingford et al., 2001; Webb and Miller, 2006). Surgical wounding of *Xenopus* tissue in the process of explant dissection was not observed to induce calcium waves (Wallingford et al., 2001), but it is not known whether calcium signaling is a factor during mesendoderm migration in vivo or in cultured explants. One way to address this question would be through the use of fluorescent calcium sensors in the same manner as previously performed for slightly later stages of development (Wallingford et al., 2001). It would be ideal to monitor calcium signaling in the intact embryo, as done in zebrafish embryos (Gilland et al., 1999), but the opacity of the gastrulating *Xenopus* embryo makes this very difficult. However, the use of mesendoderm explants for such a study is not only technically feasible, but has the added advantage of being amenable to combination with other analyses including traction force microscopy. Correlation of calcium signaling with a read-out of traction forces may provide additional insight into the relationship between the chemical and physical environments in the migrating tissue.

Although there are extracellular mechanisms for the propagation of calcium waves (Osipchuk and Cahalan, 1992), the typical mode of transmission is via gap

junctions (Sanderson et al., 1994). There are also many other signals that can be passed by gap junctions (e.g. cAMP or inositol triphosphate), some of which feed into calcium signaling pathways (Sanderson et al., 1994). To examine gap junctional communication in the mesendoderm tissue, the gap junction permeable fluorescent dye, lucifer yellow (or a fluorescently labeled dextran as a negative control), could be microinjected into cells within a migrating mesendoderm explant. The spread of the dye could then be monitored by fluorescent microscopy to determine the extent of intercellular communication through gap junction channels (Landesman et al., 2000). If such communication is evident, its influence on collective migration could be assessed by inhibiting gap junctions by addition of carbenoxolone or other inhibitory drugs (Li et al., 2009). Although this would block electrical coupling in addition to prevention of transmission of calcium or other signals, any effects of gap junction inhibition on migration could be clarified with more specific studies in the future.

Collective chemotaxis

Migration of cells toward diffusible signaling molecules, termed chemotaxis, occurs in both single cells and cell groups or tissues (Rørth, 2011). However, in some cases cell-cell contact is required for chemotactic behavior. The lateral line primordium of zebrafish migrates along a track of the chemokine sdf1 (also known as Cxcl12a) (David et al., 2002). Both single cells and tissue are responsive to sdf1 but the sdf1 track has no intrinsic directionality and directional migration requires an intact tissue (Haas and Gilmour, 2006). Directional migration is achieved through the generation of a chemotactic gradient by the tissue itself, through polarized internalization of

differentially expressed chemokine receptors (Donà et al., 2013). Cell-cell contacts are also critical for migration of *Xenopus* mesendoderm cells on substrates thought to contain a gradient of platelet derived growth factor (PDGF), and PDGF signaling is required for normal migration of the mesendoderm tissue (Nagel et al., 2004). However, the existence of a gradient of PDGF in the extracellular matrix of the blastocoel roof has yet to be clearly demonstrated so it is possible that PDGF signaling through ligand independent pathways is a contributing factor. Furthermore, the mechanism by which cell-cell contacts influence the response of mesendoderm cells to PDGF signaling is not clear. It would be interesting to determine whether or not cell-cell contacts are required for migration of mesendoderm cells up a defined gradient of PDGF. Such a gradient could be created simply using a point source (pipette) of PDGF or more precisely in a microfluidic chamber (Skoge et al., 2010). It would also be useful to define the mechanisms by which cell-cell contact alters the response of mesendoderm cells to PDGF signaling. Does the mesendoderm tissue create its own gradient, as in the zebrafish lateral line primordium? Is the PDGF signal integrated over multiple cells to allow sensation of a shallow gradient?

5.4 Adhesive networks and collective migration

We know that the cells of the mesendoderm tissue interact with their environment through cell-cell and cell-ECM adhesions. How then do cells integrate mechanical and chemical information from these multiple inputs? The necessary mechanical linkage and Newtonian balance of forces between the two adhesion types have already been discussed (see section 5.2), but the means by which forces and signals are transduced is also

important to consider. In Chapter 1, I addressed many of the common mechanisms for crosstalk between adhesion complexes and argued that the term "crosstalk" is not truly sufficient to describe the complicated network of interactions taking place inside a cell. I find it now relevant to revisit some of these concepts, to expand on this discussion in light of the data presented in Chapters 2 and 3, and to incorporate some of the preliminary findings presented in the Appendices.

Signaling through FAK

The literature on the functions of FAK is vast and covers many distinct aspects of cellular biology. FAK is important for promoting cell survival and proliferation in response to "outside-in" integrin signaling and is necessary for regulation of adhesion and migration on ECM substrates through a plethora of intermediate signaling pathways (Fig. 5.2) (Parsons, 2003; Schaller, 2010). Signaling through FAK can regulate cytoskeletal dynamics and contractility, thus altering the mechanical properties of a cell or tissue and contributing to modulation of both cell-ECM and cell-cell adhesions (de Rooij et al., 2005; Fabry et al., 2011). FAK has also been shown to have indirect effects on cell-cell adhesion through Rho family GTPases (Playford et al., 2008; Yano et al., 2004).

Preliminary examination of cell-cell interactions in FAK morphant cells revealed cell sorting behaviors in aggregates of control and FAK morphant mesendoderm cells (Fig. A.2). These data suggest that depletion of FAK alters the way in which cells interact with one another, but do not definitively point to changes in cadherin adhesion per se. The results of attachment assays and analyses of cell spreading on C-cadherin coated substrates support the notion that FAK is involved in regulating cadherin-

mediated adhesion (Fig. A.3). However, some of the changes are subtle and in each assay there is room for alternate interpretation of the results. For example, cell sorting and cell spreading are both likely to be affected by changes in contractility or cortical tension and sorting behaviors could be dependent on interactions with Fn assembled during the aggregation process. A simple control for the latter would be to immunostain fixed aggregates with an antibody directed against Fn and to look for the presence of fibrils and for any differences between Fn assembly in each possible pairing of control and Fak morphant cells. Alternate methods of analyzing the strength of cell-cell adhesions include pipette (Martinez-Rico et al., 2010) or atomic force microscopy (AFM) (Arboleda-Estudillo et al., 2010; Krieg et al., 2008) based assays. Quantification of traction forces on a cadherin-coated substrate (e.g. mPADs used in Fig. 3.14) could also be used as a measure of adhesion (Ganz et al., 2006).

Although FAK is typically localized to integrin-based focal contacts, there is some limited evidence that it may also be present at cell-cell adhesions (Crawford et al., 2003; Playford et al., 2008; Yano et al., 2004). I observed FAK punctae at what appeared to be nascent cell-cell contacts in migrating mesendoderm, but never at mature junctions (Fig. A.5C-D). This is similar to what has been previously reported in cells forming new junctions after a calcium switch (Playford et al., 2008). Biochemical evidence is suggestive of an interaction between FAK and C-cadherin but is not conclusive (Fig. A.6). An antibody directed against the extracellular domain of C-cadherin recognizes a band in immunoprecipitates of FAK but the band is smaller than would be expected for full-length cadherin. This band could be a natural degradation product, the result of a non-specific antibody interaction or, perhaps, a specific cleavage product. Further

analysis will be required to determine the nature of the biochemical interaction between FAK and C-cadherin. Together, these data suggest that FAK is important for normal cell-cell interactions but the mechanisms by which it acts are not yet clear.

Rho family GTPases

Rho family GTPases such as Rho and Rac are signaling intermediates that feature prominently in pathways downstream of cadherin- and integrin-based adhesions and are also involved in the regulation of adhesion (see Chapter 1 or Weber et al., 2011). There are many studies demonstrating the importance of Rho family GTPases in collective cell movements (Khalil and Friedl, 2010; Theveneau and Mayor, 2013). It is important to note that the functions of these proteins are dictated by their activity and by their subcellular localization (Bishop and Hall, 2000; Spiering and Hodgson, 2011). Both subcellular and supracellular (across the tissue) organization of RhoA activity is associated with distribution of traction forces in collectively migrating epithelial cells (Reffay et al., 2014). Local activation of Rac is sufficient to redirect groups of migrating border cells in the *Drosophila* oocyte (Wang et al., 2010). Furthermore, local induction of Rac disrupts intermediate filaments and induces lamellipodial protrusions (Helfand et al., 2011). Given that keratin intermediate filaments are typically localized toward the rear of each cell in the migrating mesendoderm, it is tempting to suppose that activation of Rac by integrin-mediated signaling may be acting to suppress keratin assembly at the leading edge, thereby setting up anterior-posterior protrusive polarity.

One way to address this hypothesis is to look for gradients in the activity of Rac within migrating mesendoderm explants. This can be achieved using the current

iterations of the elegant FRET (Forster resonance energy transfer) based sensors devised by the Hahn group (Hodgson et al., 2010). It will also be interesting to examine the relationship between tension on cadherin- and integrin-based adhesions and the activity and localization of Rac, Rho and Cdc42. Preliminary data suggests that Rac protein levels (and activity) decrease in response to force on cadherin adhesions (data not shown). It is technically challenging to directly examine the localization of active Rac in cells subject to stretch (see Chapter 4) or bead pull (see Chapter 2). However, visualization of active Rac in migrating mesendoderm explants is feasible and could be used in combination with maps of traction forces within the migrating tissue to estimate effects of traction and intercellular forces on Rac activity. Local inhibition of Rac in conjunction with live imaging of fluorescently tagged keratin filaments would also provide new insight into the relationship between Rac activity and the polarity of migrating mesendoderm.

Cytoskeletal linkages

Although it is clear that actin, microtubules and intermediate filaments are all important for the normal function and migration of cells, the extent to which each cytoskeletal network contributes to adhesive crosstalk in the migrating mesendoderm is an open question. The actin filament network in mesendoderm cells appears to be insensitive to the presence or absence of cell-cell adhesion (Fig. 2.2B-C). We observed no dramatic differences in the organization of filaments in the cell body or protrusions in single cells compared with those in an intact tissue. Actin is of course linked to both cell-cell and cell-ECM junctions (Maruthamuthu et al., 2010), and is known to be important

for mechanosensation at both integrin- and cadherin-based adhesions (Huveneers and de Rooij, 2013; Ross et al., 2013). The actin network does not appear to be essential for resisting force applied to cadherins but is important for maintaining adhesion of cells to the Fn substrate (Fig. 2.2A). These data suggest that actin is not a primary component of the mechanosensitive cadherin complex. However, none of the data presented here preclude a role for actin in mediating adhesive crosstalk in the migrating mesendoderm. In contrast to actin, keratin filaments are highly sensitive to tissue context (Fig. 2.3A-D) and are definitely important for mechanical sensitivity and polarity of mesendoderm (Fig. 2.5). Intermediate filaments are also linked to both cell-cell and cell-ECM adhesions but no roles have yet been proposed for this filament network in crosstalk between the two adhesion types (see Chapter 1 or Weber et al., 2011).

The organization and function of microtubules within the mesendoderm has not yet been comprehensively addressed. Preliminary evidence suggests that, as with actin, there are not significant differences between the organizations of microtubules in single cells compared with cells in the intact tissue (data not shown). Initial studies also found that the localization of centrosomes in cells in the migrating mesendoderm tissue seems to be random (data not shown). There is no correlation observed between centrosome (or Golgi body, data not shown) orientation and migratory direction. Although it is has been shown that directional migration (Kupfer et al., 1982), geometric constraint (Pouthas et al., 2008), and cadherin adhesions (Dupin et al., 2009) can mediate positioning of the centrosome, this is likely a result of polarity and not necessary for polarized movement (Ueda et al., 1997). Together these data suggest that microtubules are not organized by cell-cell contacts or tissue tension. However, no analysis of tissue level organization of

microtubules has yet been conducted and no studies have been conducted to determine their involvement in communication between cell-cell and cell-ECM adhesions in the mesendoderm.

5.5 Interactions and functions of cytoskeletal networks

We have established that the organization of keratin is sensitive to mechanical tension, but we do not yet understand how the organization of the filament network is generated, nor do we know how it interacts with the actin network. In the previous section I discussed mechanisms by which Rho family GTPases might contribute to the organization of the keratin filaments within collectively migrating cells and compared the organization of the actin and keratin networks. The assembly and organization of keratin filaments are thought to also be dependent on actin (Kölsch et al., 2009; Wöll et al., 2005), suggesting that the two filament systems may be co-patterned within the cell. This does not appear to be the case in mesendoderm cells. Co-expression of fluorescently tagged keratin and the actin binding protein moesin revealed little overlap between the two filament networks (Fig. A.8A). Furthermore, although depletion of FAK alters the organization of actin filaments in protrusions and increases the abundance of stress fibers, these phenotypes could be considered subtle in comparison with the disruption observed in the keratin network (Fig. A.8B). These results indicate that the organization of keratin filaments is not fully dependent on the actin network but some preliminary evidence suggests that depletion of keratin may have a severe effect on actin organization (data not shown).

The formation of supracellular cables of actin (data not shown) and keratin (Fig. 2.11C, 3,12B) along the leading edge of migrating mesendoderm may be regulated by means distinct from those regulating the assembly of keratin "baskets" in the rear of each cell. Although disordered keratin filaments are evident within Pkg morphant mesendoderm cells, keratin cabling along the leading edge of the tissue remains and is perhaps even more prominent than in control tissues (Fig. 2.11D). This indicates that linkage of keratin filaments to cadherins through Pkg is not required for assembly and maintenance of the leading edge cable. How else might keratin filaments be anchored? One possibility is that these keratin filaments are interacting with actin either directly (Green et al., 1987) or indirectly through linker proteins such as plectins (Sonnenberg and Liem, 2007). Ultrastructural analysis of the leading edge of migrating mesendoderm by transmission electron microscopy (TEM) could help to determine what type of junction or interaction is taking place where keratin cables intersect with cell-cell contacts. Inhibition of plectins by injection of antisense morpholinos may also provide insight into the linkage between keratin and actin both at the leading edge and throughout the cell.

Role of actin and keratin cables at the leading edge

What is the function of the supracellular cables of actin and keratin at the leading edge of the migrating mesendoderm? Others have observed similar bands of actin across multicellular "fingers" of epithelial cells migrating into free space and proposed that the actin cables served to constrain the tissue and restrict the formation of new leader cells (Reffay et al., 2014). Actin and keratin cables could serve to maintain the integrity of the migrating tissue and to resist lateral tension. The cables could also be important for the

continuity of the leading edge. Loss of cabling in FAK morphant mesendoderm is correlated with discontinuity of the leading edge of the tissue (Fig. 3.9B, 3.12C-D). Acute photo-ablation of actin and keratin filaments could be used to test these hypotheses directly. This could be performed either by nonspecific laser surgery to cut both filament networks together or using targeted ablation techniques such as chromophore assisted light inactivation (CALI) to sever filament networks individually (Jacobson et al., 2008; Reffay et al., 2014; Takemoto et al., 2013). CALI could also be used to target and ablate the linkages of these networks to adhesions through Pkg, β-catenin, vinculin or other linker proteins. These acute perturbations allow dissection of signals required for establishment of tissue organization and polarity from those required for maintenance of collective migration.

5.6 The search for mechanosensors

One of the main goals of the work presented in Chapter 4 is the identification of proteins that act as mechanosensors. The precise definition of a mechanosensor is somewhat contentious but I have defined it as a protein that is directly acted upon by a mechanical stimulus and that converts this mechanical signal into a chemical one. Deletion or inhibition of proteins can provide evidence of function in mechanically sensitive signaling pathways, but proving that a protein senses and transduces mechanical forces is quite difficult. The CS-MS protocol described in Chapter 4 is an attempt to do just that. CS-MS identifies proteins that undergo conformational changes in response to a mechanical stimulus. However, even this method is insufficient to determine whether a protein is undergoing conformational change in direct response to mechanical stimulation

or in response to a downstream chemical signaling cue. Some studies have stretched individual proteins directly (Little et al., 2008; Sawada et al., 2006) and found that they generate a chemical signal in response to stretch, but these stretch events are artificial and do not prove that such an event takes place in a cell or tissue. Generation of conformation sensitive FRET sensors (Grashoff et al., 2010; Margadant et al., 2011; Smith et al., 2007) and conformation specific antibodies (Yonemura et al., 2010) are technically very challenging but can be used to confirm the results of screens (e.g. CS-MS) or targeted queries (e.g. application of stretch to single proteins).

Certain identification of a mechanosensor then requires many steps. First, one must determine the native mechanical environment of the cell and the protein in question. What type and magnitude of forces might the candidate protein be exposed to? Does the protein undergo a conformational change in response to applied force? Is there a change in signaling by the protein (e.g. phosphorylation, binding to effector proteins) following application of force? Does the protein undergo a conformational change in its endogenous environment? Is the protein required for the signal transduction in response to the applied force? Ideally these last questions are addressed in a physiologically relevant environment such as a developing embryo or intact tissue. Last but not least, does inhibition of the force sensation mechanism (i.e. conformational change) abrogate transduction of the mechanically induced signal? Although not every step is necessarily applicable to all mechanosensor candidates, answering any one of these questions is a difficult proposition. Thus, although some have come very close (Yonemura et al., 2010), no proteins have yet been identified that satisfy the definition of a mechanosensor.

5.7 Conclusion

This work describes the identification of four members of the network of proteins mediating and directing collective migration of mesendoderm cells in the developing *Xenopus* embryo: C-cadherin, keratin, plakoglobin and FAK. Each of these proteins is required for the tension-mediated self-organization of the mesendoderm tissue. The studies presented here highlight the importance of the integration of signals from multiple sources (e.g. cell-cell and cell-ECM adhesions, mechanical and chemical stimuli) and translation of those signals into coordinated cell behaviors. The search for proteins that sense and transduce forces remains incomplete, but will serve as a stepping stone for continued investigation. Finally, although this work was conducted in an effort to understand cellular interactions during development, the resulting knowledge may help to elucidate mechanisms mediating wound healing, collective invasion of tumor cells and other pathophysiological migration events.

Figure 5.1

A proposed model of the adhesive signaling network in collectively migrating mesendoderm. The mesendoderm migrates as a wedge shaped tissue across fibronectin matrix assembled by the cells of the blastocoel roof. The illustration shows a cross section of the migrating tissue, along with key components of the adhesive network. Proteins are color coded according to the key at left. Arrow denotes direction of migration.

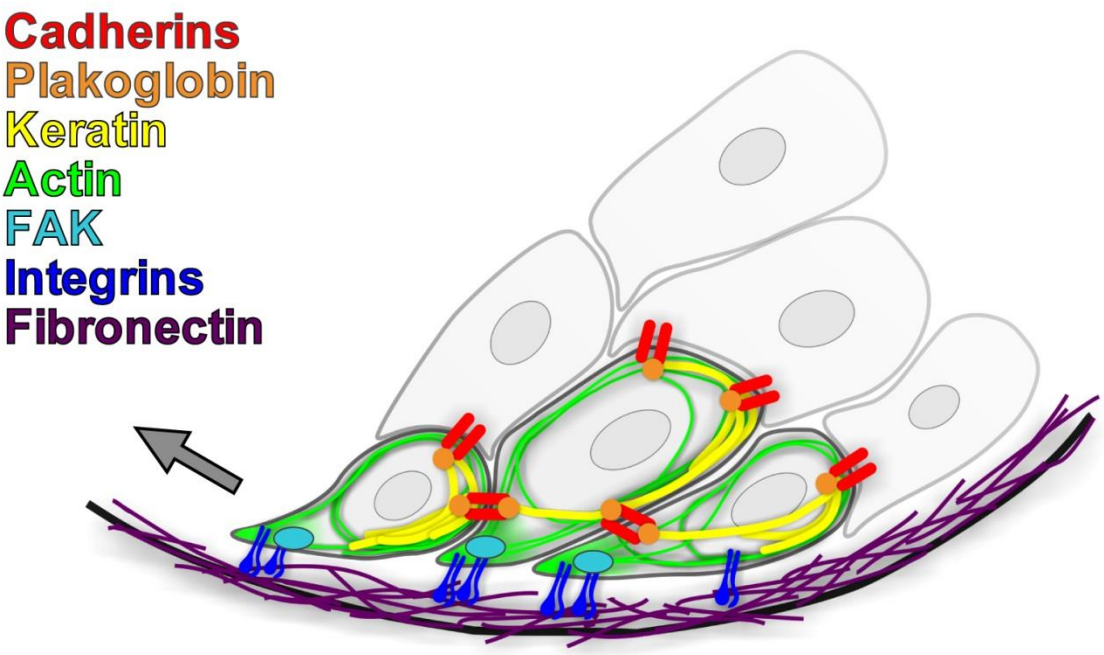
Cadherins
Plakoglobin
Keratin
Actin
FAK
Integrins
Fibronectin

Figure 5.2

FAK signaling network. FAK integrates signals from integrins and growth factor receptors and regulates proliferation, cell survival, cell-cell adhesion and cell-ECM adhesion and migration. Positive (arrows) and negative (bars) interactions are indicated. Solid lines indicate direct interactions, dashed lines indicate indirect or uncertain interactions. Yellow highlighting indicates cellular processes that modulate cell-cell adhesion, blue highlighting indicates cellular processes that modulate cell-ECM adhesion and migration.

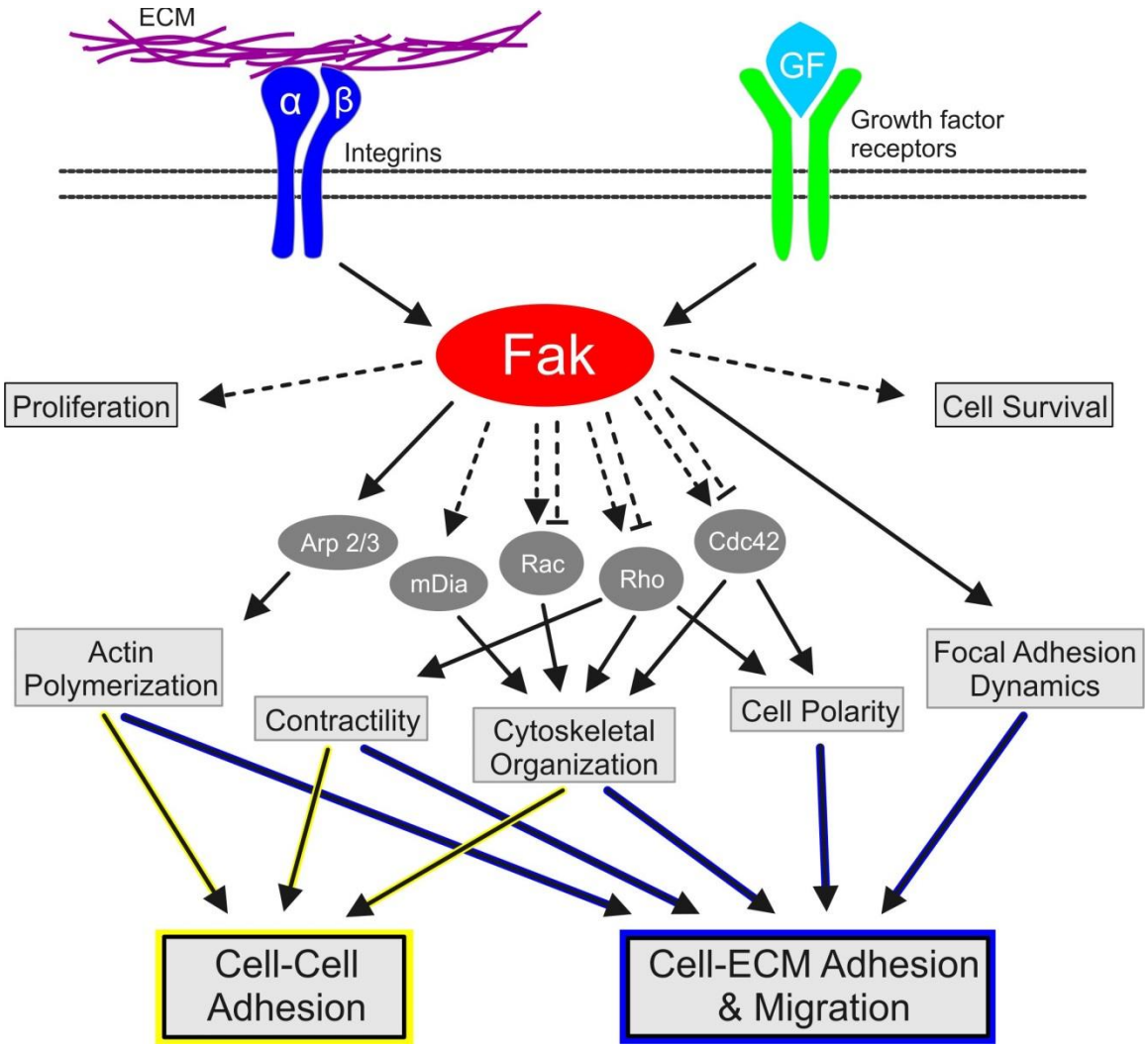
ECM
α
β
Integrins
GF
Growth factor receptors
Fak
Proliferation
Cell Survival
Arp 2/3
mDia
Rac
Rho
Cdc42
Actin Polymerization
Contractility
Cytoskeletal Organization
Cell Polarity
Focal Adhesion Dynamics
Cell-Cell Adhesion
Cell-ECM Adhesion & Migration

Literature Cited

Abercrombie, M., Heaysman, J.E.M., 1953. Observations on the social behaviour of cells in tissue culture. I. Speed of movement of chick heart fibroblasts in relation to their mutual contacts. Exp. Cell Res. 5, 111–131.

Abercrombie, M., Heaysman, J.E.M., 1954. Observations on the social behaviour of cells in tissue culture. II. "Monolayering" of fibroblasts. Exp. Cell Res. 6, 293–306.

Acehan, D., Petzold, C., Gumper, I., Sabatini, D.D., Müller, E.J., Cowin, P., Stokes, D.L., 2008. Plakoglobin is required for effective intermediate filament anchorage to desmosomes. J. Invest. Dermatol. 128, 2665–75.

Aebersold, R., Mann, M., 2003. Mass spectrometry-based proteomics. Nature 422, 198–207.

Aman, A., Piotrowski, T., 2011. Cell-cell signaling interactions coordinate multiple cell behaviors that drive morphogenesis of the lateral line. Cell Adh. Migr. 5, 499–508.

Angres, B., Müller, A.H.J., Kellermann, J., Hausen, P., 1991. Differential expression of two cadherins in Xenopus laevis. Development 111, 829–44.

Arboleda-Estudillo, Y., Krieg, M., Stühmer, J., Licata, N.A., Muller, D.J., Heisenberg, C.-P., 2010. Movement directionality in collective migration of germ layer progenitors. Curr. Biol. 20, 161–9.

Arregui, C., Pathre, P., Lilien, J., Balsamo, J., 2000. The nonreceptor tyrosine kinase fer mediates cross-talk between N-cadherin and β1-integrins. J. Cell Biol. 149, 1263–74.

Avizienyte, E., Fincham, V.J., Brunton, V.G., Frame, M.C., 2004. Src SH3/2 domain-mediated peripheral accumulation of Src and phospho-myosin is linked to deregulation of E-cadherin and the epithelial-mesenchymal transition. Mol. Biol. Cell 15, 2794–803.

Avizienyte, E., Wyke, A.W., Jones, R.J., McLean, G.W., Westhoff, M.A., Brunton, V.G., Frame, M.C., 2002. Src-induced de-regulation of E-cadherin in colon cancer cells requires integrin signalling. Nat. Cell Biol. 4, 632–8.

Baker, B.M., Chen, C.S., 2012. Deconstructing the third dimension: how 3D culture microenvironments alter cellular cues. J. Cell Sci. 125, 3015–24.

Balzac, F., Avolio, M., Degani, S., Kaverina, I., Torti, M., Silengo, L., Small, J.V., Retta, S.F., 2005. E-cadherin endocytosis regulates the activity of Rap1: a traffic light GTPase at the crossroads between cadherin and integrin function. J. Cell Sci. 118, 4765–83.

Bass, M.D., Morgan, M.R., Roach, K.A., Settleman, J., Goryachev, A.B., Humphries, M.J., 2008. p190RhoGAP is the convergence point of adhesion signals from α5β1 integrin and syndecan-4. J. Cell Biol. 181, 1013–26.

Behrens, J., Vakaet, L., Friis, R., Winterhager, E., Van Roy, F., Mareel, M.M., Birchmeier, W., 1993. Loss of epithelial differentiation and gain of invasiveness correlates with tyrosine phosphorylation of the E-cadherin/β-catenin complex in cells transformed with a temperature-sensitive v-SRC gene. J. Cell Biol. 120, 757–66.

Beil, M., Micoulet, A., von Wichert, G., Paschke, S., Walther, P., Omary, M.B., Van Veldhoven, P.P., Gern, U., Wolff-Hieber, E., Eggermann, J., Waltenberger, J., Adler, G., Spatz, J.P., Seufferlein, T., 2003. Sphingosylphosphorylcholine regulates keratin network architecture and visco-elastic properties of human cancer cells. Nat. Cell Biol. 5, 803–11.

Benedito, R., Roca, C., Sörensen, I., Adams, S., Gossler, A., Fruttiger, M., Adams, R.H., 2009. The notch ligands Dll4 and Jagged1 have opposing effects on angiogenesis. Cell 137, 1124–35.

Beningo, K.A., Hamao, K., Dembo, M., Wang, Y.-L., Hosoya, H., 2006. Traction forces of fibroblasts are regulated by the Rho-dependent kinase but not by the myosin light chain kinase. Arch. Biochem. Biophys. 456, 224–31.

Bershadsky, A.D., Kozlov, M., Geiger, B., 2006. Adhesion-mediated mechanosensitivity: a time to experiment, and a time to theorize. Curr. Opin. Cell Biol. 18, 472–81.

Besson, A., Wilson, T.L., Yong, V.W., 2002. The anchoring protein RACK1 links protein kinase Cε to integrin β chains: requirements for adhesion and motility. J. Biol. Chem. 277, 22073–84.

Bhadriraju, K., Yang, M.T., Alom Ruiz, S., Pirone, D.M., Tan, J.L., Chen, C.S., 2007. Activation of ROCK by RhoA is regulated by cell adhesion, shape, and cytoskeletal tension. Exp. Cell Res. 313, 3616–23.

Bhattacharya, R., Gonzalez, A.M., Debiase, P.J., Trejo, H.E., Goldman, R.D., Flitney, F.W., Jones, J.C.R., 2009. Recruitment of vimentin to the cell surface by β3 integrin and plectin mediates adhesion strength. J. Cell Sci. 122, 1390–400.

Bishop, A.L., Hall, A., 2000. Rho GTPases and their effector proteins. Biochem. J. 348, 241–55.

Block, E.R., Matela, A.R., SundarRaj, N., Iszkula, E.R., Klarlund, J.K., 2004. Wounding induces motility in sheets of corneal epithelial cells through loss of spatial constraints: role of heparin-binding epidermal growth factor-like growth factor signaling. J. Biol. Chem. 279, 24307–12.

Block, E.R., Tolino, M.A., Lozano, J.S., Lathrop, K.L., Sullenberger, R.S., Mazie, A.R., Klarlund, J.K., 2010. Free edges in epithelial cell sheets stimulate epidermal growth factor receptor signaling. Mol. Biol. Cell 21, 2172–2181.

Boghaert, E., Gleghorn, J.P., Lee, K., Gjorevski, N., Radisky, D.C., Nelson, C.M., 2012. Host epithelial geometry regulates breast cancer cell invasiveness. Proc. Natl. Acad. Sci. U. S. A. 109, 19632–7.

Bolós, V., Mira, E., Martínez-Poveda, B., Luxán, G., Cañamero, M., Martínez-A, C., Mañes, S., de la Pompa, J.L., 2013. Notch activation stimulates migration of breast cancer cells and promotes tumor growth. Breast cancer Res. 15, R54.

Bonné, S., Gilbert, B., Hatzfeld, M., Chen, X., Green, K.J., van Roy, F., 2003. Defining desmosomal plakophilin-3 interactions. J. Cell Biol. 161, 403–16.

Bordeleau, F., Galarneau, L., Gilbert, S., Loranger, A., Marceau, N., 2010. Keratin 8/18 modulation of protein kinase C-mediated integrin-dependent adhesion and migration of liver epithelial cells. Mol. Biol. Cell 21, 1698–1713.

Bordeleau, F., Myrand Lapierre, M.-E., Sheng, Y., Marceau, N., 2012. Keratin 8/18 Regulation of Cell Stiffness-Extracellular Matrix Interplay through Modulation of Rho-Mediated Actin Cytoskeleton Dynamics. PLoS One 6, e38780.

Borghi, N., Lowndes, M., Maruthamuthu, V., Gardel, M.L., Nelson, W.J., 2010. Regulation of cell motile behavior by crosstalk between cadherin- and integrin-mediated adhesions. Proc. Natl. Acad. Sci. U. S. A. 107, 13324–13329.

Borghi, N., Sorokina, M., Shcherbakova, O.G., Weis, W.I., Pruitt, B.L., Nelson, W.J., Dunn, A.R., 2012. E-cadherin is under constitutive actomyosin-generated tension that is increased at cell-cell contacts upon externally applied stretch. Proc. Natl. Acad. Sci. U. S. A. 109, 12568–73.

Bornslaeger, E.A., Godsel, L.M., Corcoran, C.M., Park, J.K., Hatzfeld, M., Kowalczyk, A.P., Green, K.J., 2001. Plakophilin 1 interferes with plakoglobin binding to desmoplakin, yet together with plakoglobin promotes clustering of desmosomal plaque complexes at cell-cell borders. J. Cell Sci. 114, 727–38.

Braga, V.M.M., Yap, A.S., 2005. The challenges of abundance: epithelial junctions and small GTPase signalling. Curr. Opin. Cell Biol. 17, 466–74.

Brieher, W.M., Gumbiner, B.M., 1994. Regulation of C-cadherin function during activin induced morphogenesis of animal caps. J. Cell Biol. 126, 519–27.

Bugyi, B., Carlier, M.-F., 2010. Control of actin filament treadmilling in cell motility. Annu. Rev. Biophys. 39, 449–70.

Burridge, K., Sastry, S.K., Sallee, J.L., 2006. Regulation of cell adhesion by protein-tyrosine phosphatases. I. Cell-matrix adhesion. J. Biol. Chem. 281, 15593–6.

Burridge, K., Wennerberg, K., 2004. Rho and Rac take center stage. Cell 116, 167–79.

Busch, T., Armacki, M., Eiseler, T., Joodi, G., Temme, C., Jansen, J., von Wichert, G., Omary, M.B., Spatz, J.P., Seufferlein, T., 2012. Keratin 8 phosphorylation regulates keratin reorganization and migration of epithelial tumor cells. J. Cell Sci. 125, 2148–59.

Byzova, T. V., Goldman, C.K., Pampori, N., Thomas, K.A., Bett, A., Shattil, S.J., Plow, E.F., 2000. A mechanism for modulation of cellular responses to VEGF: activation of the integrins. Mol. Cell 6, 851–60.

Calalb, M.B., Polte, T.R., Hanks, S.K., 1995. Tyrosine phosphorylation of focal adhesion kinase at sites in the catalytic domain regulates kinase activity: a role for Src family kinases. Mol. Cell. Biol. 15, 954–63.

Canonici, A., Steelant, W., Rigot, V., Khomitch-Baud, A., Boutaghou-Cherid, H., Bruyneel, E., Van Roy, F., Garrouste, F., Pommier, G., André, F., 2008. Insulin-like growth factor-I receptor, E-cadherin and αv integrin form a dynamic complex under the control of α-catenin. Int. J. Cancer 122, 572–82.

Capaldo, C.T., Farkas, A.E., Nusrat, A., 2014. Epithelial adhesive junctions. F1000Prime Rep. 6, 1–4.

Carmeliet, P., Lampugnani, M.-G., Moons, L., Breviario, F., Compernolle, V., Bono, F., Balconi, G., Spagnuolo, R., Oosthuyse, B., Dewerchin, M., Zanetti, A., Angellilo, A., Mattot, V., Nuyens, D., Lutgens, E., Clotman, F., de Ruiter, M.C., Gittenberger-de Groot, A., Poelmann, R., Lupu, F., Herbert, J.-M., Collen, D., Dejana, E., 1999. Targeted deficiency or cytosolic truncation of the VE-cadherin gene in mice impairs VEGF-mediated endothelial survival and angiogenesis. Cell 98, 147–57.

Carmona-Fontaine, C., Matthews, H.K., Kuriyama, S., Moreno, M., Dunn, G.A., Parsons, M., Stern, C.D., Mayor, R., 2008. Contact inhibition of locomotion in vivo controls neural crest directional migration. Nature 456, 957–61.

Carmona-Fontaine, C., Theveneau, E., Tzekou, A., Tada, M., Woods, M., Page, K.M., Parsons, M., Lambris, J.D., Mayor, R., 2011. Complement fragment C3a controls mutual cell attraction during collective cell migration. Dev. Cell 21, 1026–37.

Chan, C.E., Odde, D.J., 2008. Traction dynamics of filopodia on compliant substrates. Science 322, 1687–91.

Chang, F., Lemmon, C.A., Park, D., Romer, L.H., 2007. FAK potentiates Rac1 activation and localization to matrix adhesion sites: a role for βPIX. Mol. Biol. Cell 18, 253–264.

Chang, L., Goldman, R.D., 2004. Intermediate filaments mediate cytoskeletal crosstalk. Nat. Rev. Mol. Cell Biol. 5, 601–13.

Chappuis-Flament, S., 2001. Multiple cadherin extracellular repeats mediate homophilic binding and adhesion. J. Cell Biol. 154, 231–243.

Chartier, N.T., Lainé, M., Gout, S., Pawlak, G., Marie, C.A., Matos, P., Block, M.R., Jacquier-Sarlin, M.R., 2006. Laminin-5-integrin interaction signals through PI 3-kinase and Rac1b to promote assembly of adherens junctions in HT-29 cells. J. Cell Sci. 119, 31–46.

Chattopadhyay, N., Wang, Z., Ashman, L.K., Brady-Kalnay, S.M., Kreidberg, J.A., 2003. α3β1 integrin-CD151, a component of the cadherin-catenin complex, regulates PTPμ expression and cell-cell adhesion. J. Cell Biol. 163, 1351–62.

Chausovsky, A., Bershadsky, A.D., Borisy, G.G., 2000. Cadherin-mediated regulation of microtubule dynamics. Nat. Cell Biol. 2, 797–804.

Cheeseman, I.M., Desai, A., 2005. A combined approach for the localization and tandem affinity purification of protein complexes from metazoans. Sci. STKE 2005, 1–15.

Cheeseman, I.M., Niessen, S., Anderson, S., Hyndman, F., Yates, J.R., Oegema, K., Desai, A., 2004. A conserved protein network controls assembly of the outer kinetochore and its ability to sustain tension. Genes Dev. 18, 2255–68.

Chen, B.-H., Tzen, J.T.C., Bresnick, A.R., Chen, H.-C., 2002. Roles of Rho-associated kinase and myosin light chain kinase in morphological and migratory defects of focal adhesion kinase-null cells. J. Biol. Chem. 277, 33857–63.

Chen, H., Cohen, D.M., Choudhury, D.M., Kioka, N., Craig, S.W., 2005. Spatial distribution and functional significance of activated vinculin in living cells. J. Cell Biol. 169, 459–70.

Chiba, A., Keshishian, H., 1996. Neuronal pathfinding and recognition: roles of cell adhesion molecules. Dev. Biol. 180, 424–32.

Chigurupati, S., Arumugam, T. V., Son, T.G., Lathia, J.D., Jameel, S., Mughal, M.R., Tang, S.-C., Jo, D.-G., Camandola, S., Giunta, M., Rakova, I., McDonnell, N., Miele, L., Mattson, M.P., Poosala, S., 2007. Involvement of notch signaling in wound healing. PLoS One 2, e1167.

Choi, H.-J., Gross, J.C., Pokutta, S., Weis, W.I., 2009. Interactions of plakoglobin and β-catenin with desmosomal cadherins: basis of selective exclusion of α- and β-catenin from desmosomes. J. Biol. Chem. 284, 31776–88.

Chu, Y.-S., Thomas, W.A., Eder, O., Pincet, F., Perez, E., Thiery, J.P., Dufour, S., 2004. Force measurements in E-cadherin-mediated cell doublets reveal rapid adhesion strengthened by actin cytoskeleton remodeling through Rac and Cdc42. J. Cell Biol. 167, 1183–94.

Clarke, E.J., Allan, V.J., 2003. Cytokeratin intermediate filament organisation and dynamics in the vegetal cortex of living Xenopus laevis oocytes and eggs. Cell Motil. Cytoskeleton 56, 13–26.

Colakoğlu, G., Brown, A., 2009. Intermediate filaments exchange subunits along their length and elongate by end-to-end annealing. J. Cell Biol. 185, 769–77.

Conover, J.C., Doetsch, F., Garcia-Verdugo, J.-M., Gale, N.W., Yancopoulos, G.D., Alvarez-Buylla, A., 2000. Disruption of Eph/ephrin signaling affects migration and proliferation in the adult subventricular zone. Nat. Neurosci. 3, 1091–7.

Coulombe, P.A., Hutton, M.E., Vassar, R., Fuchs, E., 1991. A function for keratins and a common thread among different types of epidermolysis bullosa simplex diseases. J. Cell Biol. 115, 1661–74.

Crawford, B.D., Henry, C.A., Clason, T.A., Becker, A.L., Hille, M.B., 2003. Activity and distribution of paxillin, focal adhesion kinase, and cadherin indicate cooperative roles during zebrafish morphogenesis. Mol. Biol. Cell 14, 3065–81.

Dambly-Chaudière, C., Cubedo, N., Ghysen, A., 2007. Control of cell migration in the development of the posterior lateral line: antagonistic interactions between the chemokine receptors CXCR4 and CXCR7/RDC1. BMC Dev. Biol. 7, 23.

David, N.B., Sapède, D., Saint-Etienne, L., Thisse, C., Thisse, B., Dambly-Chaudière, C., Rosa, F.M., Ghysen, A., 2002. Molecular basis of cell migration in the fish lateral line: role of the chemokine receptor CXCR4 and of its ligand, SDF1. Proc. Natl. Acad. Sci. U. S. A. 99, 16297–302.

Davidson, L.A., Hoffstrom, B.G., Keller, R., DeSimone, D.W., 2002. Mesendoderm extension and mantle closure in Xenopus laevis gastrulation: combined roles for integrin α5β1, fibronectin, and tissue geometry. Dev. Biol. 242, 109–29.

Davidson, L.A., Keller, R., DeSimone, D.W., 2004a. Assembly and remodeling of the fibrillar fibronectin extracellular matrix during gastrulation and neurulation in Xenopus laevis. Dev. Dyn. 231, 888–95.

Davidson, L.A., Keller, R., DeSimone, D.W., 2004b. Patterning and tissue movements in a novel explant preparation of the marginal zone of Xenopus laevis. Gene Expr. Patterns 4, 457–66.

Davidson, L.A., Marsden, M., Keller, R., DeSimone, D.W., 2006. Integrin α5β1 and fibronectin regulate polarized cell protrusions required for Xenopus convergence and extension. Curr. Biol. 16, 833–44.

De Hoffmann, E., Stroobant, V., 2007. Mass Spectrometry: Principles and Applications. John Wiley and Sons.

De Rooij, J., Kerstens, A., Danuser, G., Schwartz, M.A., Waterman-Storer, C.M., 2005. Integrin-dependent actomyosin contraction regulates epithelial cell scattering. J. Cell Biol. 171, 153–64.

Defranco, B.H., Nickel, B.M., Baty, C.J., Martinez, J.S., Gay, V.L., Sandulache, V.C., Hackam, D.J., Murray, S.A., 2008. Migrating cells retain gap junction plaque structure and function. Cell Commun. Adhes. 15, 273–88.

Delanoe-Ayari, H., Kurdi, R. Al, Vallade, M., Gulino-Debrac, D., Riveline, D., 2004. Membrane and acto-myosin tension promote clustering of adhesion proteins. Proc. Natl. Acad. Sci. U. S. A. 101, 2229–34.

Desai, R.A., Gao, L., Raghavan, S., Liu, W.F., Chen, C.S., 2009. Cell polarity triggered by cell-cell adhesion via E-cadherin. J. Cell Sci. 122, 905–11.

Desai, R.A., Gopal, S.B., Chen, S., Chen, C.S., 2013. Contact inhibition of locomotion probabilities drive solitary versus collective cell migration. J. R. Soc. Interface 10, 20130717.

Desai, S.P., Bhatia, S.N., Toner, M., Irimia, D., 2013. Mitochondrial localization and the persistent migration of epithelial cancer cells. Biophys. J. 104, 2077–88.

Doherty, J.T., Conlon, F.L., Mack, C.P., Taylor, J.M., 2010. Focal adhesion kinase is essential for cardiac looping and multichamber heart formation. Genesis 48, 492–504.

Donà, E., Barry, J.D., Valentin, G., Quirin, C., Khmelinskii, A., Kunze, A., Durdu, S., Newton, L.R., Fernandez-Minan, A., Huber, W., Knop, M., Gilmour, D., 2013. Directional tissue migration through a self-generated chemokine gradient. Nature 503, 285–9.

Doyle, A.D., Wang, F.W., Matsumoto, K., Yamada, K.M., 2009. One-dimensional topography underlies three-dimensional fibrillar cell migration. J. Cell Biol. 184, 481–90.

Duchek, P., Rørth, P., 2001. Guidance of cell migration by EGF receptor signaling during Drosophila oogenesis. Science 291, 131–3.

Duchek, P., Somogyi, K., Jékely, G., Beccari, S., Rørth, P., 2001. Guidance of cell migration by the Drosophila PDGF/VEGF receptor. Cell 107, 17–26.

Dumbauld, D.W., Shin, H., Gallant, N.D., Michael, K.E., Radhakrishna, H., García, A.J., 2010. Contractility modulates cell adhesion strengthening through focal adhesion kinase and assembly of vinculin-containing focal adhesions. J. Cell. Physiol. 223, 746–56.

Dumortier, J.G., Martin, S., Meyer, D., Rosa, F.M., David, N.B., 2012. Collective mesendoderm migration relies on an intrinsic directionality signal transmitted through cell contacts. Proc. Natl. Acad. Sci. U. S. A. 109, 16945–50.

Dupin, I., Camand, E., Etienne-Manneville, S., 2009. Classical cadherins control nucleus and centrosome position and cell polarity. J. Cell Biol. 185, 779–86.

Dzamba, B.J., Jakab, K.R., Marsden, M., Schwartz, M.A., DeSimone, D.W., 2009. Cadherin adhesion, tissue tension, and noncanonical Wnt signaling regulate fibronectin matrix organization. Dev. Cell 16, 421–32.

Ehrlich, J.S., Hansen, M.D.H., Nelson, W.J., 2002. Spatio-temporal regulation of Rac1 localization and lamellipodia dynamics during epithelial cell-cell adhesion. Dev. Cell 3, 259–70.

El Sayegh, T.Y., Arora, P.D., Fan, L., Laschinger, C.A., Greer, P.A., McCulloch, C.A., Kapus, A., 2005. Phosphorylation of N-cadherin-associated cortactin by Fer kinase regulates N-cadherin mobility and intercellular adhesion strength. Mol. Biol. Cell 16, 5514–5527.

Elias, L.A.B., Wang, D.D., Kriegstein, A.R., 2007. Gap junction adhesion is necessary for radial migration in the neocortex. Nature 448, 901–7.

Engler, A.J., Carag-Krieger, C., Johnson, C.P., Raab, M., Tang, H.-Y., Speicher, D.W., Sanger, J.W., Sanger, J.M., Discher, D.E., 2008. Embryonic cardiomyocytes beat best on a matrix with heart-like elasticity: scar-like rigidity inhibits beating. J. Cell Sci. 121, 3794–802.

Engler, A.J., Sen, S., Sweeney, H.L., Discher, D.E., 2006. Matrix elasticity directs stem cell lineage specification. Cell 126, 677–89.

Etienne-Manneville, S., Hall, A., 2002. Rho GTPases in cell biology. Nature 420, 629–35.

Eyckmans, J., Boudou, T., Yu, X., Chen, C.S., 2011. A hitchhiker's guide to mechanobiology. Dev. Cell 21, 35–47.

Ezratty, E.J., Partridge, M.A., Gundersen, G.G., 2005. Microtubule-induced focal adhesion disassembly is mediated by dynamin and focal adhesion kinase. Nat. Cell Biol. 7, 581–90.

Fabry, B., Klemm, A.H., Kienle, S., Schäffer, T.E., Goldmann, W.H., 2011. Focal adhesion kinase stabilizes the cytoskeleton. Biophys. J. 101, 2131–8.

Farge, E., 2003. Mechanical induction of Twist in the Drosophila foregut/stomodeal primordium. Curr. Biol. 13, 1365–1377.

Farooqui, R., Fenteany, G., 2005. Multiple rows of cells behind an epithelial wound edge extend cryptic lamellipodia to collectively drive cell-sheet movement. J. Cell Sci. 118, 51–63.

Fonar, Y., Gutkovich, Y.E., Root, H., Malyarova, A., Aamar, E., Golubovskaya, V.M., Elias, S., Elkouby, Y.M., Frank, D., 2011. Focal adhesion kinase protein regulates Wnt3a gene expression to control cell fate specification in the developing neural plate. Mol. Biol. Cell 22, 2409–21.

Forman, J.R., Clarke, J., 2007. Mechanical unfolding of proteins: insights into biology, structure and folding. Curr. Opin. Struct. Biol. 17, 58–66.

Fouquet, B., Herrmann, H., Franz, J.K., Franke, W.W., 1988. Expression of intermediate filament proteins during development of Xenopus laevis. III. Identification of mRNAs encoding cytokeratins typical of complex epithelia. Development 104, 533–48.

Fournier, A.K., Campbell, L.E., Castagnino, P., Liu, W.F., Chung, B.M., Weaver, V.M., Chen, C.S., Assoian, R.K., 2008. Rac-dependent cyclin D1 gene expression regulated by cadherin- and integrin-mediated adhesion. J. Cell Sci. 121, 226–33.

Franz, J.K., Franke, W.W., 1986. Cloning of cDNA and amino acid sequence of a cytokeratin expressed in oocytes of Xenopus laevis. Proc. Natl. Acad. Sci. U. S. A. 83, 6475–9.

Franz, J.K., Gall, L., Williams, M.A., Picheral, B., Franke, W.W., 1983. Intermediate-size filaments in a germ cell: Expression of cytokeratins in oocytes and eggs of the frog Xenopus. Proc. Natl. Acad. Sci. U. S. A. 80, 6254–8.

Fredberg, J.J., Trepat, X., 2011. Plithotaxis and emergent dynamics in collective cellular migration. Trends Cell Biol.

Frenzel, E.M., Johnson, R.G., 1996. Gap junction formation between cultured embryonic lens cells is inhibited by antibody to N-cadherin. Dev. Biol. 179, 1–16.

Friedl, P., Gilmour, D., 2009. Collective cell migration in morphogenesis, regeneration and cancer. Nat. Rev. Mol. Cell Biol. 10, 445–57.

Friedl, P., Locker, J., Sahai, E., Segall, J.E., 2012. Classifying collective cancer cell invasion. Nat. Cell Biol. 14, 777–83.

Friedman, J.R., Nunnari, J., 2014. Mitochondrial form and function. Nature 505, 335–43.

Fudge, D.S., Gardner, K.H., Forsyth, V.T., Riekel, C., Gosline, J.M., 2003. The mechanical properties of hydrated intermediate filaments: insights from hagfish slime threads. Biophys. J. 85, 2015–27.

Furuta, Y., Ilić, D., Kanazawa, S., Takeda, N., Yamamoto, T., Aizawa, S., 1995. Mesodermal defect in late phase of gastrulation by a targeted mutation of focal adhesion kinase, FAK. Oncogene 11, 1989–95.

Gabbiani, G., Chaponnier, C., Huttner, I., 1978. Cytoplasmic filaments and gap junctions in epithelial cells and myofibroblasts during wound healing. J. Cell Biol. 76, 561–8.

Galloway, C.A., Yoon, Y., 2012. What comes first, misshape or dysfunction? The view from metabolic excess. J. Gen. Physiol. 139, 455–63.

Ganz, A., Lambert, M., Saez, A., Silberzan, P., Buguin, A., Mège, R.-M., Ladoux, B., 2006. Traction forces exerted through N-cadherin contacts. Biol. Cell 98, 721–30.

Gao, L., McBeath, R., Chen, C.S., 2010. Stem cell shape regulates a chondrogenic versus myogenic fate through Rac1 and N-cadherin. Stem Cells 28, 564–72.

Geiger, B., Spatz, J.P., Bershadsky, A.D., 2009. Environmental sensing through focal adhesions. Nat. Rev. Mol. Cell Biol. 10, 21–33.

Georges-Labouesse, E., George, E.L., Rayburn, H., Hynes, R.O., 1996. Mesodermal development in mouse embryos mutant for fibronectin. Dev. Dyn. 207, 145–56.

Giannone, G., Sheetz, M.P., 2006. Substrate rigidity and force define form through tyrosine phosphatase and kinase pathways. Trends Cell Biol. 16, 213–23.

Gilland, E., Miller, A.L., Karplus, E., Baker, R., Webb, S.E., 1999. Imaging of multicellular large-scale rhythmic calcium waves during zebrafish gastrulation. Proc. Natl. Acad. Sci. U. S. A. 96, 157–61.

Gingras, A.R., Vogel, K.-P., Steinhoff, H.-J., Ziegler, W.H., Patel, B., Emsley, J., Critchley, D.R., Roberts, G.C.K., Barsukov, I.L., 2006. Structural and dynamic characterization of a vinculin binding site in the talin rod. Biochemistry 45, 1805–17.

Godsel, L.M., Hobbs, R.P., Green, K.J., 2008. Intermediate filament assembly: dynamics to disease. Trends Cell Biol. 18, 28–37.

Grashoff, C., Hoffman, B.D., Brenner, M.D., Zhou, R., Parsons, M., Yang, M.T., McLean, M.A., Sligar, S.G., Chen, C.S., Ha, T., Schwartz, M.A., 2010. Measuring mechanical tension across vinculin reveals regulation of focal adhesion dynamics. Nature 466, 263–6.

Green, K.J., Geiger, B., Jones, J.C.R., Talian, J.C., Goldman, R.D., 1987. The relationship between intermediate filaments and microfilaments before and during the formation of desmosomes and adherens-type junctions in mouse epidermal keratinocytes. J. Cell Biol. 104, 1389–402.

Gu, J., Tamura, M., Pankov, R., Danen, E.H.J., Takino, T., Matsumoto, K., Yamada, K.M., 1999. Shc and FAK differentially regulate cell motility and directionality modulated by PTEN. J. Cell Biol. 146, 389–403.

Guarino, M., 2007. Epithelial-mesenchymal transition and tumour invasion. Int. J. Biochem. Cell Biol. 39, 2153–60.

Gygi, S.P., Corthals, G.L., Zhang, Y., Rochon, Y., Aebersold, R., 2000. Evaluation of two-dimensional gel electrophoresis-based proteome analysis technology. Proc. Natl. Acad. Sci. U. S. A. 97, 9390–5.

Haas, P., Gilmour, D., 2006. Chemokine signaling mediates self-organizing tissue migration in the zebrafish lateral line. Dev. Cell 10, 673–80.

Hall, A., 1998. Rho GTPases and the actin cytoskeleton. Science 279, 509–14.

Hammer, Ø., Harper, D.A.T., Ryan, P.D., 2001. PAST: Paleontological Statistics software package for education and data analysis. Palaeontol. Electron. 4, 1–9.

Hanks, S.K., Calalb, M.B., Harper, M.C., Patel, S.K., 1992. Focal adhesion protein-tyrosine kinase phosphorylated in response to cell attachment to fibronectin. Proc. Natl. Acad. Sci. U. S. A. 89, 8487–91.

Harrison, D.G., Widder, J., Grumbach, I., Chen, W., Weber, M., Searles, C., 2006. Endothelial mechanotransduction, nitric oxide and vascular inflammation. J. Intern. Med. 259, 351–63.

Hatzfeld, M., Haffner, C., Schulze, K., Vinzens, U., 2000. The function of plakophilin 1 in desmosome assembly and actin filament organization. J. Cell Biol. 149, 209–22.

Heasman, J., Ginsberg, D., Geiger, B., Goldstone, K., Pratt, T., Yoshida-Noro, C., Wylie, C., 1994. A functional test for maternally inherited cadherin in Xenopus shows its importance in cell adhesion at the blastula stage. Development 120, 49–57.

Helfand, B.T., Mendez, M.G., Murthy, S.N.P., Shumaker, D.K., Grin, B., Mahammad, S., Aebi, U., Wedig, T., Wu, Y.I., Hahn, K.M., Inagaki, M., Herrmann, H., Goldman, R.D., 2011. Vimentin organization modulates the formation of lamellipodia. Mol. Biol. Cell 22, 1274–1289.

Hellström, M., Phng, L.-K., Hofmann, J.J., Wallgard, E., Coultas, L., Lindblom, P., Alva, J., Nilsson, A.-K., Karlsson, L., Gaiano, N., Yoon, K., Rossant, J., Iruela-Arispe, M.L., Kalén, M., Gerhardt, H., Betsholtz, C., 2007. Dll4 signalling through Notch1 regulates formation of tip cells during angiogenesis. Nature 445, 776–80.

Henry, C.A., Crawford, B.D., Yan, Y.-L., Postlethwait, J., Cooper, M.S., Hille, M.B., 2001. Roles for zebrafish focal adhesion kinase in notochord and somite morphogenesis. Dev. Biol. 240, 474–87.

Hens, M.D., DeSimone, D.W., 1995. Molecular analysis and developmental expression of the focal adhesion kinase pp125FAK in Xenopus laevis. Dev. Biol. 170, 274–88.

Hirano, S., Nose, A., Hatta, K., Kawakami, A., Takeichi, M., 1987. Calcium-dependent cell-cell adhesion molecules (cadherins): subclass specificities and possible involvement of actin bundles. J. Cell Biol. 105, 2501–10.

Hodgson, L., Shen, F., Hahn, K.M., 2010. Biosensors for characterizing the dynamics of Rho family GTPases in living cells. Curr. Protoc. cell Biol. 46, 14.11.1–26.

Hodivala, K.J., Watt, F.M., 1994. Evidence that cadherins play a role in the downregulation of integrin expression that occurs during keratinocyte terminal differentiation. J. Cell Biol. 124, 589–600.

Hofmann, I., Franke, W.W., 1997. Heterotypic interactions and filament assembly of type I and type II cytokeratins in vitro: viscometry and determinations of relative affinities. Eur. J. Cell Biol. 72, 122–32.

Hotta, A., Kawakatsu, T., Nakatani, T., Sato, T., Matsui, C., Sukezane, T., Akagi, T., Hamaji, T., Grigoriev, I., Akhmanova, A., Takai, Y., Mimori-Kiyosue, Y., 2010. Laminin-based cell adhesion anchors microtubule plus ends to the epithelial cell basal cortex through LL5α/β. J. Cell Biol. 189, 901–17.

Hsu, M.-Y., Andl, T., Li, G., Meinkoth, J.L., Herlyn, M., 2000. Cadherin repertoire determines partner-specific gap junctional communication during melanoma progression. J. Cell Sci. 113 (Pt 9, 1535–42.

Huang, G.Y., Cooper, E.S., Waldo, K., Kirby, M.L., Gilula, N.B., Lo, C.W., 1998. Gap junction-mediated cell-cell communication modulates mouse neural crest migration. J. Cell Biol. 143, 1725–34.

Huveneers, S., Danen, E.H.J., 2009. Adhesion signaling - crosstalk between integrins, Src and Rho. J. Cell Sci. 122, 1059–1069.

Huveneers, S., de Rooij, J., 2013. Mechanosensitive systems at the cadherin-F-actin interface. J. Cell Sci. 126, 403–13.

Ikeya, T., Hayashi, S., 1999. Interplay of Notch and FGF signaling restricts cell fate and MAPK activation in the Drosophila trachea. Development 126, 4455–63.

Ilić, D., Furuta, Y., Kanazawa, S., Takeda, N., Sobue, K., Nakatsuji, N., Nomura, S., Fujimoto, J., Okada, M., Yamamoto, T., Aizawa, S., 1995. Reduced cell motility and enhanced focal adhesion contact formation in cells from FAK-deficient mice. Nature 377, 539–44.

Ilić, D., Kovacic, B., Johkura, K., Schlaepfer, D.D., Tomasević, N., Han, Q., Kim, J.-B., Howerton, K., Baumbusch, C., Ogiwara, N., Streblow, D.N., Nelson, J.A., Dazin, P., Shino, Y., Sasaki, K., Damsky, C.H., 2004. FAK promotes organization of fibronectin matrix and fibrillar adhesions. J. Cell Sci. 117, 177–87.

Illés, A., Enyedi, B., Tamás, P., Balázs, A., Bogel, G., Lukács, M., Buday, L., 2006. Cortactin is required for integrin-mediated cell spreading. Immunol. Lett. 104, 124–30.

Jaalouk, D.E., Lammerding, J., 2009. Mechanotransduction gone awry. Nat. Rev. Mol. Cell Biol. 10, 63–73.

Jacobson, K., Rajfur, Z., Vitriol, E., Hahn, K.M., 2008. Chromophore-assisted laser inactivation in cell biology. Trends Cell Biol. 18, 443–50.

Jefferson, J.J., Leung, C.L., Liem, R.K.H., 2004. Plakins: goliaths that link cell junctions and the cytoskeleton. Nat. Rev. Mol. Cell Biol. 5, 542–53.

Jiang, G., Huang, A.H., Cai, Y., Tanase, M., Sheetz, M.P., 2006. Rigidity sensing at the leading edge through αvβ3 integrins and RPTPα. Biophys. J. 90, 1804–9.

Johnson, C.P., Tang, H.-Y., Carag, C., Speicher, D.W., Discher, D.E., 2007. Forced unfolding of proteins within cells. Science 317, 663–6.

Jongen, W.M.F., Fitzgerald, D.J., Asamoto, M., Piccoli, C., Slaga, T.J., Gros, D., Takeichi, M., Yamasaki, H., 1991. Regulation of connexin 43-mediated gap junctional intercellular communication by Ca2+ in mouse epidermal cells is controlled by E-cadherin. J. Cell Biol. 114, 545–55.

Joos, T.O., Whittaker, C.A., Meng, F., DeSimone, D.W., Gnau, V., Hausen, P., 1995. Integrin α5 during early development of Xenopus laevis. Mech. Dev. 50, 187–99.

Jülich, D., Geisler, R., Holley, S.A., 2005. Integrin α5 and delta/notch signaling have complementary spatiotemporal requirements during zebrafish somitogenesis. Dev. Cell 8, 575–86.

Kang, H.-G., Jenabi, J.M., Zhang, J., Keshelava, N., Shimada, H., May, W.A., Ng, T., Reynolds, C.P., Triche, T.J., Sorensen, P.H.B., 2007. E-cadherin cell-cell adhesion in ewing tumor cells mediates suppression of anoikis through activation of the ErbB4 tyrosine kinase. Cancer Res. 67, 3094–105.

Keller, R., 2002. Shaping the vertebrate body plan by polarized embryonic cell movements. Science 298, 1950–4.

Keller, R., 2005. Cell migration during gastrulation. Curr. Opin. Cell Biol. 17, 533–41.

Keller, R., 2012. Physical biology returns to morphogenesis. Science 338, 201–3.

Keller, R., Davidson, L.A., Edlund, A., Elul, T., Ezin, M., Shook, D., Skoglund, P., 2000. Mechanisms of convergence and extension by cell intercalation. Philos. Trans. R. Soc. Lond. B. Biol. Sci. 355, 897–922.

Khalil, A.A., Friedl, P., 2010. Determinants of leader cells in collective cell migration. Integr. Biol. 2, 568–74.

Kim, J.H., Serra-Picamal, X., Tambe, D.T., Zhou, E.H., Park, C.Y., Sadati, M., Park, J.-A., Krishnan, R., Gweon, B., Millet, E., Butler, J.P., Trepat, X., Fredberg, J.J., 2013. Propulsion and navigation within the advancing monolayer sheet. Nat. Mater. 12, 856–63.

Kitt, K.N., Nelson, W.J., 2011. Rapid suppression of activated Rac1 by cadherins and nectins during de novo cell-cell adhesion. PLoS One 6, e17841.

Klarlund, J.K., Block, E.R., 2011. Free edges in epithelia as cues for motility. Cell Adh. Migr. 5, 106–110.

Klymkowsky, M.W., Shook, D., Maynell, L.A., 1992. Evidence that the deep keratin filament systems of the Xenopus embryo act to ensure normal gastrulation. Proc. Natl. Acad. Sci. U. S. A. 89, 8736–40.

Knudsen, K.A., Wheelock, M.J., 1992. Plakoglobin, or an 83-kD homologue distinct from β-catenin, interacts with E-cadherin and N-cadherin. J. Cell Biol. 118, 671–9.

Kolega, J., 1981. The movement of cell clusters in vitro: morphology and directionality. J. Cell Sci. 49, 15–32.

Kolodkin, A.L., Tessier-Lavigne, M., 2011. Mechanisms and molecules of neuronal wiring: a primer. Cold Spring Harb. Perspect. Biol. 3, 1–14.

Kölsch, A., Windoffer, R., Leube, R.E., 2009. Actin-dependent dynamics of keratin filament precursors. Cell Motil. Cytoskeleton 66, 976–85.

Korobova, F., Gauvin, T.J., Higgs, H.N., 2014. A role for myosin II in mammalian mitochondrial fission. Curr. Biol. 24, 409–14.

Kostic, A., Sheetz, M.P., 2006. Fibronectin rigidity response through Fyn and p130Cas recruitment to the leading edge. Mol. Biol. Cell 17, 2684–2695.

Kouklis, P.D., Hutton, E., Fuchs, E., 1994. Making a connection: direct binding between keratin intermediate filaments and desmosomal proteins. J. Cell Biol. 127, 1049–60.

Kowalczyk, A.P., Bornslaeger, E.A., Borgwardt, J.E., Palka, H.L., Dhaliwal, A.S., Corcoran, C.M., Denning, M.F., Green, K.J., 1997. The amino-terminal domain of desmoplakin binds to plakoglobin and clusters desmosomal cadherin-plakoglobin complexes. J. Cell Biol. 139, 773–84.

Kowalczyk, A.P., Navarro, P., Dejana, E., Bornslaeger, E.A., Green, K.J., Kopp, D.S., Borgwardt, J.E., 1998. VE-cadherin and desmoplakin are assembled into dermal microvascular endothelial intercellular junctions: a pivotal role for plakoglobin in the recruitment of desmoplakin to intercellular junctions. J. Cell Sci. 111, 3045–57.

Kozlowski, C., Srayko, M., Nedelec, F., 2007. Cortical microtubule contacts position the spindle in C. elegans embryos. Cell 129, 499–510.

Kragtorp, K.A., Miller, J.R., 2006. Regulation of somitogenesis by Ena/VASP proteins and FAK during Xenopus development. Development 133, 685–95.

Kreplak, L., Herrmann, H., Aebi, U., 2008. Tensile properties of single desmin intermediate filaments. Biophys. J. 94, 2790–9.

Krieg, M., Arboleda-Estudillo, Y., Puech, P.-H., Käfer, J., Graner, F., Müller, D.J., Heisenberg, C.-P., 2008. Tensile forces govern germ-layer organization in zebrafish. Nat. Cell Biol. 10, 429–36.

Kühl, M., Wedlich, D., 1996. Xenopus cadherins: sorting out types and functions in embryogenesis. Dev. Dyn. 207, 121–34.

Kuijper, S., Turner, C.J., Adams, R.H., 2007. Regulation of angiogenesis by Eph-ephrin interactions. TCM 17, 145–51.

Kupfer, A., Louvard, D., Singer, S.J., 1982. Polarization of the Golgi apparatus and the microtubule-organizing center in cultured fibroblasts at the edge of an experimental wound. Proc. Natl. Acad. Sci. U. S. A. 79, 2603–7.

Ladoux, B., Anon, E., Lambert, M., Rabodzey, A., Hersen, P., Buguin, A., Silberzan, P., Mège, R.-M., 2010. Strength dependence of cadherin-mediated adhesions. Biophys. J. 98, 534–542.

Landesman, Y., Goodenough, D.A., Paul, D.L., 2000. Gap junctional communication in the early Xenopus embryo. J. Cell Biol. 150, 929–36.

Larsson, C., 2006. Protein kinase C and the regulation of the actin cytoskeleton. Cell. Signal. 18, 276–84.

Lauble, H., Stout, C.D., 1995. Steric and conformational features of the aconitase mechanism. Proteins 22, 1–11.

Le Duc, Q., Shi, Q., Blonk, I., Sonnenberg, A., Wang, N., Leckband, D.E., de Rooij, J., 2010. Vinculin potentiates E-cadherin mechanosensing and is recruited to actin-anchored sites within adherens junctions in a myosin II-dependent manner. J. Cell Biol. 189, 1107–15.

Leckband, D.E., Le Duc, Q., Wang, N., De Rooij, J., 2011. Mechanotransduction at cadherin-mediated adhesions. Curr. Opin. Cell Biol. 23, 523–30.

Lecuit, T., Lenne, P.-F., 2007. Cell surface mechanics and the control of cell shape, tissue patterns and morphogenesis. Nat. Rev. Mol. Cell Biol. 8, 633–44.

Lee, C.-H., Gumbiner, B.M., 1995. Disruption of gastrulation movements in Xenopus by a dominant-negative mutant for C-cadherin. Dev. Biol. 171, 363–73.

Lee, H.-H., Tien, S.-C., Jou, T.-S., Chang, Y.-C., Jhong, J.-G., Chang, Z.-F., 2010. Src-dependent phosphorylation of ROCK participates in regulation of focal adhesion dynamics. J. Cell Sci. 123, 3368–77.

Legant, W.R., Miller, J.S., Blakely, B.L., Cohen, D.M., Genin, G.M., Chen, C.S., 2010. Measurement of mechanical tractions exerted by cells in three-dimensional matrices. Nat. Methods 7, 969–71.

Leonard, M., Chan, Y., Menko, A.S., 2008. Identification of a novel intermediate filament-linked N-cadherin/γ-catenin complex involved in the establishment of the cytoarchitecture of differentiated lens fiber cells. Dev. Biol. 319, 298–308.

Levental, K.R., Yu, H., Kass, L., Lakins, J.N., Egeblad, M., Erler, J.T., Fong, S.F.T., Csiszar, K., Giaccia, A., Weninger, W.J., Yamauchi, M., Gasser, D.L., Weaver, V.M., 2009. Matrix crosslinking forces tumor progression by enhancing integrin signaling. Cell 139, 891–906.

Li, W.-C., Roberts, A., Soffe, S.R., 2009. Locomotor rhythm maintenance: electrical coupling among premotor excitatory interneurons in the brainstem and spinal cord of young Xenopus tadpoles. J. Physiol. 587, 1677–93.

Lim, S.-T., Chen, X.L., Tomar, A., Miller, N.L.G., Yoo, J., Schlaepfer, D.D., 2010. Knock-in mutation reveals an essential role for focal adhesion kinase activity in blood vessel morphogenesis and cell motility-polarity but not cell proliferation. J. Biol. Chem. 285, 21526–36.

Lim, Y., Lim, S.-T., Tomar, A., Gardel, M.L., Bernard-Trifilo, J.A., Chen, X.L., Uryu, S.A., Canete-Soler, R., Zhai, J., Lin, H., Schlaepfer, W.W., Nalbant, P., Bokoch, G., Ilić, D., Waterman-Storer, C.M., Schlaepfer, D.D., 2008. PyK2 and FAK connections to p190Rho guanine nucleotide exchange factor regulate RhoA activity, focal adhesion formation, and cell motility. J. Cell Biol. 180, 187–203.

Lin, J.H.C., Takano, T., Cotrina, M.L., Arcuino, G., Kang, J., Liu, S., Gao, Q., Jiang, L., Li, F., Lichtenberg-Frate, H., Haubrich, S., Willecke, K., Goldman, S.A., Nedergaard, M., 2002. Connexin 43 enhances the adhesivity and mediates the invasion of malignant glioma cells. J. Neurosci. 22, 4302–11.

Liska, A.J., Popov, A. V., Sunyaev, S., Coughlin, P., Habermann, B., Shevchenko, A., Bork, P., Karsenti, E., Shevchenko, A., 2004. Homology-based functional proteomics by mass spectrometry: application to the Xenopus microtubule-associated proteome. Proteomics 4, 2707–21.

Little, W.C., Schwartlander, R., Smith, M.L., Gourdon, D., Vogel, V., 2009. Stretched extracellular matrix proteins turn fouling and are functionally rescued by the chaperones albumin and casein. Nano Lett. 9, 4158–67.

Little, W.C., Smith, M.L., Ebneter, U., Vogel, V., 2008. Assay to mechanically tune and optically probe fibrillar fibronectin conformations from fully relaxed to breakage. Matrix Biol. 27, 451–61.

Liu, W.F., Nelson, C.M., Tan, J.L., Chen, C.S., 2007. Cadherins, RhoA, and Rac1 are differentially required for stretch-mediated proliferation in endothelial versus smooth muscle cells. Circ. Res. 101, e44–52.

Liu, Y., Sweet, D.T., Irani-Tehrani, M., Maeda, N., Tzima, E., 2008. Shc coordinates signals from intercellular junctions and integrins to regulate flow-induced inflammation. J. Cell Biol. 182, 185–96.

Liu, Z., Tan, J.L., Cohen, D.M., Yang, M.T., Sniadecki, N.J., Ruiz, S.A., Nelson, C.M., Chen, C.S., 2010. Mechanical tugging force regulates the size of cell-cell junctions. Proc. Natl. Acad. Sci. U. S. A. 107, 9944–49.

Llense, F., Martín-Blanco, E., 2008. JNK signaling controls border cell cluster integrity and collective cell migration. Curr. Biol. 18, 538–44.

Llimargas, M., 1999. The Notch pathway helps to pattern the tips of the Drosophila tracheal branches by selecting cell fates. Development 126, 2355–64.

Londono, C., Loureiro, M.J., Slater, B., Lucker, P.B., Soleas, J., Sathananthan, S., Aitchison, J.S., Kabla, A.J., McGuigan, A.P., 2014. Nonautonomous contact guidance signaling during collective cell migration. Proc. Natl. Acad. Sci.

Long, H.A., Boczonadi, V., McInroy, L., Goldberg, M., Määttä, A., 2006. Periplakin-dependent re-organisation of keratin cytoskeleton and loss of collective migration in keratin-8-downregulated epithelial sheets. J. Cell Sci. 119, 5147–59.

Machacek, M., Hodgson, L., Welch, C., Elliott, H., Pertz, O., Nalbant, P., Abell, A., Johnson, G.L., Hahn, K.M., Danuser, G., 2009. Coordination of Rho GTPase activities during cell protrusion. Nature 461, 99–103.

Malovannaya, A., Li, Y., Bulynko, Y., Jung, S.Y., Wang, Y., Lanz, R.B., O'Malley, B.W., Qin, J., 2010. Streamlined analysis schema for high-throughput identification of endogenous protein complexes. Proc. Natl. Acad. Sci. U. S. A. 107, 2431–6.

Mammoto, T., Ingber, D.E., 2010. Mechanical control of tissue and organ development. Development 137, 1407–20.

Margadant, F., Chew, L.L., Hu, X., Yu, H., Bate, N., Zhang, X., Sheetz, M.P., 2011. Mechanotransduction in vivo by repeated talin stretch-relaxation events depends upon vinculin. PLoS Biol. 9, e1001223.

Marsden, M., DeSimone, D.W., 2001. Regulation of cell polarity, radial intercalation and epiboly in Xenopus: novel roles for integrin and fibronectin. Development 128, 3635–47.

Marsden, M., DeSimone, D.W., 2003. Integrin-ECM interactions regulate cadherin-dependent cell adhesion and are required for convergent extension in Xenopus. Curr. Biol. 13, 1182–91.

Martinez-Rico, C., Pincet, F., Thiery, J.P., Dufour, S., 2010. Integrins stimulate E-cadherin-mediated intercellular adhesion by regulating Src-kinase activation and actomyosin contractility. J. Cell Sci. 123, 712–722.

Maruthamuthu, V., Aratyn-Schaus, Y., Gardel, M.L., 2010. Conserved F-actin dynamics and force transmission at cell adhesions. Curr. Opin. Cell Biol. 22, 583–588.

Maruthamuthu, V., Sabass, B., Schwarz, U.S., Gardel, M.L., 2011. Cell-ECM traction force modulates endogenous tension at cell-cell contacts. Proc. Natl. Acad. Sci. U. S. A. 108, 4708–13.

Matsuda, M., Chitnis, A.B., 2010. Atoh1a expression must be restricted by Notch signaling for effective morphogenesis of the posterior lateral line primordium in zebrafish. Development 137, 3477–87.

Mbemba, F., Houbion, A., Raes, M., Remacle, J., 1985. Subcellular localization and modification with ageing of glutathione, glutathione peroxidase and glutathione reductase activities in human fibroblasts. Biochim. Biophys. Acta 838, 211–20.

McBeath, R., Pirone, D.M., Nelson, C.M., Bhadriraju, K., Chen, C.S., 2004. Cell shape, cytoskeletal tension, and RhoA regulate stem cell lineage commitment. Dev. Cell 6, 483–95.

McDonald, J.A., Pinheiro, E.M., Kadlec, L., Schupbach, T., Montell, D.J., 2006. Multiple EGFR ligands participate in guiding migrating border cells. Dev. Biol. 296, 94–103.

McDonald, J.A., Pinheiro, E.M., Montell, D.J., 2003. PVF1, a PDGF/VEGF homolog, is sufficient to guide border cells and interacts genetically with Taiman. Development 130, 3469–78.

McGarry, J.G., Maguire, P., Campbell, V.A., O'Connell, B.C., Prendergast, P.J., Jarvis, S.P., 2008. Stimulation of nitric oxide mechanotransduction in single osteoblasts using atomic force microscopy. J. Orthop. Res. 26, 513–21.

McLachlan, R.W., Kraemer, A., Helwani, F.M., Kovacs, E.M., Yap, A.S., 2007. E-cadherin adhesion activates c-Src signaling at cell-cell contacts. Mol. Biol. Cell 18, 3214–3223.

Meng, W., Mushika, Y., Ichii, T., Takeichi, M., 2008. Anchorage of microtubule minus ends to adherens junctions regulates epithelial cell-cell contacts. Cell 135, 948–59.

Merriam, J.M., Rubenstein, A.B., Klymkowsky, M.W., 1997. Cytoplasmically anchored plakoglobin induces a WNT-like phenotype in Xenopus. Dev. Biol. 185, 67–81.

Mertz, A.F., Che, Y., Banerjee, S., Goldstein, J.M., Rosowski, K.A., Revilla, S.F., Niessen, C.M., Marchetti, M.C., Dufresne, E.R., Horsley, V., 2013. Cadherin-based intercellular adhesions organize epithelial cell-matrix traction forces. Proc. Natl. Acad. Sci. 110, 842–7.

Messina, G., Blasi, C., La Rocca, S.A., Pompili, M., Calconi, A., Grossi, M., 2005. p27 Kip1 acts downstream of N-cadherin-mediated cell adhesion to promote myogenesis beyond cell cycle regulation. Mol. Biol. Cell 16, 1469–1480.

Miravet, S., Piedra, J., Castaño, J., Raurell, I., Francí, C., Duñach, M., García de Herreros, A., 2003. Tyrosine phosphorylation of plakoglobin causes contrary effects on its association with desmosomes and adherens junction components and modulates β-catenin-mediated transcription. Mol. Cell. Biol. 23, 7391–7402.

Mitra, S.K., Hanson, D.A., Schlaepfer, D.D., 2005. Focal adhesion kinase: in command and control of cell motility. Nat. Rev. Mol. Cell Biol. 6, 56–68.

Moissoglu, K., Schwartz, M.A., 2006. Integrin signalling in directed cell migration. Biol. Cell 98, 547–55.

Monier-Gavelle, F., Duband, J.-L., 1997. Cross talk between adhesion molecules: control of N-cadherin activity by intracellular signals elicited by β1 and β3 integrins in migrating neural crest cells. J. Cell Biol. 137, 1663–1681.

Montell, D.J., Yoon, W.H., Starz-Gaiano, M., 2012. Group choreography: mechanisms orchestrating the collective movement of border cells. Nat. Rev. Mol. Cell Biol. 13, 631–45.

Moore, S.W., Roca-Cusachs, P., Sheetz, M.P., 2010. Stretchy proteins on stretchy substrates: the important elements of integrin-mediated rigidity sensing. Dev. Cell 19, 194–206.

Mourton, T., Hellberg, C.B., Burden-Gulley, S.M., Hinman, J., Rhee, A., Brady-Kalnay, S.M., 2001. The PTPμ protein-tyrosine phosphatase binds and recruits the scaffolding protein RACK1 to cell-cell contacts. J. Biol. Chem. 276, 14896–901.

Müller, E.J., Williamson, L., Kolly, C., Suter, M.M., 2008. Outside-in signaling through integrins and cadherins: a central mechanism to control epidermal growth and differentiation? J. Invest. Dermatol. 128, 501–16.

Muller-Marschhausen, K., Waschke, J., Drenckhahn, D., 2008. Physiological hydrostatic pressure protects endothelial monolayer integrity. Am. J. Physiol. cell Physiol. 294, 324–332.

Murrell, M., Kamm, R.D., Matsudaira, P., 2011. Substrate viscosity enhances correlation in epithelial sheet movement. Biophys. J. 101, 297–306.

Myers, J.P., Robles, E., Ducharme-Smith, A., Gomez, T.M., 2012. Focal adhesion kinase modulates Cdc42 activity downstream of positive and negative axon guidance cues. J. Cell Sci. 125, 2918–29.

Na, S., Collin, O., Chowdhury, F., Tay, B., Ouyang, M., Wang, Y., Wang, N., 2008. Rapid signal transduction in living cells is a unique feature of mechanotransduction. Proc. Natl. Acad. Sci. U. S. A. 105, 6626–31.

Nagel, M., Tahinci, E., Symes, K., Winklbauer, R., 2004. Guidance of mesoderm cell migration in the Xenopus gastrula requires PDGF signaling. Development 131, 2727–36.

Nakatsuji, N., Johnson, K.E., 1982. Cell locomotion in vitro by Xenopus laevis gastrula mesodermal cells. Cell Motil. 2, 149–61.

Nelson, W.J., 2008. Regulation of cell-cell adhesion by the cadherin-catenin complex. Biochem. Soc. Trans. 36, 149–55.

Nern, A., Zhu, Y., Zipursky, S.L., 2008. Local N-cadherin interactions mediate distinct steps in the targeting of lamina neurons. Neuron 58, 34–41.

Ng, M.R., Besser, A., Danuser, G., Brugge, J.S., 2012. Substrate stiffness regulates cadherin-dependent collective migration through myosin-II contractility. J. Cell Biol. 199, 545–63.

Nieuwkoop, P.D., Faber, J., 1994. Normal table of Xenopus laevis (Daudin). Garland Publishing Inc, New York.

Niewiadomska, P., Godt, D., Tepass, U., 1999. DE-Cadherin is required for intercellular motility during drosophila oogenesis. J. Cell Biol. 144, 533–48.

Ninomiya, H., Elinson, R.P., Winklbauer, R., 2004. Antero-posterior tissue polarity links mesoderm convergent extension to axial patterning. Nature 430, 364–7.

Nobes, C.D., Hall, A., 1999. Rho GTPases control polarity, protrusion, and adhesion during cell movement. J. Cell Biol. 144, 1235–44.

Noren, N.K., Niessen, C.M., Gumbiner, B.M., Burridge, K., 2001. Cadherin engagement regulates Rho family GTPases. J. Biol. Chem. 276, 33305–8.

Ohashi, T., Sugaya, Y., Sakamoto, N., Sato, M., 2007. Hydrostatic pressure influences morphology and expression of VE-cadherin of vascular endothelial cells. J. Biomech. 40, 2399–405.

Oliveira, R., Christov, C., Guillamo, J.S., de Boüard, S., Palfi, S., Venance, L., Tardy, M., Peschanski, M., 2005. Contribution of gap junctional communication between tumor cells and astroglia to the invasion of the brain parenchyma by human glioblastomas. BMC Cell Biol. 6, 7.

Onodera, T., Sakai, T., Hsu, J.C., Matsumoto, K., Chiorini, J.A., Yamada, K.M., 2010. Btbd7 regulates epithelial cell dynamics and branching morphogenesis. Science 329, 562–565.

Orr, A.W., Helmke, B.P., Blackman, B.R., Schwartz, M.A., 2006. Mechanisms of mechanotransduction. Dev. Cell 10, 11–20.

Osipchuk, Y., Cahalan, M., 1992. Cell-to-cell spread of calcium signals mediated by ATP receptors in mast cells. Nature 359, 241–4.

Oviedo-Orta, E., Errington, R.J., Evans, W.H., 2002. Gap junction intercellular communication during lymphocyte transendothelial migration. Cell Biol. Int. 26, 253–263.

Owen, K.A., Pixley, F.J., Thomas, K.S., Vicente-Manzanares, M., Ray, B.J., Horwitz, A.F., Parsons, J.T., Beggs, H.E., Stanley, E.R., Bouton, A.H., 2007. Regulation of lamellipodial persistence, adhesion turnover, and motility in macrophages by focal adhesion kinase. J. Cell Biol. 179, 1275–87.

Papachroni, K.K., Karatzas, D.N., Papavassiliou, K.A., Basdra, E.K., Papavassiliou, A.G., 2009. Mechanotransduction in osteoblast regulation and bone disease. Trends Mol. Med. 15, 208–16.

Papusheva, E., Heisenberg, C.-P., 2010. Spatial organization of adhesion: force-dependent regulation and function in tissue morphogenesis. EMBO J. 29, 2753–68.

Parsons, J.T., 2003. Focal adhesion kinase: the first ten years. J. Cell Sci. 116, 1409–16.

Pathak, A., Kumar, S., 2012. Independent regulation of tumor cell migration by matrix stiffness and confinement. Proc. Natl. Acad. Sci. U. S. A. 109, 10334–9.

Pathre, P., Arregui, C., Wampler, T., Kue, I., Leung, T., Lilien, J., Balsamo, J., 2001. PTP1B regulates neurite extension mediated by cell-cell and cell-matrix adhesion molecules. J. Neurosci. Res. 63, 143–50.

Perez-Moreno, M., Fuchs, E., 2006. Catenins: keeping cells from getting their signals crossed. Dev. Cell 11, 601–12.

Petridou, N.I., Stylianou, P., Christodoulou, N., Rhoads, D., Guan, J.-L., Skourides, P.A., 2012. Activation of endogenous FAK via expression of its amino terminal domain in Xenopus embryos. PLoS One 7, e42577.

Petridou, N.I., Stylianou, P., Skourides, P.A., 2013. A dominant-negative provides new insights into FAK regulation and function in early embryonic morphogenesis. Development 140, 4266–76.

Phng, L.-K., Gerhardt, H., 2009. Angiogenesis: a team effort coordinated by notch. Dev. Cell 16, 196–208.

Playford, M.P., Schaller, M.D., 2004. The interplay between Src and integrins in normal and tumor biology. Oncogene 23, 7928–7946.

Playford, M.P., Vadali, K., Cai, X., Burridge, K., Schaller, M.D., 2008. Focal adhesion kinase regulates cell-cell contact formation in epithelial cells via modulation of Rho. Exp. Cell Res. 314, 3187–97.

Poliakov, A., Cotrina, M., Wilkinson, D.G., 2004. Diverse roles of eph receptors and ephrins in the regulation of cell migration and tissue assembly. Dev. Cell 7, 465–80.

Pollard, T.D., Borisy, G.G., 2003. Cellular motility driven by assembly and disassembly of actin filaments. Cell 112, 453–65.

Pollmann, M.-A., Shao, Q., Laird, D.W., Sandig, M., 2005. Connexin 43 mediated gap junctional communication enhances breast tumor cell diapedesis in culture. Breast Cancer Res. 7, R522–34.

Poujade, M., Grasland-Mongrain, E., Hertzog, A., Jouanneau, J., Chavrier, P., Ladoux, B., Buguin, A., Silberzan, P., 2007. Collective migration of an epithelial monolayer in response to a model wound. Proc. Natl. Acad. Sci. 104, 15988–93.

Pouthas, F., Girard, P., Lecaudey, V., Ly, T.B.N., Gilmour, D., Boulin, C., Pepperkok, R., Reynaud, E.G., 2008. In migrating cells, the Golgi complex and the position of the centrosome depend on geometrical constraints of the substratum. J. Cell Sci. 121, 2406–14.

Prasad, M., Montell, D.J., 2007. Cellular and molecular mechanisms of border cell migration analyzed using time-lapse live-cell imaging. Dev. Cell 12, 997–1005.

Rabilloud, T., Chevallet, M., Luche, S., Lelong, C., 2010. Two-dimensional gel electrophoresis in proteomics: Past, present and future. J. Proteomics 73, 2064–77.

Ramms, L., Fabris, G., Windoffer, R., Schwarz, N., Springer, R., Zhou, C., Lazar, J., Stiefel, S., Hersch, N., Schnakenberg, U., Magin, T.M., Leube, R.E., Merkel, R., Hoffmann, B., 2013. Keratins as the main component for the mechanical integrity of keratinocytes. Proc. Natl. Acad. Sci. U. S. A. 110, 18513–8.

Ramos, J.W., DeSimone, D.W., 1996. Xenopus embryonic cell adhesion to fibronectin: position-specific activation of RGD/synergy site-dependent migratory behavior at gastrulation. J. Cell Biol. 134, 227–40.

Ramos, J.W., Whittaker, C.A., DeSimone, D.W., 1996. Integrin-dependent adhesive activity is spatially controlled by inductive signals at gastrulation. Development 122, 2873–83.

Rappsilber, J., 2011. The beginning of a beautiful friendship: cross-linking/mass spectrometry and modelling of proteins and multi-protein complexes. J. Struct. Biol. 173, 530–40.

Rauzi, M., Verant, P., Lecuit, T., Lenne, P.-F., 2008. Nature and anisotropy of cortical forces orienting Drosophila tissue morphogenesis. Nat. Cell Biol. 10, 1401–10.

Ravichandran, K.S., 2001. Signaling via Shc family adapter proteins. Oncogene 20, 6322–30.

Reffay, M., Parrini, M.C., Cochet-Escartin, O., Ladoux, B., Buguin, A., Coscoy, S., Amblard, F., Camonis, J., Silberzan, P., 2014. Interplay of RhoA and mechanical forces in collective cell migration driven by leader cells. Nat. Cell Biol. 16, 217–223.

Reffay, M., Petitjean, L., Coscoy, S., Grasland-Mongrain, E., Amblard, F., Buguin, A., Silberzan, P., 2011. Orientation and polarity in collectively migrating cell structures: statics and dynamics. Biophys. J. 100, 2566–75.

Ren, G., Helwani, F.M., Verma, S., McLachlan, R.W., Weed, S.A., Yap, A.S., 2009. Cortactin is a functional target of E-cadherin-activated Src family kinases in MCF7 epithelial monolayers. J. Biol. Chem. 284, 18913–18922.

Ren, X.-D., Kiosses, W.B., Schwartz, M.A., 1999. Regulation of the small GTP-binding protein Rho by cell adhesion and the cytoskeleton. EMBO J. 18, 578–85.

Ren, X.-D., Kiosses, W.B., Sieg, D.J., Otey, C.A., Schlaepfer, D.D., Schwartz, M.A., 2000. Focal adhesion kinase suppresses Rho activity to promote focal adhesion turnover. J. Cell Sci. 113, 3673–8.

Retta, S.F., Balzac, F., Avolio, M., 2006. Rap1: a turnabout for the crosstalk between cadherins and integrins. Eur. J. Cell Biol. 85, 283–93.

Ricca, B.L., Venugopalan, G., Fletcher, D.A., 2013. To pull or be pulled: parsing the multiple modes of mechanotransduction. Curr. Opin. Cell Biol. 25, 558–64.

Rigaut, G., Shevchenko, A., Rutz, B., Wilm, M., Mann, M., Séraphin, B., 1999. A generic protein purification method for protein complex characterization and proteome exploration. Nat. Biotechnol. 17, 1030–2.

Riveline, D., Zamir, E., Balaban, N.Q., Schwarz, U.S., Ishizaki, T., Narumiya, S., Kam, Z., Geiger, B., Bershadsky, A.D., 2001. Focal contacts as mechanosensors: externally applied local mechanical force induces growth of focal contacts by an mDia1-dependent and ROCK-independent mechanism. J. Cell Biol. 153, 1175–86.

Roberts, B.J., Wahl, J.K., Johnson, K.R., Pashaj, A., 2011. Desmosome dynamics in migrating epithelial cells requires the actin cytoskeleton. Exp. Cell Res. 317, 2814–2822.

Roca, C., Adams, R.H., 2007. Regulation of vascular morphogenesis by Notch signaling. Genes Dev. 21, 2511–24.

Roca-Cusachs, P., Sunyer, R., Trepat, X., 2013. Mechanical guidance of cell migration: lessons from chemotaxis. Curr. Opin. Cell Biol. 25, 543–9.

Rørth, P., 2011. Whence directionality: guidance mechanisms in solitary and collective cell migration. Dev. Cell 20, 9–18.

Ross, T.D., Coon, B.G., Yun, S., Baeyens, N., Tanaka, K., Ouyang, M., Schwartz, M.A., 2013. Integrins in mechanotransduction. Curr. Opin. Cell Biol. 25, 613–8.

Roura, S., Miravet, S., Piedra, J., Garcia de Herreros, A., Dunach, M., 1999. Regulation of E-cadherin/ catenin association by tyrosine phosphorylation. J. Biol. Chem. 274, 36734–40.

Rozario, T., DeSimone, D.W., 2010. The extracellular matrix in development and morphogenesis: a dynamic view. Dev. Biol. 341, 126–40.

Rozario, T., Dzamba, B.J., Weber, G.F., Davidson, L.A., DeSimone, D.W., 2009. The physical state of fibronectin matrix differentially regulates morphogenetic movements in vivo. Dev. Biol. 327, 386–98.

Sahai, E., Marshall, C.J., 2002. ROCK and Dia have opposing effects on adherens junctions downstream of Rho. Nat. Cell Biol. 4, 408–15.

Sahlgren, C., Gustafsson, M. V., Jin, S., Poellinger, L., Lendahl, U., 2008. Notch signaling mediates hypoxia-induced tumor cell migration and invasion. Proc. Natl. Acad. Sci. U. S. A. 105, 6392–7.

Sallee, J.L., Wittchen, E.S., Burridge, K., 2006. Regulation of cell adhesion by protein-tyrosine phosphatases: II. Cell-cell adhesion. J. Biol. Chem. 281, 16189–92.

Sammak, P.J., Hinman, L.E., Tran, P.O., Sjaastad, M.D., Machen, T.E., 1997. How do injured cells communicate with the surviving cell monolayer? J. Cell Sci. 110, 465–75.

Sanderson, M.J., Charles, A.C., Boitano, S., Dirksen, E.R., 1994. Mechanisms and function of intercellular calcium signaling. Mol. Cell. Endocrinol. 98, 173–87.

Sangrar, W., Gao, Y., Scott, M., Truesdell, P., Greer, P.A., 2007. Fer-mediated cortactin phosphorylation is associated with efficient fibroblast migration and is dependent on reactive oxygen species generation during integrin-mediated cell adhesion. Mol. Cell. Biol. 27, 6140–52.

Sawada, Y., Tamada, M., Dubin-Thaler, B.J., Cherniavskaya, O., Sakai, R., Tanaka, S., Sheetz, M.P., 2006. Force sensing by mechanical extension of the Src family kinase substrate p130Cas. Cell 127, 1015–26.

Schaller, M.D., 2010. Cellular functions of FAK kinases: insight into molecular mechanisms and novel functions. J. Cell Sci. 123, 1007–1013.

Schaller, M.D., Borgman, C.A., Cobb, B.S., Vines, R.R., Reynolds, A.B., Parsons, J.T., 1992. pp125FAK a structurally distinctive protein-tyrosine kinase associated with focal adhesions. Proc. Natl. Acad. Sci. U. S. A. 89, 5192–6.

Schindelin, J., Arganda-Carreras, I., Frise, E., Kaynig, V., Longair, M., Pietzsch, T., Preibisch, S., Rueden, C., Saalfeld, S., Schmid, B., Tinevez, J.-Y., White, D.J., Hartenstein, V., Eliceiri, K., Tomancak, P., Cardona, A., 2012. Fiji: an open-source platform for biological-image analysis. Nat. Methods 9, 676–82.

Schlaepfer, D.D., Hauck, C.R., Sieg, D.J., 1999. Signaling through focal adhesion kinase. Prog. Biophys. Mol. Biol. 71, 435–478.

Schlaepfer, D.D., Mitra, S.K., Ilić, D., 2004. Control of motile and invasive cell phenotypes by focal adhesion kinase. Biochim. Biophys. Acta 1692, 77–102.

Schneider, S., Herrenknecht, K., Butz, S., Kemler, R., Hausen, P., 1993. Catenins in Xenopus embryogenesis and their relation to the cadherin-mediated cell-cell adhesion system. Development 118, 629–40.

Schober, M., Raghavan, S., Nikolova, M., Polak, L., Pasolli, H.A., Beggs, H.E., Reichardt, L.F., Fuchs, E., 2007. Focal adhesion kinase modulates tension signaling to control actin and focal adhesion dynamics. J. Cell Biol. 176, 667–80.

Schober, M., Rebay, I., Perrimon, N., 2005. Function of the ETS transcription factor Yan in border cell migration. Development 132, 3493–504.

Schwartz, E.A., Bizios, R., Medow, M.S., Gerritsen, M.E., 1999. Exposure of human vascular endothelial cells to sustained hydrostatic pressure stimulates proliferation : involvement of the v integrins. Circ. Res. 84, 315–322.

Schwartz, M.A., Assoian, R.K., 2001. Integrins and cell proliferation: regulation of cyclin-dependent kinases via cytoplasmic signaling pathways. J. Cell Sci. 114, 2553–60.

Schwartz, M.A., DeSimone, D.W., 2008. Cell adhesion receptors in mechanotransduction. Curr. Opin. Cell Biol. 20, 551–6.

Serra-Picamal, X., Conte, V., Vincent, R., Anon, E., Tambe, D.T., Bazellieres, E., Butler, J.P., Fredberg, J.J., Trepat, X., 2012. Mechanical waves during tissue expansion. Nat. Phys. 8, 628–634.

Serrels, B., Serrels, A., Brunton, V.G., Holt, M., McLean, G.W., Gray, C.H., Jones, G.E., Frame, M.C., 2007. Focal adhesion kinase controls actin assembly via a FERM-mediated interaction with the Arp2/3 complex. Nat. Cell Biol. 9, 1046–56.

Sestan, N., Artavanis-Tsakonas, S., Rakic, P., 1999. Contact-dependent inhibition of cortical neurite growth mediated by notch signaling. Science 286, 741–6.

Shay-Salit, A., Shushy, M., Wolfovitz, E., Yahav, H., Breviario, F., Dejana, E., Resnick, N., 2002. VEGF receptor 2 and the adherens junction as a mechanical transducer in vascular endothelial cells. Proc. Natl. Acad. Sci. U. S. A. 99, 9462–7.

Shewan, A.M., Maddugoda, M., Kraemer, A., Stehbens, S.J., Verma, S., Kovacs, E.M., Yap, A.S., 2005. Myosin 2 is a key Rho kinase target necessary for the local concentration of E-cadherin at cell–cell contacts. Mol. Biol. Cell 16, 4531–4542.

Shikanai, M., Nakajima, K., Kawauchi, T., 2011. N-cadherin regulates radial glial fiber-dependent migration of cortical locomoting neurons. Commun. Integr. Biol. 4, 326–30.

Shook, D., Keller, R., 2003. Mechanisms, mechanics and function of epithelial–mesenchymal transitions in early development. Mech. Dev. 120, 1351–83.

Sieg, D.J., Hauck, C.R., Schlaepfer, D.D., 1999. Required role of focal adhesion kinase (FAK) for integrin-stimulated cell migration. J. Cell Sci. 112, 2677–91.

Siekmann, A.F., Lawson, N.D., 2007. Notch signalling limits angiogenic cell behaviour in developing zebrafish arteries. Nature 445, 781–4.

Sive, H.L., Grainger, R.M., Harland, R.M., 2000. Early development of Xenopus laevis : a laboratory manual. Cold Spring Harbor Laboratory Press, Cold Spring Harbor, NY.

Skoge, M., Adler, M., Groisman, A., Levine, H., Loomis, W.F., Rappel, W.-J., 2010. Gradient sensing in defined chemotactic fields. Integr. Biol. 2, 659–68.

Smith, M.L., Gourdon, D., Little, W.C., Kubow, K.E., Eguiluz, R.A., Luna-Morris, S., Vogel, V., 2007. Force-induced unfolding of fibronectin in the extracellular matrix of living cells. PLoS Biol. 5, e268.

Somogyi, K., Rørth, P., 2004. Evidence for tension-based regulation of Drosophila MAL and SRF during invasive cell migration. Dev. Cell 7, 85–93.

Sonnenberg, A., Liem, R.K.H., 2007. Plakins in development and disease. Exp. Cell Res. 313, 2189–203.

Spiering, D., Hodgson, L., 2011. Dynamics of the Rho-family small GTPases in actin regulation and motility. Cell Adh. Migr. 5, 170–180.

Steneberg, P., Hemphälä, J., Samakovlis, C., 1999. Dpp and Notch specify the fusion cell fate in the dorsal branches of the Drosophila trachea. Mech. Dev. 87, 153–63.

Stoker, A.W., 2005. Protein tyrosine phosphatases and signalling. J. Endocrinol. 185, 19–33.

Stylianou, P., Skourides, P.A., 2009. Imaging morphogenesis, in Xenopus with Quantum Dot nanocrystals. Mech. Dev. 126, 828–41.

Symes, K., Smith, J.C., 1987. Gastrulation movements provide an early marker of mesoderm induction in Xenopus laevis. Development 101, 339–49.

Symowicz, J., Adley, B.P., Gleason, K.J., Johnson, J.J., Ghosh, S., Fishman, D.A., Hudson, L.G., Stack, M.S., 2007. Engagement of collagen-binding integrins promotes matrix metalloproteinase-9-dependent E-cadherin ectodomain shedding in ovarian carcinoma cells. Cancer Res. 67, 2030–9.

Taddei, M.L., Chiarugi, P., Cirri, P., Buricchi, F., Fiaschi, T., Giannoni, E., Talini, D., Cozzi, G., Formigli, L., Raugei, G., Ramponi, G., 2002. β-catenin interacts with low-molecular-weight protein tyrosine phosphatase leading to cadherin-mediated cell-cell adhesion increase. Cancer Res. 62, 6489–6499.

Takemoto, K., Matsuda, T., Sakai, N., Fu, D., Noda, M., Uchiyama, S., Kotera, I., Arai, Y., Horiuchi, M., Fukui, K., Ayabe, T., Inagaki, F., Suzuki, H., Nagai, T., 2013. SuperNova, a monomeric photosensitizing fluorescent protein for chromophore-assisted light inactivation. Sci. Rep. 3, 2629.

Tambe, D.T., Hardin, C.C., Angelini, T.E., Rajendran, K., Park, C.Y., Serra-Picamal, X., Zhou, E.H., Zaman, M.H., Butler, J.P., Weitz, D.A., Fredberg, J.J., Trepat, X., 2011. Collective cell guidance by cooperative intercellular forces. Nat. Mater. 10, 469–75.

Teddy, J.M., Kulesa, P.M., 2004. In vivo evidence for short- and long-range cell communication in cranial neural crest cells. Development 131, 6141–51.

Theisen, C.S., Wahl, J.K., Johnson, K.R., Wheelock, M.J., 2007. NHERF links the N-cadherin/catenin complex to the platelet-derived growth factor receptor to modulate the actin cytoskeleton and regulate cell motility. Mol. Biol. Cell 18, 1220–32.

Theveneau, E., Marchant, L., Kuriyama, S., Gull, M., Moepps, B., Parsons, M., Mayor, R., 2010. Collective chemotaxis requires contact-dependent cell polarity. Dev. Cell 19, 39–53.

Theveneau, E., Mayor, R., 2012. Cadherins in collective cell migration of mesenchymal cells. Curr. Opin. Cell Biol. 24, 677–84.

Theveneau, E., Mayor, R., 2013. Collective cell migration of epithelial and mesenchymal cells. Cell. Mol. Life Sci. 70, 3481–92.

Theveneau, E., Steventon, B., Scarpa, E., Garcia, S., Trepat, X., Streit, A., Mayor, R., 2013. Chase-and-run between adjacent cell populations promotes directional collective migration. Nat. Cell Biol. 15, 763–72.

Tilghman, R.W., Slack-Davis, J.K., Sergina, N., Martin, K.H., Iwanicki, M., Hershey, E.D., Beggs, H.E., Reichardt, L.F., Parsons, J.T., 2005. Focal adhesion kinase is required for the spatial organization of the leading edge in migrating cells. J. Cell Sci. 118, 2613–23.

Todorović, V., Desai, B. V., Schroeder Patterson, M.J., Amargo, E. V., Dubash, A.D., Yin, T., Jones, J.C.R., Green, K.J., 2010. Plakoglobin regulates cell motility through Rho- and fibronectin-dependent Src signaling. J. Cell Sci. 123, 3576–86.

Tomar, A., Lim, S.-T., Lim, Y., Schlaepfer, D.D., 2009. A FAK-p120RasGAP-p190RhoGAP complex regulates polarity in migrating cells. J. Cell Sci. 122, 1852–62.

Torpey, N., Wylie, C., Heasman, J., 1992. Function of maternal cytokeratin in Xenopus development. Nature 357, 413–5.

Tórtora, V., Quijano, C., Freeman, B., Radi, R., Castro, L., 2007. Mitochondrial aconitase reaction with nitric oxide, S-nitrosoglutathione, and peroxynitrite: mechanisms and relative contributions to aconitase inactivation. Free Radic. Biol. Med. 42, 1075–88.

Trepat, X., Wasserman, M.R., Angelini, T.E., Millet, E., Weitz, D.A., Butler, J.P., Fredberg, J.J., 2009. Physical forces during collective cell migration. Nat. Phys. 5, 426–430.

Tsuruta, D., Jones, J.C.R., 2003. The vimentin cytoskeleton regulates focal contact size and adhesion of endothelial cells subjected to shear stress. J. Cell Sci. 116, 4977–84.

Tzima, E., Irani-Tehrani, M., Kiosses, W.B., Dejana, E., Schultz, D.A., Engelhardt, B., Cao, G., DeLisser, H., Schwartz, M.A., 2005. A mechanosensory complex that mediates the endothelial cell response to fluid shear stress. Nature 437, 426–31.

Ueda, M., Gräf, R., MacWilliams, H.K., Schliwa, M., Euteneuer, U., 1997. Centrosome positioning and directionality of cell movements. Proc. Natl. Acad. Sci. U. S. A. 94, 9674–8.

Ursell, T.S., Klug, W.S., Phillips, R., 2009. Morphology and interaction between lipid domains. Proc. Natl. Acad. Sci. U. S. A. 106, 13301–6.

Van Aelst, L., Symons, M., 2002. Role of Rho family GTPases in epithelial morphogenesis. Genes Dev. 16, 1032–1054.

Van Horssen, R., Galjart, N., Rens, J.A.P., Eggermont, A.M.M., ten Hagen, T.L.M., 2006. Differential effects of matrix and growth factors on endothelial and fibroblast motility: application of a modified cell migration assay. J. Cell. Biochem. 99, 1536–52.

Vedula, S.R.K., Hirata, H., Nai, M.H., Brugués, A., Toyama, Y., Trepat, X., Lim, C.T., Ladoux, B., 2014. Epithelial bridges maintain tissue integrity during collective cell migration. Nat. Mater. 13, 87–96.

Vedula, S.R.K., Leong, M.C., Lai, T.L., Hersen, P., Kabla, A.J., Lim, C.T., Ladoux, B., 2012. Emerging modes of collective cell migration induced by geometrical constraints. Proc. Natl. Acad. Sci. U. S. A. 109, 12974–9.

Vedula, S.R.K., Ravasio, A., Lim, C.T., Ladoux, B., 2013. Collective cell migration: a mechanistic perspective. Physiology 28, 370–9.

Wallingford, J.B., Ewald, A.J., Harland, R.M., Fraser, S.E., 2001. Calcium signaling during convergent extension in Xenopus. Curr. Biol. 11, 652–61.

Wang, H., Radjendirane, V., Wary, K.K., Chakrabarty, S., 2004. Transforming growth factor β regulates cell-cell adhesion through extracellular matrix remodeling and activation of focal adhesion kinase in human colon carcinoma Moser cells. Oncogene 23, 5558–61.

Wang, H.-B., Dembo, M., Hanks, S.K., Wang, Y.-L., 2001. Focal adhesion kinase is involved in mechanosensing during fibroblast migration. Proc. Natl. Acad. Sci. U. S. A. 98, 11295–300.

Wang, X., Adam, J.C., Montell, D.J., 2007. Spatially localized Kuzbanian required for specific activation of Notch during border cell migration. Dev. Biol. 301, 532–40.

Wang, X., He, L., Wu, Y.I., Hahn, K.M., Montell, D.J., 2010. Light-mediated activation reveals a key role for Rac in collective guidance of cell movement in vivo. Nat. Cell Biol. 12, 591–7.

Warner, S.J., Longmore, G.D., 2009. Cdc42 antagonizes Rho1 activity at adherens junctions to limit epithelial cell apical tension. J. Cell Biol. 187, 119–33.

Watanabe, T., Sato, K., Kaibuchi, K., 2009. Cadherin-mediated intercellular adhesion and signaling cascades involving small GTPases. Cold Spring Harb. Perspect. Biol. 1, a003020.

Watt, F.M., 2002. Role of integrins in regulating epidermal adhesion, growth and differentiation. EMBO J. 21, 3919–26.

Webb, D.J., Donais, K., Whitmore, L.A., Thomas, S.M., Turner, C.E., Parsons, J.T., Horwitz, A.F., 2004. FAK-Src signalling through paxillin, ERK and MLCK regulates adhesion disassembly. Nat. Cell Biol. 6, 154–61.

Webb, S.E., Miller, A.L., 2006. Ca2+ signaling and early embryonic patterning during the blastula and gastrula periods of zebrafish and Xenopus development. Biochim. Biophys. Acta 1763, 1192–208.

Weber, G.F., Bjerke, M.A., DeSimone, D.W., 2011. Integrins and cadherins join forces to form adhesive networks. J. Cell Sci. 124, 1183–93.

Weber, G.F., Bjerke, M.A., DeSimone, D.W., 2012. A mechanoresponsive cadherin-keratin complex directs polarized protrusive behavior and collective cell migration. Dev. Cell 22, 104–15.

Wildenberg, G.A., Dohn, M.R., Carnahan, R.H., Davis, M.A., Lobdell, N.A., Settleman, J., Reynolds, A.B., 2006. p120-catenin and p190RhoGAP regulate cell-cell adhesion by coordinating antagonism between Rac and Rho. Cell 127, 1027–39.

Wilson, E., Sudhir, K., Ives, H.E., 1995. Mechanical strain of rat vascular smooth muscle cells is sensed by specific extracellular matrix/integrin interactions. J. Clin. Invest. 96, 2364–72.

Winklbauer, R., 1990. Mesodermal cell migration during Xenopus gastrulation. Dev. Biol. 142, 155–168.

Winklbauer, R., 2009. Cell adhesion in amphibian gastrulation. Int. Rev. Cell Mol. Biol. 278, 215–75.

Winklbauer, R., Selchow, A., 1992. Motile behavior and protrusive activity of migratory mesoderm cells from the Xenopus gastrula. Dev. Biol. 150, 335–51.

Winklbauer, R., Selchow, A., Nagel, M., Angres, B., 1992. Cell interaction and its role in mesoderm cell migration during Xenopus gastrulation. Dev. Dyn. 195, 290–302.

Wolf, K., Wu, Y.I., Liu, Y., Geiger, J., Tam, E., Overall, C., Stack, M.S., Friedl, P., 2007. Multi-step pericellular proteolysis controls the transition from individual to collective cancer cell invasion. Nat. Cell Biol. 9, 893–904.

Wöll, S., Windoffer, R., Leube, R.E., 2005. Dissection of keratin dynamics: different contributions of the actin and microtubule systems. Eur. J. Cell Biol. 84, 311–28.

Wong, P., Coulombe, P.A., 2003. Loss of keratin 6 (K6) proteins reveals a function for intermediate filaments during wound repair. J. Cell Biol. 163, 327–37.

Wozniak, M.A., Chen, C.S., 2009. Mechanotransduction in development: a growing role for contractility. Nat. Rev. Mol. Cell Biol. 10, 34–43.

Xu, X., Francis, R., Wei, C.J., Linask, K.L., Lo, C.W., 2006. Connexin 43-mediated modulation of polarized cell movement and the directional migration of cardiac neural crest cells. Development 133, 3629–39.

Xu, X., Li, W.E., Huang, G.Y., Meyer, R., Chen, T., Luo, Y., Thomas, M.P., Radice, G.L., Lo, C.W., 2001. Modulation of mouse neural crest cell motility by N-cadherin and connexin 43 gap junctions. J. Cell Biol. 154, 217–30.

Yamada, S., Nelson, W.J., 2007. Localized zones of Rho and Rac activities drive initiation and expansion of epithelial cell-cell adhesion. J. Cell Biol. 178, 517–27.

Yamada, S., Wirtz, D., Coulombe, P.A., 2002. Pairwise assembly determines the intrinsic potential for self-organization and mechanical properties of keratin filaments. Mol. Biol. Cell 13, 382–91.

Yang, J.T., Rayburn, H., Hynes, R.O., 1993. Embryonic mesodermal defects in α5 integrin-deficient mice. Development 119, 1093–105.

Yang, M.T., Fu, J., Wang, Y.-K., Desai, R.A., Chen, C.S., 2011. Assaying stem cell mechanobiology on microfabricated elastomeric substrates with geometrically modulated rigidity. Nat. Protoc. 6, 187–213.

Yang, X., Chrisman, H., Weijer, C.J., 2008. PDGF signalling controls the migration of mesoderm cells during chick gastrulation by regulating N-cadherin expression. Development 135, 3521–30.

Yano, H., Mazaki, Y., Kurokawa, K., Hanks, S.K., Matsuda, M., Sabe, H., 2004. Roles played by a subset of integrin signaling molecules in cadherin-based cell-cell adhesion. J. Cell Biol. 166, 283–95.

Yin, T., Getsios, S., Caldelari, R., Kowalczyk, A.P., Müller, E.J., Jones, J.C.R., Green, K.J., 2005. Plakoglobin suppresses keratinocyte motility through both cell-cell adhesion-dependent and -independent mechanisms. Proc. Natl. Acad. Sci. U. S. A. 102, 5420–5.

Yonemura, S., Wada, Y., Watanabe, T., Nagafuchi, A., Shibata, M., 2010. α-Catenin as a tension transducer that induces adherens junction development. Nat. Cell Biol. 12, 533–42.

Zhong, C., Kinch, M.S., Burridge, K., 1997. Rho-stimulated contractility contributes to the fibroblastic phenotype of Ras-transformed epithelial cells. Mol. Biol. Cell 8, 2329–44.

Zhurinsky, J., Shtutman, M., Ben-Ze'ev, A., 2000. Plakoglobin and β-catenin: protein interactions, regulation and biological roles. J. Cell Sci. 113, 3127–39.